

B186
4

0

AGARD-R-702

AGARD-R-702

ADA121013

AGARD

ADVISORY GROUP FOR AEROSPACE RESEARCH & DEVELOPMENT

7 RUE ANCELEE 92200 NEUILLY SUR SEINE FRANCE

AGARD REPORT No. 702

Compendium of Unsteady Aerodynamic Measurements

DTIC
SELECTE
NOV 2 1982
A

This document has been approved
for public release and sale; its
distribution is unlimited.

NORTH ATLANTIC TREATY ORGANIZATION



DISTRIBUTION AND AVAILABILITY
ON BACK COVER

DTIC FILE COPY

82 11 02 130

NORTH ATLANTIC TREATY ORGANIZATION
ADVISORY GROUP FOR AEROSPACE RESEARCH AND DEVELOPMENT
(ORGANISATION DU TRAITE DE L'ATLANTIQUE NORD)

AGARD Report No.702
COMPENDIUM OF UNSTEADY AERODYNAMIC MEASUREMENTS

This Report was sponsored by the Structures and Materials Panel of AGARD.

THE MISSION OF AGARD

The mission of AGARD is to bring together the leading personalities of the NATO nations in the fields of science and technology relating to aerospace for the following purposes:

- Exchanging of scientific and technical information;
- Continuously stimulating advances in the aerospace sciences relevant to strengthening the common defence posture;
- Improving the co-operation among member nations in aerospace research and development;
- Providing scientific and technical advice and assistance to the North Atlantic Military Committee in the field of aerospace research and development;
- Rendering scientific and technical assistance, as requested, to other NATO bodies and to member nations in connection with research and development problems in the aerospace field;
- Providing assistance to member nations for the purpose of increasing their scientific and technical potential;
- Recommending effective ways for the member nations to use their research and development capabilities for the common benefit of the NATO community.

The highest authority within AGARD is the National Delegates Board consisting of officially appointed senior representatives from each member nation. The mission of AGARD is carried out through the Panels which are composed of experts appointed by the National Delegates, the Consultant and Exchange Programme and the Aerospace Applications Studies Programme. The results of AGARD work are reported to the member nations and the NATO Authorities through the AGARD series of publications of which this is one.

Participation in AGARD activities is by invitation only and is normally limited to citizens of the NATO nations.

The content of this publication has been reproduced directly from material supplied by AGARD or the authors.

Published August 1982

Copyright © AGARD 1982
All Rights Reserved

ISBN 92-835-1430-0



Printed by Technical Editing and Reproduction Ltd
5-11 Mortimer Street, London W1N 7RH

PREFACE

The Subcommittee on Aeroelasticity of the AGARD Structures and Materials Panel (SMP) has produced two recent publications on the AGARD Standard Configurations for Aeroelastic Applications of Transonic Unsteady Aerodynamics: AGARD Advisory Report 156, "AGARD Two-Dimensional Aeroelastic Configurations" and AGARD Advisory Report 167, "AGARD Three-Dimensional Aeroelastic Configurations."

Now that the AGARD has established standard aeroelastic configurations, the next effort is to encourage aeroelasticians in the NATO countries to develop improved methods of predicting transonic unsteady aerodynamics and aeroelastic response and to evaluate them with respect to the AGARD configurations. This Compendium assists that development and evaluation by collecting the known unsteady aerodynamic experimental data for the AGARD configurations. It is due mainly to the efforts of Mr Norman Lambourne, recently of the Royal Aeronautical Establishment, with Mr H C Garner of the RAE as a major collaborator.

The next phases will come under the guidance of facilitators for aeroelasticity:

France: Mr R. Dat
ONERA
29 Avenue de la Division LeClerc
92 Chatillon
Paris

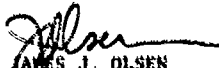
Germany: Dr W. Geissler
DFVLR-AVA
Bunsenstrasse 10
3400 Gottingen

Netherlands: Mr R. Zwaan
NLR
Anthony Fokkerweg 2
Amsterdam 1017

United Kingdom: Mr H C Garner
RAE
Farnborough, Hants GU14 6TD

United States: Dr J. Edwards
NASA Langley Research Center
MS 340
Hampton VA 23665

These facilitators will encourage contributions and communications among investigators in the NATO countries for a few key two-dimensional and three-dimensional standard configurations. They will present progress reports to the AGARD Structures and Materials Panel (SMP) in the Autumn of 1983. The effort will culminate in a Specialists' Meeting on "Transonic Unsteady Aerodynamics and Aeroelastic Application" at the SMP meeting in Fall 84. We encourage scientists in the NATO countries to communicate with one of the above facilitators to coordinate their contributions.


JAMES J. OLSEN
Chairman
AGARD/SMP Subcommittee on Aeroelasticity



Accession For	
NO. 156	<input checked="" type="checkbox"/>
156	<input type="checkbox"/>
Classified	<input type="checkbox"/>
Justification	<input type="checkbox"/>
Distribution	
Availability Code	<input type="checkbox"/>
Avail. Status	<input type="checkbox"/>
Dist. Special	<input type="checkbox"/>
A	

COMPENDIUM OF UNSTEADY AERODYNAMIC MEASUREMENTS

SUMMARY

The Compendium contains a selection of wind-tunnel measurements made on some of the AGARD Aeroelastic Configurations already chosen as computational test cases. Presentation of the numerical data in the form of separate Data Sets is preceded by a general review that discusses the various aspects concerning experimental measurements and comparisons with theoretical computations.

CONTENTS

	Page
GENERAL REVIEW by N.C. Lambourne	
1 Introduction	0-1
2 Guide to Compendium	0-1
3 General nature of unsteady data	0-2
4 Notation	0-3
5 Experimental procedures and interpretation of results	0-7
6 Tunnel interference	0-11
7 Uncertainties of experimental data	0-13
8 Comparison between theory and experiment	0-15
9 Suggestions for future experiments	0-16
References	0-17
Tables	0-18
Illustrations	0-20
DATA SETS	
2-D Configurations	
1 NACA 64A006. Oscillating flap by R.J. Zwaan, NLR	1-1
2 NACA 64A010 (NASA Ames model). Oscillatory pitching by Sanford S. Davis, NASA Ames	2-1
3 NACA 0012. Oscillatory and transient pitching by R.H. Landon, ARA	3-1
4 NLR 7301 supercritical airfoil. Oscillatory pitching and oscillating flap by R.J. Zwaan, NLR	4-1
5 NLR 7301 supercritical airfoil. Oscillatory pitching by Sanford S. Davis, NASA Ames	5-1
3-D Configurations	
6 RAE Wing A. Oscillating flap by D.G. Mabey, RAE	6-1
7 NORA model. Oscillation about swept axis by N.C. Lambourne	7-1

Further Data Sets may be issued later, as addenda, when experimental results for other configurations become available.

Note: Although the General Review and the Data Sets are separate contributions, a consistent scheme of numbering the pages, references, tables and figures is used throughout the Compendium. Thus, for instance Table m.n is the nth table of Data Set m. For the General Review m = 0.

GENERAL REVIEW

by

N. C. Lambourne*

1 INTRODUCTION

Interest in the kind of unsteady aerodynamics considered here arises from the need for information relevant to the aeroelastic stability of aircraft. The continuing need for studies is due to design developments extending to different types of flow and to new structural configurations. At present there is special interest in transonic and separated flows, in wings specially designed for supercritical flow, and in surfaces operating as part of active control systems.

Advances in computational fluid dynamics are giving impetus to the development of new theoretical methods for unsteady aerodynamics. The development of satisfactory methods, whilst depending ultimately on comparisons with experiment, is considerably helped by comparisons between one computational method and another. To assist these developments a Working Group of the AGARD Structures and Materials Panel has already chosen a series of 2-D and 3-D configurations and for each a set of test cases, including a priority subset, to be used for comparisons. These test cases are fully identified in Refs 0.1 and 0.2, which are the documents that have set the scene for the present Compendium. The chosen configurations are known as the AGARD Aeroelastic Configurations and it is now convenient to denote the chosen cases associated with them as the Computational Test (or CT) Cases.

Although some of the configurations and some of the CT Cases were chosen purely for theoretical interest and do not have experimental counterparts, others were chosen because they had been, or were shortly to be, the subject of unsteady measurements. For the most part, these measurements had been made independently by various researchers and the resulting data are situated at separate locations or in diverse documents. The present Compendium was conceived with the idea of collecting into a single document the experimental data most important for the proposed comparisons.

Whilst the prime purpose is the presentation of numerical data, it seemed desirable to include information about the experiments themselves and to mention their more important results. Also, when experimental data are to be used for numerical comparisons, some indication of their reliability is needed; for this reason a general discussion of the various experimental procedures and the limitations of experimental data is included.

For the presentation of the material, it has been found convenient to follow the kind of arrangement already used in an AGARD document, Ref 0.3, giving a data base for steady aerodynamics.

2 GUIDE TO COMPENDIUM

The complete list of AGARD Aeroelastic Configurations is given in Table 0.1. For those configurations having Data Sets in this Compendium this table also gives the CT Case numbers (as defined in Refs 0.1 and 0.2) for which there are experimental data. For those configurations not having Data Sets the present position regarding the experiments is stated. It is intended to issue further Data Sets whenever possible.

The Compendium consists of a General Review, of which this present section is part, followed by seven self-contained Data Sets. Each Data Set provides:

- means for identifying and locating all the unsteady measurements that could be made available;
- a brief overview of the salient features of the experimental results;
- numerical data from those tests that relate directly to the CT Cases.

Also, by means of a standard form, each Data Set gives key information about the test equipment and test conditions - information that may be found important when comparing experimental and theoretical results.

It is hoped that the information contained in the Data Sets will satisfy the theoretician through the first stages of comparing calculation with experiment. At some later stage the need may arise for comparisons with experimental cases beyond those selected to correspond with the CT Cases. It is for that reason that each Set lists all the experimental tests for which data could be made available if requested from the original source.

The tables presenting the numerical data are mostly copies of computer listings from the original data banks. Therefore the forms and notations differ across the various Data Sets. To have reformatted the data to a standard notation and lay-out would

* Preparation of the Review and editing of the Compendium was funded by US Air Force Office of Scientific Research, European Office of Aerospace Research and Development.

have required much labour and incurred the risk of introducing errors - apart from which, a familiarity gained with the original form makes for easy communication if similar data are required for additional cases.

It will be seen from Table 0.1 that the present Data Sets extend over a range of 2-D section shapes and 3-D planforms. The unsteady model motions are basically either some form of rigid-body pitching or control-surface rotation; they are mostly small-amplitude oscillations, although Data Set 3 includes large-amplitude oscillatory and transient motions. The experimental cases also include a variety of types of subsonic and transonic flow, but it is necessary to refer to the Data Sets themselves for detailed specifications.

It may be noted that not every CT Case has an experimental counterpart.

2.1 Correspondence between experimental and computational cases

Although it is true that the related CT Cases were chosen from the available experimental tests, the degree of relationship between them differs over the complete series.

The type of unsteady motion is basically the same for corresponding experimental and computation cases. In some CT Cases the specification of parameters such as amplitude, frequency, Mach number, Reynolds number, model incidence and flap angle are in exact agreement with the experiments. But for Data Sets 4 and 5, which both relate to the super-critical aerofoil NLR 7301, there are differences between the experimental and CT values of model mean incidence α_m and Mach number M as shown in Table 0.2.

With regard to Data Set 4, the explanation is straightforward. The airfoil was designed by a hodograph theory which predicted shock-free flow at $M = 0.721$ and $\alpha_m = -0.19$ deg. In the NLR experiments this type of flow did not occur for those theoretical values of M and α_m but was approximated as closely as possible for a different combination: $M = 0.744$ and $\alpha_m = 0.85$ deg. The differences were mainly due to viscous effects and tunnel interference. Thus the CT specifications were chosen such that theory would produce flows similar to those observed in the experiments, on the argument that these specifications will compensate for the two effects.

The situation with regard to Data Set 5 is rather more complicated because, at the time the CT Cases were chosen, these data, generated at NASA Ames, were not available. As in the NLR tests, the experiments from which the data are abstracted were run for combinations of M and α_m which gave classes of steady flow corresponding to those predicted by the aerofoil design theory using the CT specifications. Thus the cases of Data Set 5 can be related to the CT Cases on the basis of similar flows but for this Set the values of the frequency parameters do not match the CT Cases exactly.

Data Sets 4 and 5 form a unique combination in providing independent measurements of comparable data for the same aerofoil. However, as shown in Table 0.2 there are differences between the Reynolds numbers for the two sets and also differences in regard to the use of boundary-layer transition trips. In addition there is an appreciable difference between the two ratios of tunnel to model size, which as discussed later, may be important in connection with the effects of tunnel interference. Examples of comparisons between these two Data Sets are discussed in section 7.

Certain implications arising from the differences between the experimental and CT specifications will be discussed later in section 8.

3 GENERAL NATURE OF UNSTEADY DATA

The practical requirement is for aerodynamic information for lifting surfaces and control surfaces undergoing arbitrary time-dependent displacements or deformations. Basic studies are usually centred on 2-D or 3-D model configurations performing prescribed unsteady motions in a uniform stream with steady perturbations.

In considering the general forms of the aerodynamic quantities it is convenient to restrict the discussion to pressures, the quantities that are measured. Since it is the distribution of pressure that determines the resultant forces and moments it will be readily appreciated that similar remarks can apply to quantities such as lift, pitching moment and control-surface hinge-moment. For the time being discussion will be concerned with pressure denoted by p , the introduction of non-dimensional coefficients being left until later.

For a given model configuration in a given flow, interest lies in the pressure distributions associated with an unsteady change in a model displacement parameter ϕ , which is a general coordinate to denote angle of pitch, control-surface deflection or some other quantity defining the unsteady motion. The basic problem is to determine $p(t)$ for the prescribed time-wise variation $\phi(t)$.

Experiments are sometimes made with non-harmonic forms of $\phi(t)$, and indeed Data Set 3 includes tests in which incidence is increased approximately linearly with time, but most unsteady experiments have been made for oscillatory conditions. Although there are special interests in large-amplitude motions, the main concern is with small

perturbations and the most usual form of testing is with small-amplitude continuous harmonic oscillations. For this reason it is the pressure quantities relating to harmonic oscillations that will now be discussed.

We consider a rigid model undergoing oscillatory pitching motion. In addition to specifying Mach number and Reynolds number, the condition of the model is defined by

- a mean condition about which the oscillation occurs, specified by a mean incidence α_m ;
- an oscillatory motion specified by the sinusoid $\phi = \phi_0 \sin \omega t$.

Associated with this oscillatory condition will be the following classes of pressure quantity:

- steady pressure for the steady mean condition;
- unsteady pressure for the oscillatory condition: this includes a mean and an oscillatory component;
- steady pressures resulting from steady model positions which correspond to successive instantaneous positions during the unsteady excursions.

When a system can be regarded as linear (p varying linearly with ϕ) there are just four kinds of pressure quantities to be determined:

- (1) steady pressure p_s for the steady mean condition identical with p_m the mean pressure during the oscillation;
- (2) in-phase component normalised by motion amplitude, p'/ϕ_0 ;
- (3) in-quadrature component normalised by motion amplitude, p''/ϕ_0 ;
- (4) steady pressure derivative, $dp/d\phi$.

As an alternative, a modulus and a phase angle can replace the in-phase and in-quadrature components.

The distribution of p_s characterizes the type of flow, which in many respects influences the oscillatory and derivative pressures. Components p'/ϕ_0 and p''/ϕ_0 are, in general, dependent on the frequency of oscillation, and their variations with frequency give an indication of the effects of unsteady aerodynamics. In a linear system the derivative $dp/d\phi$ is the zero-frequency equivalent of p'/ϕ_0 , and provides a useful datum from which the effects of unsteadiness can be assessed.

When non-linearities are present, the pressure variation can be expressed as the Fourier series:

$$p(t) = p_m + p' \sin \omega t + p'' \cos \omega t + p_1' \sin 2\omega t + p_1'' \cos 2\omega t$$

plus higher harmonics. In the general non-linear case the Fourier coefficients are not necessarily proportional to the motion amplitude ϕ_0 , and the mean pressure p_m is not necessarily the same as the steady pressure p_s . Also the steady derivative $dp/d\phi$ needs to be replaced by another concept which will be discussed in the following section.

For attached flow serious non-linearities in pressure usually occur only for positions close to either a leading-edge, a flap hinge-line or a shockwave. Consequently being localised, the non-linearities tend to disappear when the pressures are integrated to give forces and moments. It is for this reason that even when non-linearity is present, practical interest continues to be centred on the fundamental components p'/ϕ_0 and p''/ϕ_0 . In most of the experiments included here, no attempt was made to measure any of the higher harmonics although large non-linearities were known to be occurring at a shockwave.

4 NOTATION

Various symbolic notations are used in the documents from which the information in the Data Sets has been obtained. Because the data listings are presented in their original form, it is necessary to explain the individual notations in each Data Set.

Some uniformity in notation is however desirable for future discussions and for this reason Bland, in Refs 0.1 and 0.2, has recommended a basic notation. This has been extended in this Compendium and, although the data listings retain their original forms, a move towards a standard notation has been made in preparing the diagrams and descriptive material for the Data Sets.

The following scheme is consistent with that proposed by Bland although there are a few minor changes. The sign conventions and some of the major definitions are shown in Fig 0.1 reproduced from Ref 0.2. The present scheme includes the basic notation and an extension to deal with the unsteady aerodynamic quantities.

BASIC NOTATION

Model geometry

local chord: c
 root chord: c_r
 model span: s
 full-span aspect ratio: AR
 sweepback angle: Λ
 taper ratio: $\lambda = \text{tip chord}/\text{root chord}$
 streamwise position aft of root leading edge: x
 chordwise position aft of local leading edge: ξc
 spanwise position: ns
 local position of pitching axis: x_a
 local position of flap hinge: x_δ
 incidence: α
 flap angle: δ (measured in a streamwise section)

Stream

Mach number: M
 Reynolds number based on root chord: Re
 velocity: V
 static pressure: p_∞
 total pressure: p_t
 dynamic pressure: q
 total temperature: T_0
 ratio of specific heats: γ

Model pressure (steady or instantaneous values)

surface pressure: p
 pressure coefficient: $C_p = (p - p_\infty)/q$
 pressure ratio: p/p_t
 pressure resultant loading: $\Delta C_p = (C_p \text{ lower} - C_p \text{ upper})$

Model surface flow

local Mach number M_L determined from a measured pressure ratio by the isentropic relation:

$$M_L = \left\{ \frac{2}{(\gamma - 1)} \left[\left(\frac{p}{p_t} \right)^{-(\gamma - 1)/\gamma} - 1 \right] \right\}^{1/2}$$

Section force coefficients

$$\text{lift: } c_l = \int_0^1 \Delta C_p d(x/c)$$

$$\text{pitching moment: } c_m = \int_0^1 \Delta C_p (x_a/c - x/c) d(x/c)$$

(Note: This definition of c_m is more general than that in Fig 0.1 because it relates to the moment about point x_a which need not be the same as x_δ about which the model is pitching.)

$$\text{flap lift: } c_{lf} = \int_{x_\delta/c}^1 \Delta C_p d(x/c)$$

Section force coefficients (concluded)

$$\text{flap hinge moment: } c_h = \int_{x_\delta/c}^1 \Delta C_p (x_\delta/c - x/c) d(x/c)$$

UNSTEADY NOTATION

Model motiontime: t non-dimensional time: $\tau \equiv 2Vt/c$ general coordinate for model motion: ϕ arbitrary motion: $\phi(t)$ or $\phi(\tau)$ oscillatory motion: $\phi = \phi_0 \sin \omega t$ (or $\phi_0 \cos \omega t$)oscillatory amplitude: ϕ_0 representing α_0 , δ_0 or θ_0 (Data Set 7)mean incidence during an oscillation: α_m mean flap angle during an oscillation: δ_m oscillation frequency: f (Hz), or $2\pi f \equiv \omega$ (rad s⁻¹)reduced frequency: $k = \omega c/2V$, or $\omega c_r/2V$ Unsteady pressures

For an arbitrary model motion $\phi = \phi(\tau)$, the time-wise variation of instantaneous pressure is defined as

$$C_p(\tau) = (p(\tau) - p_\infty)/q$$

Oscillatory pressures

For the oscillatory motion $\phi = \phi_0 \sin \omega t$, a general equation for oscillatory pressure is

$$p(t) = p_m + p' \sin \omega t + p'' \cos \omega t + p_1' \sin 2\omega t + p_1'' \cos 2\omega t + \text{etc}$$

or the alternative,

$$p(t) = p_m \pm [p_0 \sin(\omega t + \epsilon_0) + p_1 \sin(2\omega t + \epsilon_1) + \text{etc}]$$

The sign outside the brackets in the last equation is a matter of choice. However, it is most convenient to choose the negative sign for the upper surface of the model and the positive for the lower, then usually the phase angles ϵ_0 in degrees for both surfaces will tend to zero, and not 180 deg, as the frequency tends to zero. Also this choice of signs is consistent with the usual method of plotting chordwise distributions of oscillatory pressure.

Mean pressure during oscillation: $C_{pm} = (p_m - p_\infty)/q$

Fundamental (1st harmonic) amplitude-normalised components

in-phase (or real component): $C_p'/\phi_0 = p'/q\phi_0$

in-quadrature (or imaginary component): $C_p''/\phi_0 = p''/q\phi_0$

Where an oscillatory quantity can be expressed as a complex amplitude a bar is used thus:

$$\text{complex amplitude: } \bar{C}_p/\phi_0 = (C_p'/\phi_0) + i(C_p''/\phi_0) = \pm (|\bar{C}_p|/\phi_0)^{1\epsilon_0}$$

$$\text{modulus: } |\bar{C}_p|/\phi_0 = [(C_p'/\phi_0)^2 + (C_p''/\phi_0)^2]^{1/2}$$

$$\text{phase angle: } \epsilon_0 = \tan^{-1}(C_p''/C_p')$$

Following the recommendation of Ref 0.1 the motion normalised quantities defined above are represented by a combined symbol including the normalising amplitude ϕ_0 , which in particular cases will be replaced by α_0 , θ_0 or δ_0 . It should be noted that in some existing notations the normalising amplitude is omitted from the symbolic representation. Thus an existing notation may use C_p' and C_p'' respectively for the quantities C_p'/ϕ_0 and C_p''/ϕ_0 per radian as now proposed.

The (n+1)th harmonic

in-phase component: $C'_{pn}/\phi_0 = P'_n/q\phi_0$

in-quadrature component: $C''_{pn}/\phi_0 = P''_n/q\phi_0$

complex amplitude: $\bar{C}_{pn}/\phi_0 = (C'_{pn}/\phi_0) + i(C''_{pn}/\phi_0) = \pm (|\bar{C}_{pn}|/\phi_0) e^{i\epsilon_n}$ with modulus $|\bar{C}_{pn}|/\phi_0$ and phase angle ϵ_n .

Unsteady forces and moments

The sectional unsteady forces and moments are obtained from the pressures by integration of the separate in-phase and in-quadrature components. The amplitude normalised coefficients are represented symbolically by using c_l, c_m, c_h etc in place of C_p . Thus \bar{c}_l/ϕ_0 represents the normalised complex amplitude of lift.

Use of p_t rather than q as a non-dimensionalising factor

In the preceding notation, apart from pressure ratio p/p_t in the expression for local Mach number M_L , all the aerodynamic pressure and force quantities have been divided by q to make them non-dimensional. An alternative which, as will be discussed in section 8, has advantages in certain circumstances is to use p_t in place of q . Thus the complex pressure amplitude $\bar{p}/p_t\phi_0$ is an alternative to \bar{C}_p/ϕ_0 . Of course the two forms are related through the stream Mach number by the relation:

$$p_t/q = \left[1 + \frac{1}{2}(\gamma-1)M^2 \right]^{\gamma/(\gamma-1)} / \frac{1}{2}\gamma M^2.$$

Units

Incidence, control angle, amplitude of angular motion and phase angle are conventionally specified in degrees. Oscillatory pressure or force when normalised by an angular motion are usually specified 'per radian'. The amplitude of a linear motion is preferably made non-dimensional by dividing by a model dimension.

Quasi-steady and steady perturbation pressures

Several kinds of steady, or quasi-steady, quantities are used as equivalent quantities to provide comparisons with the unsteady ones; the application in the linear case of the steady quantity $dC_p/d\phi$ has already been mentioned. The following discussion is intended to clarify the distinctions between the various forms these quantities can take.

The term 'quasi-steady' is usually applied to all such quantities but for the identification of experimental data it would seem preferable for this term to be applied only to those quantities that are measured in the same way as unsteady quantities but for slow rates of change. Such a quasi-steady oscillation, denoted by $k \rightarrow 0$ would yield for each in-phase component a quasi-steady value, for instance $(C'_p/\phi_0)_{qs}$. Data Sets 6 and 7 both include measurements for comparatively low-frequency oscillations which are regarded as quasi-steady.

The term 'steady perturbation pressure' is a better description of those quantities obtained by steady pressure measurements made for two or more stationary conditions of the model close to the mean condition. The simplest of these is an approximation to the derivative $dC_p/d\phi$ obtained from measured steady pressures C_{p-} and C_{p+} corresponding respectively to the two conditions $-\phi_1$ and $+\phi_1$. The quantity taken to be comparable with the unsteady in-phase component C'_p/ϕ_0 is then $dC_p/d\phi = (C_{p+} - C_{p-})/2\phi_1$ with the deflection ϕ_1 chosen to be the same as, or related to, the amplitude of oscillation ϕ_0 . Data Sets 1 and 4 contain data obtained in this manner.

More detailed information could be obtained if measurements are made for several increments of ϕ_1 so that the form of steady $C_p(\phi)$ over the oscillation amplitude is revealed. Then an average slope $dC_p/d\phi$ could be obtained, say, by 'least squares'.

To make allowance for non-linearities it is in principle possible to extend the measurements further so that they become equivalent to the steady quasi-oscillation $\phi = \phi_0 \sin \psi$, with $0 < \psi < \pi/2$. Provided the chosen values of ψ are sufficiently numerous, the measured steady pressures can be regarded as sampled data from which the fundamental and higher harmonic values can be calculated. In particular such measurements would yield a steady quantity $(C'_p/\phi_0)_s$ which is directly comparable with its unsteady counterpart C'_p/ϕ_0 . Although none of the present Data Sets contains quasi-oscillatory

quantities of this nature, it may be possible to derive such quantities from data available from the original sources.

In short, under the customary generic title 'quasi-steady', three of the possible kinds of quantity comparable with the unsteady C_p'/ϕ_0 are:

- (1) Low-frequency equivalent $(C_p'/\phi_0)_{qs}$ measured for $k \rightarrow 0$;
- (2) Steady derivative $\delta C_p'/\delta \phi$, or $dC_p'/d\phi$;
- (3) Steady quasi-oscillatory quantity $(C_p'/\phi_0)_s$.

In many cases a low-frequency change will become equivalent to a series of steady conditions as the rate of change is reduced. But there are special circumstances where this is not so - where even the slowest rate of change includes an unsteady event. Such a situation occurs when the motion, however slow, leads to the onset of flow separation where the actual process of shedding vorticity occupies a period of time largely independent of the rate of change. That is the condition $k \rightarrow 0$ is not always the same as the condition $k = 0$.

In addition to the fundamental differences in the form of these three quantities it may be necessary to take into account the differences between the method used to measure (1) and that used to measure the steady pressures from which (2) and (3) are derived. Sometimes different instrumentation is employed to obtain unsteady and steady measurements, in which case also, the unsteady and steady measuring positions may not be the same. Thus, whilst $(C_p'/\phi_0)_{qs}$ and the unsteady C_p'/ϕ_0 are obtained with the same instrumentation, a comparison between C_p'/ϕ_0 and a steady perturbation quantity may involve different measuring systems and different accuracies.

5 EXPERIMENTAL PROCEDURES AND INTERPRETATION OF RESULTS

The intention here is to give a brief account of some of the procedures commonly adopted in the experimental measurements and, by so doing, to draw attention to the possible limitations of the data. It is also hoped that this account will lead to an appreciation of the significance of the details of the test equipment and test conditions that are given in a standard form in each Data Set. A more extensive account of experimental techniques used in unsteady aerodynamics is contained in Ref 0.4.

Each series of tests involves a model, equipment to provide the required unsteady motion, instrumentation to measure the model motion and pressure distributions, and a wind tunnel to provide the appropriate test conditions.

The characteristics of the tunnel and the interference effects produced are of especial importance and form the subject of section 6.

5.1 Model motion

In each of the present experiments the model was designed to perform rigid-body motion. All the 2-D aerofoil models (Data Sets 1 to 5) were stiff enough to be regarded as rigid, but for the half-models of Data Sets 6 and 7, flexibility led to the basic applied motion being augmented by a small amount of elastic distortion dependant on oscillation frequency and aerodynamic loading.

The model motion, even when elastic deformation occurs, is usually defined by the output of a displacement transducer arranged to measure the motion reference coordinate ϕ , and to provide a time-varying electrical signal which is used as a phase reference for harmonic analysis. When the model cannot be regarded as rigid, some assessment of the actual motion which includes the unsteady deformation may be obtained from a distribution of accelerometers installed inside the model. By this means the true motion can be related to the measurements of ϕ .

5.2 Measurement of pressure

There are various schemes for measuring surface pressures. All of them depend on one or more pressure transducers to provide electrical outputs which are the actual quantities that are processed and eventually measured. Sometimes, as in Data Sets 2, 5, 6 and 7, two different systems are used in the same experiment: one to measure pressures in the steady state, the other for measurements in unsteady conditions. Then the steady and unsteady distributions may not be measured for the same positions, as in Data Set 7. One type of unsteady measuring system uses small transducers installed within the model and connected to orifices at the model surface. But in another system, as used for Data Sets 1 and 4, unsteady pressures are piped to a location outside the tunnel and switched in sequence to a single transducer. With any system the measurement that is sought is the surface pressure which would be acting at the position of the orifice: what is actually measured is the pressure acting at the diaphragm of the transducer. Therefore, unless the transducer is actually part of the surface there is always a question about the transfer function between the pressure acting at the orifice and that at the transducer. In systems where the unsteady pressures are piped to a distant measuring device, the determination of these transfer functions is a vital part of the calibration. When the transducer is situated very close to the orifice and the enclosed volume of air is small, the effects of transmission are usually neglected. However, a feature, which is common

to all systems and very difficult to simulate in bench calibrations, is the effect of the flow across the orifice.

Whether or not the transfer function between orifice and transducer diaphragm is significant, the calibration factor relating the unsteady electrical output to unsteady pressure is of paramount importance. Whereas good standards of steady pressure are commonplace, there is no readily available definitive standard for oscillatory pressure. Although the experimenters will have taken great care over this matter, it is easily appreciated that a systematic error in the calibration could lead to undisclosed errors in all the measurements of a series.

5.2 Signal processing

In oscillatory tests, the electrical signals from the pressure transducers are usually processed in some manner to yield harmonic components phase-referenced to the signal representing the motion coordinate ϕ . However this is not so for Data Set 3 in which the pressure and motion signals are sampled to provide instantaneous values at a series of known time-intervals.

It is unnecessary to describe in detail the methods of processing the electrical signals, but it is important to be aware of the nature of the signals and to understand the kind of quantities that result from the processing. Almost inevitably the signal from a transducer sensing an aerodynamic pressure includes, in addition to the wanted signal, random-like fluctuations from various sources. Transonic tunnels with their slotted or perforated walls are prone to produce stream flows with some degree of inherent unsteadiness. Model flows which are supercritical, or separated, may themselves provide another source of unsteady disturbance. Thus even when the model is stationary the pressure signals may include fluctuations. When the model is undergoing a prescribed unsteady motion the complete pressure signal will represent a combination of random fluctuations and the response to the motion.

Depending on the type of signal processing employed, the result could be

- an instantaneous value;
- a time-average;
- a cycle-average of instantaneous samples taken at corresponding times in a number of cycles;
- a series of harmonic components obtained by Fourier analysis over either a whole number of cycles or a certain period of time.

Steady pressures are usually measured as averages over short periods of time. In general, time or cycle averaging is beneficial in reducing, if not always eliminating, the effect of random fluctuations. In some circumstances, where the unsteady process under investigation itself includes some form of randomness, averaging can obscure features of the individual cycles. Because the experiments from which Data Set 3 was extracted included an element of randomness in each cyclic onset of flow separation, both quasi-steady and unsteady pressures were measured as instantaneous values.

5.3 Occurrence and effects of extraneous fluctuations

When extraneous pressure fluctuations, independent of the applied model motion, are produced by an instability of the flow over the model they are a proper feature of the flow phenomenon and as such should appear in the results and require theoretical modelling. It is for this reason that items 5.11 or 5.12 of the test specification have been requested in each Data Set.

When the fluctuations are the result of turbulence or other unsteadiness in the tunnel flow it is desirable for their effects to be reduced by averaging. Whether they can be completely eliminated by averaging depends on whether they are linearly superposed on the pressure response to the prescribed motion or whether there is some form of non-linear interaction. In highly non-linear situations in the close vicinity of a shockwave, extraneous fluctuations can lead to erroneous data. Examples of such interference are mentioned in Refs 0.4 and 0.5.

5.4 Non-linearities

For small excursions away from the mean condition the pressure over much of the model surface will vary linearly with steady displacement ϕ . Exceptions to this become evident when measurements are made near to a leading edge or a control-surface hinge-line, or close to a shockwave. Non-linearities in the steady pressure variation are accompanied by the presence of higher harmonic components under oscillatory conditions; the manner in which these are produced in the close neighbourhood of a shockwave has been described in Refs 0.6 and 0.7.

Measurements of harmonic components are often limited to the fundamental on the grounds that this is the only component of importance in practical problems of aero-elasticity. Only Data Set 4 includes any numerical data for higher harmonics although Fig 6.6 of Data Set 6 gives graphical information on the spectral content of the pressures for transonic flow. Also Data Sets 2 and 5 include instantaneous pressures over a cycle of oscillation, which show non-linear features.

If in some circumstances the presence of higher harmonics in the oscillatory pressures is found to be independent of chordwise position, it is advisable before attributing these to non-linear aerodynamics to verify that the model motion is truly simple harmonic. This comment is relevant to any Fourier analysis that might be made on the instantaneous data presented in Data Set 3 which gives information on the harmonic distortion in the model motion.

When non-linearity is present, the values of the amplitude-normalised quantities C_p'/ϕ_0 and C_p''/ϕ_0 and the steady quantity $\delta C_p/\delta\phi$ are liable to be dependent on the displacement amplitude. This point needs to be borne in mind before placing too much emphasis on the peak values of these quantities obtained at the position of a shockwave. Interesting examples of amplitude dependence are shown in Fig 2.3 of Data Set 2 and Fig 5.7 of Data Set 5.

Irregularities in the chordwise distribution of the oscillatory pressure components are sometimes found near to the leading edge. These may be due to non-linearities associated with a local separation or with the disturbance produced by a transition-trip. Such irregularities usually appear only for small amplitudes, and disappear when the amplitude is increased.

To summarize, indications of non-linearity include:

- non-linearity in $C_p(\phi)$;
- amplitude effects on the fundamental components C_p'/ϕ_0 and C_p''/ϕ_0 ;
- non-sinusoidal time histories;
- higher harmonic components from Fourier analysis;
- irregularities in chordwise distributions of the oscillatory components.

5.5 Reduced frequency

The exact values of the test frequencies are often chosen for practical reasons such as the need to avoid unwanted resonances of the model or its supports. Almost invariably, tests are made for sets of fixed frequencies of oscillation so that for each constant frequency the reduced frequency k , varies with Mach number M and stream total temperature T_0 . For a fixed M , k varies inversely with $\sqrt{T_0(K)}$. Total temperature in a tunnel is not always closely controlled so that the value of k can vary during a tunnel run, but even in an extreme case where temperature changes from 25°C to 35°C the value of k would change by only 2%. Such a change is hardly likely to have a serious effect on the unsteady aerodynamics.

No uniform procedure has been adopted in specifying the test values of k . When either an average or a nominal value is quoted for each combination of M and f , it will be appreciated that the true value may differ by a few percent.

Tests made with substantially different values of frequency are included in most series of measurements. For rigid models the interpretation of the results is straightforward, but if model flexibility is significant, care has to be taken to eliminate any effects of changes in the oscillation mode with frequency.

5.6 Mach number and model incidence

These are the main parameters that define the basic flow from which the unsteady changes are made. In some cases the actual incidences and tunnel Mach numbers may be found to be slightly different from the specified nominal values.

For models with symmetrical sections, the datum incidence $\alpha = 0$ is usually set to align with the known flow direction of the tunnel. For models having sections that are not symmetrical the method of setting incidence is given in item 5.7 or 5.9 of the specification in each Data Set.

Where measurements of tunnel Mach number and model incidence are subject to standard corrections for wall interference, the details are given in item 9.6 of each specification.

5.7 Tunnel pressure and Reynolds number variations

The Reynolds number for a test depends on the pressure and temperature of the flow in the tunnel. Usually flow temperature is not closely controlled so that there may be small variations in Reynolds number throughout a series of tests. For those test series where tunnel total pressure remains constant, the Reynolds number is different for each Mach number. In tunnels where total pressure can be changed, variation of this quantity provides a means of obtaining data over a range of Reynolds number for each Mach number.

But as well as changing Reynolds number, alteration of total pressure can produce side-effects which, unless recognised and taken into account, may lead to apparent trends with Reynolds number that are in fact spurious.

For instance, an increase in total pressure means an increase in all the unsteady pressures, with a consequent improvement in the measurement accuracy. This in turn may mean a reduction in random errors and result in smoother pressure distributions. Also a change in total pressure alters the mean pressure level at which the transducers are operating and, in the presence of non-linearity, this can lead to a change of transducer sensitivity factor. If not accounted for in the calibration this could appear as a spurious Reynolds number effect.

An increase in the aerodynamic loading on the model is also produced by increasing the total pressure, and if the flexibility of the model is significant, this can lead to distortion of the model and to modifications to the mode of oscillatory motion. Data Sets 2 and 5 include data for a range of Reynolds numbers, but for these there is no possibility of unwanted aeroelastic effects because of the rigidity of the 2-D models.

5.8 Transition fixing and Reynolds number

Most of the tests were made for Reynolds numbers less than full-scale. To avoid unwanted effects associated with laminar boundary layers, trips to fix the transition position were fitted to some of the models. No trips were fitted for the measurements of Data Set 3 because the Reynolds numbers of the tests matched those of the full-scale helicopter blades to which the experiments were directed. Data Sets 1, 6 and 7 present numerical data for only models with transition trips, whilst for the experiments of Data Sets 2 and 5 no trips were attached. Data Set 4 gives information about the effects of fixing transition; in this Set transition was fixed for some cases and for others it was free. Data Set 6 contains a brief discussion of transition fixing in terms of increasing the thickness of the boundary layer, and provides graphical information about the effect this has on the unsteady loading produced by an oscillating control surface.

Data Sets 4 and 5 which give measurements for models having the same aerofoil shape, offer comparisons, as already shown in Table 0.2, between (a) tests with transition fixed at comparatively low Reynolds number, and (b) tests with free transition for a range of Reynolds number. Some of these comparisons will be discussed in section 7.

The desirability of fixing transition and the best position in the chord for attaching the trips are debatable matters. On the one hand if transition remains free, a laminar boundary layer may lead to types of flow separation and shockwave boundary-layer interactions that are unrepresentative of full-scale. Also it is possible that, when natural transition is delayed to a rearward position of the chord, the cyclic excursions of the transition point due to a model oscillation may engender non-typical oscillatory pressures of no practical interest. On the other hand when transition trips are used, the turbulent boundary so produced is usually too thick over the rearward part of the chord, thus over-emphasizing viscous effects which can be especially serious for a trailing-edge control, see Fig 6.4.

With regard to tests with over-thick boundary layers, Binion, Ref 0.8, points out that with modern designs of wings, even at high Reynolds number, viscous effects are likely to be so large that worthwhile calculation methods must be able to take these effects into account. The conclusion then is, albeit for steady conditions, that provided the class of flow is representative, tests with thick boundary layers do provide a useful challenge to theoretical computations. The objective of fixing transition therefore depends to some extent on whether the experiments are aimed at providing data appropriate to full-scale Reynolds numbers, or providing data to validate viscous calculations.

5.9 Accuracy of measurements

The accuracy with which the relevant quantities are measured is clearly an important matter although, as will be discussed in subsequent sections, the quality and reliability of experimental data involve wider considerations concerning the test environments.

It may be taken for granted that steady pressure, Mach number, incidence, steady deflections and oscillation frequency are measured with adequate accuracy. It is the accuracies of unsteady pressure quantities such as C_p'/ρ_0 and C_p''/ρ_0 that give cause for concern. Each of these quantities is derived from separate measurements of small changes in pressure and small displacements of the model. The measurements are made with instrumentation operating under dynamic, not steady conditions, and their accuracy depends crucially on the calibration procedure. It is easily seen that a systematic error in the measurement of a pressure harmonic component, or of a motion amplitude, could affect the whole set of measurements.

Whereas the resolution of the instrumentation or the day-to-day repeatability, both of which set limits to the accuracy, are fairly easy to determine, the overall accuracy of a measurement is extremely difficult to quantify. Usually the most that can be expected is a statement to the effect that the measurement of quantity A is no better than x percent. Such statements are usually made on personal, and to some extent intuitive, assessments based on the experience of the experimenter. To demand more would be unreasonable, for a thorough analysis of possible errors could easily entail as much work as the measurements themselves.

6 TUNNEL INTERFERENCE

All measurements obtained from wind tunnels are liable to suffer from the effects of tunnel interference. That is, the data obtained may differ from those which would be obtained with the same model moving in a free and uniform atmosphere. With that as a broad definition, the various sources of interference are:

- (1) Wall constraint on the flow.
- (2) Shockwave reflections from the walls.
- (3) Side-wall boundary layers in 2-D tests.
- (4) Reflection-plane boundary layer in half-model tests.
- (5) Support interference in complete model tests.
- (6) Flow fluctuations inherent in the tunnel flow.
- (7) Curtailment of wake vorticity by tunnel corner, shockwave or fan.
- (8) Reflection of acoustic disturbances at the walls.
- (9) Occurrence of tunnel resonance.
- (10) Acoustic disturbances propagated through a plenum chamber.

Items (1) to (6) affect both steady and unsteady measurements, whereas items (7) to (10) are peculiar to unsteady conditions. General accounts of the effects of interference on unsteady measurements are given in Refs 0.4 and 0.5. Of all the possible causes of interference, the only ones likely to be important to the present data are the constraint and reflection properties of the walls (items (1), (2) and (8)) and, if flow separation occurs at the model, the effects of the side-wall and reflection-plane boundary layers (items (3) and (4)). Tunnel resonance is known to be possible in 2-D tests (Ref 0.9) but no occurrences are reported in any of the Data Sets.

Because of its more complicated nature, interference on unsteady measurements is poorly understood in comparison with interference on steady measurements. Since some part of the total effect on an unsteady measurement can be attributed to steady interference - indeed for supercritical conditions the steady effect may be the major contribution - it is important to clarify the distinction and see how much of the total effect can be accounted for by steady considerations.

Consider for the moment a specific event in which a model initially at a steady incidence α_A is rapidly moved to a new steady incidence α_B . After sufficient time has elapsed we can assume that the flow has reached a new steady state appropriate to the new steady incidence. If the event occurs in a wind tunnel, the initial flow for α_A and the final flow for α_B are both subject to steady interference. The manner in which the flow changes with time, and indeed the time taken for the flow to approach its final steady state are subject to unsteady interference. The totality of the interference on the unsteady event is a combination of these steady and unsteady contributions.

For the more usual type of unsteady test where the model is given an oscillation of small amplitude ϕ_0 about a mean incidence α_m and conditions are linear, the aerodynamic pressure characteristics are fully described by

- (1) C_p for steady α_m .
- (2) $(|\bar{C}_p|/\phi_0)_{qs}$, the amplitude for a quasi-steady oscillation identical with $dC_p/d\phi$.
- (3) Variations with frequency of amplitude $|\bar{C}_p|/\phi_0$ and phase angle ϵ_0 .

Quantities (1) and (2) are affected by only steady interference and provided these effects can be accounted for, the only unsteady effects are those concerning the phase angle and variations with frequency, (3).

A crucial question is whether the aerodynamic measurements can be corrected for the interference effects. For supercritical flows simple forms of correction are generally impossible, but it is still helpful to approach the question from the standpoint of purely subsonic flow. Classical theory for steady subsonic flow regards wall constraint as consisting, in effect, of incremental changes in

- stream velocity due to blockage;
- model incidence due to induced upwash;
- lift and pitching moment due to streamline curvature.

On this simple basis, which neglects buoyancy effects due to the streamwise gradient of blockage, the condition of a model in a tunnel can be regarded as equivalent to the

condition in free air of another model with a different camber set at a different incidence in a stream of modified velocity. For subsonic conditions values of the incremental changes can be obtained by theoretical calculations if the boundary conditions at the walls can be mathematically defined or if the wall pressures are known, or possibly by empirical means if the wall conditions are unknown.

The concept of an equivalent free-air system suggests, if the effects of streamline curvature are simplified, that the steady part of the wall constraint affecting oscillatory measurements might be equivalent to changes in stream Mach number and mean incidence. This leads to a possible basis for making comparisons between theory and experiment which will be discussed later in section 8.

For the oscillatory type of test mentioned previously a possible correction procedure would consist of applying corrections to:

- (1) M and α_m - to account for steady interference on the mean condition;
- (2) $(|\bar{c}_p|/\phi_0)_{qs}$ - to account for steady interference on the quasi-steady perturbation;
- (3) $|\bar{c}_p|/\phi_0$ and ϵ_0 - to account for the unsteady interference.

The procedure is illustrated schematically in Fig 0.2 which shows a hypothetical variation of $|\bar{c}_p|/\phi_0$ and ϵ_0 with reduced frequency k . It is assumed that the measured steady C_p obtained for the steady condition (M, α_m) would be obtained in free air for another steady condition $(M, \alpha_m)'$. The curves labelled 1 are those measured in the tunnel for (M, α_m) ; those labelled 2 would be obtained in free air for the mean condition $(M, \alpha_m)'$. Steady interference is responsible for the displacement Δ_1 . If curve 1A is drawn parallel to curve 1; or more strictly to give Δ_1 proportional to the modulus of total lift, then the additional and unsteady interference effects are represented by Δ_2 and Δ_3 . Ability to apply corrections to the measurements requires knowledge of the translation from (M, α_m) to $(M, \alpha_m)'$ and the values of Δ_1 , Δ_2 and Δ_3 .

For subsonic conditions, corrections to M and α_m and corrections of the type Δ_1 applicable to lift and moment may be obtained theoretically or empirically. In principle, corrections of types Δ_2 and Δ_3 could be obtained from the extensions of classical interference theory to unsteady conditions, as described in Ref 0.10. But, as for the steady corrections, the calculations depend on an adequate definition of the wall boundary conditions which, for the unsteady case, includes time dependence.*

For the present data, any purely theoretical forms of interference corrections are liable to be unreliable because of inadequate definition of boundary conditions for the ventilated walls of the tunnels in which the data were obtained.

Broadly speaking, the steady constraint effects in a ventilated tunnel depend on the degree of ventilation; in principle at least, careful matching of the wall geometry and wall porosity to the model geometry could result in negligible interference (see for instance Ref 0.11). More usually, the measured slope of the steady lift curve for a particular model will be too large or too small depending on whether the tunnel walls are 'too closed' or 'too open'. Also it is to be expected that the larger the model is relative to the tunnel, the greater is the influence of wall constraint.

Even if the wall boundary conditions can be adequately defined, theoretical corrections to the measurements are simply not possible for supercritical flow conditions. A useful discussion of steady interference under transonic conditions is given by Binion, Ref 0.8. He points out that, where the supercritical region is no longer small with respect to the tunnel dimensions, the effect of wall constraint can no longer be regarded in the classical terms of blockage, upwash and streamline curvature; instead it must be regarded as a complicated distortion of the flow field which can strongly influence the shockwave and separation patterns. In which case, there may no longer be an equivalent free-air condition corresponding to the model in the tunnel.

It is unfortunate that the foregoing discussion has done little except describe the difficulties of making corrections to the measured unsteady data.

In none of the Data Sets are any corrections made for unsteady interference but in some Sets, steady-based corrections are either made, or the method for applying them is described. In Data Set 4, although the presented data include no interference corrections whatsoever, formulae are given for making corrections to the incidence, and to the lift and moment for steady conditions. In Data Sets 4 and 5, as already explained in section 2.1, some adjustments have been made between the experimental values of M and α_m and those chosen for the CT Cases; to some extent these adjustments are intended to account for the steady interference effects.

* Addendum: The author's attention has been drawn to recent methods of including the effect of the walls in unsteady calculations for aerofoils and controls (see Refs 0.13, 0.14).

Data Set 5 comprises results obtained with a model having the same basic shape as the model of Data Set 4 - two examples of comparisons between the sets will be discussed in section 7. In making other comparisons between the two Sets it should be noted that, in addition to the differences shown in Table 0.2, the ratios of tunnel height to model chord are 3.1 for Data Set 4 and 6.7 for Data Set 5. However, because of the beneficial effect of wall ventilation, which to some unknown degree applies to both tunnels, it cannot without further analysis be concluded that the interference effects on Data Set 4 are necessarily larger than those on Data Set 5.

In Data Set 3 where the unsteady data are presented as instantaneous values of C_p and sectional force coefficients for instantaneous values of incidence α , the tabulated values of the incidence and the force coefficients, but not C_p , have been corrected for tunnel constraint as if each instantaneous value were obtained for a steady condition.

Data Set 7 is unique in being abstracted from an investigation into tunnel interference. In the light of the evidence obtained from several tunnels it is believed that the data for the two largest tunnels are free from any large effects due to tunnel constraint interference.

7 UNCERTAINTIES OF EXPERIMENTAL DATA

If experimental results are used only as qualitative information questions of accuracy and reliability hardly arise. But when making quantitative comparisons the user of experimental data will certainly want to know the confidence that can be placed on the measured values. Basically the question is how well do the measured unsteady aerodynamic quantities relate to the specified configuration, its motion, and to the test conditions defined by parameters such as M , Re , α_m and k . The answer is seldom straightforward. It depends not only on the accuracy of the measurements and the manufacturing accuracy of the physical model but also on the appropriateness of the wind-tunnel test conditions and the uncertainties of wind-tunnel interference. In critical situations in the presence of shockwaves or separations the answer also requires knowledge of the sensitivity of the measured data to small changes in the parameters.

A general insight into the uncertainties of measurements and an idea of the confidence that can be placed in experimental data can be obtained from a comparison of results obtained in different ways. For instance, confidence in the technique of unsteady pressure measurement was obtained when, on several occasions in the past, different organisations made comparative measurements using their own forms of instrumentation. Usually, however, such comparisons are not completely independent because they use either the same model, or the same tunnel, or both.

Examples of comparisons obtained with the same model in two different tunnels, thus providing evidence of the effects of tunnel interference, are given by Figs 7.20 and 7.21 of Data Set 7. In these comparisons the model was small in relation to the sizes of the tunnels; unfortunately the confidence gained by these comparisons does not necessarily apply to every other situation. In the same Data Set, Figs 7.16 to 7.19, also provide evidence of the sensitivity of the measured oscillatory pressures to small changes of M and α_m for some examples of transonic flow.

The two investigations from which Data Sets 4 and 5 are drawn provide a rare opportunity for comparing two independent sets of measurements. The data available for comparison relate to oscillatory pitching of the NLR 7301 supercritical airfoil. It is important to note that the two sets were obtained with different physical models in different wind tunnels by different experimenters using different instrumentation. As such the two experiments were completely independent.

At the outset, before making comparisons of the measured data, there are three points to be noted; firstly, there are differences in the degree to which each physical model represents the design shape of the NLR 7301 aerofoil; secondly, in neither case has there been any attempt to apply tunnel interference corrections to the measured unsteady data; and thirdly, there are no exact correspondences between the parametric conditions of the two tests.

Fig 0.3 provides comparisons between the measured and the design ordinates for a portion of the upper surface of each physical model. The ordinates for the NLR physical model are taken from Tables 4.1 and 4.2 of the present document; those for the Ames model are taken from Ref 5.4 which mentions that, owing to an expansion of the manufacturing mould, the model is slightly thicker than it should be. The same report also contains a suggestion, which is supported by Fig 0.3, that the surface of the model is not as smooth as the design shape.

Two examples of data comparisons will now be discussed. Not only do they provide evidence of the kind of uncertainties surrounding experimental data, but they provide a foretaste of situations requiring judgements to be made when comparing calculated and experimental results. In each example the unsteady quantities being compared are the distributions of the oscillatory pressure components, C_p'/α_0 and C_p''/α_0 , for the upper surface only. The different tests are identified by the NLR Run No. or the Ames Dynamic Index.

The first example, chosen because of the aerodynamic simplicity of purely subsonic flow for $M = 0.5$, relates to CT Case 2. The three tests being compared are identified:

Test	M	α_m (deg)	α_0 (deg)	k	$Re \times 10^{-6}$	Transition
NLR 1301	0.498	0.85	0.4	0.26	1.7	Fixed at 0.3c
Ames 185	0.508	0.58	0.5	0.20	2.3	Free
Ames 170	0.508	0.58	0.5	0.20	9.3	Free

The steady pressure distributions are shown in Fig 0.4a. Whilst examining these it may be noted that there is adequate agreement between the test Mach numbers and that, because the flow is subsonic, no great significance need be attached to the small difference in the values of α_m . Also it is reasonable to regard the difference between the Reynolds number of the NLR test and that of the Ames 185 test as not being too large. Although in both the Ames tests transition remained free, it was fixed in the NLR tests, but it is important to note that the roughness band was as far downstream as $x = 0.3c$. Since it appears from a comparison of the Ames and NLR steady pressures that fixing transition causes no dramatic changes downstream of the band, it seems reasonable to conclude that the band has no significant upstream effect. Thus the results from the Ames 185 test should be comparable with those from the NLR test at least ahead of $x = 0.3c$. In fact, comparison of the steady pressures shows that although there is a disagreement between the Ames and the NLR pressures at the lower surface, the three sets of results for the upper surface are in reasonable agreement in regard to the basic shape, but that there are more irregularities in the Ames distribution, possibly because of surface waviness.

Before comparing the oscillatory measurements, it should be noted that the difference between the Ames and the NLR values of k would not be expected to lead to significant changes in the real component C'_p/a_0 , although it would have a small effect on the imaginary component, C''_p/a_0 . The distributions of the oscillatory components are shown in Fig 0.4b and c. With regard to C'_p/a_0 , in the region ahead of $x = 0.3c$ there are considerable differences both between the two Ames sets and between the Ames and NLR sets. The dip in the region $0.1c < x < 0.3c$ is well established by three points in the Ames test at the higher Re , but is only just in evidence with a single point at the lower Re . This is mentioned in the Introduction to Data Set 5 where it is concluded that this dip is not spurious but must be attributed to a viscous effect. Interestingly the NLR distribution for an even lower Re also shows a single-point dip.

For the distribution of the imaginary component, C''_p/a_0 the main difference is the vertical displacement between the similarly shaped distributions of NLR and Ames tests. This can be ascribed partly to the known influence of changing k from 0.20 to 0.26. Another contributory factor may be differences between the unsteady effects of wall interference in the two tunnels.

The second example is a comparison of tests that relate closely to CT Case 8 which corresponds to a supercritical design case. The tests chosen for comparison are:

Test	M	α_m (deg)	α_0 (deg)	k	$Re \times 10^{-6}$	Transition
NLR 6708	0.744	0.85	0.6	0.18	2.2	Free
Ames 191	0.752	0.37	0.5	0.20	3.3	Free
Ames 148	0.751	0.37	0.5	0.20	11.4	Free

All the tests were made without fixing transition and the Reynolds numbers for the NLR test and the Ames 191 are sufficiently close for the viscous characteristics of these two tests to be comparable. The third set, Ames 148, is included to show the effects of a large increase in Reynolds number.

There are differences between the NLR and Ames tests in regard to Mach number and mean incidence. As already explained in section 2.1 these differences are deliberate, each (M, α_m) combination having been chosen by the experimenter during preliminary trials to achieve a steady flow that matched the flow calculated by an inviscid theory for the supercritical design case. In a sense, the differences in the parametric settings in the NLR and Ames tunnels can be regarded as compensating to some extent for the differences in steady interference effects and for the differences in the shapes of the models.

The distributions of local Mach number, M_L , for the steady mean incidences, as shown in Fig 0.5a, have the same general shape, are in reasonable agreement on the general level of M_L in the supercritical region and agree on the chordwise position, $x = 0.6c$, at which the deceleration from supercritical flow occurs. However, as for the subsonic example, the Ames distributions have a waviness over the forward half of the chord that is not present in the NLR distribution. Also there are significant differences in the deceleration gradients $dM_L/d(x/c)$ where the abrupt deceleration begins.

Comparisons of the oscillatory pressures are shown in Fig 0.5b and c. Each set of results include peaks in $-C'_p/a_0$ and $-C''_p/a_0$ close to the beginning of the deceleration

from supercritical flow, the highest Re producing the highest peaks. Whilst the waviness in the Ames distributions is not unexpected in view of the waviness in the M_L distributions, there are serious differences between the Ames and NLR results in regard to the mean level of C'_p/α_0 in the region $0.3c < x < 0.6c$.

Also there are serious differences for both C'_p/α_0 and C''_p/α_0 in the region $0.6c < x < 1.0c$ where, surprisingly, it is the Ames results for the higher, and not the lower, Re that agree better with the NLR results. It is remarkable that over the rear of the chord, $0.7c < x < 1.0c$, there are such large differences between the three sets of unsteady pressures when the steady pressures there are in relatively good agreement. Probably the explanation is that the unsteady pressures over the rear part of the chord are dependent on the convection of the vorticity generated by the unsteady processes occurring upstream - in the present case the unsteady behaviour where the supercritical flow is first decelerated. In other words, over the rear of the chord, the effects of changing test conditions on the unsteady pressures are more likely to correlate with the effects of the changes on the steady pressures at more forward, rather than local, positions.

It will now be clear that both of the previous examples include discrepancies that cannot readily be attributed to differences in the models or in the test parameters. Since the ratio of tunnel height to model chord is 6.7 for the Ames tests and 3.1 for the NLR tests it is tempting to ascribe at least some of the discrepancies to differences in tunnel interference and furthermore to give more 'weight' to the data from the tunnel with the larger ratio. However, whilst interference may indeed be the reason, without further evidence and analysis it may be better to regard the differences simply as typical uncertainties inherent in unsteady wind-tunnel measurements.

8 COMPARISON BETWEEN THEORY AND EXPERIMENT

The use of experimental data as qualitative information requires no special comment - it is when the data are to be used for numerical comparisons with theoretical computations that difficulties arise.

The principal aim of computational development is naturally directed towards full-scale aircraft. One of the difficulties in making comparisons with wind-tunnel results arises because the experiments include features, particularly tunnel interference, which have no counterparts in the aircraft situation. The difficulties of applying interference corrections to the measurements have already been discussed. If no assurance can be given that the interference effects on a particular set of data are negligible, either theory must be diverted from its main aim and extended to include a mathematical representation of the tunnel boundaries in the computational model: or, if that is not possible, the probable importance of the effects must be assessed from whatever information on the subject has become available when the comparisons are being made.

A full specification of an unsteady experiment in a tunnel includes:

Model and basic flow

Model shape;
Oscillatory motion: mode, amplitude and frequency;
Stream Mach number, M ;
Mean incidence, α_m (also possibly mean flap angle, δ_m);

Viscous characteristics

Reynolds number;
Transition position;

Tunnel boundary characteristics

Wall geometry;
Ventilation properties.

Comparative computations can vary in type from (a) those that include only the model and basic flow, to (b) those that include the full experimental specification. But at the start of any programme of comparison it is most likely that the chosen type of computation will omit the tunnel boundaries; furthermore the computational model may not fully represent the viscous characteristics of the experiment. In this case, apart from the shape of the model and the oscillatory motion, the main parameters entering the computation will be M and α_m . If tunnel interference (or viscosity) has had a serious effect on the measurements, then it is hardly likely that computations made for the experimental specification $(M, \alpha_m)_E$ will yield results in agreement with the experiment.

In the particular case when a shockwave is present, it is clear that the experimental and theoretical distributions of unsteady pressure will not agree unless there is already an agreement with regard to the mean position and strength of the shock. But more generally for all types of flow, it would seem that an agreement on the steady pressure distribution is a prerequisite to an agreement on the unsteady pressures.

Whilst it may be true that there is generally no free-air equivalent of the tunnel condition, it is possible that an improved comparison of unsteady pressure may result if the calculations are made for a different condition $(M, \alpha_m)_C$ which gives better agreement

for the steady pressure distributions. In effect, the comparison will no longer be based on identities of stream Mach number and mean incidence but instead on similarity of the steady pressure distributions or, more aptly, on similarity of the distributions of local Mach number M_L . If such a method of comparison is adopted, steady computations would need to be made over ranges of M and α_m to seek some agreement in the distributions of M_L before any unsteady calculations are performed. As previously mentioned in section 2.1, such adjustments to the steady mean conditions have already been suggested for the supercritical design case for the NLR 7301 airfoil of Data Sets 4 and 5.

A caution is necessary here. Should a theoretical condition $(M, \alpha_m)_C$ be found that gives an M_L distribution exactly matching that of an experimental condition $(M, \alpha_m)_E$, thus supposedly compensating for the steady interference effects, it does not follow that the compensation extends to the unsteady interference or even to the interference on a quasi-steady change. This should be clear from Fig 0.2. The point needs to be kept in mind when making unsteady comparisons between theory and measurements for the steady-matched supercritical design cases of Data Sets 4 and 5.

When a comparison is made across an appreciable difference in stream Mach number, there is a question of choice concerning the form of the non-dimensional unsteady aerodynamic quantities that are to be compared. This arises because local Mach number M_L is related uniquely to p/p_t but not to C_p : obtaining identity in the values of M_L entails a difference in the values of C_p . Then, since in effect p/p_t rather than C_p is being used for the steady matching, it would seem more appropriate for the comparison of unsteady data to be made for non-dimensional quantities such as $\bar{p}/p_t \phi_0$ (already mentioned in section 4) rather than the conventional quantities typified by $\bar{C}_p/\phi_0 \equiv \bar{p}/q\phi_0$. To give an example: if the two stream Mach numbers over which the comparison is being made are $M = 0.80$ and $M = 0.85$, then an exact agreement between the values of $\bar{p}/p_t \phi_0$ would entail a difference of approximately 7% in the corresponding values of \bar{C}_p/ϕ_0 . However, for small differences in M , the matter is usually unimportant, particularly if the differences lie within the range of experimental uncertainty. Note that the unsteady measurements of Data Set 7 are presented as values of $\bar{p}/p_t \phi_0$ because they were originally used for comparisons between different tunnels.

The preceding discussion has assumed that the tunnel walls are not taken into account in the calculations. If the intention is to include the tunnel boundaries in the computational model it may be difficult to define a mathematical boundary condition sufficiently representative of the ventilated walls of the experiment. It may then be desirable to make separate calculations for each of the two extreme conditions representing closed and open boundaries, as has been done in Ref 0.12 and possibly make a third calculation for some intermediate homogeneous boundary condition.

In summary, the basis on which the experimental and computational unsteady data are compared may take any of the following forms:

- Same class of flow;
- Similarity of M_L distribution;
- Identity of basic flow parameters (M, α_m) . Possibly also identity of viscous parameters, Re and transition position;
- Full experimental specification including the tunnel boundaries.

9 SUGGESTIONS FOR FUTURE EXPERIMENTS

The need for further experimental data will naturally depend on the early comparisons with the present data. If the agreement is good, the only question to arise would be whether all the significant features associated with full-scale aircraft had been catered for. In this connection it will be noted that, although a supercritical section is included in the Compendium, there are no data for a supercritical wing. However, this omission will be overcome when oscillatory pressure measurements become available for the LANN wing whose geometry and CT Cases are defined in Ref 0.2.

In the more likely event of differences being found between the computations and the experiments, there may be a need for new experiments. Before discussing what form these should take, it needs to be noted that the experimental programmes from which the present Data Sets were abstracted predate the choice of the CT Cases. Not all the experiments were specifically designed to provide data for the kind of close numerical comparisons now proposed.

In future it may be desirable to give more attention to overcoming the uncertainties of tunnel interference, say by including in any new tests the effects of changing the characteristics of the tunnel walls. The desirability of fixing transition needs to be re-examined. There could be advantages in making measurements of boundary-layer thickness under steady conditions so that these could be related to viscous calculations. Also it may be necessary to take more account of, or to place greater restraint on, the elastic distortions when 3-D configurations are being tested.

In addition there are two general matters that merit discussion and which to some extent are interrelated. These are (1) the form of the comparisons and (2) the method of communicating the experimental data.

Regarding the first of these matters, it is evident that the importance of variation of the main parameters was fully recognized when the CT Cases were selected. Completion of the computations for all cases for a configuration and their comparison with experiment is intended to demonstrate how well theory can cope with the different situations. But the intervals between consecutive values of the parameters are necessarily rather wide so that the comparisons tend to appear as a series of single-point correspondences. That is, for each case the experimental results for a particular condition $(M, \alpha_m)_E$ will be compared with computed results for the same or a related condition $(M, \alpha_m)_C$. Whilst single-point comparisons may be satisfactory for comparing one computational method with another, they may not be ideal for comparing computation with experiment: one reason being the inevitable uncertainties and sensitivities of the experimental results. It would be preferable to make comparisons of the variations of the aerodynamic quantities with the main parameters such as M and α_m , in the immediate vicinity of the corresponding condition (M, α_m) , thereby taking account of the parametric sensitivities. In practice this could mean a comparison between, on the one hand the data for a pivotal condition, and on the other, data for a mesh of points surrounding the pivot point. Whether in a planned programme, the matrix of data is provided by the computations or the experiments will probably depend to some extent on the relative costs of computation and experiment. On this matter it is noted that although the capital cost of mounting an experiment is large, the running cost of additional measurements may be relatively low.

The possibility of using a greater quantity of experimental data leads to a consideration of the second matter, the means by which the data are communicated. It is obvious that printed tables cannot be used until they have been read and some manual action performed. This procedure is acceptable provided the listings are not too extensive, but the labour involved, quite apart from the amount of paper required, inhibits the use of large amounts of data in this form. Rather than printed tables it is suggested that in future the data be communicated by computer-readable magnetic tape. To give an example of the practicality of this suggestion, all the results of the NORA tests from two large tunnels, some 177 cases in all, can be made available on a standard 200 mm diameter magnetic tape. By using this means of communication, a computer available to the theoretician could present visual displays of the effects of parametric variations and indeed show the comparisons themselves.

REFERENCES

- 0.1 S.R. Bland: "AGARD two-dimensional aeroelastic configurations." AGARD AR 156, August 1979
- 0.2 S.R. Bland: "AGARD three-dimensional aeroelastic configurations." AGARD AR 167, March 1982
- 0.3 "Experimental data base for computer program assessment." AGARD AR 138, May 1979
- 0.4 N.C. Lambourne: "Experimental techniques in unsteady aerodynamics." Lecture 10 in Special Course on Unsteady Aerodynamics, AGARD AR 679, March 1980
- 0.5 N.C. Lambourne: "Wind tunnel wall interference in unsteady transonic testing." Contribution to Lecture Series on Unsteady Airloads and Aeroelastic Problems in Separated and Transonic Flow. Von-Karman Institute, Rhode-St-Genese, Belgium, March 1981
- 0.6 H. Tijdeman: "Investigations of the transonic flow around oscillating airfoils." NLR TR 77090U (1977)
- 0.7 N.C. Lambourne, B.L. Walsh: "Pressure measurements on a wing oscillating in super-critical flow." RAE Technical Report 79074 (1979)
- 0.8 T.W. Binion: "Limitations of available data." Section 2 of Ref 0.3 (above)
- 0.9 D.G. Mabey: "The resonance frequencies of ventilated wind tunnels." ARC R&M 3841 (1978)
- 0.10 W.E.A. Acum: "Interference effects in unsteady experiments." Chapter IV of Subsonic Wind Tunnel Wall Corrections (Ed. H.C. Garner), AGARDograph 109 (1966)
- 0.11 H.C. Garner: "Theoretical use of variable porosity in slotted tunnels for minimizing wall interference on dynamic measurements." ARC R&M 3706 (1971)
- 0.12 W.F. Ballhaus, P.M. Goojarian: "Efficient solution of unsteady transonic flows about airfoils." AGARD CP-226, Paper 14 (1977)
- 0.13 J. Fromme, M. Goldberg: "Unsteady two dimensional airloads acting on oscillating thin airfoils in subsonic ventilated wind tunnels." NASA CR 2967 (1978)
- 0.14 J. Fromme, M. Goldberg, J. Werth: "Two dimensional aerodynamic interference effects on oscillating airfoils with flaps in ventilated subsonic wind tunnels." NASA CR 3210 (1979)

Table 0.1

THE AGARD AEROELASTIC CONFIGURATIONS

Configuration	Motion	Experimental data	
		Source	Present position
<u>2-Dimensional</u> Parabolic arc	Pitch and plunge oscillations	-	No experiments
NACA 64A006	Flap oscillation	NLR	Data Set 1. CT Cases 1,2,3,5,6,7,8*,10*,11
NACA 64A010 NASA Ames model	Pitch oscillation	Ames	Data Set 2. CT Cases 1,2,3,4,5,6*,7,8,9,10*
NACA 0012	Pitch oscillation and transient	ARA	Data Set 3. CT Cases 1*,2,3,5,6,7,8*
MBB-A3	Pitch and plunge oscillations	MBB	Steady data only
DO A1	Pitch oscillation	-	No experiments
NLR 7301	Pitch oscillation	NLR	Data Set 4. CT Cases 1,2,3,4,5,6,8*
		Ames	Data Set 5. CT Cases 1,2,3,4,5,6,7,8*,9
	Flap oscillation	NLR	Data Set 4. CT Cases 10,11,12,14
<u>3-Dimensional</u> Rectangular wing	Pitch oscillation about 2 axes	RAE	Experiments planned for 1984
RAE wing A	Pitch oscillation	RAE	Possibility of future experiments
	Flap oscillation	RAE	Data Set 6. CT Cases 4,5,8,9*,11
NORA model	Oscillation about swept axis	GARTEur [†]	Data Set 7. CT Cases 1,2*,3,4,5*,6*,7,8,9
ZKP wing	Flap oscillation	VFW	Data available in 1983
LANN wing	Pitch oscillation	NLR	Data probably available in 1983

* Denotes the priority cases for computational tests.

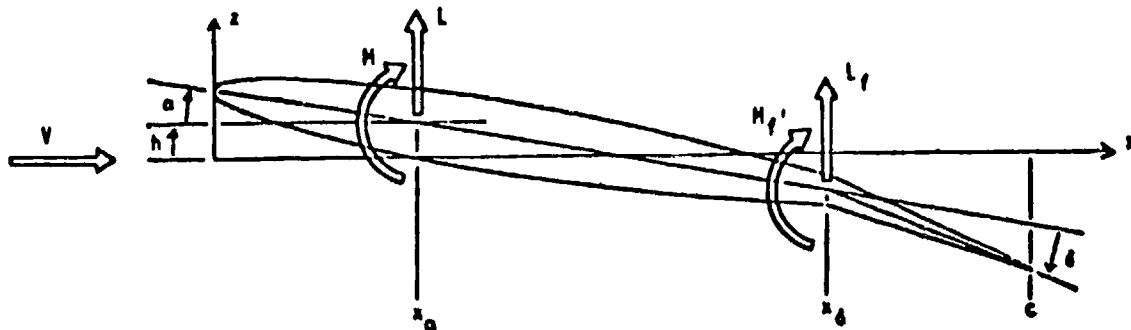
[†] The NORA experiments were made under the auspices of the Group for Aeronautical Research and Technology in Europe.

Table 0.2

NLR 7301 AEROFOIL PITCHING ABOUT 0.4c

Flow	Case	Run No. or DI	M	α_m	α_0	k	$Re \times 10^{-6}$	Transition
Subsonic	<u>CT Case 1</u>	-	0.500	0.40	0.5	0.098	-	-
	Data Set 4	1601	0.499	0.85	0.55	0.098	1.70	Fixed
	Data Set 5 {	184	0.508	0.58	0.50	0.050	2.53	Free
		168	0.505	0.58	0.51	0.049	9.33	Free
	<u>CT Case 2</u>	-	0.500	0.40	0.5	0.263	-	-
	Data Set 4	1301	0.498	0.85	0.44	0.262	1.70	Fixed
Data Set 5 {	185	0.508	0.58	0.50	0.197	2.53	Free	
	170	0.505	0.58	0.50	0.198	9.33	Free	
Transonic with shock	<u>CT Case 3</u>	-	0.700	2.00	0.5	0.072	-	-
	Data Set 4	3805	0.696	3.00	0.42	0.072	2.11	Fixed
	Data Set 5 {	204	0.710	2.53	0.50	0.050	3.14	Free
		197	0.700	2.53	0.49	0.050	12.0	Free
	<u>CT Case 4</u>	-	0.700	2.00	1.0	0.072	-	-
	Data Set 4	3905	0.696	3.00	0.98	0.072	2.11	Fixed
	Data Set 5 {	206	0.710	2.53	1.01	0.050	3.14	Free
		199	0.700	2.53	1.01	0.050	12.0	Free
	<u>CT Case 5</u>	-	0.700	2.00	0.5	0.192	-	-
Data Set 4	52705	0.695	3.00	0.55	0.192	2.12	Fixed	
Data Set 5 {	205	0.710	2.53	0.58	0.199	3.14	Free	
	198	0.700	2.53	0.49	0.201	12.0	Free	
Super- critical design	<u>CT Case 6</u>	-	0.721	-0.19	0.5	0.068	-	-
	Data Set 4	9608	0.744	0.85	0.46	0.068	2.23	Free
	Data Set 5 {	190	0.752	0.37	0.50	0.050	3.30	Free
		132	0.752	0.37	0.50	0.050	6.20	Free
		144	0.751	0.37	0.50	0.050	11.4	Free
	<u>CT Case 7</u>	-	0.721	-0.19	1.0	0.068	-	-
	Data Set 4	-	-	-	No measurements		-	-
	Data Set 5 {	136	0.752	0.37	1.01	0.050	6.20	Free
		150	0.751	0.37	1.00	0.050	11.4	Free
	<u>CT Case 8*</u>	-	0.721	-0.19	0.5	0.181	-	-
	Data Set 4	6708	0.744	0.85	0.61	0.181	2.22	Free
	Data Set 5 {	191	0.752	0.37	0.50	0.200	3.30	Free
	134	0.752	0.37	0.49	0.200	6.20	Free	
	148	0.751	0.37	0.50	0.201	11.4	Free	
<u>CT Case 9</u>	-	0.721	-0.19	0.5	0.453	-	-	
Data Set 4	-	-	-	No measurements		-	-	
Data Set 5 {	135	0.752	0.37	0.50	0.300	6.20	Free	
	149	0.751	0.37	0.50	0.301	11.4	Free	

* Denotes a priority case for computations



$$q = 1/2 \rho V^2$$

$$C_p = \frac{p - p_\infty}{q}$$

$$\Delta C_p = C_{p, \text{lower}} - C_{p, \text{upper}}$$

$$L = q c c_l$$

$$L_f = q c c_{l, f}$$

$$M = q c^2 c_m$$

$$M_f = q c^2 c_m$$

$$C_L = \frac{2}{S} \int_0^b c c_l dy$$

$$C_M = \frac{2}{3c_r} \int_0^b c^2 c_m dy$$

$$C_M = \frac{2}{3c_r} \int_{\text{control span}} c^2 c_m dy$$

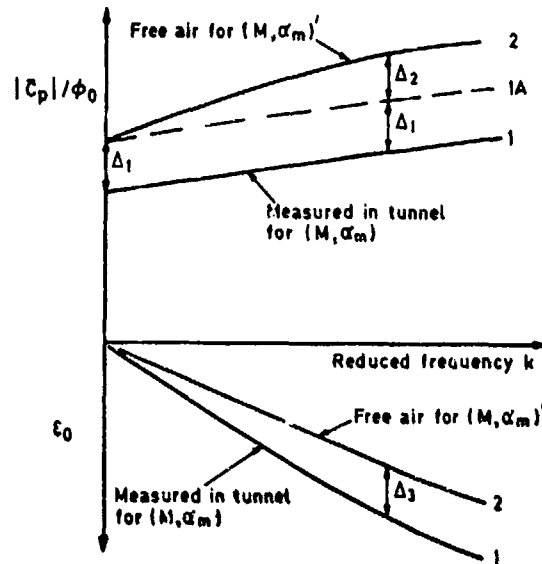
$$c_l = \oint_{\text{airfoil}} C_p dt = \int_0^1 \Delta C_p dt$$

$$c_m = \oint_{\text{airfoil}} C_p (x_a/c - t - z/c + dz/dx) dt = \int_0^1 \Delta C_p (x_a/c - t) dt$$

$$c_{l, f} = \oint_{\text{flap}} C_p dt = \int_{x_b/c}^1 \Delta C_p dt$$

$$c_m = \oint_{\text{flap}} C_p (x_b/c - t - z/c + dz/dx) dt = \int_{x_b/c}^1 \Delta C_p (x_b/c - t) dt$$

Fig 0.1 Wing section and total force and moment definitions from Ref 0.2



It is assumed that a steady condition (M, α_m) in the tunnel is equivalent to a steady condition $(M, \alpha_m)'$ in free air.
 Displacement Δ_1 is an effect of steady interference;
 Δ_2 and Δ_3 are the effects of unsteady interference

Fig 0.2 Schematic diagram illustrating tunnel interference on the modulus and phase of oscillatory pressure

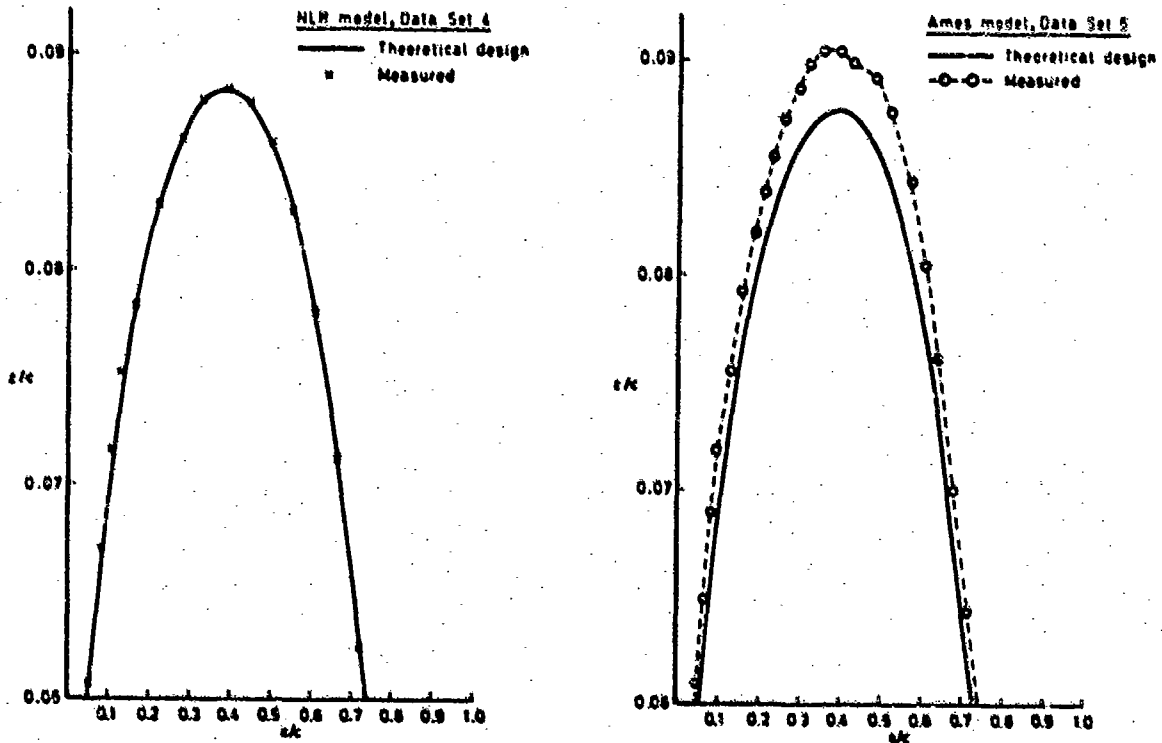


Fig 0.3 NLR 7301 Airfoil. Comparison between physical models and design shape. Profile height z/c for part of upper surface. (Note: the base line used to define z is not the same for both models; this is irrelevant to the comparisons)

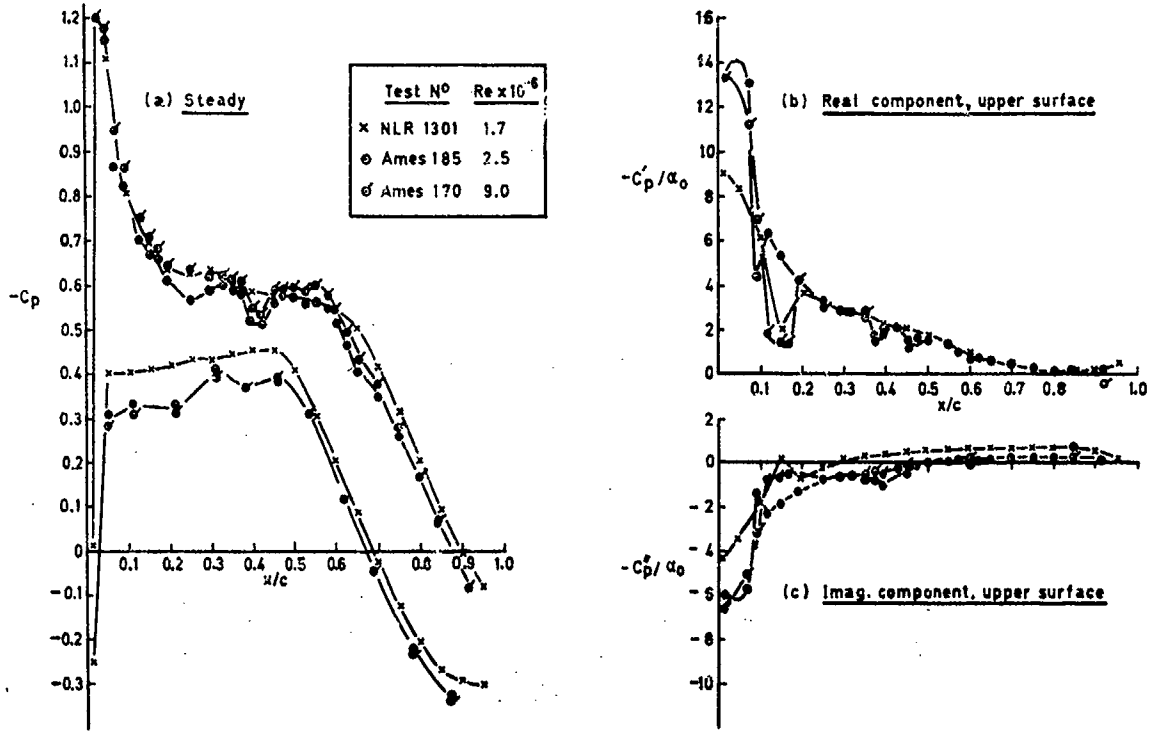


Fig 0.4 NLR 7301 Airfoil. Comparison of NLR and Ames data relating to CT Case 2 (subsonic M = 0.5)

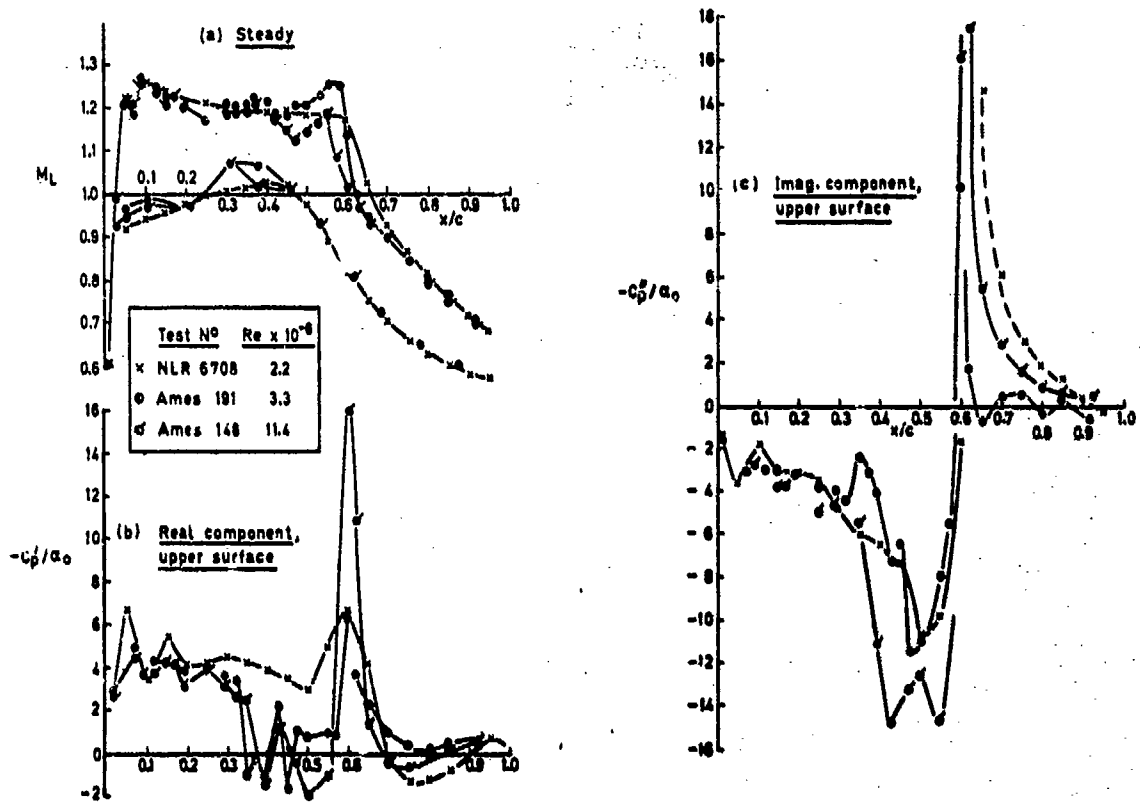


Fig 0.5 NLR 7301 Airfoil. Comparison of NLR and Ames data relating to CT Case 8 (Supercritical design case)

DATA SET 1

NACA 64A006 OSCILLATING FLAP

by

R.J. Zwaan, NLR

INTRODUCTION

The wind tunnel model which had a NACA 64A006 airfoil section, was fitted with a trailing-edge flap of 25 per cent of the chord. The maximum thickness of this symmetrical airfoil is 6 per cent and is located at about 28 per cent of the chord. During the test the main surface was clamped at the wind tunnel side walls, whereas the flap could be driven in a harmonic motion about an axis at 75 per cent of the chord. The flap had no aerodynamic balance.

In the set of two-dimensional aeroelastic configurations this airfoil represents the category of small thickness and conventional airfoils (roof-top type). The characteristics are illustrated in figure 1.1, presenting the development of the steady and unsteady pressure distributions with Mach number for a given frequency. Passing the critical Mach number, $M^* \approx 0.85$, the measured unsteady pressure distributions start to deviate from the calculated distributions under the influence of shocks at both sides. The calculated results are based on lifting surface theory.

Lift and moment coefficients are given in figure 1.2 for a frequency of 120 Hz. An at least qualitative agreement exists between experiment and theory up to $M \approx 0.85$. Results are also given for $k = 0$, see figure 1.3. The differences between experiment and theory are appreciably larger now, which can be ascribed partly to tunnel wall interference.

1	AIRFOIL	
1.1	Designation	NACA 64A006
1.2	Type of airfoil	Roof top, 6 % thick, symmetrical
1.3	Geometry	See Table 1.1
1.4	Design condition	Not applicable
1.5	Additional remarks	-
1.6	References on airfoil	Ref. 1.1
2	MODEL GEOMETRY	
2.1	Chord length	0.18 m
2.2	Span	0.42 m
2.3	Actual model coordinates and accuracy of measurements	See Table 1.2
2.4	Flap: hinge and gap details	Hinge axis at 0.75 c; gap width 0.1 mm
2.5	Additional remarks	-
2.6	References on model	-
3	WIND TUNNEL	
3.1	Designation	NLR Pilot Tunnel
3.2	Type of tunnel	Continuous, closed circuit
3.3	Test section dimensions	Rectangular; see Fig. 1.4 height 0.35 m, width 0.42 m
3.4	Type of roof and floor	10 % slotted top and bottom walls, separate top and bottom plenums
3.5	Type of side walls	Solid side walls
3.6	Ventilation geometry	See Fig. 1.4
3.7	Thickness of side wall boundary layer	Thickness 10 % of test section semi-width, no special treatment
3.8	Thickness of boundary layers at roof and floor	Not measured; probably comparable with side wall boundary layers
3.9	Method of measuring Mach number	Derived from static pressure measured upstream of model and from total pressure measured in settling chamber
3.10	Uniformity of Mach number over test section	See Fig. 1.5
3.11	Sources and levels of noise or turbulence in empty tunnel	Turbulence/noise level, see Fig. 1.6
3.12	Tunnel resonances	No evidence

3.13	Additional remarks	For two-dimensionality of the flow see Ref. 1.3
3.14	References on tunnel	Ref. 1.2
4	MODEL MOTION	
4.1	Mode of applied motion	Flap oscillation
4.2	Range of amplitude	$\delta_0 \approx 1^\circ$
4.3	Range of frequency	$f = 0$ to 120 Hz; $k = 0$ to 0.4
4.4	Method of application	Electrodynamic excitation at both sides of the flap, using adjustable spring stiffness
4.5	Purity of applied motion	Checked by spectral analysis; no data stored
4.6	Natural frequencies and normal modes of model	No interference with natural vibration modes
4.7	Static or dynamic elastic distortion during tests	Negligible
4.8	Additional remarks	-
5	TEST CONDITIONS	
5.1	Tunnel height/model chord ratio	3.1
5.2	Tunnel width/model chord ratio	2.3
5.3	Range of Mach number	$M = 0.5$ to 1.0
5.4	Range of tunnel total pressure	Atmospheric
5.5	Range of tunnel total temperature	313 ± 1 K
5.6	Range of model steady, or mean, incidence	$\alpha_m: -4^\circ$ to 0° ; $\delta_m: -3^\circ$ to 3°
5.7	Definition of model incidence	Zero incidence defined by matching upper and lower static pressure distribution (applicable because of airfoil symmetry)
5.8	Position of transition, if free	Not applicable
5.9	Position and type of trip, if transition fixed	2.5 mm strip of carborundum grains at 0.1 c
5.10	For mixed flow, position of sonic boundary in relation to roof and floor	Not measured
5.11	Flow instabilities during tests	No evidence
5.12	Additional remarks	-
5.13	References describing tests	Ref. 1.4
6	MEASUREMENTS AND OBSERVATIONS	
6.1	Steady pressures for the mean conditions	<input checked="" type="checkbox"/>
6.2	Steady pressures for small changes from the mean conditions	<input checked="" type="checkbox"/>
6.3	Quasi-steady pressures	<input type="checkbox"/>
6.4	Unsteady pressures	<input checked="" type="checkbox"/>
6.5	Steady forces for the mean conditions	{measured directly integrated press. <input checked="" type="checkbox"/>
6.6	Steady forces for small changes from the mean conditions	{measured directly integrated press. <input checked="" type="checkbox"/>
6.7	Quasi-steady forces	{measured directly integrated press. <input type="checkbox"/>
6.8	Unsteady forces	{measured directly integrated press. <input checked="" type="checkbox"/>
6.9	Measurement of actual motion at points on model	<input checked="" type="checkbox"/>
6.10	Observation or measurement of boundary layer properties	<input type="checkbox"/>
6.11	Visualization of surface flow	<input type="checkbox"/>
6.12	Visualization of shockwave movements	<input checked="" type="checkbox"/>
6.13	Additional remarks	<input type="checkbox"/>

7	INSTRUMENTATION	
	7.1 Steady pressures	
	7.1.1 Position of orifices spanwise and chordwise	See 7.2.1
	7.1.2 Type of measuring system	See 7.2.3
	7.2 Unsteady pressures	
	7.2.1 Position of orifices spanwise and chordwise	See Fig: 1.7 and 1.8
	7.2.2 Diameter of orifices	0.8 mm
	7.2.3 Type of measuring system	38 pressure tubes + 6 in situ pressure transducers
	7.2.4 Type of transducers	± 2.5 psi and ± 5 psi Statham differential pressure transducers, and ± 5 psi Kulite miniature pressure transducers
	7.2.5 Principle and accuracy of calibration	Calibration uses transfer functions of pressure tubes, see Ref. 1.4; for accuracy see 9.10
	7.3 Model motion	
	7.3.1 Method of measurement	See Fig. 1.7
	7.3.2 Accuracy	See 9.10
	7.4 Processing of unsteady measurements	
	7.4.1 Method of acquiring and processing measurements	See Fig. 1.9
	7.4.2 Type of analysis	Signal analysis of TFA over 20 cycles for $f = 30$ Hz and 60 cycles for $f = 120$ Hz
	7.4.3 Unsteady pressure quantities obtained and accuracies achieved	Fundamental harmonics; for accuracy see 9.10
	7.4.4 Method of integration to obtain forces	Trapezoidal rule
	7.5 Additional remarks	-
	7.6 References on techniques	Refs 1.4, 1.5
8	DATA PRESENTATION	
	8.1 Test cases for which data could be made available	Table 1.3
	8.2 Test cases for which data are included in this document	Table 1.4
	8.3 Steady pressures	Mean pressures in Tables 1.5 to 1.18
	8.4 Quasi-steady or steady perturbation pressures	Steady pressure derivatives in Tables 1.5, 1.8, 1.11, 1.14 and 1.17
	8.5 Unsteady pressures	Tables 1.6, 1.7, 1.9, 1.10, 1.12, 1.13, 1.15, 1.16 and 1.18
	8.6 Steady forces or moments	-
	8.7 Quasi-steady or steady perturbation forces	See 8.4
	8.8 Unsteady forces and moments	See 8.5
	8.9 Other forms in which data could be made available if required	-
	8.10 References giving other presentations of data	Ref. 1.6
9	COMMENTS ON DATA	
	9.1 Accuracy	
	9.1.1 Mach number	± 0.002
	9.1.2 Steady incidence	$\pm 0.02^\circ$
	9.1.3 Reduced frequency	± 0.0005
	9.1.4 Steady pressure coefficients	Not known
	9.1.5 Steady pressure derivatives	Not known
	9.1.6 Unsteady pressure coefficients	Not known
	9.2 Sensitivity to small changes of parameter	No evidence
	9.3 Spanwise variations	No evidence
	9.4 Non-linearities	Part of analysis of experimental results; see Ref. 1.4

9.5	Influence of tunnel total pressure	-
9.6	Wall interference corrections	No corrections included
9.7	Other relevant tests on <u>same model</u>	None
9.8	Relevant tests on other model of nominally the <u>same</u> airfoil	Unknown
9.9	Any remarks relevant to comparison between experiment and theory	Comparisons of experiment and theory including various calculation methods are given in Ref. 4
9.10	Additional remarks	No systematic investigations of separate accuracies have been performed; accuracy of lift and moment coefficients is estimated to be 5 to 10 per cent in magnitude and 3 to 6 degrees in phase angle
9.11	References on discussion of data	Refs 1.4, 1.7

10 PERSONAL CONTACT FOR FURTHER INFORMATION

R.J. Zwaan, National Aerospace Laboratory (NLR), Anthony Fokkerweg 2, 1059 CM Amsterdam, The Netherlands

11 LIST OF REFERENCES

- 1.1 I.H. Abbott Theory of wing sections
A.E. von Doenhoff Dover Publications, Inc., New York, 1959
- 1.2 J. Zwaaneveld Principal data of the NLL Pilot Tunnel
NLL Report MP 185, 1959
- 1.3 H.A. Dambrink Investigation of the 2-dimensionality of the flow around a profile in the NLR 0.55x0.42 m² transonic wind tunnel
NLR Memorandum AC-72-018, 1972
- 1.4 H. Tijdeman Investigations of the transonic flow around oscillating airfoils
NLR TR 77090 U, 1977
- 1.5 P.H. Fuykschot DXDRA - Data logger for dynamic measurements
L.J.M. Joosten NLR MP 69012 U, 1969
- 1.6 H. Tijdeman Results of pressure measurements on an airfoil with oscillating flap in two-dimensional high subsonic and transonic flow (zero incidence and zero mean flap position)
P. Schippers NLR TR 73078 U, 1973
- 1.7 R. Houwink Some remarks on boundary layer effects on unsteady airloads
AGARD-CP-296, 1981
- 1.8 S.R. Bland AGARD Two-dimensional aeroelastic configurations
AGARD-AR-156, 1979

12 NOTATION AND LIST OF SYMBOLS

DATA SET	STANDARD
ALPHA	mean wing incidence, α_m , deg
C	flap amplitude, δ_o , deg; see Note 2 below
CP	steady mean pressure coefficient, C_p
DCP	oscillatory pressure coefficient ($k \neq 0$), tabulated as REal, IMaginary, MODulus and ARGument, equivalent to $-\bar{C}_p/\delta_o$, in which $\bar{C}_p/\delta_o = (C_p/\delta_o) + i(C_p''/\delta_o)$. RE, IM, MOD in rad ⁻¹ , ARG in deg. If $k = 0$, then DCP = $-(C_p(+\delta_o) - C_p(-\delta_o))/2\delta_o$
DELTA	mean flap angle, δ_m , deg
F	frequency, f, Hz
K	reduced frequency, $k = \pi fc/V$
KC, k_c	oscillatory wing lift coefficient, $\bar{C}_L/\omega\delta_o$, rad ⁻¹
M	mean local Mach number, M_L
MC, m_c	oscillatory wing pitching moment coefficient (about 0.25 c), $-2 \bar{C}_m/\omega\delta_o$, rad ⁻¹
NC, n_c	oscillatory flap hinge moment coefficient, $-2 \bar{C}_h/\omega\delta_o$, rad ⁻¹
PO	total pressure, p_t , Pa
Q	dynamic pressure, q, Pa
RC	oscillatory flap lift coefficient, $\bar{C}_{L_f}/\omega\delta$, rad ⁻¹
RE	Reynolds number based on wing chord, Re
+	(suffix) upper side
-	(suffix) lower side

* (superscript) critical value

Note 1: Symbols not mentioned here conform to the notation in the General Review

Note 2: The oscillatory motion is defined as $\delta = \delta_0 \sin \omega t$, in accordance with the General Review. The equation for a corresponding oscillatory pressure reads:

$$p(t) = p_m + p' \sin \omega t + p'' \cos \omega t + \text{etc.}$$

Similar expressions hold for the aerodynamic coefficients.

TABLE 1.1

Contour data of the NACA 64A006 airfoil

x (% c)	z (% c)	x (% c)	z (% c)
0	0	40	2.999
0.5	0.485	45	2.945
0.75	0.585	50	2.825
1.25	0.739	55	2.653
2.5	1.016	60	2.438
5.0	1.399	65	2.188
7.5	1.684	70	1.907
10	1.919	75	1.602
15	2.283	80	1.285
20	2.557	85	0.967
25	2.757	90	0.649
30	2.896	95	0.331
35	2.977	100	0.013

L.E. radius: 0.246 % c

TABLE 1.2

Actual contour data of the NACA 64A006 airfoil (measures per cent of chord)

x	z _{upper}	z _{lower}
1.25	0.742	-0.742
2.50	1.025	-1.025
5.00	1.405	-1.405
7.50	1.686	-1.686
10.00	1.919	-1.922
15.00	2.283	-2.283
20.00	2.558	-2.555
25.00	2.758	-2.758
30.00	2.894	-2.889
35.00	2.975	-2.969
40.00	2.991	-2.989
45.00	2.942	-2.936
50.00	2.822	-2.819
55.00	2.655	-2.642
60.00	2.430	-2.425
65.00	2.194	-2.169
70.00	1.908	-1.894
75.00	-	-
80.00	1.310	-1.310
85.00	0.989	-0.989
90.00	0.668	-0.668
95.00	0.346	-0.346
100.00	0.027	-0.027

TABLE 1.3

Test program for the NACA 64A006 airfoil with flap

Test condition	FREQ. (Hz)	MACH NUMBER												
		.50	.75	.775	.80	.825	.85	.875	.90	.92	.94	.96	.98	1.00
$\alpha_{flap} = 0^\circ$ $\delta_{flap} = 0^\circ$	0	x	x		x	x	x	x	x	x	x	x	x	x
	10	x				x	x	x	x					
	20	x					x							
	30	x			x	x	x	x	x			x		
	90	x				x	x	x	x			x		
120	x	x	x	x	x	x	x	x	x	x	x	x	x	x
$\alpha_{flap} = 0^\circ$ $\delta_{flap} = 3^\circ$	0	x	x		x	x	x	x	x	x	x	x	x	x
	30	x				x	x	x	x					
	120	x	x	x	x	x	x	x			x	x		
$\alpha_{flap} = -2^\circ$ $\delta_{flap} = 0^\circ$	0	x	x		x	x	x	x	x	x	x			
	30	x				x	x	x	x					
	120	x	x	x	x	x	x	x	x	x				
$\alpha_{flap} = -2^\circ$ $\delta_{flap} = 3^\circ$	0	x	x	x	x	x	x	x	x	x	x			
	30	x				x	x	x	x					
	120	x	x	x	x	x	x	x			x			
$\alpha_{flap} = -2^\circ$ $\delta_{flap} = -3^\circ$	0	x	x	x	x	x	x	x	x	x	x			
	30	x				x	x	x						
	120	x	x	x	x	x	x							
$\alpha_{flap} = -4^\circ$ $\delta_{flap} = 0^\circ$	0	x	x	x	x	x	x	x	x	x				
	10	x					x							
	30	x					x							
	120	x	x	x	x	x	x	x	x					

AMPLITUDE OF OSCILLATION: $\delta_0 = 1$ DEG

TABLE 1.4

Test cases for the NACA 64A006 airfoil with flap included in Data Set 1

Flow	CT Case				Data Set 1						
	No	M	δ_o	k	Run No	M	δ_o	δ_m	k	Re $\times 10^{-6}$	Table
Subsonic	z1	0.800	1.5	0	-	0.800	1.5	0	0	2.34	1.5
	1	0.800	1.0	0.064	40904	0.794	1.09	0.15	0.064	2.32	1.6
	2	0.800	1.0	0.253	40807	0.804	1.11	0.00	0.253	2.35	1.7
	z2	0.825	1.5	0	-	0.825	1.5	0	0	2.36	1.8
	3	0.825	1.0	0.062	40905	0.824	1.09	0.15	0.062	2.36	1.9
	4	0.825	2.0	0.062	No measurement						
5	0.825	1.0	0.248	40305	0.822	0.95	0.20	0.248	2.28	1.10	
Transonic	z3	0.850	1.5	0	-	0.850	1.5	0	0	2.39	1.11
	6	0.850	1.0	0.060	40906	0.853	1.10	0.16	0.060	2.40	1.12
	7	0.850	1.0	0.240	40806	0.854	1.05	0.02	0.240	2.41	1.13
	z4	0.875	1.5	0	-	0.875	1.5	0	0	2.43	1.14
	8*	0.875	1.0	0.059	40907	0.877	1.13	0.15	0.059	2.43	1.15
	9*	0.875	2.0	0.059	No measurement						
	10*	0.875	1.0	0.234	40807	0.879	1.08	0.01	0.234	2.44	1.16
	z5	0.960	1.5	0	-	0.960	1.5	0	0	2.51	1.17
	11	0.960	1.0	0.054	40911	0.966	1.03	0.00	0.054	2.53	1.18
	12	0.960	1.0	0.214	No measurement						
								0.18			

Remarks on Table 1.4

Cases z1 to z5 are extra to the computational cases identified in reference 1.8. They correspond to zero-frequency ($k = 0$) experimental data that are closely related to the CT Cases for which $k \neq 0$. The asterisks denote Priority Cases.

In all cases $\alpha_m = 0$. Transition is fixed at 0.15 c.

TABLE 1.5

M = .800

F = 0

ALPHA = 0.00

KC = 1.32

DELTA = 0.00

MC = .612

C = 1.5

NC = .0372

UPPERSIDE

LOWERSIDE

X/C	CP +	M +	RE	IM	DCP +	CP -	M -	RE	IM	DCP -
.010	-.005	.A02	3.552	0.0	.029	.787	-3.609	0.0		
.050	-.154	.A70	2.292	0.0	-.143	.865	-2.253	0.0		
.100	-.192	.A87	1.833	0.0	-.179	.881	-1.833	0.0		
.200	-.236	.907	1.690	0.0	-.238	.908	-1.719	0.0		
.300	-.268	.922	1.719	0.0	-.273	.924	-1.852	0.0		
.400	-.290	.932	1.890	0.0	-.293	.933	-2.005	0.0		
.450	-.276	.926	1.967	0.0	-.267	.921	-1.986	0.0		
.500	-.249	.913	1.890	0.0	-.250	.914	-2.024	0.0		
.550	-.216	.898	1.948	0.0	-.213	.897	-1.986	0.0		
.600	-.179	.881	2.005	0.0	-.176	.880	-2.158	0.0		
.650	-.150	.868	2.215	0.0	-.144	.865	-2.349	0.0		
.700	-.114	.854	2.597	0.0	-.103	.847	-2.616	0.0		
.725	-.104	.847	2.941	0.0	-.084	.838	-2.826	0.0		
.750	-.096	.843	4.431	0.0	.007	.797	-7.086	0.0		
.775	-.071	.832	3.458	0.0	-.053	.824	-3.724	0.0		
.800	-.046	.821	2.807	0.0	-.034	.815	-2.769	0.0		
.850	-.010	.805	1.661	0.0	-.004	.802	-1.699	0.0		
.900	.023	.790	.974	0.0	.010	.786	-.974	0.0		
.950	.067	.770	.459	0.0	.072	.768	-.477	0.0		

TABLE 1.6

RUNNO 40904

M = .794 F= 30.0 ALPHA= 0
 PO= 10429 DELTA= .15
 RE= 2.32E6 K= .064 C= 1.09
 Q = 3037.30

KC= RE IM RC= RE IM X5= 1.334E-3 1
 MC= .640 .010 NC= .0385 .0028 X6= 1.346E-3 0

X/C	CP+	M+	UPPERSIDE				DCP+	CP-	M-	LOWERSIDE			
			RE	IM	MOD	ARG				RE	IM	MOD	ARG
.010	-0.035	.811	.671	-1.474	1.619	-65	.077	.759	-0.736	1.554	1.719	115	
.050	-0.175	.873	.342	-0.753	.827	-66	-0.120	.847	-0.678	1.050	1.250	123	
.100	-0.226	.897	.657	-0.853	1.077	-52	-0.166	.867	-0.737	.895	1.159	129	
.200	-0.252	.909	.991	-0.787	1.266	-38	-0.222	.893	-1.115	.826	1.387	143	
.300	-0.279	.921	1.245	-0.683	1.420	-29	-0.256	.908	-1.276	.708	1.459	151	
.400	-0.304	.932	1.628	-0.554	1.719	-19	-0.279	.919	-1.578	.605	1.690	159	
.450	-0.287	.925	1.744	-0.403	1.790	-13	-0.260	.910	-1.665	.490	1.736	164	
.500	-0.263	.914	1.826	-0.301	1.850	-9	-0.235	.898	-1.825	.379	1.864	168	
.550	-0.222	.895	1.915	-0.198	1.925	-6	-0.199	.882	-1.927	.288	1.948	172	
.600	-0.190	.881	2.034	-0.113	2.038	-3	-0.165	.867	-2.105	.185	2.113	175	
.650	-0.159	.866	2.155	-0.136	2.159	-4	-0.127	.850	-2.302	.118	2.305	177	
.700	-0.125	.851	2.258	-0.253	2.272	-6	-0.089	.833	-2.649	.043	2.650	179	
.725	-0.108	.844	2.658	-0.213	2.667	-5	-0.071	.825	-2.885	.023	2.885	180	
.750	-0.068	.825	4.948	.409	4.965	5	.013	.787	-5.276	1.571	5.505	163	
.775	-0.085	.833	4.097	.224	4.103	3	-0.030	.806	-3.821	-0.047	3.822	181	
.800	-0.058	.821	3.038	.335	3.057	6	-0.018	.801	-2.943	-0.141	2.946	183	
.850	-0.018	.803	1.751	.212	1.764	7	.006	.790	-1.738	-0.042	1.739	181	
.900	.021	.786	.959	.100	.964	6	.038	.776	-1.066	-0.090	1.069	185	
.950	.069	.764	.374	.013	.374	2	.080	.757	-0.581	-0.043	.583	185	

TABLE 1.7

RUNNO 40807

M = .804 F= 120.0 ALPHA= 0
 PO= 10484 DELTA=-9.00
 RE= 2.35E6 K= .253 C= 1.11
 Q = 3097.83

KC= RE IM RC= RE IM
 MC= .830 -0.394 NC= .3090 .0480
 .756 -0.019 NC= .0419 .0115

X/C	CP+	M+	UPPERSIDE				DCP+	CP-	M-	LOWERSIDE			
			RE	IM	MOD	ARG				RE	IM	MOD	ARG
.010	-0.031	.818	-1.001	-0.899	1.346	-138	.068	.774	1.043	.914	1.387	41	
.050	-0.173	.882	-0.494	-0.510	.710	-134	-0.124	.860	.661	.704	.926	49	
.100	-0.225	.906	-0.416	-0.768	.873	-118	-0.171	.882	.476	.647	.971	61	
.200	-0.252	.919	-0.081	-1.121	1.124	-94	-0.225	.906	.061	1.126	1.127	67	
.300	-0.280	.932	.428	-1.351	1.417	-72	-0.257	.921	-0.448	1.276	1.352	109	
.400	-0.306	.944	1.240	-1.468	1.921	-50	-0.282	.933	-1.100	1.307	1.708	130	
.450	-0.289	.936	1.647	-1.277	2.084	-38	-0.267	.926	-1.335	1.199	1.795	138	
.500	-0.261	.923	1.943	-1.118	2.242	-30	-0.238	.912	-1.668	1.044	1.968	148	
.550	-0.223	.905	2.146	-0.900	2.327	-23	-0.203	.896	-1.906	.924	2.118	154	
.600	-0.188	.889	2.336	-0.629	2.420	-15	-0.168	.880	-2.217	.664	2.315	163	
.650	-0.158	.875	2.582	-0.428	2.617	-9	-0.132	.864	-2.556	.923	2.609	168	
.700	-0.126	.861	2.729	-0.180	2.735	-4	-0.095	.847	-2.978	.290	2.992	174	
.725	-0.108	.852	3.259	-0.139	3.262	-2	-0.076	.838	-3.286	.212	3.293	176	
.750	-0.045	.824	7.188	.060	7.188	0	.008	.890	-6.507	.214	6.510	178	
.775	-0.083	.841	4.427	.134	4.429	2	-0.038	.821	-3.953	-0.189	3.957	183	
.800	-0.055	.828	3.339	.446	3.368	8	-0.026	.816	-3.099	-0.374	3.121	187	
.850	-0.017	.811	1.986	.488	2.045	14	-0.001	.804	-1.833	-0.437	1.885	193	
.900	.020	.794	1.105	.407	1.178	20	.032	.789	-1.121	-0.444	1.206	202	
.950	.066	.773	.431	.228	.487	28	.074	.770	-0.498	-0.273	.566	209	

TABLE 1.8

M = .825 F = 0 ALPHA = 0.00 KC = 1.35
 DELTA = 0.00 MC = .640
 C = 1.5 NC = .0380

X/C	UPPERSIDE				LOWERSIDE			
	CP +	M +	DCP +		CP -	M -	DCP -	
			RE	IM			RE	IM
.010	.017	.817	3.132	0.0	.039	.807	-3.208	0.0
.050	-.146	.894	2.081	0.0	-.141	.891	-2.139	0.0
.100	-.188	.914	1.680	0.0	-.181	.910	-1.757	0.0
.200	-.246	.942	1.623	0.0	-.247	.942	-1.719	0.0
.300	-.283	.959	1.852	0.0	-.289	.962	-1.910	0.0
.400	-.321	.978	2.349	0.0	-.326	.980	-2.349	0.0
.450	-.300	.968	2.311	0.0	-.294	.965	-2.292	0.0
.500	-.265	.951	2.081	0.0	-.263	.950	-2.177	0.0
.550	-.225	.931	2.062	0.0	-.224	.931	-2.158	0.0
.600	-.187	.913	2.177	0.0	-.184	.912	-2.253	0.0
.650	-.151	.896	2.406	0.0	-.147	.894	-2.463	0.0
.700	-.119	.881	2.750	0.0	-.104	.874	-2.712	0.0
.725	-.103	.873	3.132	0.0	-.084	.864	-2.922	0.0
.750	-.092	.868	4.660	0.0	.007	.822	-7.219	0.0
.775	-.068	.857	3.991	0.0	-.051	.849	-3.839	0.0
.800	-.042	.845	2.845	0.0	-.032	.840	-2.884	0.0
.850	-.006	.828	1.661	0.0	.002	.824	-1.699	0.0
.900	.029	.811	.935	0.0	.036	.808	-.974	0.0
.950	.072	.791	.439	0.0	.079	.788	-.401	0.0

TABLE 1.9

RUNNO 40905

M = .824 F = 30.0 ALPHA = 0
 P0 = 10426 DELTA = .15
 RE = 2.36E6 K = .062 C = 1.09
 Q = 3175.36

KC = RE 1.068 IM -0.260 RO = RE .2863 IM .0195
 MC = .681 .022 NO = .0395 .0041

X/C	CP*	M*	UPPERSIDE				LOWERSIDE					
			DCP*		MOD	ARG	DCP*		MOD	ARG		
			RE	IM			RE	IM				
.010	-0.011	.831	.517	-1.351	1.446	-69	.088	.782	-0.529	1.384	1.491	111
.050	-0.169	.905	.273	-0.707	.758	-69	-0.116	.878	-0.562	.999	1.147	119
.100	-0.223	.931	.559	-0.839	1.008	-56	-0.168	.902	-0.608	.915	1.151	127
.200	-0.258	.948	.908	-0.844	1.240	-43	-0.235	.934	-1.067	.901	1.396	140
.300	-0.294	.966	1.308	-0.793	1.538	-31	-0.275	.953	-1.354	.817	1.582	149
.400	-0.329	.983	1.956	-0.715	2.082	-20	-0.308	.969	-1.877	.754	2.023	158
.450	-0.312	.975	2.107	-0.467	2.158	-12	-0.284	.958	-1.940	.378	2.025	161
.500	-0.278	.958	2.113	-0.271	2.130	-7	-0.254	.943	-2.030	.391	2.057	169
.550	-0.233	.936	2.065	-0.143	2.069	-4	-0.212	.923	-2.102	.262	2.119	173
.600	-0.194	.918	2.147	-0.048	2.148	-1	-0.171	.903	-2.246	.141	2.250	176
.650	-0.162	.902	2.271	-0.053	2.272	-1	-0.134	.886	-2.447	.050	2.447	179
.700	-0.129	.887	2.346	-0.182	2.353	-4	-0.092	.866	-2.771	-0.042	2.771	181
.725	-0.112	.878	2.780	-0.133	2.783	-3	-0.072	.857	-2.994	-0.044	2.995	181
.750	-0.068	.858	5.091	.547	5.120	6	.017	.815	-5.417	1.590	5.645	184
.775	-0.086	.866	4.289	.363	4.304	5	-0.029	.836	-4.000	-0.133	4.003	182
.800	-0.058	.853	3.173	.468	3.207	8	-0.016	.831	-3.079	-0.202	3.085	184
.850	-0.014	.832	1.805	.288	1.828	9	.008	.819	-1.793	-0.092	1.795	183
.900	.024	.815	.967	.135	.977	8	.043	.803	-1.089	-0.128	1.096	187
.950	.073	.791	.381	.032	.382	5	.084	.784	-0.492	-0.061	.496	181

TABLE 1.10

RUNNO 40305

M = .822 F = 120.0 ALPHA = 0
 P0 = 10069 DELTA = 120
 RE = 2.28E6 K = 248 C = 195
 Q = 3056.41

KC = .865 -0.480 RC = .3462 .8481
 MC = .861 -0.064 NC = .0477 .0120

X/C	CP+	M+	UPPERSIDE				DCP+	CP-	M-	LOWERSIDE			
			RE	IM	MOD	ARG				DCP-	RE	IM	MOD
.010	.002	.821	-1.336	-0.490	1.423	-160	.064	.792	1.437	.496	1.521	19	
.050	-0.157	.896	-0.661	-0.285	.720	-157	-0.135	.885	.978	.433	1.070	24	
.100	-0.217	.925	-0.734	-0.588	.940	-141	-0.185	.909	.849	.673	1.083	38	
.200	-0.257	.944	-0.566	-1.074	1.214	-118	-0.247	.938	.608	1.233	1.374	64	
.300	-0.293	.961	.138	-1.765	1.770	-85	-0.285	.956	-0.048	1.690	1.691	92	
.400	-0.329	.979	1.462	-2.225	2.662	-57	-0.319	.973	-1.291	2.051	2.424	122	
.450	-0.307	.968	2.104	-1.836	2.792	-41	-0.296	.962	-1.683	1.754	2.431	134	
.500	-0.270	.950	2.333	-1.416	2.730	-31	-0.258	.944	-2.112	1.399	2.533	146	
.550	-0.229	.930	2.577	-1.087	2.797	-23	-0.220	.925	-2.314	1.165	2.591	153	
.600	-0.193	.913	2.747	-0.745	2.846	-15	-0.179	.906	-2.586	.843	2.720	162	
.650	-0.161	.898	2.967	-0.489	3.007	-9	-0.142	.888	-2.869	.654	2.943	167	
.700	-0.126	.882	2.956	-0.230	2.965	-4	-0.104	.870	-3.307	.354	3.326	174	
.725	-0.106	.872	3.445	-0.194	3.451	-3	-0.081	.859	-3.571	.248	3.580	176	
.750	-0.061	.851	6.850	-0.178	6.853	-1	.017	.814	-7.104	.136	7.105	179	
.775	-0.080	.860	4.901	.086	4.901	1	-0.045	.843	-4.696	-0.106	4.698	181	
.800	-0.052	.847	3.740	.440	3.766	7	-0.029	.835	-3.638	-0.338	3.654	185	
.850	-0.013	.829	2.224	.501	2.280	13	-0.000	.822	-2.121	-0.483	2.175	193	
.900	.024	.811	1.194	.429	1.268	20	.034	.806	-1.329	-0.466	1.408	199	
.950	.071	.789	.455	.246	.517	28	.041	.784	-0.607	-0.296	.675	206	

TABLE 1.11

M = .850 F = 0 ALPHA = 0.00 KC = 1.41
 DELTA = 0.00 MC = .745
 C = 1.5 NC = .0358

X/C	CP +	M +	UPPERSIDE		DCP +	CP -	M -	LOWERSIDE	
			RE	IM				DCP -	RE
.010	.043	.829	2.731	0.0	0.0	.062	.820	-2.654	0.0
.050	-0.134	.916	1.814	0.0	0.0	-0.130	.914	-1.745	0.0
.100	-0.190	.938	1.451	0.0	0.0	-0.175	.936	-1.444	0.0
.200	-0.254	.976	1.449	0.0	0.0	-0.264	.981	-1.585	0.0
.300	-0.304	1.001	1.714	0.0	0.0	-0.317	1.008	-1.948	0.0
.400	-0.375	1.038	2.444	0.0	0.0	-0.344	1.043	-2.554	0.0
.450	-0.340	1.020	3.704	0.0	0.0	-0.362	1.031	-4.049	0.0
.500	-0.283	.990	4.794	0.0	0.0	-0.242	.990	-5.042	0.0
.550	-0.237	.967	1.837	0.0	0.0	-0.216	.967	-2.062	0.0
.600	-0.191	.944	1.984	0.0	0.0	-0.190	.943	-1.986	0.0
.650	-0.152	.925	2.257	0.0	0.0	-0.147	.922	-2.234	0.0
.700	-0.115	.906	2.654	0.0	0.0	-0.105	.901	-2.674	0.0
.725	-0.100	.899	3.094	0.0	0.0	-0.042	.890	-2.884	0.0
.750	-0.090	.894	4.660	0.0	0.0	.011	.845	-7.105	0.0
.775	-0.065	.882	4.049	0.0	0.0	-0.047	.873	-3.877	0.0
.800	-0.039	.869	2.884	0.0	0.0	-0.029	.864	-2.922	0.0
.850	0.000	.850	1.400	0.0	0.0	.007	.847	-1.680	0.0
.900	.017	.832	.944	0.0	0.0	.044	.829	-0.974	0.0
.950	.082	.810	.439	0.0	0.0	.047	.808	-0.401	0.0

TABLE 1.12

RUNNO 40906

M = .853 F = 30.0 ALPHA = 0
 P = 1.425 DELTA = .16
 RE = 2.40E6 K = .060 C = 1.10
 Q = 3302.42

RE IM RC IM
 KC = 1.119 -0.278 KC = .2887 .0284
 MC = .732 .029 MC = .0393 .0056

X/C	CP+	M+	UPPERSIDE				LOWERSIDE					
			RE	IM	MOD	ARG	RE	IM	MOD	ARG		
.010	.015	.845	.292	-1.137	1.174	-76	.104	.803	-0.340	1.212	1.258	106
.050	-0.156	.929	.153	-0.602	.621	-76	-0.107	.907	-0.373	.867	.944	113
.100	-0.220	.961	.343	-0.737	.813	-65	-0.166	.937	-0.507	.867	1.005	120
.200	-0.273	.988	.621	-0.843	1.047	-54	-0.244	.976	-0.828	.979	1.282	130
.300	-0.321	1.013	.998	-0.951	1.379	-44	-0.296	1.002	-1.155	.998	1.526	139
.400	-0.392	1.050	1.721	-1.059	2.021	-32	-0.354	1.033	-2.351	1.311	2.691	151
.450	-0.377	1.042	4.088	-1.770	4.454	-23	-0.329	1.019	-3.773	1.312	3.995	161
.500	-0.311	1.008	4.276	-0.332	4.289	-4	-0.265	.986	-2.161	.170	2.167	176
.550	-0.240	.972	1.884	.334	1.913	10	-0.221	.964	-2.149	.090	2.151	178
.600	-0.198	.951	1.975	.236	1.989	7	-0.174	.941	-2.265	.023	2.265	179
.650	-0.160	.932	2.193	.161	2.199	4	-0.133	.920	-2.466	-0.047	2.466	181
.700	-0.125	.914	2.384	-0.037	2.384	-1	-0.088	.898	-2.804	-0.114	2.807	182
.725	-0.106	.905	2.837	-0.000	2.837	-0	-0.068	.888	-3.028	-0.141	3.031	183
.750	-0.064	.884	5.195	.660	5.237	7	.020	.844	-5.510	1.582	5.733	164
.775	-0.080	.892	4.426	.483	4.453	6	-0.026	.867	-4.083	-0.228	4.089	183
.800	-0.052	.878	3.235	.578	3.286	10	-0.013	.860	-3.114	-0.300	3.128	185
.850	-0.007	.856	1.812	.363	1.847	11	.014	.847	-1.796	-0.164	1.804	185
.900	.034	.836	.955	.175	.971	10	.047	.831	-1.063	-0.177	1.077	189
.950	.082	.813	.360	.040	.362	6	.092	.810	-0.465	-0.081	.472	190

TABLE 1.13

RUNNO 40806

M = .854 F = 120.0 ALPHA = 0
 P = 10479 DELTA = .02
 RE = 2.41E6 K = .240 C = 1.05
 Q = 3320.06

RE IM RC IM
 KC = .797 -0.551 KC = .3814 .0651
 MC = .923 -0.147 MC = .0475 .0146

X/C	CP+	M+	UPPERSIDE				LOWERSIDE					
			RE	IM	MOD	ARG	RE	IM	MOD	ARG		
.010	.019	.844	-1.224	.262	1.252	-192	.094	.808	1.220	-0.280	1.251	347
.050	-0.152	.929	-0.851	.181	.875	-196	-0.114	.910	.908	-0.116	.913	353
.100	-0.214	.960	-0.891	.055	.893	-184	-0.169	.937	.989	.039	.990	2
.200	-0.267	.986	-1.213	-0.339	1.260	-164	-0.245	.975	1.116	.633	1.283	30
.300	-0.314	1.011	-1.354	-1.330	1.897	-136	-0.301	1.004	1.008	1.498	1.805	56
.400	-0.372	1.041	-0.325	-3.083	3.100	-96	-0.354	1.032	-0.250	3.063	3.073	95
.450	-0.367	1.038	1.399	-4.719	4.922	-73	-0.342	1.026	-1.513	4.335	4.592	109
.500	-0.330	1.019	3.214	-5.418	6.300	-59	-0.280	.993	-3.476	2.969	4.571	140
.550	-0.236	.971	3.841	-1.564	4.147	-22	-0.220	.963	-3.243	1.189	3.454	160
.600	-0.190	.948	3.538	-0.633	3.594	-10	-0.178	.942	-3.274	.679	3.343	168
.650	-0.156	.930	3.489	-0.367	3.508	-6	-0.136	.921	-3.374	.506	3.412	171
.700	-0.124	.915	3.485	-0.060	3.486	-1	-0.093	.899	-3.587	.185	3.591	177
.725	-0.102	.903	3.856	-0.016	3.856	-0	-0.074	.890	-3.860	.089	3.861	179
.750	-0.044	.875	7.724	.194	7.726	1	.021	.843	-7.010	-0.283	7.015	182
.775	-0.079	.893	5.129	.229	5.134	3	-0.031	.869	-4.597	-0.276	4.605	183
.800	-0.051	.879	3.946	.589	3.990	8	-0.018	.862	-3.637	-0.516	3.673	188
.850	-0.008	.857	2.246	.614	2.329	15	.012	.848	-2.116	-0.586	2.196	195
.900	.032	.838	1.232	.510	1.333	22	.046	.832	-1.260	-0.570	1.383	204
.950	.082	.814	.467	.261	.535	29	.086	.811	-0.526	-0.348	.629	214

TABLE 1.14

M = .875 F = 0 ALPHA = 0.00 KC = 1.57
 DELTA = 0.00 MC = 1.000
 C = 1.5 NC = .0336

X/C	UPPERSIDE				LOWERSIDE			
	CP +	M +	DCP +		CP -	M -	DCP -	
			RE	IM			RE	IM
.010	.069	.840	1.948	0.0	.088	.831	-1.948	0.0
.050	-.114	.933	1.317	0.0	-.109	.930	-1.337	0.0
.100	-.163	.958	.955	0.0	-.160	.957	-.993	0.0
.200	-.251	1.004	.897	0.0	-.256	1.007	-.974	0.0
.300	-.318	1.040	1.203	0.0	-.325	1.044	-1.298	0.0
.400	-.395	1.082	1.146	0.0	-.404	1.087	-1.260	0.0
.450	-.435	1.104	1.356	0.0	-.435	1.104	-1.585	0.0
.500	-.468	1.123	5.118	0.0	-.471	1.125	-5.290	0.0
.550	-.408	1.089	6.551	0.0	-.384	1.076	-6.761	0.0
.600	-.166	.960	7.640	0.0	-.163	.958	-7.888	0.0
.650	-.124	.938	5.882	0.0	-.119	.936	-5.233	0.0
.700	-.094	.923	2.311	0.0	-.081	.916	-2.406	0.0
.725	-.081	.916	2.483	0.0	-.062	.906	-2.406	0.0
.750	-.075	.913	4.106	0.0	.029	.860	-6.436	0.0
.775	-.051	.901	3.648	0.0	-.029	.890	-3.304	0.0
.800	-.028	.889	2.654	0.0	-.011	.881	-2.502	0.0
.850	.013	.868	1.508	0.0	.022	.864	-1.528	0.0
.900	.049	.850	.802	0.0	.058	.846	-.802	0.0
.950	.094	.828	.362	0.0	.100	.825	-.286	0.0

TABLE 1.15

RUNNO 40907

M = .877 F = 30.0 ALPHA = 0
 P0 = 10425 DELTA = .15
 RE = 2.43E6 K = .039 C = 1.13
 Q = 3403.23

KC = 1.166 RE IM RC = 2.719 IM X5 = 1.375E-3 0
 MC = .866 -0.063 NC = .8364 .8101 X6 = 1.395E-3 0

X/C	UPPERSIDE				LOWERSIDE							
	CP+	M+	DCP+		CP-	M-	DCP-					
			RE	IM	MOD	ARG	RE	IM	MOD	ARG		
.010	.048	.851	.071	0.024	.827	-85	.127	.815	-0.084	.889	.893	95
.050	-0.130	.942	.015	-0.425	.426	-88	-0.091	.926	-0.123	.639	.651	101
.100	-0.195	.976	.117	-0.464	.479	-76	-0.151	.957	-0.224	.671	.707	108
.200	-0.263	1.011	.206	-0.516	.556	-68	-0.242	1.004	-0.380	.748	.839	117
.300	-0.334	1.050	.355	-0.778	.855	-65	-0.308	1.040	-0.522	.821	.973	122
.400	-0.406	1.089	.521	-0.832	.981	-58	-0.386	1.083	-0.695	.898	1.135	128
.450	-0.450	1.114	.656	-0.857	1.080	-53	-0.426	1.105	-0.965	.938	1.368	136
.500	-0.476	1.129	1.210	-1.040	1.596	-41	-0.364	1.071	-5.728	3.401	6.661	149
.550	-0.351	1.059	7.760	-5.047	9.257	-33	-0.291	1.031	-7.755	4.112	8.777	152
.600	-0.262	1.011	7.810	-3.794	8.683	-26	-0.178	.971	-4.027	.672	4.028	179
.650	-0.154	.955	3.871	.199	3.876	3	-0.114	.937	-2.142	-0.792	2.283	200
.700	-0.100	.927	2.265	.567	2.335	14	-0.071	.915	-2.433	-0.657	2.520	195
.725	-0.082	.917	2.560	.660	2.629	13	-0.050	.905	-2.780	-0.561	2.836	191
.750	-0.048	.900	4.891	1.172	5.029	13	.036	.861	-5.451	.965	5.536	170
.775	-0.063	.908	4.125	1.888	4.246	14	-0.089	.884	-3.889	-0.438	3.939	189
.800	-0.035	.894	3.046	.947	3.198	17	.083	.878	-2.964	-0.688	3.028	192
.850	.007	.872	1.586	.898	1.706	19	.020	.864	-1.784	-0.348	1.738	182
.900	.048	.851	.883	.384	.938	19	.062	.848	-0.958	-0.294	1.042	187
.950	.064	.828	.384	.168	.378	16	.166	.827	-0.128	-.413	.413	187

TABLE 1.16

RUNNO 40807

M = .879 F = 120.0 ALPHA = 0
 P0 = 10474 DELTA = .01
 RE = 2.44E6 K = .234 C = 1.08
 Q = 3426.23

KC = .579 IM = -0.479 RC = .3998 IM = .0592
 MC = .757 -0.327 NC = .0552 IM = .0148

X/C	CP+	M+	UPPERSIDE				DCP+	CP-	M-	LOWERSIDE			
			RE	IM	RC	IM				DCP-	DCP-	RC	IM
.010	.052	.852	-0.375	.422	.564	-229	.118	.82	.393	-1.441	.591	312	
.050	-0.129	.945	-0.146	.213	.258	-236	-0.096	.928	.270	-0.308	.410	311	
.100	-0.194	.979	-0.176	.213	.276	-230	-0.152	.958	.284	-1.312	.421	312	
.200	-0.262	1.015	-0.216	.192	.289	-222	-0.243	1.006	.415	-0.312	.519	323	
.300	-0.330	1.051	-0.336	.231	.408	-214	-0.311	1.042	.683	-0.228	.720	342	
.400	-0.406	1.093	-0.669	.187	.695	-196	-0.385	1.083	.858	-0.087	.862	354	
.450	-0.445	1.115	-0.795	.078	.799	-186	-0.424	1.104	1.211	.33	1.255	15	
.500	-0.467	1.128	-1.389	-0.752	1.579	-152	-0.363	1.071	3.179	4.753	5.718	56	
.550	-0.356	1.065	-3.250	-6.962	7.683	-115	-0.292	1.032	.977	7.526	7.550	86	
.600	-0.244	1.005	1.224	-7.095	7.200	-80	-0.193	.979	-3.824	4.949	6.254	128	
.650	-0.148	.955	4.090	-2.598	4.846	-32	-0.118	.940	-4.577	1.605	4.850	161	
.700	-0.103	.931	4.239	-0.825	4.318	-11	-0.073	.917	-4.569	.480	4.594	174	
.725	-0.083	.921	4.625	-0.489	4.651	-6	-0.054	.907	-4.564	.271	4.572	177	
.750	-0.025	.891	8.368	-0.211	8.371	-1	.038	.860	-7.141	.059	7.141	180	
.775	-0.064	.911	5.768	-0.015	5.768	-0	-0.013	.886	-5.277	-0.203	5.281	182	
.800	-0.037	.898	4.482	.472	4.506	6	-0.000	.880	-4.239	-0.463	4.264	186	
.850	.005	.876	2.628	.571	2.690	12	.026	.866	-2.490	-0.631	2.569	194	
.900	.045	.856	1.391	.496	1.477	20	.060	.849	-1.480	-0.626	1.607	203	
.950	.092	.832	.534	.269	.598	27	.101	.829	-0.657	-0.398	.768	211	

TABLE 1.17

M = .960 F = 0 ALPHA = 0.00 KC = .07
 DELTA = 0.00 MC = -.183
 C = 1.5 NC = -.0219

X/C	CP +	M +	UPPERSIDE				CP -	M -	LOWERSIDE			
			RE	IM	RC	IM			DCP -	DCP -	RC	IM
.010	.178	.861	.038	0.0	.217	.839	-.152	0.0				
.050	-.007	.964	0.000	0.0	.013	.953	-.114	0.0				
.100	-.034	.982	-.038	0.0	-.032	.978	-.114	0.0				
.200	-.175	1.062	-.010	0.0	-.127	1.033	-.133	0.0				
.300	-.219	1.089	-.057	0.0	-.219	1.049	-.114	0.0				
.400	-.305	1.147	-.057	0.0	-.304	1.141	-.133	0.0				
.450	-.346	1.168	-.034	0.0	-.342	1.146	-.133	0.0				
.500	-.381	1.191	-.076	0.0	-.378	1.189	-.152	0.0				
.550	-.405	1.207	-.057	0.0	-.407	1.208	-.133	0.0				
.600	-.421	1.218	-.057	0.0	-.425	1.220	-.133	0.0				
.650	-.435	1.227	-.038	0.0	-.439	1.230	-.152	0.0				
.700	-.447	1.235	-.038	0.0	-.450	1.237	-.152	0.0				
.725	-.448	1.236	-.057	0.0	-.456	1.242	-.171	0.0				
.750	-.486	1.267	.744	0.0	-.743	1.193	-1.967	0.0				
.775	-.471	1.252	3.094	0.0	-.442	1.232	-3.266	0.0				
.800	-.463	1.246	2.540	0.0	-.442	1.232	-3.189	0.0				
.850	-.212	1.084	.038	0.0	-.378	1.186	-2.081	0.0				
.900	-.013	.967	.955	0.0	-.058	.993	.802	0.0				
.950	.070	.921	1.146	0.0	.053	.930	.210	0.0				

TABLE 1.18

RUNNO 40911

M = .966 F = 30.0 ALPHA = 0
 PO = 10472 DELTA = .18
 RE = 2.53E6 K = .054 C = 1.03
 Q = 3759.58

KC = .173 .083 RC = .1510 .0932
 MC = .178 .108 NC = .0104 .0203

X/C	CP+	M+	UPPERSIDE				LOWERSIDE					
			RE	IM	MOD	ARG	RE	IM	MOD	ARG		
.010	.171	.870	.016	-.024	.029	-56	.229	.838	-0.038	.034	.081	138
.050	-0.013	.973	.004	-.019	.019	-78	.014	.959	-0.027	.017	.032	149
.100	-0.061	1.001	.003	-.014	.014	-79	-0.037	.988	-0.018	.008	.019	157
.200	-0.125	1.039	-0.020	.005	.021	-195	-0.135	1.046	-0.014	-0.005	.015	200
.300	-0.236	1.106	.003	-0.005	.006	-59	-0.226	1.102	-0.010	.008	.020	165
.400	-0.313	1.155	.013	-0.019	.023	-55	-0.305	1.151	-0.011	.012	.016	132
.450	-0.354	1.181	.017	-0.024	.029	-54	-0.348	1.179	-0.040	.020	.044	154
.500	-0.388	1.204	.017	-0.015	.023	-40	-0.376	1.197	-0.025	.028	.038	131
.550	-0.412	1.220	.025	-0.023	.034	-42	-0.404	1.216	-0.038	.061	.030	179
.600	-0.430	1.232	.023	-0.019	.030	-40	-0.422	1.228	-0.036	.019	.041	152
.650	-0.448	1.245	.002	-0.010	.011	-80	-0.437	1.239	-0.033	.035	.048	133
.700	-0.466	1.253	.013	-0.023	.027	-61	-0.447	1.245	-0.049	.017	.051	161
.725	-0.465	1.257	.026	-0.029	.038	-49	-0.452	1.249	-0.064	.025	.064	176
.750	-0.456	1.250	1.498	-0.185	1.509	-7	-0.420	1.227	-1.931	.729	2.064	159
.775	-0.488	1.273	4.594	.297	4.604	4	-0.418	1.226	-4.674	-0.557	4.787	187
.800	-0.476	1.264	3.822	.419	3.845	6	-0.416	1.225	-4.717	-0.659	4.762	188
.850	-0.169	1.065	-2.897	1.024	3.072	-199	-0.246	1.114	.300	-2.852	2.073	278
.900	-0.012	.973	.833	.903	1.158	44	-0.023	.980	.469	-0.785	1.031	310
.950	.057	.934	1.367	.000	1.367	0	.063	.931	.688	-0.135	.788	311

NACA 64A006 AIRFOIL

$\alpha_m = 0$ $\delta_m = 0$

EXP. \bullet UPPER SURFACE \circ LOWER SURFACE AMPLITUDE 1° DEG

— THIN-AIRFOIL THEORY

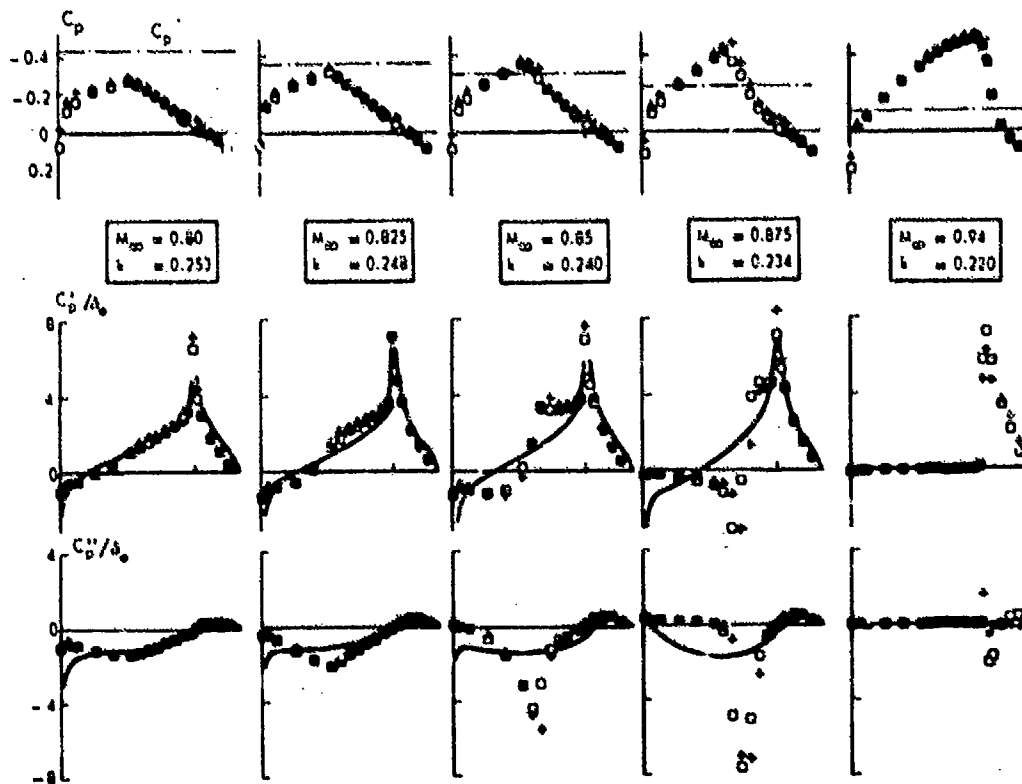


Fig. 1.1 Development of mean steady and unsteady pressure distributions with Mach number ($f = 120$ Hz)

NACA 64 A 006 AIRFOIL
 ○ EXPERIMENT
 — THIN-AIRFOIL THEORY

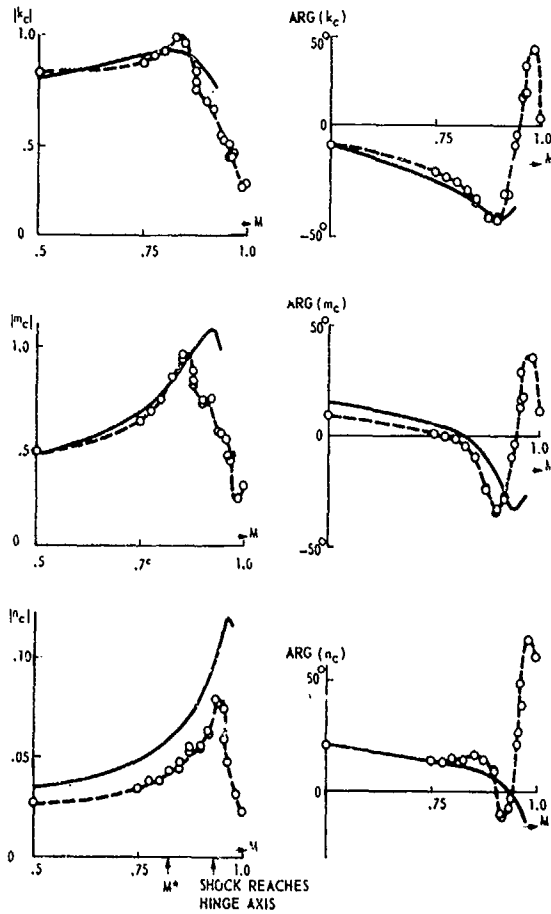


Fig. 1.2 Unsteady aerodynamic coefficients as a function of Mach number ($f = 120$ Hz)

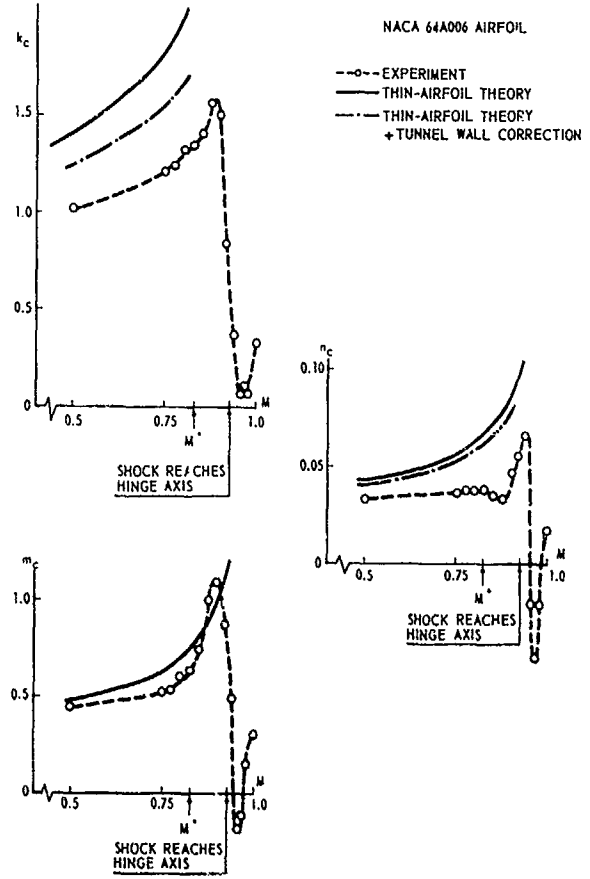


Fig. 1.3 Steady aerodynamic derivatives as a function of Mach number

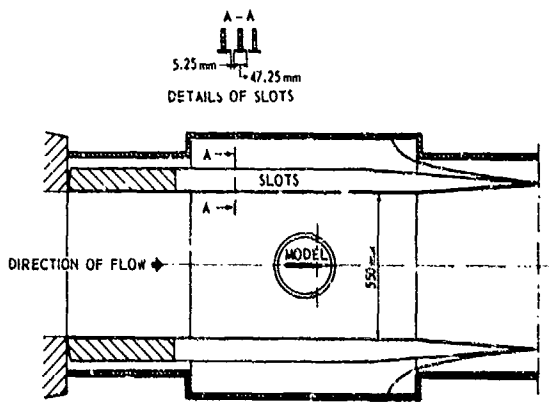


Fig. 1.4 Transonic test section of the NLR Pilot Tunnel

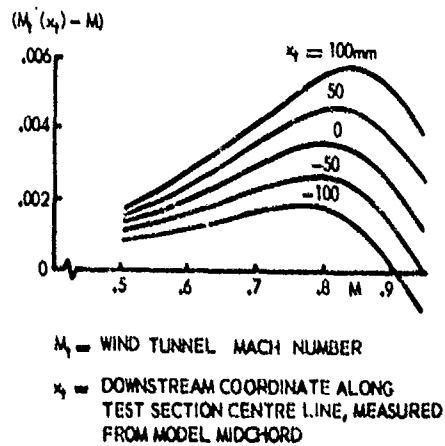


Fig. 1.5 Mach number distribution in NLR Pilot Tunnel test section

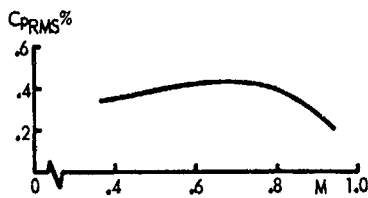


Fig. 1.6 Noise level in NLR Pilot Tunnel test section

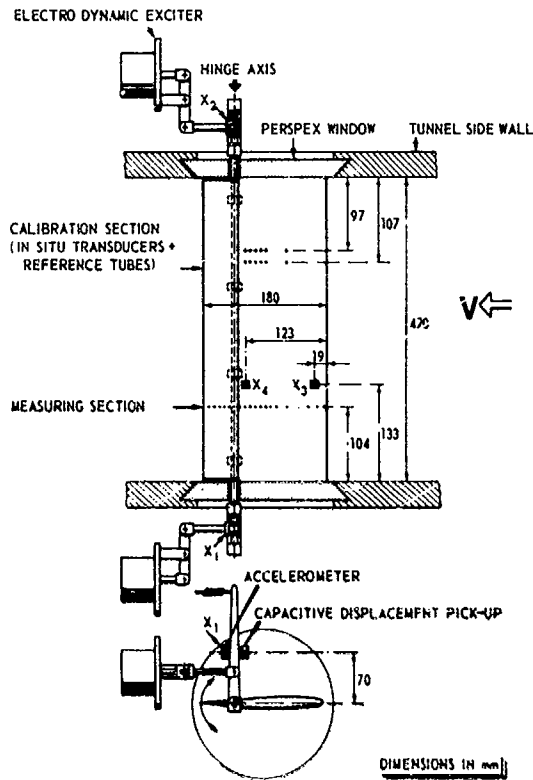
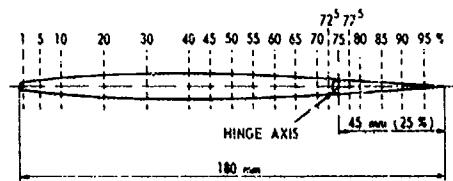


Fig. 1.7 Test set-up and instrumentation of the NACA 64A006 airfoil with flap



MEASURING SECTION (BOTH UPPER AND LOWER SURFACE)	
No. 1	x/c = .01
2	.05
3	.10
4	.20
5	.30
6	.40
7	.45
8	.50
9	.55
10	.60

CALIBRATION SECTION (UPPER SURFACE ONLY)	
No. 1	x/c = .30
2	.50
3	.55
4	.60
5	.65
6	.70

Fig. 1.8 Location of pressure orifices on the NACA 64A006 airfoil with flap

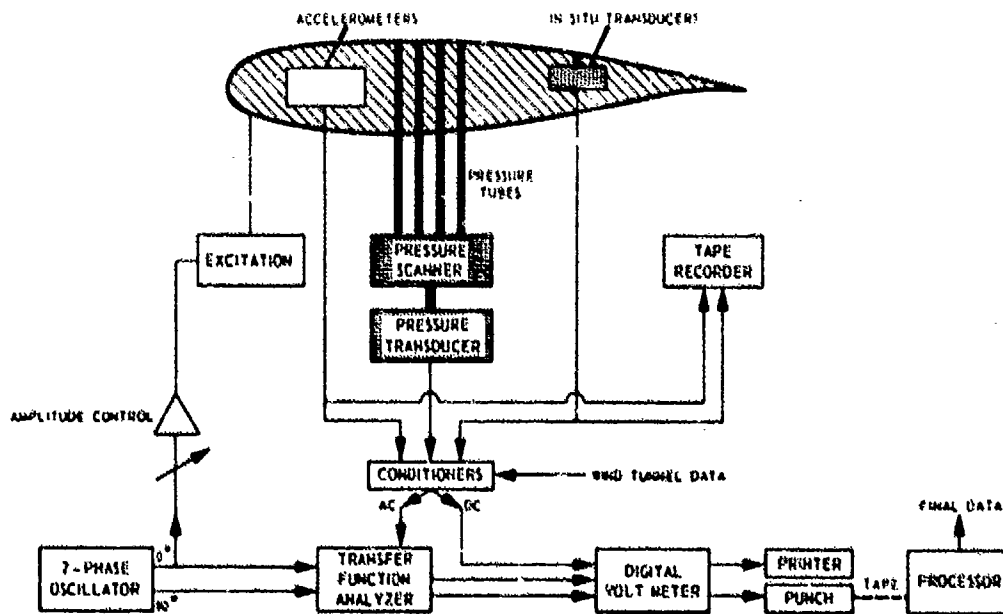


Fig. 1.9 Block diagram of measuring equipment

DATA SET 2

NACA 64A010 (NASA AMES MODEL) OSCILLATORY PITCHING

by

Sanford S. Davis, NASA Ames

INTRODUCTION AND DISCUSSION

The test program on the oscillating NACA 64A010 airfoil was designed to expand the existing unsteady aerodynamic test envelope to a higher Reynolds number and more diverse flow conditions. The data base for this airfoil, as reported in Ref. 2.1, contains 114 different combinations of Mach number, Reynolds number, mean angle of attack, oscillation frequency, and motion mode. A subset of 66 runs corresponds to the motion of pitching about a nominal axis at 0.25c. The purpose of this Data Set is to present the matrix of test conditions corresponding to these 66 runs, to tabulate numerical data belonging to the ten AGARD CT Cases supplemented by a shock-stall case (SSC) of special interest, and to present an overview of certain parametric variations of the data. The data should be useful in ascertaining the performance of those numerical codes that predict unsteady transonic flows with shock-wave boundary-layer interactions.

Each combination of motion mode and the five input parameters M , α_m , Re , α_0 , and k are identified with a unique number - the dynamic index (DI). The output was the measured instantaneous chordwise pressure distribution on the airfoil. These data were digitized and processed on-line (Ref. 2.2) into a form that was suitable for interpretation and analysis. Subsequent off-line processing converted the data into the conventional normalized quantities presented in this Data Set. The notation generally follows that advocated as the AGARD standard. The nomenclature used here and an explanation of the table headings are included in Section 12 of this Data Set.

The following processed data are included for each of the AGARD CT Cases:

- A. Steady upper and lower surface pressure distributions.
- B. Fundamental frequency upper and lower surface pressure distributions.
- C. Steady lift and moment coefficients.
- D. Fundamental frequency lift and moment coefficients.

The following detailed data are presented for AGARD CT Case 6 only:

- E. Instantaneous upper surface pressure distribution.
- F. Instantaneous lift and moment coefficients.

Some of the data have been presented and/or discussed in previous publications. Items A, B, C, and D were included in the tabulated and graphical data of Ref. 2.1. The data were compared among themselves and with theory in Refs. 2.3 to 2.6.

Table 2.1 presents a complete list of the entire test program in chronological order. Table 2.2 shows the subset of 66 DI's considered in this Data Set. A small subset of 10 DI's, designated in Ref. 2.7 as AGARD CT Cases and the extra shock-stall case (SSC), are identified in Table 2.3 along with the relevant flow parameters. A sketch of the oscillating airfoil test apparatus is shown in Fig. 2.1. The experimental arrangement is described in detail in Refs. 2.1 and 2.8.

Tabulated data for the AGARD CT Cases and the SSC are presented in varying detail in Tables 2.4 to 2.18. Table 2.4 shows the steady values and the fundamental frequency complex amplitudes of lift and moment. (Note that the real and imaginary parts of the complex numbers in Table 2.4 are identical to the single- and double-primed quantities in the standard AGARD notation.) The mean and fundamental frequency pressure distributions are tabulated in Tables 2.5 to 2.14 and 2.17. These data are taken directly from the microfiche records enclosed in Ref. 2.1. A more basic data set, representing the instantaneous load on the airfoil, is presented in Table 2.15 for CT Case 6. Along with these data, the fundamental frequency component of the lift and moment is included for comparison and reference. The most detailed data set, from which all the previous data were derived, is the instantaneous pressure distribution. These data are presented in Table 2.16 in the form of chordwise pressure distributions at 6° phase increments for CT Case 6. The value of phase shown at the head of each column may be correlated with the nondimensional time, or the load, by cross-checking with Table 2.15.

With these AGARD CT data, one should be able to verify in detail the predictive capability of all inviscid codes and those viscous codes that include mild shock-wave/boundary-layer interactions. In Ref. 2.6 CT Case 6 was thoroughly analyzed and, being selected for priority analysis in Ref. 2.7, should be the first transonic case to compute.

Some of the first harmonic data were investigated for parametric trends. These data are presented in graphical form in Figs. 2.2 to 2.5. Fig. 2.2 shows the effect of varying Mach number with other parameters held constant. As the steady shock wave develops (uppermost row), the unsteady pressure distribution evolves into the peaked distribution usually associated with transonic flow. Although the unsteady pressure drops at $M = 0.84$, compared to $M = 0.80$, one should not consider this to be a typical response with increasing velocity in the transonic speed range. The data in Fig. 2.2 are presented at a reduced frequency $k = 0.2$, which is high enough to reduce the shock motion considerably. The interaction

between frequency and shock strength may be such that this dramatic drop in peak loading would not occur at lower values of k . Unfortunately, data at other frequencies were not measured at $M = 0.84$ so cross-trends cannot be determined experimentally.

Figure 2.3 shows the effect of varying the oscillation amplitude with other parameters held constant. Following the conventional notation, the pressure data (output) is normalized by the oscillation amplitude (input) to indicate the linearity of the response. Data presented in Ref. 2.4 showed that the force coefficients were linear functions of α_0 , but the individual pressure data do not seem to follow this trend. The shock-wave excursions, being minimal at lower oscillation amplitudes, induce peaked unsteady pressure distributions. However, at higher oscillation amplitudes the increased shock motion affects a larger portion of the airfoil. The net result is a balance in the loads even though the individual distributions vary. It is expected that this trend holds at other oscillation frequencies.

Figure 2.4 shows the frequency variation with other parameters held constant. As reported in Ref. 2.4, the pressure peaks and leading edge loading all decrease with increasing frequency. The trend is smoothly varying for this transonic flow condition, but this may not hold true for other conditions, such as shock-induced separation. For further discussions, refer to Refs. 2.3 and 2.5.

Figure 2.5 shows that scale effect is quite minimal for this flow condition. Sublimation photographs indicate that transition occurs at the shock wave at $Re = 3.3 \times 10^6$, while leading edge transition was observed at $Re = 12.6 \times 10^6$. Even though the point of transition varies widely, the unsteady pressure distributions are similar over the entire Reynolds number range. This benign behavior should not be considered a general rule; airfoil geometry and other mean flow conditions may be important factors (see Ref. 2.5).

The complete unsteady pressure distribution is shown in Fig. 2.6 for CT Cases 4 and 6. Certain features are common at both low and high frequencies: pure sinusoidal motion upstream of the shock wave, severe harmonic distortion at the shock, and minimal response towards the trailing edge region. The distorted wave forms in the shock region are caused by the frequency-dependent shock motion. These pressure data can be considered typical of that induced by unseparated, transonic flow over an oscillating airfoil. Although harmonic distortion is evident over part of the airfoil, the forces and moments are almost pure sinusoids.

ADDENDUM - A SHOCK-STALL CASE (SSC)

The AGARD CT Cases for this configuration refer to mean flows without separation. A more severe challenge to computational methods is the case where the airfoil pitches about a steady flow condition that supports a stronger shock wave. Some data from DI 89, a case not included in the AGARD Series but specified in Table 2.3, is presented for analysis and computational verification.

The fundamental frequency and steady pressure distributions are tabulated in Table 2.17 and the instantaneous pressure distribution in Table 2.18. Figure 2.7 depicts the complete unsteady pressure distribution on the upper surface at two frequencies. There is much more harmonic distortion, and the contrast with Fig. 2.6 is striking. The low frequency data at the shock wave in Fig. 2.7 are 180° out of phase when compared with CT Case 4 in Fig. 2.6, and a strong unsteady response persists to the trailing edge. Unlike the unseparated flows of the CT Cases, these complex flows require full Navier-Stokes modeling to predict both the steady shock wave position and the subsequent time-dependent motion.

1 AIRFOIL	
1.1 Designation	NACA 64A010 (NASA Ames Model)
1.2 Type of airfoil	Conventional - Laminar Flow
1.3 Geometry	Refer to Ref. 2.8 for theoretical profile
1.4 Design condition	
1.5 Additional remarks	
1.6 References on airfoil	Ref. 2.8
2 MODEL GEOMETRY	
2.1 Chord length	0.50 m (19.685 in.)
2.2 Span	1.35 m (53.2 in.)
2.3 Actual model coordinates and accuracy of measurement	Refer to AGARD-AR-156 (Ref. 2.7)
2.4 Flap: hinge and gap details	None
2.5 Additional remarks	Model mounted between splitter plates - see Fig. 2.1
2.6 References on model	Refs. 2.1, 2.2, and 2.9
3 WIND TUNNEL	
3.1 Designation	NASA Ames 11- X 11-Foot Transonic Wind Tunnel
3.2 Type of tunnel	Closed return, variable density
3.3 Test section dimensions	3.35 X 3.35 X 6.7 m (11 X 11 X 22 ft.)
3.4 Type of roof and floor	Baffled slot

3	WIND TUNNEL (Continued)	
3.5	Type of side walls	Same as 3.4
3.6	Ventilation geometry	1.78 cm (0.7 in.) slots, 24.4 cm (9.63 in.) slats. Open area ratio ~ 8% between splitters
3.7	Thickness of side wall boundary layer	Very thin due to splitters
3.8	Thickness of boundary layers at roof and floor	Approx. 7.6 cm (3 in.)
3.9	Method of measuring Mach number	Static taps on splitters, see Refs. 2.2 and 2.9
3.10	Uniformity of Mach number over test section	± 0.002
3.11	Sources of levels of noise or turbulence in empty tunnel	Not investigated
3.12	Tunnel resonances	None noted
3.13	Additional remarks	
3.14	References on tunnel	Ref. 2.2 and 2.9
4	MODEL MOTION	
4.1	Mode of applied motion	Pitching nominally about 0.25c and 0.50c, also plunging
4.2	Range of amplitude	$\pm 0-2$ deg; ± 1 cm
4.3	Range of frequency	0-60 Hz
4.4	Method of application	Four graphite epoxy push-pull rods with differential motion of forward and aft pair, Fig. 2.1
4.5	Purity of applied motion	Pure sinusoids
4.6	Natural frequencies and normal modes of model	Lowest mode: torsion at 60 Hz
4.7	Static or dynamic elastic distortion during tests	Not measured
4.8	Additional remarks	
5	TEST CONDITIONS	
5.1	Tunnel height/model chord ratio	3.35 m/0.50 m = 6.7
5.2	Tunnel width/model chord ratio	1.35 m/0.50 m = 2.7 (between splitter plates)
5.3	Range of Mach number	0.5-0.85
5.4	Range of tunnel total pressure	50 kN/m ² - 225 kN/m ² (0.5-2.25 ATM)
5.5	Range of tunnel total temperature	290 K - 320 K
5.6	Range of model steady, or mean, incidence	0-4 deg
5.7	Definition of model incidence	Chord line relative to wind tunnel
5.8	Position of transition, if free	Limited transition studies were attempted using a sublimating material. At $M = 0.5$, $\alpha = 0$, irregular patterns were observed without a definitive transi- tion point. At $M = 0.8$, $\alpha = 0$, $Re = 12.6 \times 10^6$ transition was observed at $x/c = 0.05$. At $M = 0.8$, $\alpha = 0$, $Re = 3.4 \times 10^6$ transition was observed at $x/c = 0.5$ (the shock wave).
5.9	Position and type of trip, if transition fixed	
5.10	For mixed flow, position of sonic boundary in relation to roof and floor	Not measured
5.11	Flow instabilities during tests	--
5.12	Additional remarks	--
5.13	References describing tests	--
6	MEASUREMENTS AND OBSERVATIONS	
6.1	Steady pressures for the mean conditions	/
6.2	Steady pressures for small changes from the mean conditions	-
6.3	Quasi-steady pressures	-
6.4	Unsteady pressures	/

6	MEASUREMENTS AND OBSERVATIONS (Continued)		
6.5	Steady forces for the mean conditions	measured directly	—
		integrated pressures	✓
6.6	Steady forces for small changes from the mean conditions	measured directly	—
		integrated pressures	—
6.7	Quasi-steady forces	measured directly	—
		integrated pressures	—
6.8	Unsteady forces	measured directly	—
		integrated pressures	✓
6.9	Measurement of actual motion at points on model		✓
6.10	Observation or measurement of boundary layer properties		limited
6.11	Visualization of surface flow		✓
6.12	Visualization of shockwave movements		—
6.13	Additional remarks		—
7	INSTRUMENTATION		
7.1	Steady pressures		
7.1.1	Position of orifices spanwise and chordwise	Mid-span, 20 upper, 20 lower; see Table 2.5 for locations	
7.1.2	Type of measuring system	Pneumatic	
7.2	Unsteady pressures		
7.2.1	Position of orifices spanwise and chordwise	Mid-span, 20 upper, 20 lower, see Table 2.5 for locations	
7.2.2	Diameter of orifices	1.02 mm (0.040 in.)	
7.2.3	Type of measuring system	Strain-gauge-type miniature pressure transducers installed close to orifice with minimum cavities.	
7.2.4	Type of transducers	Kulite model XCQL-7A-093.	
7.2.5	Principle and accuracy of calibration	On-line calibrations. Up to 2% change in static sensitivity before and after run allowed	
7.3	Model motion		
7.3.1	Method of measurement	Motion of four push-pull rods with LVDT (reactive-type) transducers. Phase synchronism checked with wing-mounted accelerometers	
7.3.2	Accuracy	~ 1%	
7.4	Processing of unsteady measurements		
7.4.1	Method of acquiring and processing measurements	Real-time digitization with on-line calibration and diagnostics. Signal averaging over about 100 cycles to suppress random noise (if present). Variable sampling time adjusted to yield 60 data points per cycle.	
7.4.2	Type of analysis	On-line processing for frequency content of pressure distributions and comparisons with linear theory and other data.	
7.4.3	Unsteady pressure quantities obtained and accuracies achieved	Signal-averaged (essentially instantaneous) pressured distributions. Harmonic analysis of pressure distributions.	
7.4.4	Method of integration to obtain forces	Numerical quadratures (see Appendix A of Ref. 2.1)	
7.5	Additional remarks		
7.6	References on techniques	Ref. 2.2	
8	DATA PRESENTATION		
8.1	Test cases for which data could be made available	Tables 2.1 and 2.2	
8.2	Test cases for which data are included in this document	Table 2.3	
8.3	Steady pressures	Tables 2.5 to 2.14 and 2.17	
8.4	Quasi-steady or steady perturbation pressures	N/A	
8.5	Unsteady pressures	Tables 2.5 to 2.14 and 2.16 to 2.18	
8.6	Steady forces or moments	None	

- 8 DATA PRESENTATION (Continued)
- 8.7 Quasi-steady or steady perturbation forces N/A
- 8.8 Unsteady forces and moments Tables 2.4 and 2.15
- 8.9 Other forms in which data could be made available if required Magnetic tape
- 8.10 References giving other presentations of data Refs. 2.1 to 2.6
- 9 COMMENTS ON DATA
- 9.1 Accuracy
- 9.1.1 Mach number ± 0.002
- 9.1.2 Steady incidence ± 0.05 deg.
- 9.1.3 Reduced frequency ± 0.005
- 9.1.4 Steady pressure coefficients 1%
- 9.1.5 Steady pressure derivatives N/A
- 9.1.6 Unsteady pressure coefficients 2%
- 9.2 Sensitivity to small changes of parameter No evidence of undue sensitivity, see Figs. 2.2 to 2.5
- 9.3 Spanwise variations Probably small
- 9.4 Nonlinearities Depends on data set
- 9.5 Influence of tunnel total pressure Minimal on model distortion
- 9.6 Wall interference corrections No corrections made
- 9.7 Other relevant tests on *same model* None
- 9.8 Relevant tests on other models of nominally the *same* aerofoil. None
- 9.9 Any remarks relevant to comparison between experiment and theory Ref. 2.4, 2.6
- 9.10 Additional remarks
- 9.11 References on discussion of data Refs. 2.1 to 2.6
- 10 PERSONAL CONTACT FOR FURTHER INFORMATION
- Sanford Davis, Aerodynamics Division, NASA Ames Research Center, Moffett Field, CA 94035
- 11 REFERENCES
- 2.1 S. Davis and G. Malcolm Experimental Unsteady Aerodynamics of Conventional and Supercritical Airfoils. NASA TM-81221, Aug. 1980.
- 2.2 S. Davis Computer/Experiment Integration for Unsteady Aerodynamic Research. Intl. Congress on Instrumentation in Aerospace Simulation Facilities, ICIAS '79 Record, Sept. 1979, pp. 237-250.
- 2.3 S. Davis and G. Malcolm Unsteady Aerodynamics of Conventional and Supercritical Airfoils. AIAA Paper 80-734, Seattle, WA, May 1980.
- 2.4 S. Davis and G. Malcolm Transonic Shock-Wave/Boundary-Layer Interactions on an Oscillating Airfoil. AIAA Journal, Vol. 18, No. 11, Nov. 1980, pp. 1306-1312.
- 2.5 S. Davis Experimental Studies of Scale Effects on Oscillating Airfoils at Transonic Speeds. AGARD-CP-296, Feb. 1981, pp. 9-1 to 9-6.
- 2.6 W. Chyu, S. Davis and K. S. Chang Calculation of Unsteady Transonic Flow over an Airfoil. AIAA Journal, Vol. 19, No. 6, June 1981, pp. 684-690.
- 2.7 S. R. Bland AGARD Two-Dimensional Aeroelastic Configurations. AGARD-AR-156, Aug. 1979.
- 2.8 I. Abbott, and A. Von Doenhoff Theory of Wing Sections. Dover Pub., New York, 1959.
- 2.9 G. Malcolm and S. Davis New NASA-Ames Wind Tunnel Techniques for Studying Airplane Spin and Two-Dimensional Unsteady Aerodynamics. In Dynamic Stability Parameters. AGARD CP-235, Nov. 1978, pp. 3-1 to 3-12.

12 NOTATION AND EXPLANATION OF TABLES*

GENERAL NOTATION

C, c	chord of airfoil, m
DI	dynamic index, data identification number
f, FREQ	frequency, Hz
k, K	reduced (nondimensional) frequency, $\frac{\omega c}{2V}$
M	free-stream Mach number
Re, RE	Reynolds number (based on chord)
t	time, s
V	free-stream velocity, m/s
X, x	distance along airfoil, m
x_α/c	pitch axis position relative to leading edge
$\alpha(t)$	Instantaneous incidence, $\deg(\alpha_m + \alpha_o \cos \omega t)$
α_m	mean incidence, deg
α_o	oscillatory pitch amplitude, deg
ω	radian frequency, rad/s ($=2\pi f$)

TABLE 2.4

C_L	steady lift, +ve up [c_L]
C_M	steady moment, +ve nose up about 0.25c [c_m]
$C_{L,\alpha}$	normalized complex amplitude of lift coefficient, +ve up, per radian [$c'_L/\alpha_o + ic''_L/\alpha_o$]
$C_{M,\alpha}$	normalized complex amplitude of moment coefficient, +ve noseup, about 0.25c, per radian [$c'_m/\alpha_o + ic''_m/\alpha_o$]

TABLES 2.5 to 2.14 and 2.17

ALPHA	mean incidence, deg [α_m]
PTOT	total pressure, N/m^2 [P_t]
PINF	static pressure, N/m^2 [P_∞]
QINF	dynamic pressure, N/m^2 [q]
CPU(CPL)	steady upper (lower) surface pressure coefficient [c_p]
CPU,A (CPL,A)	normalized complex amplitude of upper (lower) surface fundamental frequency pressure coefficient, per radian [$c'_p/\alpha_o + ic''_p/\alpha_o$]

TABLE 2.15

TAU	nondimensional time [$\tau = 2Vt/c$]
WT	phase angle re $\alpha(t)_{\max}$ [ωt]
ALPHA	oscillatory incidence [$\alpha_o \cos \omega t$]
CL UP	upper surface contribution to c_L
CL LO	lower surface contribution to c_L
CL	instantaneous lift coefficient [$c_L(t)$]
CLN=1	instantaneous value of fundamental frequency component of lift coefficient
CM UP	upper surface contribution to c_m
CM LO	lower surface contribution to c_m
CM	instantaneous moment coefficient, +re noseup, about 0.25c [$c_m(t)$]
CMN=1	instantaneous value of fundamental frequency component of moment coefficient

TABLES 2.16, 2.18

PHASE	phase angle re $\alpha(t)_{\max}$ [ωt]
ALPHA	oscillatory incidence [$\alpha_o \cos(\omega t)$]
CP	instantaneous pressure coefficient [$c_p(t)$]

* Square-bracketed quantities indicate standard AGARD notation.

TABLE 2.1. DATA BASE FOR NACA 64A010 AIRFOIL

DI	M	α , deg	$Re \times 10^{-6}$	Motion	f, Hz	k
1	0.489	0.03	2.51	Plunging 0.35 cm (0.137 in.)	5.0	0.048
2	.489	.01	2.50	Pitching 0.94 deg about $x_{\alpha}/c = 0.236$	20.8	.200
3	.488	.00	2.50	Pitching .95 deg about $x_{\alpha}/c = .512$	20.8	.200
4	.489	.01	2.31	Plunging 1.01 cm (0.396 in.)	20.8	.200
5	.490	-.01	2.52	Pitching .96 deg about $x_{\alpha}/c = .507$	26.0	.249
6	.490	-.01	2.52	Pitching .96 deg about $x_{\alpha}/c = .238$	15.7	.151
7	.490	-.01	2.52	Pitching .96 deg about $x_{\alpha}/c = .233$	10.4	.100
8	.490	-.01	2.52	Pitching .97 deg about $x_{\alpha}/c = .230$	5.2	.050
9	.490	-.01	2.52	Pitching 1.01 deg about $x_{\alpha}/c = .224$	2.6	.025
10	.490	-.01	2.52	Pitching 1.98 deg about $x_{\alpha}/c = .249$	5.2	.050
11	.489	.00	2.51	Pitching 1.45 deg about $x_{\alpha}/c = .250$	20.8	.200
12	.802	.00	3.38	Pitching .94 deg about $x_{\alpha}/c = .232$	33.2	.200
13	.802	.00	3.38	Pitching 1.27 deg about $x_{\alpha}/c = .431$	33.2	.200
14	.797	-.06	3.39	Plunging .89 cm (0.349 in.)	33.1	.201
15	.797	-.06	3.39	Pitching .95 deg about $x_{\alpha}/c = .234$	41.3	.250
16	.795	.01	6.67	Pitching .96 deg about $x_{\alpha}/c = .252$	33.3	.201
17	.795	.01	6.67	Pitching .98 deg about $x_{\alpha}/c = .501$	33.3	.201
18	.795	.01	6.67	Plunging .38 cm (0.346 in.)	33.3	.201
19	.795	.01	6.67	Pitching 1.10 deg about $x_{\alpha}/c = .505$	41.6	.251
20	.497	.04	5.03	Pitching .01 deg about $x_{\alpha}/c = .046$	5.0	.047
21	.497	.04	5.03	Pitching .99 deg about $x_{\alpha}/c = .257$	21.3	.201
22	.497	.04	5.03	Pitching 1.07 deg about $x_{\alpha}/c = .504$	21.3	.201
23	.497	.04	5.03	Plunging 1.02 cm (0.400 in.)	21.3	.201
24	1.074	.00	6.58	Plunging .44 cm (0.173 in.)	5.0	.024
25	.497	1.98	5.00	Plunging .00 cm (0.000 in.)	5.0	.047
26	.502	-.22	9.98	Pitching .00 deg about $x_{\alpha}/c = .150$	5.0	.046
27	.502	-.22	9.98	Pitching .24 deg about $x_{\alpha}/c = .234$	10.8	.100
28	.502	-.22	9.98	Pitching .51 deg about $x_{\alpha}/c = .269$	10.8	.100
29	.502	-.22	9.98	Pitching 1.02 deg about $x_{\alpha}/c = .269$	10.8	.100
30	.499	-.21	9.90	Pitching .26 deg about $x_{\alpha}/c = .277$	21.5	.201
31	.499	-.13	9.89	Pitching .50 deg about $x_{\alpha}/c = .271$	21.5	.200
32	.499	-.13	9.89	Pitching 1.00 deg about $x_{\alpha}/c = .269$	21.5	.200
33	.499	-.13	9.89	Pitching 2.01 deg about $x_{\alpha}/c = .267$	21.5	.200
34	.499	-.13	9.89	Pitching 2.13 deg about $x_{\alpha}/c = .503$	21.5	.200
35	.499	-.13	9.89	Pitching 1.06 deg about $x_{\alpha}/c = .506$	21.5	.200
36	.499	-.13	9.89	Plunging 1.01 cm (0.399 in.)	21.5	.200
37	.499	-.13	9.89	Pitching 1.00 deg about $x_{\alpha}/c = .252$	26.9	.251
38	.499	-.13	9.89	Pitching 1.07 deg about $x_{\alpha}/c = .506$	26.9	.251
39	.499	-.13	9.89	Pitching 1.00 deg about $x_{\alpha}/c = .250$	16.2	.151
40	.499	-.13	9.89	Plunging 1.01 cm (0.396 in.)	16.2	.151
41	.499	-.13	9.89	Plunging 1.02 cm (0.401 in.)	10.8	.101
42	.499	-.13	9.89	Plunging 1.03 cm (0.405 in.)	5.4	.050
43	.499	-.13	9.89	Pitching 1.02 deg about $x_{\alpha}/c = .248$	5.4	.050
44	.499	-.13	9.89	Pitching 2.04 deg about $x_{\alpha}/c = .245$	10.8	.101
45	.648	-.22	11.63	Pitching .97 deg about $x_{\alpha}/c = .249$	27.8	.201
46	.744	-.22	12.31	Pitching 1.01 deg about $x_{\alpha}/c = .248$	32.0	.201
47	.796	-.21	12.56	Pitching .30 deg about $x_{\alpha}/c = .202$	17.1	.101
48	.796	-.21	12.56	Pitching .25 deg about $x_{\alpha}/c = .234$	34.2	.201
49	.796	-.21	12.56	Pitching .51 deg about $x_{\alpha}/c = .247$	17.1	.101
50	.796	-.21	12.56	Pitching .50 deg about $x_{\alpha}/c = .248$	34.2	.201
51	.796	-.21	12.56	Pitching 1.03 deg about $x_{\alpha}/c = .249$	4.2	.025
52	.796	-.21	12.56	Pitching 1.02 deg about $x_{\alpha}/c = .246$	8.6	.051
53	.796	-.21	12.56	Pitching 1.02 deg about $x_{\alpha}/c = .248$	17.2	.101
54	.796	-.21	12.56	Pitching 1.01 deg about $x_{\alpha}/c = .254$	25.7	.151
55	.796	-.21	12.56	Pitching 1.01 deg about $x_{\alpha}/c = .248$	34.4	.202
56	.796	-.21	12.56	Pitching 1.02 deg about $x_{\alpha}/c = .248$	42.0	.247
57	.796	-.21	12.56	Pitching .99 deg about $x_{\alpha}/c = .252$	51.5	.303
58	.796	-.21	12.56	Pitching 1.08 deg about $x_{\alpha}/c = .502$	42.9	.252
59	.796	-.21	12.56	Pitching 1.09 deg about $x_{\alpha}/c = .500$	34.4	.202
60	.796	-.21	12.56	Pitching 1.08 deg about $x_{\alpha}/c = .502$	17.2	.101
61	.796	-.21	12.56	Pitching 1.09 deg about $x_{\alpha}/c = .501$	8.6	.051
62	.796	-.21	12.56	Pitching 1.12 deg about $x_{\alpha}/c = .499$	4.3	.025
63	.797	-.08	12.40	Pitching 1.95 deg about $x_{\alpha}/c = .471$	34.3	.201
64	.797	-.08	12.40	Pitching 1.94 deg about $x_{\alpha}/c = .231$	34.3	.201
65	.797	-.08	12.40	Pitching 2.00 deg about $x_{\alpha}/c = .239$	17.2	.101
66	.797	-.08	12.40	Plunging 1.01 cm (0.396 in.)	34.3	.201
67	.797	-.08	12.40	Plunging 1.02 cm (0.401 in.)	25.8	.151
68	.797	-.08	12.40	Plunging 1.03 cm (0.400 in.)	17.4	.102
69	.797	-.08	12.40	Plunging 1.04 cm (0.400 in.)	8.6	.050
70	.797	-.08	12.40	Plunging 1.04 cm (0.409 in.)	4.3	.025
71	.842	.00	12.45	Pitching 1.01 deg about $x_{\alpha}/c = .248$	36.4	.202
72	.842	-.22	12.43	Pitching 1.91 deg about $x_{\alpha}/c = .247$	36.5	.202
73	.805	-.00	3.34	Pitching 1.01 deg about $x_{\alpha}/c = .247$	25.1	.149
74	.805	-.00	3.34	Plunging .44 cm (0.173 in.)	5.0	.030
75	.805	-.00	3.34	Pitching 1.02 deg about $x_{\alpha}/c = .248$	8.3	.049

TABLE 2.1. Continued.

DI	M	α_m' deg	$Re \times 10^{-6}$	Motion	f, Hz	k
76	0.805	0.00	3.34	Pitching 2.03 deg about $x_{\alpha}/c = 0.248$	8.3	0.049
77	.805	.00	3.34	Pitching 2.00 deg about $x_{\alpha}/c = .248$	33.3	.198
78	.794	.08	12.40	Pitching .64 deg about $x_{\alpha}/c = .328$	10.0	.059
79	.782	4.00	12.01	Pitching .25 deg about $x_{\alpha}/c = .232$	17.3	.102
80	.782	4.00	12.01	Pitching .25 deg about $x_{\alpha}/c = .229$	34.7	.205
81	.782	4.00	12.01	Pitching .51 deg about $x_{\alpha}/c = .244$	17.4	.103
82	.792	3.93	6.15	Pitching 1.01 deg about $x_{\alpha}/c = .247$	34.3	.203
83	.793	4.01	6.18	Pitching 1.02 deg about $x_{\alpha}/c = .248$	34.2	.202
84	.789	4.00	11.88	Pitching .51 deg about $x_{\alpha}/c = .234$	34.9	.203
85	.789	4.00	11.88	Pitching 1.04 deg about $x_{\alpha}/c = .246$	4.4	.026
86	.789	4.00	11.88	Pitching 1.03 deg about $x_{\alpha}/c = .246$	8.8	.051
87	.789	4.00	11.88	Pitching 1.02 deg about $x_{\alpha}/c = .248$	17.5	.102
88	.789	4.00	11.88	Pitching 1.01 deg about $x_{\alpha}/c = .247$	26.3	.153
89	.789	4.00	11.88	Pitching 1.01 deg about $x_{\alpha}/c = .249$	35.1	.204
90	.789	4.00	11.88	Pitching 1.01 deg about $x_{\alpha}/c = .248$	43.9	.255
91	.789	4.00	11.88	Pitching 1.00 deg about $x_{\alpha}/c = .248$	52.7	.306
92	.789	4.00	11.88	Pitching 1.08 deg about $x_{\alpha}/c = .499$	35.2	.205
93	.789	4.00	11.88	Plunging .84 cm (0.330 in.)	35.2	.205
94	.789	4.00	11.88	Pitching 1.08 deg about $x_{\alpha}/c = .501$	44.0	.256
95	.789	4.00	11.88	Pitching 2.00 deg about $x_{\alpha}/c = .245$	17.6	.102
96	.741	4.03	11.22	Pitching 1.02 deg about $x_{\alpha}/c = .246$	35.2	.215
97	.642	3.99	10.60	Pitching 1.01 deg about $x_{\alpha}/c = .247$	28.8	.203
98	.504	4.00	10.20	Pitching 1.02 deg about $x_{\alpha}/c = .249$	22.2	.199
99	.506	3.99	9.45	Pitching 1.09 deg about $x_{\alpha}/c = .499$	22.0	.198
100	.506	3.99	9.45	Plunging 1.01 cm (0.397 in.)	22.0	.198
101	.506	3.99	9.45	Pitching 1.09 deg about $x_{\alpha}/c = .302$	27.5	.247
102	.506	3.99	9.45	Pitching 2.14 deg about $x_{\alpha}/c = .502$	27.5	.247
103	.790	4.00	11.72	Pitching 2.01 deg about $x_{\alpha}/c = .243$	35.0	.203
104	.503	4.00	4.94	Pitching 1.01 deg about $x_{\alpha}/c = .245$	21.6	.199
105	.503	4.00	4.94	Pitching 1.09 deg about $x_{\alpha}/c = .499$	21.6	.199
106	.503	4.00	4.94	Plunging 1.02 cm (0.401 in.)	21.6	.199
107	.503	4.00	4.94	Pitching 1.08 deg about $x_{\alpha}/c = .502$	26.9	.248
108	.642	3.78	5.92	Pitching 1.02 deg about $x_{\alpha}/c = .250$	27.6	.203
109	.747	3.89	6.36	Pitching 1.02 deg about $x_{\alpha}/c = .247$	31.0	.197
110	.797	4.01	6.30	Pitching 1.09 deg about $x_{\alpha}/c = .500$	33.5	.201
111	.797	4.01	6.50	Plunging 1.01 cm (0.398 in.)	33.5	.201
112	.797	4.01	6.50	Pitching 1.08 deg about $x_{\alpha}/c = .502$	42.0	.252
113	.848	3.89	6.59	Pitching 1.01 deg about $x_{\alpha}/c = .248$	35.5	.201
114	.840	3.79	12.39	Pitching 1.01 deg about $x_{\alpha}/c = .248$	36.3	.202

TABLE 2.2. DATA BASE FOR NACA 64A010 AIRFOIL, PITCHING OSCILLATION ABOUT 0.25c NOMINAL, ARRANGED IN FREQUENCY SWEEPS

M	α_m' deg	$Re \times 10^{-6}$	α_0 deg	k = 0.025	k = 0.05	k = 0.10	k = 0.15	k = 0.20	k = 0.25	k = 0.30	Type of Flow
0.50	0.0	10	± 0.25			27		30			Subsonic
.50	0.0	10	± 0.50			28		31			
.50	0.0	2.5	± 1	9	8	7	6	2			
.50	0.0	5	± 1					21			
.50	0.0	10	± 1		43	29	39	32	37		
.50	0.0	2.5	± 2		10			11			
.50	0.0	10	± 2			44		33			
.65	0.0	11.6	± 1					45			
.75	0.0	12.3	± 1					46			
.80	0.0	3.3	± 1		75		73	12	15		
.80	0.0	12.5	± 0.25					48		Transonic weak shock	
.80	0.0	12.5	± 0.50		78	49		50			
.80	0.0	6.7	± 1					16			
.80	0.0	12.6	± 1	51	52	53	54	55	56		57
.80	0.0	12.4	± 2			65		64			
.85	0.0	12.4	± 1					72			
.50	4.0	4.9	± 1					104		Subsonic	
.50	4.0	10.2	± 1					98			
.65	4.0	5.9	± 1					108			
.65	4.0	10.6	± 1					97			
.75	4.0	6.4	± 1					109			
.75	4.0	11.2	± 1					96			
.80	4.0	12	± 0.25			79		80		Transonic shock stall	
.80	4.0	12	± 0.50			81		84			
.80	4.0	6.2	± 1					82			
.80	4.0	11.9	± 1	85	86	87	88	89	90		91
.80	4.0	11.9	± 2			95		103			
.85	4.0	6.6	± 1					113			

TABLE 2.3. SELECTED NASA AMES TEST DATA ASSOCIATED WITH AGARD CT CASES AND THE SHOCK STALL CASE (SSC)

CT Case	DI	M	α_m	$Re \times 10^{-6}$	α_o	f	k	x_{α}/c
1	7	0.490	-0.01	2.52	0.96	10.4	0.100	0.233
2	29	0.502	-0.22	9.98	1.02	10.8	0.100	0.269
3	51	0.796	-0.21	12.56	1.03	4.2	0.025	0.249
4	52	0.796	-0.21	12.56	1.02	8.6	0.051	0.246
5	53	0.796	-0.21	12.56	1.02	17.2	0.101	0.248
6	55	0.796	-0.21	12.56	1.01	34.4	0.202	0.248
7	57	0.796	-0.21	12.56	0.99	51.5	0.303	0.252
8	49	0.796	-0.21	12.56	0.51	12.1	0.101	0.247
9	65	0.797	-0.08	12.40	2.00	17.2	0.101	0.239
10	12	0.802	0.00	3.38	0.94	33.2	0.200	0.232
SSC	89	0.789	4.00	11.88	1.01	35.1	0.204	0.249

TABLE 2.4. STEADY AND FUNDAMENTAL FREQUENCY LIFT AND MOMENT DATA FOR SELECTED CASES

Case	DI	Steady Data		$C_{L,\alpha}$		$C_{M,\alpha}$	
		C_L	C_m				
CT1	7	0.006	-0.002	6.139	-1.149i	0.165	-0.163i
CT2	29	0.016	0.031	6.163	-1.036i	0.167	-0.201i
CT3	51	-0.029	-0.003	9.316	-1.378i	0.000	-0.102i
CT4	52	-0.029	-0.003	8.622	-2.479i	-0.005	-0.232i
CT5	53	-0.029	-0.003	6.790	-3.387i	-0.061	-0.388i
CT6	55	-0.029	-0.003	4.887	-2.521i	-0.189	-0.653i
CT7	57	-0.029	-0.003	4.635	-1.905i	-0.374	-1.023i
CT8	49	-0.029	-0.003	6.795	-3.403i	-0.195	-0.314i
CT9	65	-0.018	-0.002	6.141	-3.113i	-0.239	-0.302i
CT10	12	0.009	-0.002	5.308	-2.471i	-0.384	-0.546i
SSC	89	0.531	0.001	9.349	-0.406i	-2.068	+0.198i

TABLE 2.5. MEAN AND FUNDAMENTAL FREQUENCY PRESSURE DATA FOR AGARD CT CASE NO. 1; DYNAMIC INDEX 7

WING MODEL: NACA 64A010, CHORD: 500 METERS

WING MOTION: PITCHING 90 DEG ABOUT X/C: 233

DYNAMIC INDEX 7 STATIC INDEX 8

M 490 PTOT 50564 K 100
 ALPHA 0.01 QINF 7250 FREQ 10.4
 RE 2.91E 08 PINF 43169

.....UPPER SURFACE.....				LOWER SURFACE.....								
STEADY DATA		UNSTEADY DATA			STEADY DATA		UNSTEADY DATA						
X/C	CPU	X/C	REAL	IMAG	PHASE	X/C	CPU	X/C	REAL	IMAG	PHASE		
030	188	033	-11.722	3.045	12.111	165.10	053	188	000	808	-183	834	-18.83
052	185	052	-9.409	2.188	9.650	168.93	093	187	034	11.555	-2.879	11.508	-13.99
091	214	091	-7.293	1.635	7.572	167.54	142	238	094	8.500	-2.069	8.720	-12.23
142	259	140	-9.434	1.178	9.563	167.78	198	259	094	7.299	-1.486	7.449	-11.51
211	292	209	-4.035	7.25	4.100	169.83	244	290	141	6.840	-1.045	6.933	-10.15
243	299	243	-4.296	7.31	4.358	170.32	292	304	200	4.820	-0.745	4.977	-9.66
292	313	339	-3.368	4.44	3.401	172.16	341	308	243	3.973	-0.726	4.039	-10.38
341	326	402	-3.254	5.80	3.304	169.90	393	312	293	4.042	-0.422	4.084	-5.98
440	319	440	-1.808	6.33	2.084	182.33	440	313	341	1.408	-0.350	1.449	-13.87
487	298	488	-1.194	8.78	1.485	143.79	493	283	364	3.133	-0.958	3.134	-1.08
537	251	528	-0.444	3.45	5.84	142.28	537	237	441	1.938	-0.385	1.978	-11.24
585	197	584	-1.944	0.25	1.944	179.24	583	196	490	1.311	-0.887	1.438	-24.12
634	143	633	-1.412	0.65	1.414	-177.38	625	183	537	1.028	-0.483	1.138	-28.18
682	118	682	-1.029	0.18	1.029	178.98	679	115	582	1.488	-2.03	1.509	10.02
733	085	733	-0.960	-0.123	9.68	-172.73	734	069	631	1.820	2.48	1.638	8.84
783	020	781	-0.702	-0.136	7.15	-169.01	789	022	678	1.322	1.49	1.331	6.41
827	010	829	-0.370	-0.025	3.71	-176.21	832	015	723	1.058	1.81	1.087	8.69
874	052	872	-0.560	-0.181	5.83	-183.99	888	065	781	7.81	1.84	7.98	11.84
924	080	941	-0.113	-0.048	1.21	-158.30	941	114	831	5.88	0.50	5.90	4.87
									888	4.32	1.35	4.62	17.38
									923	1.87	0.68	1.68	20.38

TABLE 2.6. MEAN AND FUNDAMENTAL FREQUENCY PRESSURE DATA
FOR AGARD CT CASE NO. 2; DYNAMIC INDEX 29

WING MODEL: NACA 64A010, CHORD: 500 METERS

WING MOTION: PITCHING 1.02 DEG ABOUT X/C: 269

DYNAMIC INDEX 29 STATIC INDEX 24

M .502 PTOT 203152 K 100
ALPHA - 22 QINF 30199 FREQ 10.8
RE 1.00E 07 PINF 171000

-----UPPER SURFACE-----						-----LOWER SURFACE-----									
STEADY DATA			UNSTEADY DATA			STEADY DATA			UNSTEADY DATA						
---CPU---			---CPU A---			---CPL---			---CPL A---						
X/C	CPU		X/C	REAL	IMAG	MAG	PHASE	X/C	CPL		X/C	REAL	IMAG	MAG	PHASE
030	-136		033	-10.116	2.659	10.459	165.29	032	-034		034	11.019	-2.959	11.410	-15.03
091	-177		052	-7.608	1.994	7.865	165.33	093	-142		054	9.351	-2.296	9.629	-13.80
142	-223		091	-6.377	1.434	6.536	117.34	142	-227		094	6.781	-1.585	6.964	-13.16
211	-253		140	-5.231	1.181	5.362	67.28	199	-245		141	5.469	-1.172	5.593	-12.10
243	-265		209	-4.369	.791	4.440	169.75	244	-289		200	4.541	-.837	4.617	-10.45
292	-287		243	-4.026	.679	4.083	170.44	293	-298		243	4.075	-.692	4.133	-9.65
341	-304		294	-3.810	.576	3.653	171.41	341	-285		293	3.177	-.500	3.216	-8.94
399	-309		402	-3.165	.364	3.186	173.45	393	-294		341	3.099	-.387	3.123	-7.11
440	-300		440	-2.365	.226	2.395	174.60	440	-308		394	2.647	-.275	2.662	-5.94
487	-263		488	-2.020	.109	2.023	176.93	490	-278		441	2.387	-.184	2.393	-3.94
537	-228		538	-1.723	.023	1.723	179.25	537	-223		490	2.014	-.080	2.015	-2.29
585	-190		584	-1.385	-.027	1.385	-178.90	583	-183		582	1.434	.033	1.434	1.32
634	-137		633	-1.188	-.077	1.190	-176.32	625	-148		631	1.203	.062	1.204	2.95
682	-114		682	-.977	-.108	.983	-173.72	679	-111		678	.979	.112	.986	6.50
733	-081		733	-.814	-.137	.825	-170.48	734	-067		733	.759	.121	.769	9.09
787	016		781	-.613	-.160	.634	-165.39	789	-016		781	.597	.127	.611	11.98
874	055		829	-.562	-.170	.587	-163.15	832	018		831	.410	.128	.430	17.37
924	091		872	-.333	-.148	.365	-158.08	868	077		868	.316	.110	.335	19.15
			941	-.097	-.110	.147	-131.23	941	121		923	.178	.087	.180	25.95

TABLE 2.7. MEAN AND FUNDAMENTAL FREQUENCY PRESSURE DATA
FOR AGARD CT CASE NO. 3; DYNAMIC INDEX 51

WING MODEL: NACA 64A010, CHORD: 500 METERS

WING MOTION: PITCHING 1.03 DEG ABOUT X/C: 249

DYNAMIC INDEX 51 STATIC INDEX 30

M .786 PTOT 203321 K 025
ALPHA - 21 QINF 59395 FREQ 4.2
RE 1.00E 07 PINF 133812

-----UPPER SURFACE-----						-----LOWER SURFACE-----									
STEADY DATA			UNSTEADY DATA			STEADY DATA			UNSTEADY DATA						
---CPU---			---CPU A---			---CPL---			---CPL A---						
X/C	CPU		X/C	REAL	IMAG	MAG	PHASE	X/C	CPL		X/C	REAL	IMAG	MAG	PHASE
030	-086		032	-10.450	1.860	10.614	169.82	053	-207		034	12.103	-2.329	12.325	-10.98
091	-193		052	-9.641	1.700	9.809	170.03	093	-178		054	10.371	-1.880	10.540	-10.28
142	-262		091	-8.526	1.479	8.653	170.17	142	-318		084	8.826	-1.607	8.971	-10.32
211	-378		140	-7.580	1.433	7.714	169.21	199	-320		141	8.098	-1.510	8.237	-10.97
243	-418		209	-6.812	1.182	6.915	170.08	244	-457		200	7.405	-1.371	7.531	-10.49
292	-481		243	-6.812	1.229	7.020	169.93	293	-500		243	6.293	-1.113	6.391	-10.03
341	-544		294	-6.732	1.247	6.846	169.92	341	-538		293	5.256	-.981	5.348	-10.88
399	-639		402	-6.202	1.440	6.327	170.08	393	-628		341	6.343	-1.149	6.448	-10.27
440	-703		440	-6.717	1.477	6.842	170.40	440	-712		384	6.194	-1.117	6.294	-10.22
487	-864		488	-14.522	2.131	14.878	171.67	490	-777		480	15.771	-2.269	15.957	-9.26
537	-122		538	-2.656	-.123	2.659	-177.25	537	-234		582	.791	.232	.858	22.78
585	-258		584	.392	-.957	1.138	-29.20	583	-255		631	-.202	.402	.503	124.92
634	-181		633	.337	-.389	.515	-49.13	625	-198		678	-.388	.341	.502	127.20
682	-132		733	-.054	-.293	.294	-100.78	679	-137		733	-.283	.273	.393	128.04
733	-081		781	.026	-.227	.229	-83.40	734	-070		781	-.177	.208	.273	130.41
787	041		829	.092	-.210	.229	-75.41	789	-008		831	-.325	.168	.365	152.99
874	082		872	.108	-.144	.180	-93.02	832	043		888	-.212	.178	.242	151.28
924	141		941	.043	-.080	.082	-60.67	886	113		923	-.181	.062	.172	158.80
								941	170						

TABLE 2.8. MEAN AND FUNDAMENTAL FREQUENCY PRESSURE DATA FOR AGARD CT CASE NO. 4; DYNAMIC INDEX 52

WING MODEL NACA 644010. CHORD= 500 METERS

WING MOTION PITCHING 1.02 DEG ABOUT X/C= 246

DYNAMIC INDEX 52 STATIC INDEX 30

M 796 PTOT 203321 K 051
 ALPHA - 21 QINF 59395 FREQ 8.6
 RE 1.30E 07 PINF 133912

-----UPPER SURFACE-----						-----LOWER SURFACE-----									
STEADY DATA			UNSTEADY DATA			STEADY DATA			UNSTEADY DATA						
---CPU---			---CPU A---			---CPL---			---CPL A---						
X/C	CPU		X/C	REAL	IMAG	MAG	PHASE	X/C	CPL		X/C	REAL	IMAG	MAG	PHASE
030	- 086		033	-9.518	3.334	10.086	160.71	053	- 207		034	10.999	-3.944	11.685	-19.73
091	- 193		052	-8.589	2.979	9.091	160.88	093	- 175		054	9.286	-3.301	9.856	-19.57
142	- 292		091	-7.723	2.634	8.160	161.18	142	- 316		094	7.994	-2.835	8.481	-19.53
211	- 378		140	-6.821	2.449	7.247	160.26	199	- 320		141	7.267	-2.615	7.723	-19.79
243	- 418		209	-6.132	2.094	6.400	161.18	244	- 457		200	6.540	-2.340	6.946	-19.69
292	- 481		243	-6.282	2.192	6.654	160.78	293	- 500		243	5.766	-1.987	6.099	-19.01
341	- 544		294	-6.270	2.245	6.660	160.31	341	- 536		293	4.808	-1.754	5.117	-20.04
399	- 635		402	-7.275	2.494	7.690	161.09	393	- 629		341	5.825	-2.031	6.169	-19.22
440	- 703		440	-7.936	2.648	8.366	161.56	440	- 713		393	5.638	-1.968	5.972	-19.24
487	- 594		488	-13.828	3.754	14.326	164.82	490	- 777		490	13.385	-3.652	13.874	-15.26
537	- 322		538	-2.389	- 208	2.398	-175.03	537	- 334		582	6.75	591	897	41.19
585	- 258		584	860	-1.073	1.376	-51.30	583	- 255		631	- 272	746	794	110.07
634	- 181		633	153	- 717	733	-77.97	625	- 198		678	- 368	681	771	118.35
682	- 132		733	- 111	- 473	486	-103.25	679	- 137		733	- 225	514	561	113.70
733	- 061		781	- 009	- 398	398	-91.26	734	- 070		781	- 168	390	424	113.31
827	041		829	033	- 376	377	-84.95	789	- 006		831	- 275	363	455	127.18
874	092		872	083	- 284	296	-73.78	832	043		888	- 208	244	319	130.22
924	141		941	031	- 117	121	-75.08	886	113		923	- 147	130	196	138.40
								941	170						

TABLE 2.9. MEAN AND FUNDAMENTAL FREQUENCY PRESSURE DATA FOR AGARD CT CASE NO. 5; DYNAMIC INDEX 53

WING MODEL NACA 644010. CHORD= 500 METERS

WING MOTION PITCHING 1.02 DEG ABOUT X/C= 248

DYNAMIC INDEX 53 STATIC INDEX 30

M 796 PTOT 203321 K 101
 ALPHA - 21 QINF 59395 FREQ 17.2
 RE 1.30E 09 PINF 133912

-----UPPER SURFACE-----						-----LOWER SURFACE-----									
STEADY DATA			UNSTEADY DATA			STEADY DATA			UNSTEADY DATA						
---CPU---			---CPU A---			---CPL---			---CPL A---						
X/C	CPU		X/C	REAL	IMAG	MAG	PHASE	X/C	CPL		X/C	REAL	IMAG	MAG	PHASE
030	- 086		033	-7.014	4.842	8.623	145.39	053	- 207		034	8.181	-5.798	10.025	-28.29
091	- 193		052	-8.369	4.387	7.734	145.65	093	- 175		054	6.828	-4.842	8.451	-24.98
142	- 292		091	-8.781	3.898	6.972	146.02	142	- 316		094	5.842	-4.122	7.232	-24.75
211	- 378		140	-8.065	3.841	6.180	145.06	199	- 320		141	5.398	-3.758	6.574	-24.84
243	- 418		209	-4.829	3.136	5.581	145.89	244	- 457		200	4.347	-2.854	5.200	-22.29
292	- 481		243	-4.724	3.282	5.752	145.23	293	- 500		243	4.575	-3.123	5.940	-24.22
341	- 544		294	-4.850	3.301	5.702	144.84	341	- 536		293	3.649	-2.804	4.483	-25.52
399	- 635		402	-5.478	3.653	6.584	148.31	393	- 629		341	4.448	-2.943	5.349	-23.28
440	- 703		440	-8.159	3.873	7.278	147.86	440	- 713		393	4.232	-2.731	5.027	-22.84
487	- 594		488	-12.080	5.982	13.453	153.71	490	- 777		490	11.846	-4.497	12.764	-20.83
537	- 322		538	-1.801	- 838	2.005	-181.47	537	- 334		582	481	1.338	1.414	70.98
585	- 258		584	384	-1.808	1.850	-77.70	583	- 255		631	- 153	1.404	1.413	96.23
634	- 181		633	- 105	- 1.178	1.181	-95.13	625	- 198		678	- 204	1.201	1.218	99.68
682	- 132		733	- 235	- 763	799	-107.13	679	- 137		733	- 150	919	927	99.29
733	- 061		781	- 097	- 684	671	-98.24	734	- 070		781	- 117	725	744	95.08
827	041		829	- 053	- 670	652	-95.05	789	- 006		831	- 281	658	704	110.82
874	092		872	- 008	- 459	459	-91.00	832	043		888	- 174	473	564	110.24
924	141		941	018	- 178	178	-86.02	886	113		923	- 147	274	311	118.17
								941	170						

TABLE 2.10. MEAN AND FUNDAMENTAL FREQUENCY PRESSURE DATA
FOR AGARD CT CASE NO. 6; DYNAMIC INDEX 55

WING MODEL: NACA 64A010. CHORD: 500 METERS

WING MOTION: PITCHING 1.01 DEG ABOUT X/C: 248

DYNAMIC INDEX 55 STATIC INDEX 30

M 796 PTOT 203321 K 202
ALPHA - 21 QINF 59395 FREQ 34.4
RE 1.30E 07 PINF 133912

-----UPPER SURFACE-----						-----LOWER SURFACE-----										
STEADY DATA			UNSTEADY DATA			STEADY DATA			UNSTEADY DATA							
---CPU---			---CPU A---			---CPL---			---CPL A---							
X/C	CPU		X/C	REAL	IMAG	MAG	PHASE	X/C	CPL		X/C	REAL	IMAG	MAG	PHASE	
030	-086		033	-4.346	4.572	6.308	133.56	053	-207		034	4.663	-5.537	7.239	-49.90	
091	-193		052	-3.997	4.217	5.810	133.46	093	-175		054	3.979	-4.675	6.139	-49.60	
142	-292		091	-3.469	3.557	4.969	134.29	142	-316		094	3.497	-4.034	5.339	-49.79	
211	-378		140	-3.036	3.205	4.415	133.46	199	-320		141	3.236	-3.767	4.966	-49.34	
243	-418		209	-2.880	2.974	4.140	134.09	244	-457		200	2.666	-2.792	3.861	-46.32	
292	-481		243	-3.023	3.176	4.385	133.60	293	-500		243	3.075	-3.495	4.648	-48.5	
341	-544		294	-3.002	3.079	4.300	134.28	341	-536		293	2.362	-2.728	3.607	-49.10	
399	-635		402	-4.081	3.723	5.524	137.64	393	-629		341	3.173	-3.084	4.424	-44.19	
440	-703		440	-4.988	4.016	6.423	140.96	440	-713		394	3.210	-2.902	4.381	-42.89	
487	-594		488	-11.922	4.745	12.832	158.31	490	-777		490	11.825	-3.337	12.287	-15.76	
537	-322		538	-1.672	-2.138	2.714	-128.03	537	-334		532	616	2.69:	2.761	77.12	
595	-258		584	1.28	-2.800	2.803	-87.49	583	-455		631	007	2.480	2.480	89.85	
634	-181		633	-1.120	-2.064	2.068	-93.32	625	-198		678	-1.68	2.091	2.097	94.60	
692	-132		733	-0.52	-1.338	1.339	-92.22	679	-137		733	-208	1.491	1.505	97.95	
733	-061		781	0.66	-1.202	1.204	-86.85	734	-070		781	-171	1.316	1.327	97.42	
827	041		829	1.61	-1.085	1.097	-81.55	789	-008		831	-398	1.119	1.187	109.48	
874	092		872	1.56	-714	731	-77.89	832	043		888	-246	708	749	109.16	
924	141		941	0.87	-284	281	-69.84	886	113		923	-170	463	494	110.21	
								941	170							

TABLE 2.11. MEAN AND FUNDAMENTAL FREQUENCY PRESSURE DATA
FOR AGARD CT CASE NO. 7; DYNAMIC INDEX 57

WING MODEL: NACA 64A010. CHORD: 500 METERS

WING MOTION: PITCHING 9.9 DEG ABOUT X/C: 252

DYNAMIC INDEX 57 STATIC INDEX 30

M 796 PTOT 203321 K 203
ALPHA - 21 QINF 59395 FREQ 51.5
RE 1.30E 07 PINF 133912

-----UPPER SURFACE-----						-----LOWER SURFACE-----										
STEADY DATA			UNSTEADY DATA			STEADY DATA			UNSTEADY DATA							
---CPU---			---CPU A---			---CPL---			---CPL A---							
X/C	CPU		X/C	REAL	IMAG	MAG	PHASE	X/C	CPL		X/C	REAL	IMAG	MAG	PHASE	
030	-055		033	-4.071	3.043	5.081	143.28	053	-207		034	118	-4.311	4.312	-98.47	
091	-153		052	-4.071	3.484	5.346	133.35	093	-175		054	3.831	-3.38:	5.479	-45.37	
142	-292		091	-3.341	2.997	4.488	138.12	142	-316		094	3.815	-3.368	4.288	-50.13	
211	-378		140	-3.372	2.050	4.240	133.28	199	-320		141	2.847	-3.478	4.507	-50.80	
243	-418		209	-3.110	2.974	4.303	136.29	244	-457		200	2.374	-2.480	3.441	-66.37	
292	-51		243	-3.828	3.313	4.912	137.99	293	-500		243	2.508	-3.182	4.050	-61.76	
341	-544		402	-7.512	4.219	8.757	149.68	341	-536		293	2.164	-2.735	3.397	-61.76	
399	-676		447	-7.972	3.340	8.643	157.28	393	-629		341	2.640	-3.201	4.224	-50.97	
440	-703		488	-13.200	-2.98	13.204	-178.77	440	-713		394	2.455	-3.281	4.224	-62.71	
487	-594		538	-1.358	-4.719	4.911	-108.06	490	-777		490	11.899	-8.060	13.442	-78.80	
537	-222		584	5.28	-4.838	4.867	-83.78	537	-334		532	3.248	5.074	6.048	57.08	
595	-258		633	-3.384	-3.718	5.052	-131.67	583	-455		631	-231	4.500	4.508	92.94	
634	-181		733	3.66	-2.964	3.063	-75.57	625	-198		678	-892	2.362	2.360	104.78	
692	-132		781	7.28	-2.383	7.504	-72.92	679	-137		733	-1.922	2.582	2.581	120.92	
733	-061		829	4.11	-2.429	2.442	-80.40	734	-070		781	-608	2.258	2.259	108.08	
827	041		872	7.62	-1.283	1.652	-60.28	789	-008		831	-1.485	1.880	2.225	128.32	
874	092		941	4.89	-521	721	-68.28	832	043		888	-978	1.108	1.475	131.43	
924	141							886	113		923	-688	623	881	127.37	
								941	170							

TABLE 2.12. MEAN AND FUNDAMENTAL FREQUENCY PRESSURE DATA
FOR AGARD CT CASE NO. 8; DYNAMIC INDEX 49

WING MODEL: NACA 64A010, CHORD: 500 METERS

WING MOTION: PITCHING 51 DEG ABOUT X/C: 247

DYNAMIC INDEX 49 STATIC INDEX 30

M 796 PTOT 203321 K 101
ALPHA - 21 QINF 59395 FREQ 17.1
RE 1.30E 07 PINF 133912

-----UPPER SURFACE-----						-----LOWER SURFACE-----								
STEADY DATA			UNSTEADY DATA			STEADY DATA			UNSTEADY DATA					
---CPU---			---CPU, A---			---CPL---			---CPL, A---					
X/C	CPU		X/C	REAL	IMAG	MAG	PHASE	X/C	CPL	X/C	REAL	IMAG	MAG	PHASE
030	-086		.033	-5.969	4.221	7.311	144.75	052	-207	034	8.689	-5.674	10.377	-33.15
091	-193		052	-6.089	4.153	7.371	145.71	093	-175	054	6.979	-4.989	8.578	-35.56
142	-292		.091	-5.759	3.944	6.980	145.60	142	-316	.094	6.041	-4.167	7.339	-34.80
211	-378		140	-4.902	3.538	5.045	144.19	199	-320	.141	5.340	-3.828	6.571	-35.64
243	-418		.209	-4.689	3.255	5.708	145.24	244	-4.7	200	4.130	-2.819	5.000	-34.32
292	-481		.243	-4.851	3.434	5.943	144.71	293	-500	.243	5.142	-3.708	6.340	-35.80
341	-544		.294	-4.535	3.142	5.517	145.30	341	-536	.293	3.526	-2.578	4.368	-36.18
399	-635		.402	-5.050	3.330	6.049	146.61	393	-629	.341	4.290	-2.832	5.141	-33.43
440	-703		.440	-4.941	3.414	6.006	145.37	440	-713	.394	4.538	-2.983	5.431	-33.32
487	-594		.488	-18.650	10.071	21.195	151.64	490	-777	.490	10.913	-4.639	11.858	-23.03
537	-322		.538	-803	-1.572	1.765	-117.06	537	-334	.682	-115	1.710	1.714	93.84
585	-258		.584	-593	-1.987	2.073	-73.39	583	-255	.631	-402	1.502	1.555	105.00
634	-181		.633	-058	-1.149	1.151	-92.89	625	-198	.678	-284	1.190	1.224	103.42
682	-132		.733	-222	-752	784	-106.45	679	-137	.733	-194	943	962	101.61
733	-061		.781	-114	-642	652	-100.07	734	-070	.781	-091	718	724	97.25
827	041		.829	-090	-593	599	-98.67	789	-006	.831	-267	.660	712	112.08
874	092		.872	-018	-431	432	-92.40	832	043	.888	-164	.458	.486	109.70
924	141		.941	-018	-175	176	-95.86	886	113	.923	-148	.270	.308	118.78
								941	170					

TABLE 2.13. MEAN AND FUNDAMENTAL FREQUENCY PRESSURE DATA
FOR AGARD CT CASE NO. 9; DYNAMIC INDEX 65

WING MODEL: NACA 64A010, CHORD: 500 METERS

WING MOTION: PITCHING 2 00 DEG ABOUT X/C: 239

DYNAMIC INDEX 65 STATIC INDEX 31

M 797 PTOT 203185 K 101
ALPHA - 09 QINF 59423 FREQ 17.2
RE 1.24E 07 PINF 133724

-----UPPER SURFACE-----						-----LOWER SURFACE-----								
STEADY DATA			UNSTEADY DATA			STEADY DATA			UNSTEADY DATA					
---CPU---			---CPU, A---			---CPL---			---CPL, A---					
X/C	CPU		X/C	REAL	IMAG	MAG	PHASE	X/C	CPL	X/C	REAL	IMAG	MAG	PHASE
030	-099		033	-6.824	4.616	8.239	145.97	090	-021	034	6.553	-5.203	8.367	-38.48
091	-200		052	-6.624	4.830	8.025	145.84	053	-187	054	6.738	-4.585	8.150	-34.23
142	-298		091	-5.300	3.507	6.355	146.52	142	-309	094	5.818	-3.745	6.752	-33.69
211	-385		.140	-4.806	3.234	5.793	146.07	244	-450	.141	5.340	-3.573	6.425	-32.78
243	-426		.209	-4.557	3.064	5.491	146.10	293	-487	.200	4.800	-3.279	5.879	-33.50
292	-488		.243	-4.448	3.039	5.387	145.67	341	-613	.243	4.535	-2.901	5.384	-32.61
341	-551		.294	-3.123	2.918	4.274	136.98	393	-627	.293	3.469	-2.211	4.111	-32.55
399	-643		.402	-4.844	3.104	5.797	146.69	440	-713	.341	2.881	-1.824	3.495	-31.47
440	-716		.440	-5.167	3.031	5.980	149.82	490	-784	.394	4.334	-2.487	4.997	-29.85
487	-729		.488	-8.226	4.227	9.248	152.81	537	-358	.490	8.028	-2.483	8.404	-17.18
537	-323		.538	-7.658	3.392	8.375	156.12	583	-254	.682	2.184	.275	2.196	5.89
585	-254		.584	-1.227	-746	1.436	-148.73	625	-187	.631	711	836	1.098	49.63
634	-180		.633	-087	-882	864	-95.74	679	-137	.678	260	967	991	74.81
682	-130		.733	-160	-930	943	-99.78	734	-071	.733	-003	875	626	90.18
733	-060		.781	002	-851	851	-89.85	789	-008	.781	008	713	713	89.30
827	042		.829	112	-740	748	-81.43	832	042	.888	-133	448	448	108.65
874	092		.872	103	-531	541	-79.00	886	111	.923	-150	277	318	118.54
924	140		.941	086	-224	239	-49.32	941	187					

TABLE 2.16. INSTANTANEOUS PRESSURES AT UPPER-SURFACE; CT CASE NO. 6, DYNAMIC INDEX 55

	J=	1	2	3	4	5	6	7	8	9	10	11	12	13	
PHASE, DEG=		5.5	5	6.5	12.5	18.5	24.5	30.5	36.5	42.5	48.5	54.5	60.5	66.5	
ALPHA, DEG=		1.019	1.021	1.012	.991	.958	.915	.862	.800	.730	.655	.570	.481	.387	
1	X/C	*	*	*	*	*	*	*	*	*	*	*	*	*	
1		.033	-.161	-.167	-.173	-.182	-.191	-.198	-.202	-.203	-.202	-.201	-.200	-.198	-.195
2		.052	-.187	-.196	-.204	-.210	-.214	-.218	-.222	-.225	-.224	-.224	-.222	-.219	-.217
3		.091	-.254	-.259	-.265	-.269	-.272	-.275	-.277	-.277	-.278	-.277	-.275	-.271	-.264
4		.140	-.339	-.346	-.350	-.355	-.358	-.360	-.362	-.364	-.364	-.363	-.361	-.358	-.356
5		.209	-.422	-.429	-.433	-.438	-.439	-.442	-.443	-.443	-.443	-.442	-.440	-.439	-.437
6		.243	-.466	-.474	-.480	-.484	-.486	-.488	-.490	-.490	-.490	-.488	-.487	-.486	-.484
7		.294	-.530	-.535	-.541	-.546	-.549	-.551	-.554	-.555	-.554	-.553	-.552	-.550	-.549
8		.402	-.709	-.715	-.720	-.721	-.723	-.726	-.727	-.724	-.723	-.722	-.724	-.723	-.716
9		.440	-.777	-.782	-.785	-.788	-.790	-.791	-.791	-.790	-.790	-.789	-.789	-.789	-.786
10		.468	-.777	-.786	-.792	-.795	-.796	-.795	-.794	-.792	-.792	-.795	-.793	-.789	-.784
11		.538	-.349	-.350	-.352	-.346	-.342	-.340	-.337	-.334	-.328	-.322	-.313	-.304	-.299
12		.564	-.262	-.259	-.247	-.240	-.238	-.233	-.229	-.223	-.219	-.215	-.213	-.213	-.217
13		.633	-.187	-.181	-.176	-.172	-.168	-.165	-.160	-.157	-.154	-.153	-.150	-.153	-.155
14		.733	-.059	-.056	-.053	-.055	-.050	-.048	-.045	-.044	-.042	-.039	-.040	-.043	-.042
15		.781	-.008	-.004	-.002	-.000	.003	.006	.008	.007	.009	.009	.008	.007	.009
16		.829	.043	.047	.049	.055	.060	.064	.065	.067	.067	.066	.064	.061	.060
17		.872	.092	.094	.096	.098	.100	.101	.101	.102	.102	.103	.102	.102	.102
18		.941	.160	.159	.160	.161	.160	.160	.160	.160	.160	.160	.161	.162	.162
	J=	14	15	16	17	18	19	20	21	22	23	24	25	26	
PHASE, DEG=		72.5	78.5	84.5	90.5	96.5	102.5	108.5	114.5	120.5	126.5	132.5	138.5	144.5	
ALPHA, DEG=		.290	.190	.088	-.014	-.116	-.216	-.313	-.407	-.497	-.583	-.664	-.738	-.806	
1	X/C	*	*	*	*	*	*	*	*	*	*	*	*	*	
1		.033	-.190	-.185	-.179	-.171	-.164	-.157	-.146	-.137	-.126	-.115	-.099	-.087	-.072
2		.052	-.213	-.208	-.202	-.196	-.188	-.181	-.173	-.163	-.153	-.142	-.132	-.122	-.111
3		.091	-.264	-.260	-.255	-.250	-.248	-.242	-.237	-.229	-.218	-.209	-.200	-.191	-.183
4		.140	-.353	-.349	-.345	-.340	-.337	-.332	-.327	-.321	-.314	-.306	-.298	-.289	-.281
5		.209	-.435	-.431	-.428	-.423	-.419	-.416	-.411	-.405	-.399	-.392	-.385	-.377	-.370
6		.243	-.481	-.477	-.474	-.470	-.466	-.464	-.459	-.453	-.446	-.437	-.428	-.420	-.413
7		.294	-.544	-.541	-.538	-.537	-.536	-.532	-.523	-.515	-.509	-.502	-.493	-.484	-.475
8		.402	-.715	-.707	-.703	-.700	-.696	-.689	-.682	-.676	-.666	-.658	-.651	-.642	-.634
9		.440	-.783	-.781	-.778	-.774	-.769	-.763	-.757	-.749	-.742	-.738	-.733	-.725	-.718
10		.468	-.777	-.768	-.761	-.755	-.749	-.743	-.735	-.728	-.722	-.718	-.713	-.707	-.701
11		.538	-.297	-.293	-.285	-.278	-.273	-.266	-.262	-.261	-.259	-.259	-.254	-.251	-.245
12		.564	-.219	-.216	-.213	-.211	-.213	-.218	-.221	-.221	-.222	-.223	-.226	-.232	-.234
13		.633	-.153	-.148	-.147	-.150	-.151	-.155	-.150	-.146	-.151	-.153	-.148	-.158	-.161
14		.733	-.043	-.043	-.042	-.042	-.043	-.045	-.047	-.047	-.047	-.047	-.049	-.043	-.046
15		.781	.009	.009	.009	.008	.007	.010	.010	.008	.005	.007	.007	.006	.005
16		.829	.057	.056	.055	.055	.056	.058	.056	.054	.052	.052	.052	.053	.054
17		.872	.101	.101	.101	.101	.101	.101	.100	.099	.098	.098	.098	.098	.099
18		.941	.162	.160	.163	.162	.160	.158	.157	.157	.156	.156	.156	.161	.159
	J=	27	28	29	30	31	32	33	34	35	36	37	38	39	
PHASE, DEG=		150.5	156.5	162.5	168.5	174.5	180.5	186.5	192.5	198.5	204.5	210.5	216.5	222.5	
ALPHA, DEG=		-.866	-.918	-.960	-.991	-1.014	-1.018	-1.013	-.996	-.966	-.925	-.874	-.814	-.744	
1	X/C	*	*	*	*	*	*	*	*	*	*	*	*	*	
1		.033	-.057	-.063	-.062	-.065	-.070	-.072	-.064	-.061	-.067	-.062	-.064	-.061	-.061
2		.052	-.094	-.098	-.097	-.098	-.100	-.102	-.095	-.097	-.091	-.097	-.094	-.092	-.091
3		.091	-.177	-.184	-.182	-.184	-.181	-.182	-.175	-.176	-.173	-.179	-.176	-.173	-.173
4		.140	-.274	-.280	-.279	-.280	-.281	-.283	-.276	-.277	-.274	-.279	-.276	-.273	-.273
5		.209	-.382	-.388	-.386	-.388	-.385	-.387	-.380	-.381	-.378	-.383	-.380	-.377	-.377
6		.243	-.464	-.470	-.468	-.470	-.467	-.469	-.462	-.463	-.460	-.465	-.462	-.459	-.459
7		.294	-.547	-.553	-.551	-.553	-.550	-.552	-.545	-.546	-.543	-.548	-.545	-.542	-.542
8		.402	-.822	-.815	-.809	-.804	-.807	-.804	-.797	-.798	-.795	-.799	-.796	-.793	-.793
9		.440	-.897	-.889	-.883	-.878	-.881	-.878	-.871	-.872	-.869	-.873	-.870	-.867	-.867
10		.468	-.886	-.878	-.872	-.867	-.864	-.861	-.854	-.855	-.852	-.856	-.853	-.850	-.850
11		.538	-.697	-.693	-.687	-.682	-.685	-.682	-.675	-.676	-.673	-.677	-.674	-.671	-.671
12		.564	-.607	-.603	-.597	-.592	-.595	-.592	-.585	-.586	-.583	-.587	-.584	-.581	-.581
13		.633	-.515	-.511	-.505	-.500	-.503	-.500	-.493	-.494	-.491	-.495	-.492	-.489	-.489
14		.733	-.389	-.388	-.382	-.377	-.380	-.377	-.370	-.371	-.368	-.372	-.369	-.366	-.366
15		.781	-.263	-.262	-.256	-.251	-.254	-.251	-.244	-.245	-.242	-.246	-.243	-.240	-.240
16		.829	-.137	-.137	-.131	-.126	-.129	-.126	-.119	-.120	-.117	-.121	-.118	-.115	-.115
17		.872	.006	.004	.003	.002	.001	.001	.004	.004	.003	.007	.004	.001	.001
18		.941	.161	.159	.156	.154	.154	.154	.154	.154	.154	.154	.154	.154	.154
	J=	40	41	42	43	44	45	46	47	48	49	50	51	52	
PHASE, DEG=		228.5	234.5	240.5	246.5	252.5	258.5	264.5	270.5	276.5	282.5	288.5	294.5	300.5	
ALPHA, DEG=		-.668	-.585	-.496	-.402	-.303	-.202	-.098	.007	.114	.217	.319	.417	.511	
1	X/C	*	*	*	*	*	*	*	*	*	*	*	*	*	
1		.033	.010	.016	.023	.030	.038	.043	.049	.056	.063	.071	.078	.085	.093
2		.052	-.021	-.023	-.025	-.028	-.032	-.036	-.040	-.045	-.050	-.056	-.061	-.066	-.071
3		.091	-.103	-.104	-.106	-.109	-.114	-.118	-.125	-.130	-.136	-.143	-.150	-.156	-.161
4		.140	-.207	-.209	-.210	-.213	-.217	-.221	-.227	-.231	-.238	-.244	-.250	-.256	-.264
5		.209	-.297	-.298	-.299	-.301	-.304	-.307	-.313	-.317	-.322	-.328	-.334	-.340	-.346
6		.243	-.336	-.337	-.338	-.341	-.344	-.347	-.353	-.357	-.362	-.367	-.373	-.379	-.384
7		.294	-.404	-.406	-.407	-.411	-.415	-.419	-.424	-.429	-.434	-.439	-.444	-.449	-.454
8		.402	-.510	-.513	-.516	-.520	-.524	-.528	-.533	-.537	-.542	-.547	-.552	-.557	-.562
9		.440	-.554	-.557	-.560	-.564	-.568	-.572	-.577	-.581	-.586	-.591	-.596	-.601	-.606
10		.468	-.610	-.613	-.616	-.620	-.624	-.628	-.633	-.637	-.642	-.647	-.652	-.657	-.662
11		.538	-.630	-.633	-.636	-.640	-.644	-.648	-.653	-.657	-.662	-.667	-.672	-.677	-.682

TABLE 2.18 CONCLUDED.

	53	54	55	56	57	58	59	60	61	62	63	64	65	
Phase	53	54	55	56	57	58	59	60	61	62	63	64	65	
Value	53	54	55	56	57	58	59	60	61	62	63	64	65	
1	.052	-.925	-.958	-.947	-.958	-.970	-.981	-.992	-1.002	-1.012	-1.021	-1.028	-1.033	-1.037
2	.091	-.927	-.956	-.946	-.956	-.967	-.980	-.990	-.998	-1.007	-1.015	-1.021	-1.027	-1.032
3	.140	-.937	-.948	-.960	-.975	-.986	-.998	-1.010	-1.021	-1.031	-1.040	-1.047	-1.054	-1.058
4	.209	-.932	-.940	-.950	-.961	-.972	-.983	-.993	-1.003	-1.012	-1.021	-1.027	-1.034	-1.039
5	.245	-.959	-.988	-.977	-.987	-.996	-1.008	-1.017	-1.027	-1.035	-1.043	-1.049	-1.056	-1.061
6	.294	-.994	-1.009	-1.019	-1.029	-1.041	-1.052	-1.062	-1.072	-1.082	-1.091	-1.100	-1.107	-1.115
7	.539	-1.050	-1.060	-1.071	-1.084	-1.096	-1.106	-1.116	-1.129	-1.139	-1.147	-1.154	-1.161	-1.167
8	.602	-1.317	-1.326	-1.336	-1.347	-1.357	-1.370	-1.380	-1.391	-1.400	-1.410	-1.421	-1.428	-1.435
9	.640	-.955	-.959	-.946	-.954	-.961	-.968	-.976	-.984	-.991	-.996	-1.001	-1.001	-.970
10	.486	-.994	-1.005	-1.012	-1.021	-1.025	-1.031	-1.031	-.996	-.865	-.726	-.625	-.559	-.517
11	.536	-.642	-.653	-.659	-.659	-.654	-.644	-.635	-.629	-.619	-.608	-.594	-.579	-.569
12	.584	-.563	-.576	-.586	-.590	-.594	-.596	-.592	-.594	-.593	-.587	-.580	-.576	-.568
13	.633	-.471	-.493	-.513	-.528	-.538	-.549	-.552	-.560	-.562	-.562	-.562	-.560	-.556
14	.733	-.203	-.230	-.261	-.291	-.318	-.353	-.378	-.405	-.416	-.434	-.443	-.455	-.462
15	.781	-.087	-.102	-.122	-.149	-.190	-.218	-.265	-.300	-.320	-.345	-.369	-.377	-.398
16	.829	.011	.005	-.007	-.021	-.044	-.080	-.118	-.162	-.210	-.239	-.270	-.296	-.323
17	.872	.057	.057	.054	.048	.038	.021	-.012	-.050	-.084	-.124	-.159	-.197	-.224
18	.941	.126	.127	.128	.127	.124	.113	.101	.083	.057	.028	-.003	-.038	-.075

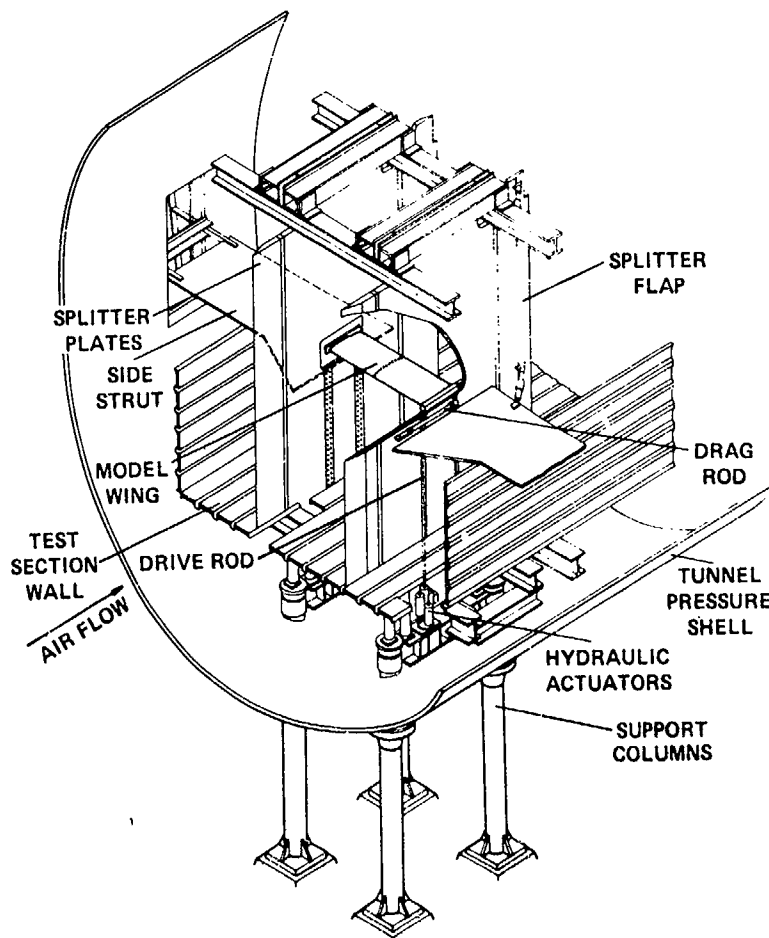


Fig. 2.1. General arrangement of oscillating airfoil test apparatus in NASA Ames 11- by 11-Foot Transonic Wind Tunnel.

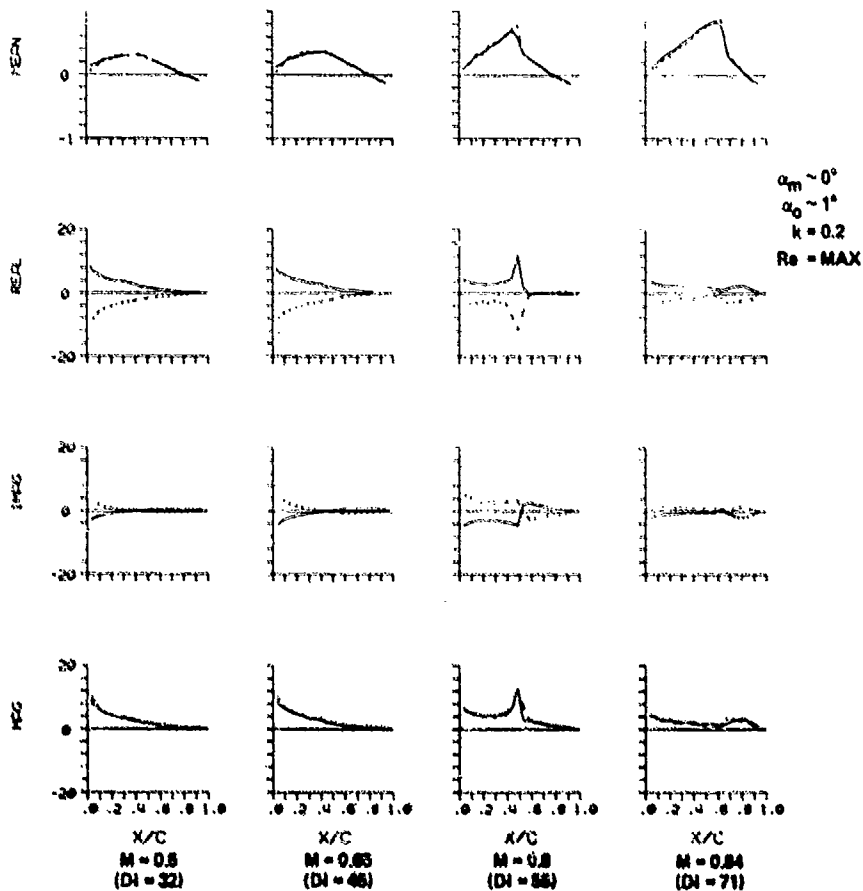


Fig. 2.2. Effect of varying Mach number.

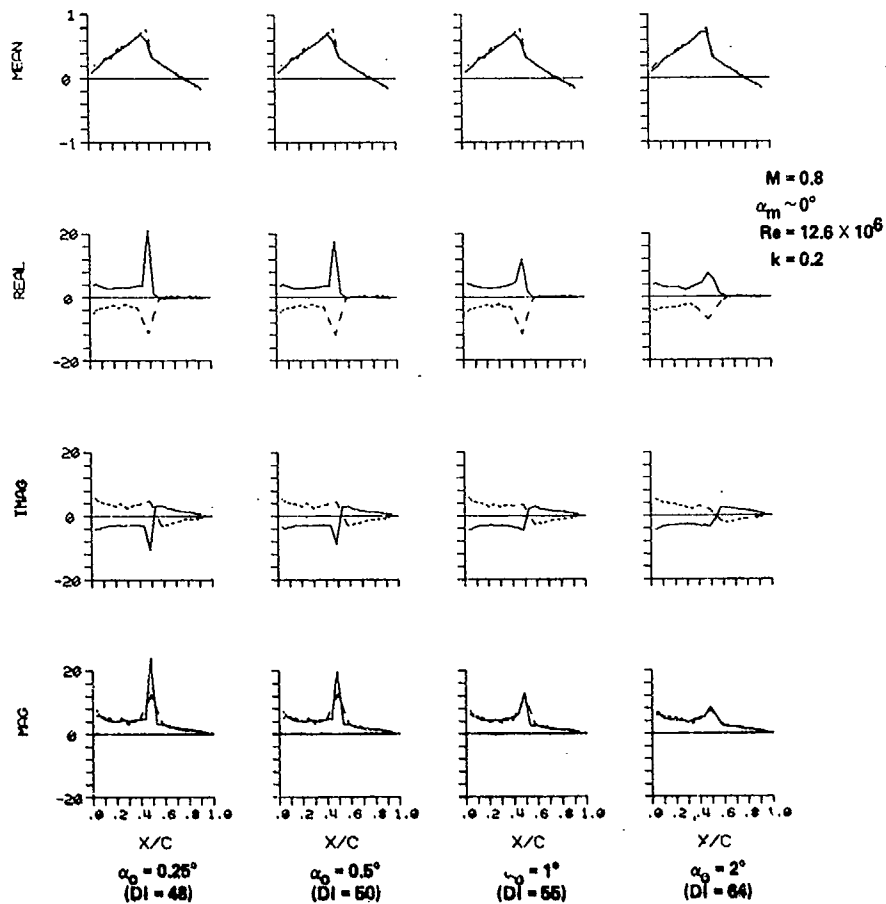


Fig. 2.3. Effect of varying oscillation amplitude.

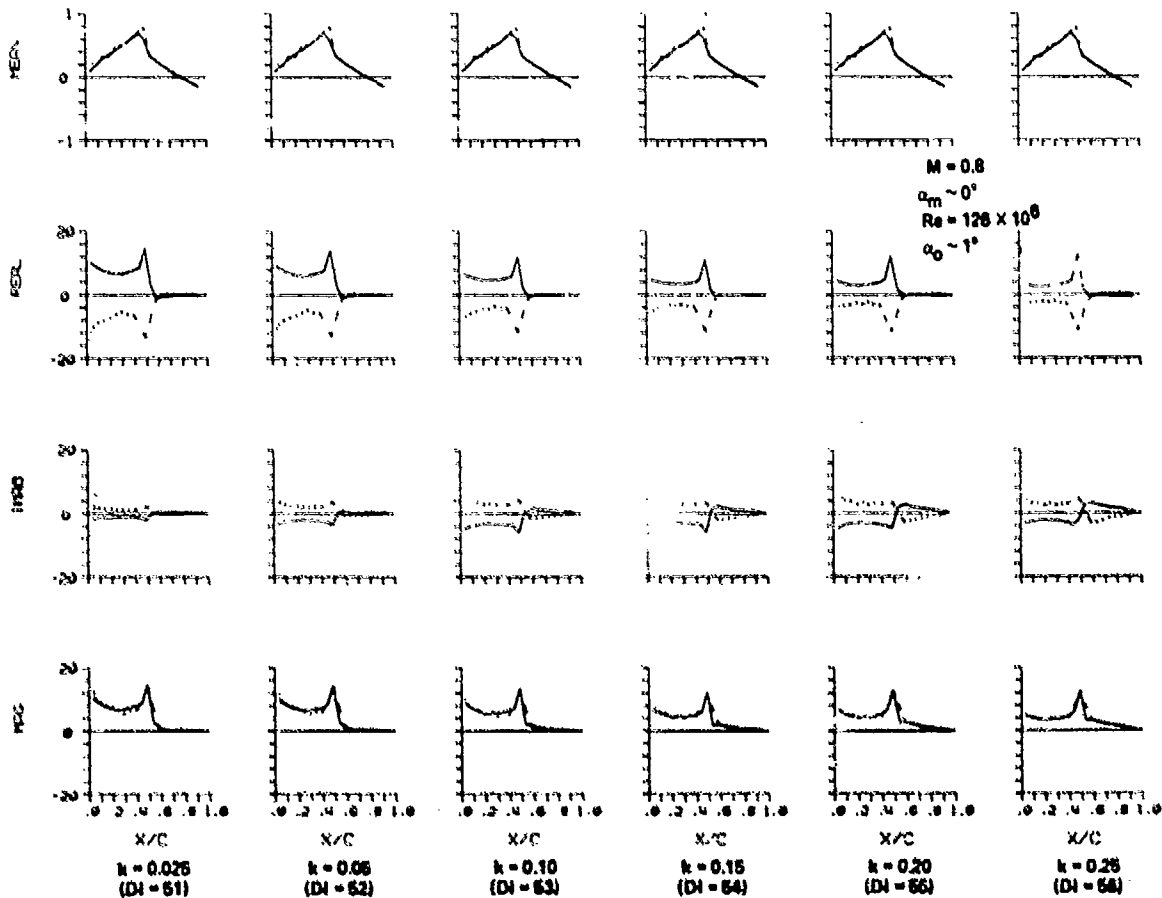


Fig. 2.4. Effect of varying frequency parameter.

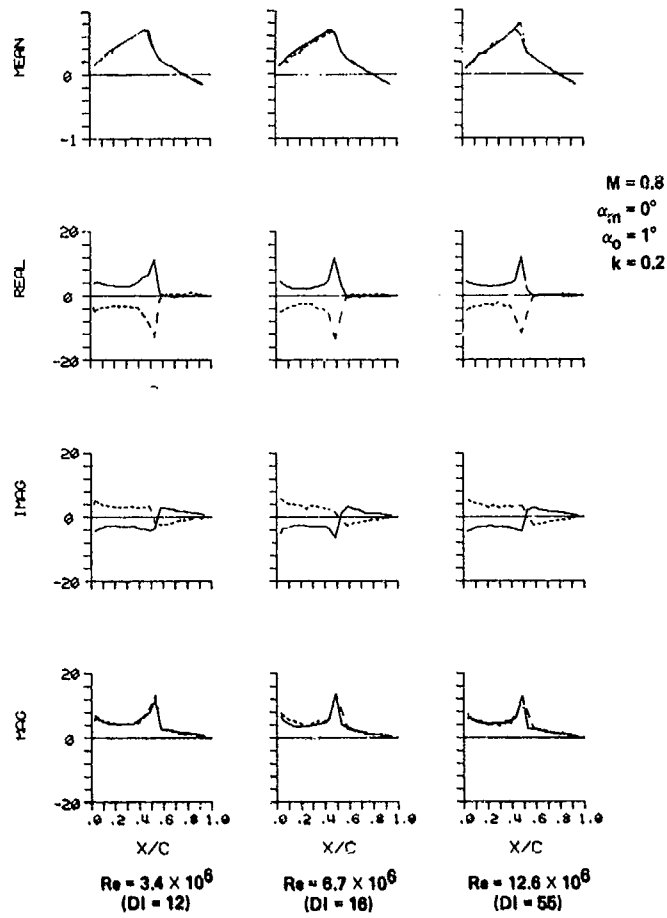


Fig. 2.5. Effect of varying Reynolds number.

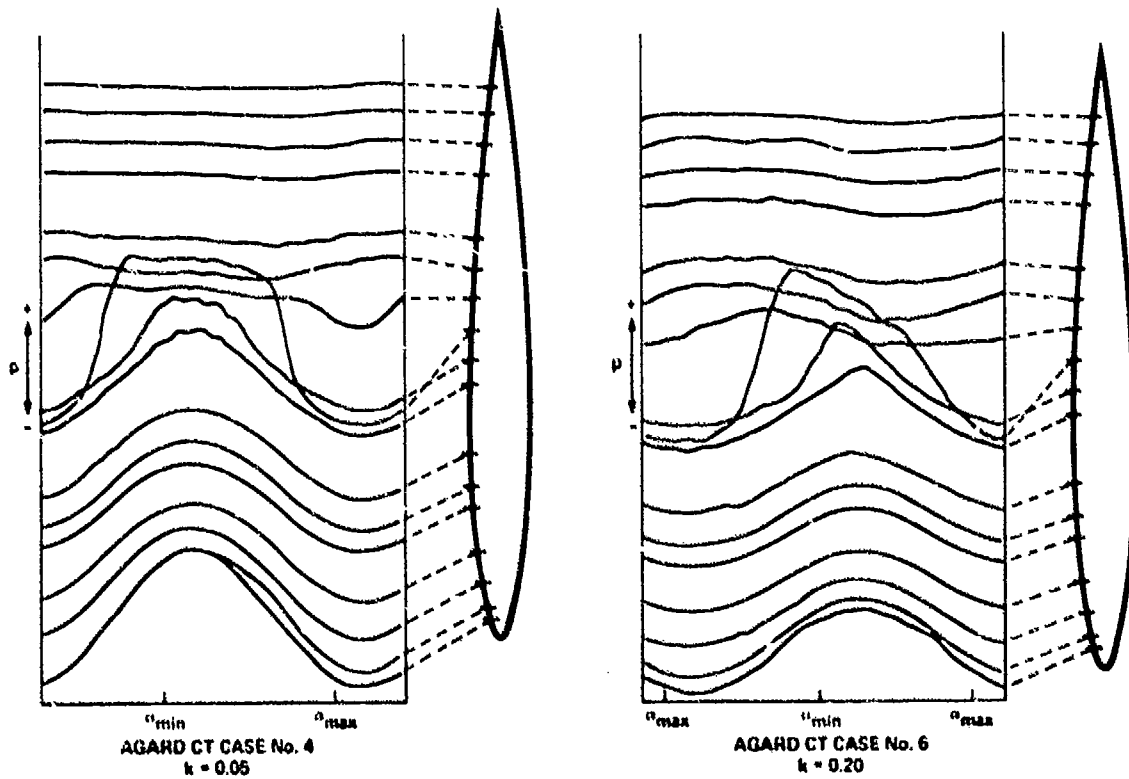


Fig. 2.6. Unsteady pressure time-histories for AGARD CT Cases 4 and 6. $M = 0.8, \alpha_m = 0^\circ$.

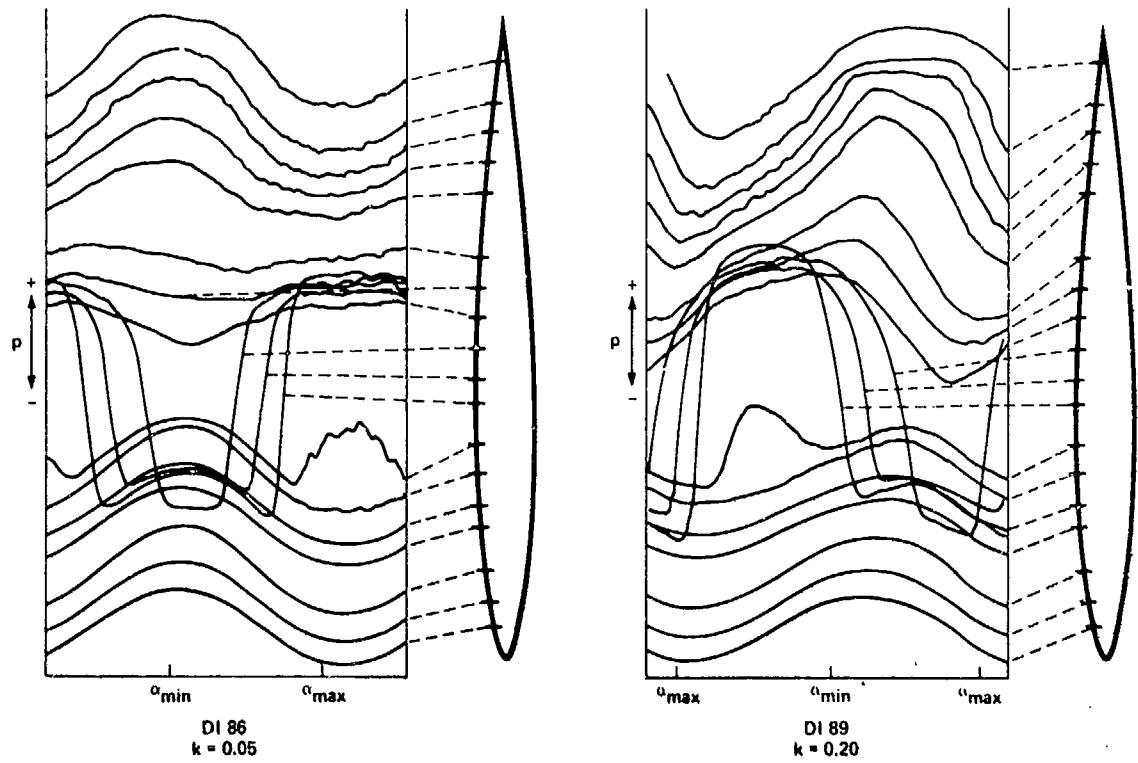


Fig. 2.7. Unsteady pressure time-histories for shock-stall case.
 $M = 0.8, \alpha_m = 4.0^\circ$.

DATA SET 3

NACA 0012. OSCILLATORY AND TRANSIENT PITCHING

by

R. H. Landon, ARA

INTRODUCTION

These results are extracted from tabulations of wing pressures resulting from the 3rd series of pitching tests about 0.25c axis made in the ARA 2-dimensional tunnel, using the pitching and heaving rig, Ref 3.1.

The main purpose of these tests was to examine the conditions of dynamic stall and recovery at scaled time rates similar to those of a typical helicopter application. Dynamic similarity was maintained also in Reynolds number; the approximately quarter scale blade section was therefore run, for all the cases reported here, at a tunnel stagnation pressure of 4 bar to match low altitude flight of the helicopter. Consequently, no artificial boundary layer transition trips were applied to the test wing.

The output of dynamic pressure transducers was sampled at fixed intervals, the instantaneous pressures and reference conditions having a matched and filtered response within 3 dB up to 460 Hz.

The results represent one specific cycle, and are not averaged over a number of cycles. The data bank at ARA contains at least 4 cycles of each dynamic condition. Ramp motions have only a single transient.

Up to 6 increments of mean incidence and amplitude, singly or in combination, could be run: the present programme called for 3 increments (called programme steps or PSTEP) of mean incidence, α_m as shown in Table 3.4.

The time-dependent results are presented without harmonic or spectral analysis. Note that the harmonic content of the pitching motion is relatively high, due to the intrusion of other modes of the drive system:

AGARD case	f (Hz)	Harmonic content and phase angle relative to the fundamental			
		First	Second	Third	Fourth
1,2,3 5	50.32	2.44%, -10°	2.45%, -39°	0.5%, -51°	0.38%, 0°
	62.5	0.22%, -13°	2.60%, -44°	0.37%, -61°	0.07%, -76°

The instantaneous Mach number varies in sympathy with the drag of the wing: the flow momentum loss changes the effective area of the choked throat that controls the flow downstream of the model, thus making speed dependent on drag. Mach number is thus given for each data point in the results.

The heave mode (no results presented here) allowed the wing to be placed up to 63.5 mm (2.5 in) above and below the tunnel centre line. Some pitching tests are reported in Ref 3.2 to show possible effects on dynamic readings of wall proximity: there has been no analysis of *unsteady* tunnel interference, but corrections appropriate to steady interference have been applied to some of the measured quantities.

Notes on the data

The ordinates of the NACA 0012 airfoil are given in Table 3.1. The chordwise and spanwise locations of the 30 pressure holes and their channel numbers are given in Table 3.2, and the arrangement of the data is explained in Table 3.3.

Ten data sets are presented to provide experimental comparison with AGARD CT Cases. These are extracted from the full set of tests identified in Tables 3.4 and 3.5.

For the priority CT Case 1 the tabulated data are presented as 32 sets of pressure coefficients at equal time intervals during a cycle of oscillation, extracted from 64 sets in the original data. For the other CT Cases of oscillatory pitch the number is reduced to 8 sets. The ramp motion and quasi-steady data have 16 points, chosen to give approximately equal incidence increments, again taken from more closely spaced original data. Tables 3.7 to 3.10 include a pitch damping factor which is irrelevant for the present purpose and its value is also shown in each of the oscillatory plots. Note also that the ramp incidence rate is an approximate or nominal value: the incidence rate $\dot{\alpha} = d\alpha/dt$ is not constant, and when calculated from different ranges of incidences, will give different values. Approximate representations of the motions in Ref 3.6 are recommended for comparative calculations at given α . No measurements were made for

strictly steady conditions, but instantaneous pressures were measured for very slow oscillations of incidence. The results of three of these quasi-steady tests are given in Tables 3.14 to 3.16.

Oscillatory pitch about 0.25c:

Related AGARD CT Case	Run No. and P step	Experimental conditions							Data table
		M	α_m (deg)	α_0 (deg)	f (Hz)	k	Re $\times 10^{-6}$	Sets	
1	87-1	0.600	2.89	2.41	50.32	0.0808	4.8	32	3.7
2	89-1	0.600	3.16	4.59	50.32	0.0811	4.8	8	3.8
3	87-3	0.600	4.86	2.44	50.32	0.0810	4.8	8	3.9
5	128-1	0.755	0.016	2.51	62.5	0.0814	5.5	8	3.10

Ramp motion about 0.25c:

Related AGARD CT Case	Run No.	Experimental conditions					Data table
		M	α range (deg)	Re $\times 10^{-6}$	Approx $\dot{\alpha}$ (deg/s)	Sets	
6	218	0.30	-0.03 to 15.54	2.7	1280	16	3.11
7	227	0.57	-0.01 to 14.80	4.6	425	16	3.12
8	230	0.56	-0.01 to 14.97	4.5	1380	16	3.13

Quasi-steady:

Run No.	M	α range in table (deg)	Re $\times 10^{-6}$	Sets	Data table
6	0.30	-0.12 to 15.55	2.6	16	3.14
11	0.58	-0.13 to 11.56	4.6	16	3.15
151	0.75	-3.27 to 3.35	5.5	16	3.16

Figs 3.2 to 3.4 show typical results extracted from Ref 3.2 for oscillatory pitching at M = 0.6 and 0.75, showing the effect of reduced frequency parameter on normal force, pitching moment and a damping factor DF. The related AGARD CT cases 1, 2, 3 and 5 are included in these figures. Figs 3.2 and 3.3 are for respective amplitudes $\alpha_0 = 2.5^\circ$ and 5.0° .

Fig 3.5 shows curves of C_N against α from the quasi-steady data and for the two ramp rates at M = 0.57 to illustrate the lag in the growth of C_N and the delayed stall under dynamic conditions.

1 AIRFOIL

1.1 Designation	NACA 0012
1.2 Type of airfoil	Symmetrical 12% thick
1.3 Geometry	See Table 3.1 and formula in Ref 3.6
1.4 Design condition	-
1.5 Additional remarks	-
1.6 References on airfoil	Refs 3.6, 3.7

2 MODEL GEOMETRY

2.1 Chord length	101.6 mm (4 in)
2.2 Span	203.2 mm (8 in)
2.3 Actual model coordinates and accuracy of measurements	See Fig 3.1 and Table 3.1. TE thickness = 0.383 mm, ie approximately 0.127 mm too thick
2.4 Flap: hinge and gap details	-
2.5 Additional remarks	-
2.6 References on model	-

- 3 WIND TUNNEL
- 3.1 Designation ARA 2-dimensional tunnel
- 3.2 Type of tunnel Intermittent blow down
- 3.3 Test section dimensions $h = 457.2$, $b = 203.2$, length = 1251 mm
- 3.4 Type of roof and floor Slotted, 3.2% open area ratio
- 3.5 Type of side walls Solid
- 3.6 Ventilation geometry Roof and floor each have 6 slots and 2 half slots at corners. Plenum chambers 133 mm deep connected by large ducts. Top and bottom walls diverge.
- 3.7 Thickness of side wall boundary layer $2\delta^*/b = 0.015$
- 3.8 Thickness of boundary layers at roof and floor Not known
- 3.9 Method of measuring Mach number Static hole in side wall 5 chords ahead of model
- 3.10 Uniformity of Mach number over test section Centre line distribution within ± 0.0015 in region of model
- 3.11 Sources and levels of noise or turbulence in empty tunnel No serious disturbances
- 3.12 Tunnel resonances No evidence
- 3.13 Additional remarks
- 3.14 References on tunnel Ref 3.8
- 4 MODEL MOTION
- 4.1 Mode of applied motion Pitching about $0.25c$, oscillation or ramp. No heave results
- 4.2 Range of amplitude Oscillation $\pm 9.5^\circ$; ramp 0 to 30° (limit 44°)
- 4.3 Range of frequency 0 to 60 Hz (limit 100 Hz)
- 4.4 Method of application Hydraulic actuator
- 4.5 Purity of applied motion See Introduction
- 4.6 Natural frequencies and normal modes of model Lowest is bending at 600 Hz
- 4.7 Static or dynamic elastic distortion during tests No significant distortion
- 4.8 Additional remarks -
- 5 TEST CONDITIONS
- 5.1 Tunnel height/model chord ratio 4.5
- 5.2 Tunnel width/model chord ratio 2.0
- 5.3 Range of Mach number 0.3 to 0.87
- 5.4 Range of tunnel total pressure 1.4-4 bar
- 5.5 Range of tunnel total temperature 260 K approximately, uncontrolled
- 5.6 Range of model steady, or mean, incidence ± 11 deg (limit 44°)
- 5.7 Definition of model incidence On chordline: datum matched on chordwise pressure distributions
- 5.8 Position of transition, if free Not known
- 5.9 Position and type of trip, if transition fixed No trip in presented data because model is consistent with full-scale helicopter blade
- 5.10 For mixed flow, position of sonic boundary in relation to roof and floor -
- 5.11 Flow instabilities during tests No simple answer: refer to ARA
- 5.12 Additional remarks Position of model $0.25c$ is 5 chords downstream of start of slots
- 5.13 References describing tests Docs 3.1, 3.2

6 MEASUREMENTS AND OBSERVATIONS

6.1	Steady pressures for the mean conditions		-
6.2	Steady pressures for small changes from the mean conditions		-
6.3	Quasi-steady pressures		✓
6.4	Unsteady pressures		✓
6.5	Steady forces for the mean conditions	measured directly	-
		integrated pressures	-
6.6	Steady forces for small changes from the mean conditions	measured directly	-
		integrated pressures	-
6.7	Quasi-steady forces	measured directly	-
		integrated pressures	✓
6.8	Unsteady forces	measured directly	-
		integrated pressures	✓
6.9	Measurement of actual motion at points on model		-
6.10	Observation or measurement of boundary layer properties		-
6.11	Visualization of surface flow		-
6.12	Visualization of shockwave movements		-
6.13	Additional remarks		-

7 INSTRUMENTATION

7.1	Steady pressures	Pressures for quasi-steady conditions measured with same system used for unsteady pressures
7.1.1	Position of orifices spanwise and chordwise	-
7.1.2	Type of measuring system	-
7.2	Unsteady pressures	
7.2.1	Position of orifices spanwise and chordwise	See Table 3.2
7.2.2	Diameter of orifices	0.25 mm
7.2.3	Type of measuring system	30 transducers in model (see Ref 3.1)
7.2.4	Type of transducers	Kulite XCQL absolute
7.2.5	Principle and accuracy of calibration	Calibrated under steady conditions against Texas Quartz Pressure Test Set. Accuracy: ± 2.7 mb
7.3	Model motion	
7.3.1	Method of measurement	Shaft encoder
7.3.2	Accuracy	Resolution: ± 0.1 deg
7.4	Processing of unsteady measurements	
7.4.1	Method of acquiring and processing measurements	Signals sampled at known time intervals, same points in cycle
7.4.2	Type of analysis	Instantaneous pressures reduced to non-dimensional coefficients
7.4.3	Unsteady pressure quantities obtained and accuracies achieved	Approximately ± 0.01 in C_p
7.4.4	Method of integration to obtain forces	Standard curve fitting procedure
7.5	Additional remarks	Tabulated C_N and C_M are corrected for wall constraint
7.6	References on techniques	Refs 3.1, 3.9, 3.10

- 8 DATA PRESENTATION
- 8.1 Test cases for which data could be made available Tables 3.4, 3.5, 3.6
- 8.2 Test cases for which data are included in this document See Introduction
- 8.3 Steady pressures -
- 8.4 Quasi-steady or steady perturbation pressures Tables 3.14, 3.15, 3.16
- 8.5 Unsteady pressures Tables 3.7 to 3.13
- 8.6 Steady forces or moments -
- 8.7 Quasi-steady or steady perturbation forces Tables 3.14, 3.15, 3.16
- 8.8 Unsteady forces and moments Tables 3.7 to 3.13
- 8.9 Other forms in which data could be made available if required None
- 8.10 References giving other presentations of data Ref 3.1
- 9 COMMENTS ON DATA
- 9.1 Accuracy
- 9.1.1 Mach number ± 0.0015
- 9.1.2 Steady incidence Instantaneous incidence to ± 0.1 deg
- 9.1.3 Reduced frequency Within about 1%
- 9.1.4 Steady pressure coefficients -
- 9.1.5 Steady pressure derivatives -
- 9.1.6 Unsteady pressure coefficients Instantaneous C_p to ± 0.01 (see Ref 3.10)
- 9.2 Sensitivity to small changes of parameter -
- 9.3 Spanwise variations Not serious for data presented here (for other cases see Ref 3.1)
- 9.4 Non-linearities -
- 9.5 Influence of tunnel total pressure -
- 9.6 Wall interference corrections Values of α , α_m , α_0 , C_N and C_m have been corrected on the basis of steady calibrations (see para 12). No corrections appear to be necessary for M .
- 9.7 Other relevant tests on *same model* -
- 9.8 Relevant tests on other models of nominally the *same* aerofoil Ref 3.11 gives steady measurements on another model of NACA 0012 in same tunnel
- 9.9 Any remarks relevant to comparison between experiment and theory -
- 9.10 Additional remarks -
- 9.11 References on discussion of data Ref 3.2
- 10 PERSONAL CONTACT FOR FURTHER INFORMATION
- Mr R.H. Landon, Aircraft Research Association Ltd, Manton Lane, Bedford MK41 7PF, England
- 11 LIST OF REFERENCES
- 3.1 R.H. Landon A description of the ARA 2-dimensional pitch and heave rig and some results from the NACA 0012 wing. ARA Memo 199, September 1977
- 3.2 Mrs M.E. Wood Results of oscillatory pitch and ramp tests on the NACA 0012 blade section. ARA Memo 220, December 1979

- 3.3 A. Harris Calibration of ARA's 2-dimensional facility using 2.8% open area liners.
April 1971, unpublished Memorandum
- 3.4 A. Harris Evidence on wall interference effects in the ARA 2-dimensional tunnel.
A.B. Haines ARA Memo 147, 1972
- 3.5 A.B. Haines An evaluation of wall interference effects in ARA's 2-dimensional tunnel.
Item 5, Tech Comm., June 1973
- 3.6 Ed. S.R. Bland AGARD two-dimensional aeroelastic configurations.
AGARD-AR-156, 1979
- 3.7 I.H. Abbott Theory of wing sections: including a summary of airfoil data.
A.E. von Doenhoff McGraw-Hill, New York, 1949
- 3.8 B.L.F. Hammond Some notes on model testing in the ARA 2-dimensional facility.
ARA Memo 170, 1975
- 3.9 R.H. Landon Some sources of error with Kulite pressure transducers in the
Mrs M.E. Wood ARA pitch/heave rig.
ARA Memo 204, 1978
- 3.10 R.H. Landon The pitch/heave rig data selection and reduction program, and
Mrs M.E. Wood Corrigendum.
ARA Memo 182, 1976
- 3.11 Mrs J. Sawyer Results of tests on aerofoil M.102/9 (NACA 0012) in the ARA
2-dimensional tunnel.
ARA Model Test Note M.102/9, 1978

12 DEFINITIONS AND EXPLANATION OF DATA TABLES

- b airfoil span and tunnel width
- c chord
- C_N normal force coefficient
- C_m pitching moment coefficient (about 0.25c)
- f frequency (Hz)
- h tunnel height
- k reduced frequency, $\omega c/2V$
- M Mach number
- q dynamic pressure
- R, Re Reynolds number
- t time (seconds)
- V velocity
- x,y,z airfoil coordinates
- α incidence
- α_m mean incidence
- α_0 pitch amplitude
- δ^* displacement thickness of boundary layer
- ω frequency (rad/s)

For each chosen case, experimental data are presented as sets of instantaneous values of the quantities C_p , C_N , C_m , α and M for particular times t (in seconds) in Tables 3.7 to 3.16.

Uncorrected coefficients C_N' and C_m' are evaluated by a curve fitting procedure from the integrals

$$C_N' = \int_0^1 (C_{pL} - C_{pU}) d(x/c)$$

$$C_m' = \int_0^1 (C_{pL} - C_{pU}) (0.25 - (x/c)) d(x/c)$$

where $C_p = (p - p_\infty)/q$ is uncorrected and the suffices L and U denote lower and upper surfaces respectively.

Oscillatory motion is defined by

$$\alpha = \alpha_m + \alpha_0 \sin(\omega t + \epsilon)$$

where ϵ is a phase angle dependent on the time datum.

The quantities α , α_m , α_0 , C_N and C_m (but not C_p) have each been corrected for tunnel constraint effects. The corrections, as derived for steady conditions in Refs 3.3, 3.4 and 3.5, are applied to each instantaneous condition as if it were steady.

Table 3.1

NACA 0012 SECTION ORDINATES

x/c	z/c
0	0
0.0050	±0.01221
0.0125	±0.01894
0.0250	±0.02615
0.0500	±0.03555
0.0750	±0.04200
0.1000	±0.04683
0.1500	±0.05345
0.2000	±0.05738
0.2500	±0.05941
0.3000	±0.06002
0.3500	±0.05949
0.4000	±0.05803
0.4500	±0.05581
0.5000	±0.05294
0.5500	±0.04952
0.6000	±0.04563
0.6500	±0.04132
0.7000	±0.03664
0.7500	±0.03160
0.8000	±0.02623
0.8500	±0.02053
0.9000	±0.01448
0.9500	±0.00807
1.0000	±0.00126

Table 3.2

NACA 0012 WING PRESSURE LOCATIONS AND CHANNEL NUMBER IDENTITIES

Upper surface			Lower surface		
Channel No.	x/c	y/b	Channel No.	x/c	y/b
1	1.0 TE	0.52	21	0 LE	0.44
2	0.9	0.51	22	0.01	0.46
3	0.8	0.48	23	0.02	0.48
4	0.7	0.49	24	0.04	0.48
5	0.6	0.5	25	0.10	0.48
6	0.5	0.5	26	0.22	0.5
7	0.4	0.5	27	0.34	0.5
8	0.3	0.5	28	0.46	0.5
9	0.2	0.51	29	0.57	0.5
10	0.15	0.48	30	0.68	0.5
11	0.125	0.48	31	0.79	0.54
12	0.1	0.49	32	0.90	0.55
13	0.075	0.5			
14	0.05	0.51			
15	0.03	0.52			
16	0.02	0.53			
17	0.01	0.55			
18	0.005	0.56			

Table 3.3

LAYOUT OF RESULTS IN TABLES 3.7 TO 3.16

C_{p1}	C_{p2}	C_{p3}	C_{p4}	C_{p5}	C_{p6}	C_{p7}	C_{p8}	C_{p9}	C_{p10}	Data point	
C_{p11}	C_{p12}	C_{p13}	C_{p14}	C_{p15}	C_{p16}	C_{p17}	C_{p18}	C_{p21}	C_{p22}	M	C_N
C_{p23}	C_{p24}	C_{p25}	C_{p26}	C_{p27}	C_{p28}	C_{p29}	C_{p30}	C_{p31}	C_{p32}	t (second)	C_m
										q (lb/ft ²)	α (deg)

where, in the arrangement above, C_{pn} is the instantaneous value of C_p for channel n (see Table 3.2). Corresponding x/c locations can be identified from the following key:

<u>Upper</u>										
1.00	0.90	0.80	0.70	0.60	0.50	0.40	0.30	0.10	0.15	
<u>Upper</u>										<u>Lower</u>
0.125	0.10	0.075	0.05	0.03	0.02	0.01	0.005	0	0.01	
<u>Lower</u>										
0.02	0.04	0.10	0.22	0.34	0.46	0.57	0.68	0.79	0.90	

Table 3.4

PARAMETERS OF OSCILLATORY PITCH CASES

ARA run No.	M	α_0 (deg)	α_m (deg)	f (Hz)	k	Re $\times 10^{-6}$	ARA run No.	M	α_0 (deg)	α_m (deg)	f (Hz)	k	Re $\times 10^{-6}$
152	0.288	8.5	4,5,6	30	0.099	2.7	178	0.598	2.5	3,4,5	30	0.050	4.9
153	0.286	8.5	7,8,9	30	0.099	2.7	179	0.593	2.5	6,8,10	30	0.050	4.9
183	0.287	8.5	10,11,12	30	0.101	2.7	180	0.597	5.0	3,4,5	30	0.050	4.9
184	0.286	7.5	6	30	0.102	2.7	202	0.600	5.0	6,9,12	30	0.049	5.0
156	0.292	9.5	6	30	0.096	2.7	87	0.600	2.5	3,4,5	50	0.081	4.9
185	0.287	9.5	6	30	0.102	2.7	88	0.595	2.5	6,8,10	50	0.082	4.9
186	0.285	Max	6	30	0.102	2.7	89	0.598	5.0	3,4,5	50	0.082	4.9
157	0.290	2.5	9,10,11	30	0.097	2.7	90	0.592	5.0	6,9,12	50	0.083	4.9
158	0.286	2.5	12,14,16	30	0.099	2.7	91	0.599	2.5	3,4,5	70	0.115	4.9
159	0.288	5.0	9,10,11	30	0.098	2.7	92	0.594	2.5	6,8,10	70	0.116	4.9
160	0.286	5.0	12,15,18	30	0.099	2.7	93	0.599	5.0	3,4,5	70	0.115	4.9
199	0.305	2.5	9,10,11	50	0.155	2.8	94	0.591	5.0	6,9,12	70	0.117	4.9
200	0.298	2.5	9,10,11	50	0.159	2.8							
188	0.285	2.5	12,14,16	50	0.168	2.6							
39	0.290	5.0	9,10,11	50	0.170	2.7	103	0.699	2.5	1,2,3	29	0.041	5.4
40	0.287	5.0	12,15,18	50	0.172	2.7	96	0.688	2.5	4,6,8	29	0.042	5.4
116	0.287	2.5	9,10,11	70	0.238	2.7	104	0.697	5.0	1,2,3	29	0.041	5.4
43	0.289	2.5	12,14,16	70	0.245	2.7	98	0.686	5.0	4,6,8	29	0.042	5.4
117	0.292	5.0	9,10,11	70	0.231	2.7	105	0.699	2.5	1,2,3	58	0.081	5.5
44	0.287	5.0	12,15,18	70	0.245	2.7	100	0.686	2.5	4,6,8	58	0.083	5.4
							106	0.696	5.0	1,2,3	58	0.082	5.4
							102	0.685	5.0	4,6,8	58	0.083	5.4
161	0.382	8.5	2,3,4	30	0.075	3.5	122	0.700	2.5	1,2,3	80	0.115	5.5
162	0.380	8.5	5,6,7	30	0.075	3.5	123	0.691	2.5	4,6,8	80	0.116	5.4
163	0.379	8.5	8,9,10	30	0.076	3.5	124	0.698	5.0	1,2,3	70	0.101	5.5
164	0.380	7.5	4	30	0.076	3.5	125	0.691	5.0	4,6,8	70	0.101	5.4
165	0.380	9.5	4	30	0.076	3.5	95	0.699	2.5	0,1,2	29	0.041	5.4
166	0.380	Max	4	30	0.076	3.5	97	0.696	5.0	0,1,2	29	0.041	5.4
201	0.398	2.5	3,9	30	0.073	3.6	99	0.697	2.5	0,1,2	58	0.082	5.4
168	0.377	2.5	10,12,14	30	0.077	3.4	101	0.693	5.0	0,1,2	58	0.082	5.4
169	0.379	5.0	6,8,10	30	0.076	3.4							
170	0.377	5.0	9,12,15	30	0.077	3.4							
59	0.377	2.5	7,8,9	50	0.126	3.3	126	0.754	2.5	0,1,2	31	0.042	5.7
60	0.383	2.5	10,12,14	50	0.128	3.3	127	0.744	2.5	3,4,5	31	0.042	5.6
61	0.380	5.0	6,8,10	50	0.127	3.4	128	0.753	2.5	0,1,2	62	0.082	5.7
62	0.380	5.0	9,12,15	50	0.128	3.4	129	0.743	2.5	3,4,5	62	0.083	5.6
63	0.381	2.5	7,8,9	70	0.182	3.5	130	0.753	2.5	0,1,2	80	0.108	5.7
64	0.378	2.5	10,12,14	70	0.184	3.4	131	0.744	2.5	3,4,5	80	0.108	5.6
65	0.378	5.0	6,8,10	70	0.184	3.4							
66	0.378	5.0	9,12,15	70	0.184	3.4							
171	0.483	8.5	0,1,2	30	0.060	4.2	138	0.805	2.5	0,1,1	33	0.041	5.9
172	0.482	8.5	3,4,5	30	0.060	4.2	203	0.816	2.5	0,1,1	33	0.041	6.0
173	0.482	8.5	6,7,8	30	0.060	4.2	204	0.802	2.5	0,1,1	33	0.041	6.0
174	0.483	2.5	5,6,7	30	0.060	4.2	139	0.794	2.5	2,2,1,3	33	0.041	5.8
175	0.481	2.5	8,10,12	30	0.061	4.2	134	0.785	2.5	0,1,1	66	0.082	5.8
176	0.483	5.0	5,6,7	30	0.060	4.2	135	0.792	2.5	2,2,1,3	66	0.081	5.8
177	0.479	5.0	9,12,15	30	0.061	4.2	136	0.799	2.5	0,1,1	80	0.101	5.9
							137	0.794	2.5	2,2,1,3	80	0.102	5.9
107	0.484	2.5	5,6,7	50	0.100	4.2	142	0.814	2.5	0,1,2	80	0.100	5.9
108	0.481	2.5	8,10,12	50	0.101	4.2	141	0.821	2.5	0,1,2	80	0.099	5.9
119	0.489	5.0	5,6,7	50	0.099	4.2	143	0.829	2.5	0,1,2	80	0.098	6.0
109	0.479	5.0	9,12,15	50	0.101	4.1	144	0.840	2.5	0,1,2	80	0.097	5.9
78	0.480	2.5	5,6,7	70	0.147	4.2	145	0.866	2.5	0,1,2	80	0.094	6.0
118	0.488	2.5	8,10,12	70	0.141	4.2	146	0.878	2.5	0,1,2	80	0.093	6.0
80	0.480	5.0	5,6,7	70	0.147	4.2	147	0.896	2.5	0,1,2	80	0.092	6.0
81	0.476	5.0	9,12,15	70	0.149	4.2							

Table 3.5

PARAMETERS OF RAMP PITCH CASES

ARA run No.		α° range	$\frac{d\alpha}{dt}$ (deg/s)	$Re \times 10^{-6}$
215	0.296	0-30	400	2.7
216	0.298	0-30	800	2.7
242	0.299	0-30	1200	2.7
218	0.294	0-30	1600	2.7
214	0.406	0-30	400	3.5
243	0.410	0-30	800	3.5
222	0.410	0-30	1200	3.6
219	0.412	0-30	1600	3.6
223	0.504	0-30	400	4.2
224	0.501	0-30	800	4.2
225	0.502	0-30	1200	4.2
226	0.496	0-30	1600	4.2
227	0.613	0-30	400	4.8
228	0.615	0-30	800	4.8
229	0.614	0-30	1200	4.8
230	0.611	0-30	1600	4.7
231	0.707	0-30	800	5.2
232	0.706	0-30	1600	5.2
233	0.761	0-30	1600	5.3
234	0.760	0-30	800	5.3
235	0.806	0-30	800	5.5
237	0.809	0-30	1600	5.5
239	0.834	0-30	800	5.7
238	0.838	0-30	1600	5.4
240	0.900	0-30	800	5.9
241	0.902	0-30	1600	5.9
236	0.812	0-30	800	5.5

Table 3.6

PARAMETERS OF QUASI-STEADY CASES

N	ARA run No.	α_0 (deg)	α_m (deg)	N	ARA run No.	α_0 (deg)	α_m (deg)
0.3	6	11	11	0.75	14	5	5
0.3	189	11	11	0.75	192	5	5
0.3	278	11	11	0.8	15	4	4
0.4	7	11	11	0.8	193	4	4
0.4	245	11	11	0.8	296	4	4
0.45	190	11	11				
0.5	9	10	10	0.4	148	0	11
0.5	279	10	10	0.6	149	0	9
0.55	46	10	10	0.7	150	0	7
0.6	11	9	9	0.75	151	0	5
0.6	280	9	9	0.3	244	0	11
0.65	12	8	8	0.5	246	0	10
0.65	191	8	8	0.6	247	0	8
0.7	13	7	7	0.7	248	0	7
0.7	281	7	7	0.8	249	0	4

Table 3.7

ARA RUN 87 PSTEP 1		AGARD CASE 1		OSC. PITCH		Damping +0.06708					
M=0.6	R=4.8*10 ⁸	$\omega_c/2V=0.0808$	$\alpha_m=2.89$	$\alpha_o=2.41$							
0.1647	-0.0007	-0.1408	-0.2437	-0.3383	-0.4547	-0.5712	-0.7231	-0.8666	-0.9290	2	
-1.0117	-1.0640	-1.1383	-1.1316	-1.1076	-0.9442	-0.7231	-0.5408	0.9766	0.6306	0.602	0.3719
0.3993	0.1580	-0.1897	-0.2488	-0.2454	-0.1948	-0.1560	-0.1070	-0.0530	0.0263	0.00000	0.0014
										1706.3	2.97
0.1562	-0.0024	-0.1493	-0.2539	-0.3501	-0.4716	-0.5965	-0.7535	-0.9172	-0.9965	4	
-1.0894	-1.1484	-1.2615	-1.2683	-1.2582	-1.0928	-0.8683	-0.6860	0.9191	0.7031	0.602	0.4267
0.4752	0.2254	-0.1358	-0.2151	-0.2134	-0.1746	-0.1391	-0.0986	-0.0497	0.0263	0.00062	0.0022
										1706.3	3.42
0.1645	0.0044	-0.1439	-0.2518	-0.3512	-0.4760	-0.6057	-0.7760	-0.9597	-1.0507	6	
-1.1519	-1.2277	-1.3979	-1.4097	-1.4148	-1.2328	-1.0103	-0.8316	0.8674	0.7747	0.602	0.4777
0.5455	0.2977	-0.0731	-0.1759	-0.1810	-0.1473	-0.1203	-0.0815	-0.0343	0.0348	0.00124	0.0043
										1708.7	3.84
0.1657	0.0078	-0.1416	-0.2519	-0.3571	-0.4879	-0.6304	-0.8070	-1.0107	-1.1024	8	
-1.2161	-1.3044	-1.5827	-1.5929	-1.5963	-1.3689	-1.1516	-0.9699	0.8138	0.8277	0.600	0.5285
0.6036	0.3538	-0.0312	-0.1348	-0.1368	-0.1314	-0.1059	-0.0720	-0.0261	0.0367	0.00187	0.0070
										1696.6	4.23
0.1594	0.0044	-0.1473	-0.2586	-0.3681	-0.4996	-0.6445	-0.8299	-1.0406	-1.1434	10	
-1.2446	-1.4333	-1.7570	-1.7772	-1.7182	-1.4772	-1.2581	-1.0878	0.7460	0.8372	0.602	0.5731
0.6449	0.4005	0.0094	-0.0968	-0.1389	-0.1187	-0.0984	-0.0647	-0.0260	0.0398	0.00249	0.0083
										1708.7	4.56
0.1632	0.0094	-0.1351	-0.2530	-0.3616	-0.4954	-0.6441	-0.8296	-1.0419	-1.1271	12	
-1.2191	-1.6887	-1.9077	-1.9043	-1.8024	-1.5817	-1.3528	-1.1940	0.6830	0.8936	0.605	0.6049
0.6880	0.4540	0.0529	-0.0641	-0.1143	-0.0976	-0.0825	-0.0558	-0.0173	0.0378	0.00311	0.0124
										1723.1	4.83
0.1537	-0.0008	-0.1571	-0.2721	-0.3871	-0.5211	-0.6807	-0.8730	-1.0791	-1.1237	14	
-1.4293	-1.9393	-2.0835	-2.0577	-1.9461	-1.7401	-1.4929	-1.3194	0.6413	0.9229	0.596	0.6485
0.7186	0.4782	0.0627	-0.0661	-0.1193	-0.1038	-0.0953	-0.0643	-0.0283	0.0301	0.00373	0.0149
										1677.4	4.98
0.1479	0.0043	-0.1493	-0.2675	-0.3803	-0.5205	-0.6778	-0.8710	-1.0556	-1.1018	16	
-1.8471	-2.0318	-2.1514	-2.1138	-1.9976	-1.8078	-1.5616	-1.3719	0.6010	0.9395	0.597	0.6717
0.7343	0.5001	0.0630	-0.0921	-0.1085	-0.0948	-0.0880	-0.0640	-0.0264	0.0300	0.00435	0.0189
										1684.6	5.11
0.1559	0.0111	-0.1387	-0.2548	-0.3659	-0.5005	-0.6520	-0.8389	-0.9887	-1.0863	18	
-2.0255	-2.0675	-2.1551	-2.1130	-2.0002	-1.8218	-1.5761	-1.3707	0.5750	0.9402	0.603	0.6725
0.7433	0.5127	0.1003	-0.0326	-0.0949	-0.0781	-0.0781	-0.0545	-0.0158	0.0364	0.00497	0.0208
										1711.1	5.09
0.1533	0.0094	-0.1429	-0.2580	-0.3697	-0.5119	-0.6643	-0.8504	-0.9926	-1.1213	20	
-2.0945	-2.1233	-2.1994	-2.1571	-2.0471	-1.8643	-1.6223	-1.3971	0.5646	0.9369	0.601	0.6756
0.7440	0.5087	0.0940	-0.0414	-0.1057	-0.1006	-0.0888	-0.0685	-0.0261	0.0297	0.00559	0.0236
										1701.5	5.05
0.1553	0.0061	-0.1430	-0.2645	-0.3642	-0.5065	-0.6591	-0.8443	-0.9918	-1.0792	22	
-2.1234	-2.1594	-2.2365	-2.1902	-2.0839	-1.8936	-1.6484	-1.4015	0.5737	0.9389	0.597	0.6694
0.7400	0.5034	0.0833	-0.0522	-0.1207	-0.1122	-0.0967	-0.0710	-0.0333	0.0301	0.00621	0.0254
										1579.7	4.82
0.1552	0.0077	-0.1381	-0.2482	-0.3567	-0.4940	-0.6432	-0.8313	-0.9906	-0.9933	24	
-1.9992	-2.1144	-2.1924	-2.1551	-2.0534	-1.8619	-1.6110	-1.3296	0.6027	0.9128	0.600	0.6422
0.7145	0.4755	0.0653	-0.0686	-0.1313	-0.1177	-0.1023	-0.0770	-0.0364	0.0247	0.00683	0.0262
										1699.1	4.54
0.1494	0.0099	-0.1426	-0.2523	-0.3603	-0.4936	-0.6354	-0.8244	-1.0101	-1.0320	26	
-1.4118	-2.0548	-2.1358	-2.1172	-2.0295	-1.8134	-1.5637	-1.2784	0.6237	0.8783	0.601	0.6039
0.6743	0.4363	0.0313	-0.0936	-0.1510	-0.1392	-0.1189	-0.0903	-0.0447	0.0194	0.00745	0.0238
										1706.4	4.17
0.1597	0.0112	-0.1373	-0.2449	-0.3524	-0.4873	-0.6256	-0.8168	-1.0216	-1.1070	28	
-1.0848	-1.9657	-2.0698	-2.0784	-2.0067	-1.7472	-1.4945	-1.2077	0.6889	0.8665	0.598	0.5739
0.6582	0.4124	0.0095	-0.1151	-0.1648	-0.1527	-0.1271	-0.0947	-0.0486	0.0231	0.00807	0.0238
										1687.0	3.80
0.1583	0.0077	-0.1328	-0.2411	-0.3427	-0.4747	-0.6067	-0.7878	-0.9892	-1.0857	30	
-1.1591	-1.3613	-1.9049	-1.9574	-1.9134	-1.6290	-1.3667	-1.0891	0.7338	0.8201	0.601	0.5269
0.6032	0.3598	-0.0380	-0.1446	-0.1903	-0.1649	-0.1396	-0.1023	-0.0532	0.0179	0.00869	0.0220
										1701.5	3.40
0.1601	0.0094	-0.1294	-0.2309	-0.3342	-0.4611	-0.5898	-0.7658	-0.9588	-1.0483	32	
-1.1923	-1.2651	-1.6663	-1.7644	-1.8068	-1.4953	-1.2279	-0.9486	0.7914	0.7796	0.601	0.4768
0.5544	0.3107	-0.0786	-0.1734	-0.2106	-0.1765	-0.1514	-0.1091	-0.0549	0.0179	0.00931	0.0192
										1701.5	3.01

(continued overleaf)

Table 3.7 (concluded)

ARA RUN 87 PSTEP 1		AGARD CASE 1 -		OSC. PITCH		Damping +0.06708					
M=0.6	R=4.8*10 ⁴	$\omega_c/2v=0.0808$	$\alpha_m=2.89$	$\alpha_o=2.41$							
0.1600	0.0043	-0.1328	-0.2360	-0.3308	-0.4493	-0.5695	-0.7370	-0.9131	-0.9943	34	
-1.1162	-1.2482	-1.4767	-1.5715	-1.6476	-1.3464	-1.0840	-0.8132	0.8472	0.7287	0.601	0.4294
0.4969	0.2582	-0.1209	-0.2089	-0.2326	-0.1988	-0.1649	-0.1209	-0.0634	0.0145	0.00994	0.0166
										1701.5	2.62
0.1698	0.0162	-0.1203	-0.2167	-0.3079	-0.4243	-0.5476	-0.7028	-0.8649	-0.9307	36	
-1.0556	-1.1653	-1.3290	-1.3881	-1.3949	-1.1467	-0.9020	-0.6421	0.9192	0.6761	0.602	0.3774
0.4432	0.2052	-0.1593	-0.2336	-0.2488	-0.2100	-0.1678	-0.1222	-0.0614	0.0213	0.01056	0.0152
										1706.3	2.24
0.1622	0.0078	-0.1280	-0.2231	-0.3097	-0.4251	-0.5405	-0.6848	-0.8342	-0.8953	38	
-1.0056	-1.0973	-1.2178	-1.2517	-1.2195	-1.0175	-0.7663	-0.5167	0.9600	0.6138	0.600	0.3342
0.3761	0.1368	-0.2112	-0.2740	-0.2808	-0.2350	-0.1908	-0.1348	-0.0686	0.0163	0.01118	0.0121
										1696.6	1.87
0.1621	0.0060	-0.1281	-0.2181	-0.2995	-0.4133	-0.5185	-0.6611	-0.7867	-0.8410	40	
-0.9530	-1.0311	-1.1177	-1.1245	-1.0718	-0.8716	-0.6271	-0.3861	0.9972	0.3440	0.599	0.2803
0.2996	0.0671	-0.2639	-0.3148	-0.3131	-0.2588	-0.2113	-0.1502	-0.0857	0.0043	0.01180	0.0128
										1696.8	1.48
0.1647	0.0094	-0.1188	-0.2083	-0.2876	-0.3973	-0.4969	-0.6252	-0.7383	-0.7855	42	
-0.8784	-0.9375	-0.9982	-0.9796	-0.9088	-0.7147	-0.4716	-0.2353	1.0340	0.4753	0.602	0.2361
0.2289	0.0044	-0.3045	-0.3450	-0.3281	-0.2657	-0.2100	-0.1475	-0.0783	0.0128	0.01242	0.0090
										1706.3	1.16
0.1712	0.0129	-0.1182	-0.2016	-0.2799	-0.3894	-0.4808	-0.5982	-0.7106	-0.7565	44	
-0.8314	-0.8876	-0.9285	-0.8910	-0.8127	-0.6084	-0.3616	-0.1216	1.0564	0.4129	0.599	0.1965
0.1678	-0.0552	-0.3497	-0.3769	-0.3480	-0.2782	-0.2237	-0.1590	-0.0898	0.0129	0.01304	0.0086
										1691.8	0.89
0.1649	0.0111	-0.1123	-0.1951	-0.2711	-0.3743	-0.4605	-0.5703	-0.6684	-0.7224	46	
-0.7748	-0.8205	-0.8492	-0.8036	-0.7089	-0.5078	-0.2661	-0.0311	1.0641	0.3525	0.601	0.1606
0.1007	-0.1072	-0.3895	-0.3996	-0.3590	-0.2897	-0.2272	-0.1613	-0.0869	0.0128	0.01366	0.0068
										1703.9	0.62
0.1669	0.0144	-0.1079	-0.1900	-0.2621	-0.3593	-0.4448	-0.5470	-0.6359	-0.6878	48	
-0.7247	-0.7582	-0.7750	-0.7197	-0.6174	-0.4096	-0.1699	0.0429	1.0670	0.2960	0.604	0.1309
0.0463	-0.1532	-0.4146	-0.4163	-0.3694	-0.2923	-0.2303	-0.1616	-0.0845	0.0161	0.01428	0.0091
										1718.3	0.50
0.1664	0.0078	-0.1183	-0.2019	-0.2752	-0.3689	-0.4593	-0.5530	-0.6349	-0.6860	50	
-0.7116	-0.7406	-0.7523	-0.6894	-0.5871	-0.3843	-0.1354	0.0698	1.0835	0.2984	0.599	0.1245
0.0095	-0.1899	-0.4422	-0.4354	-0.3826	-0.2990	-0.2325	-0.1609	-0.0876	0.0129	0.01490	0.0019
										1689.4	0.44
0.1672	0.0128	-0.1131	-0.1954	-0.2675	-0.3582	-0.4454	-0.5411	-0.6233	-0.6703	52	
-0.6972	-0.7190	-0.7240	-0.6619	-0.5596	-0.3615	-0.1131	0.0917	1.0668	0.2410	0.604	0.1166
0.0010	-0.1954	-0.4387	-0.4303	-0.3783	-0.2944	-0.2306	-0.1584	-0.0829	0.0161	0.01352	0.0019
										1715.9	0.53
0.1613	0.0044	-0.1232	-0.2066	-0.2809	-0.3720	-0.4615	-0.5560	-0.6387	-0.6809	54	
-0.7096	-0.7265	-0.7299	-0.6691	-0.5644	-0.3687	-0.1172	0.0887	1.0711	0.2525	0.602	0.1286
0.0094	-0.1914	-0.4362	-0.4277	-0.3737	-0.2927	-0.2286	-0.1594	-0.0851	0.0111	0.01614	0.0000
										1706.3	0.70
0.1647	0.0061	-0.1205	-0.2083	-0.2842	-0.3821	-0.4682	-0.5729	-0.6623	-0.6910	56	
-0.7349	-0.7484	-0.7535	-0.6944	-0.5965	-0.4108	-0.1627	0.0263	1.0711	0.2829	0.602	0.1479
0.0432	-0.1644	-0.4159	-0.4125	-0.3670	-0.2809	-0.2201	-0.1543	-0.0817	0.0128	0.01676	0.0002
										1706.3	0.96
0.1582	0.0044	-0.1292	-0.2171	-0.2931	-0.3928	-0.4892	-0.6024	-0.6920	-0.7174	58	
-0.7731	-0.7684	-0.7968	-0.7427	-0.6565	-0.4807	-0.2357	-0.0447	1.0675	0.3390	0.601	0.1845
0.1024	-0.1140	-0.3810	-0.3844	-0.3421	-0.2610	-0.2103	-0.1444	-0.0785	0.0145	0.01738	-0.0010
										1703.9	1.29
0.1689	0.0095	-0.1231	-0.2154	-0.2943	-0.3967	-0.4974	-0.6199	-0.7173	-0.7425	60	
-0.8077	-0.8314	-0.8449	-0.8012	-0.7290	-0.5545	-0.3229	-0.1298	1.0602	0.4123	0.604	0.2205
0.1773	-0.0459	-0.3296	-0.3480	-0.3161	-0.2473	-0.1936	-0.1315	-0.0660	0.0263	0.01800	-0.0005
										1712.8	1.60
0.1577	0.0010	-0.1355	-0.2282	-0.3159	-0.4238	-0.5266	-0.6347	-0.7275	-0.8080	62	
-0.8022	-0.9159	-0.9412	-0.9075	-0.8485	-0.6816	-0.4575	-0.2687	1.0325	0.4830	0.602	0.2720
0.2487	0.0161	-0.2872	-0.3193	-0.2923	-0.2316	-0.1844	-0.1254	-0.0648	0.0195	0.01862	-0.0004
										1708.7	2.12
0.1603	0.0010	-0.1397	-0.2300	-0.3279	-0.4397	-0.5482	-0.6606	-0.8177	-0.8720	64	
-0.9516	-0.9941	-1.0381	-1.0177	-0.9771	-0.8076	-0.5852	-0.4092	1.0163	0.3603	0.600	0.3211
0.3247	0.0857	-0.2397	-0.2821	-0.2719	-0.2143	-0.1719	-0.1211	-0.0634	0.0213	0.01925	0.0011
										1699.1	2.57

Table 3.8

ARA RUN 89 PSTEP 1		AGARD CASE 2		OSC. PITCH		Damping					
M=0.60	R=4.8*10 ⁶	$\omega_c/2v=0.0211$	$\alpha_m=3.16$	$\alpha_p=4.59$			+0.2455				
0.1627	0.0061	-0.1505	-0.2646	-0.3838	-0.5182	-0.6697	-0.8723	-1.0902	-1.1889	8	
-1.3285	-1.5691	-1.8937	-1.8920	-1.7677	-1.5430	-1.3200	-1.1634	0.7517	0.9185	0.599	0.6384
0.7057	0.4725	0.0622	-0.0501	-0.0978	-0.0773	-0.0654	-0.0348	-0.0024	0.0320	0.00000	0.0049
										1691.9	5.32
0.1378	-0.0078	-0.1567	-0.2800	-0.4015	-0.5419	-0.6754	-0.9253	-1.6769	-2.5089	16	
-2.5277	-2.4832	-2.5465	-2.4917	-2.3959	-2.2264	-1.9491	-1.7933	0.3312	1.0639	0.596	0.9280
0.9047	0.6958	0.2696	0.1018	0.0145	0.0008	-0.0112	-0.0026	0.0128	0.0470	0.00248	0.0258
										1682.3	7.36
0.0812	-0.0198	-0.1464	-0.2560	-0.3570	-0.4922	-0.6138	-0.7935	-1.6529	-2.3086	24	
-2.6732	-2.6578	-2.6800	-2.6355	-2.5499	-2.3770	-2.1117	-1.9662	0.2113	1.0484	0.596	0.8720
0.8910	0.6821	0.2490	0.0727	-0.0266	-0.0323	-0.0626	-0.0557	-0.0352	-0.0009	0.00496	0.0457
										1682.4	6.00
0.1562	0.0094	-0.1287	-0.2323	-0.3359	-0.4741	-0.6122	-0.8091	-0.9956	-0.9921	32	
-1.5205	-2.2389	-2.3028	-2.2873	-2.2113	-1.9557	-1.6950	-1.3254	0.6052	0.8935	0.594	0.5878
0.6811	0.4359	0.0180	-0.1218	-0.1823	-0.1719	-0.1529	-0.1132	-0.0648	0.0042	0.00745	0.0373
										1667.8	3.68
0.1677	0.0196	-0.1081	-0.1932	-0.2749	-0.3804	-0.4774	-0.6102	-0.7396	-0.7804	40	
-0.8860	-0.9711	-1.0630	-1.0306	-0.9728	-0.7651	-0.5370	-0.2698	1.0086	0.5098	0.599	0.2027
0.2596	0.0366	-0.2902	-0.3413	-0.3276	-0.2698	-0.2221	-0.1506	-0.0825	0.0111	0.00993	0.0150
										1691.9	0.86
0.1788	0.0349	-0.0802	-0.1462	-0.2072	-0.2833	-0.3510	-0.4289	-0.4678	-0.4949	48	
-0.5169	-0.5169	-0.4949	-0.3764	-0.2275	-0.0040	0.2363	0.4310	1.0877	-0.0430	0.601	0.0525
-0.2833	-0.4374	-0.6134	-0.5559	-0.4645	-0.3527	-0.2698	-0.1835	-0.0955	0.0146	0.01241	0.0047
										1701.4	-1.30
0.1680	0.0144	-0.1054	-0.1763	-0.2421	-0.3164	-0.3856	-0.4598	-0.4835	-0.4902	56	
-0.4987	-0.4750	-0.4328	-0.3215	-0.1831	0.0195	0.2676	0.4515	1.0676	-0.1426	0.601	-0.0376
-0.3738	-0.5054	-0.6489	-0.5994	-0.4565	-0.3333	-0.2573	-0.1712	-0.0885	0.0178	0.01490	-0.0073
										1706.4	0.57
0.1607	0.0129	-0.1272	-0.2210	-0.3078	-0.4159	-0.5154	-0.6434	-0.7484	-0.7855	64	
-0.8446	-0.8699	-0.8834	-0.8378	-0.7703	-0.6049	-0.3838	-0.1964	1.0644	0.4787	0.602	0.2686
0.2374	0.0112	-0.2842	-0.3095	-0.2758	-0.2116	-0.1610	-0.1070	-0.0479	0.0348	0.01738	-0.0044
										1706.3	2.38

Table 3.9

ARA RUN 87 PSTEP 3		AGARD CASE 3		OSC. PITCH		Damping					
M=0.60	R=4.8*10 ⁶	$\omega_c/2v=0.0210$	$\alpha_m=4.16$	$\alpha_p=2.44$			+0.26372				
0.1498	-0.0008	-0.1559	-0.2735	-0.3874	-0.5377	-0.6929	-0.8855	-1.0492	-1.4631	8	
-2.1453	-2.1623	-2.2748	-2.2049	-2.0993	-1.9169	-1.6748	-1.4941	0.5072	0.9846	0.598	0.7902
0.7953	0.5669	0.1475	0.0112	-0.0593	-0.0553	-0.0519	-0.0349	-0.0059	0.0436	0.00000	0.0168
										1689.4	5.35
0.1243	-0.0077	-0.1620	-0.2786	-0.3930	-0.5272	-0.6729	-0.8083	-1.0079	-2.5365	16	
-2.5640	-2.5434	-2.5691	-2.5160	-2.4320	-2.2622	-1.9965	-1.0130	0.2821	1.0430	0.596	0.9064
0.8873	0.6747	0.2512	0.0649	-0.0008	-0.0180	-0.0265	-0.0180	0.0043	0.0420	0.00248	0.0247
										1679.0	6.97
0.1163	-0.0110	-0.1485	-0.2588	-0.3657	-0.5032	-0.6373	-0.7731	-1.5573	-1.9307	24	
-2.5891	-2.5893	-2.6012	-2.5337	-2.4824	-2.3109	-2.0410	-1.8038	0.2708	1.0329	0.600	0.8480
0.8768	0.6612	0.2318	0.0654	-0.0262	-0.0415	-0.0517	-0.0449	-0.0212	0.0213	0.00496	0.0378
										1696.7	6.57
0.1428	-0.0025	-0.1427	-0.2539	-0.3564	-0.5017	-0.6483	-0.8265	-0.9274	-1.2044	32	
-2.3370	-2.4062	-2.4369	-2.3925	-2.3341	-2.1070	-1.8796	-1.5360	0.4761	0.9480	0.597	0.6985
0.7616	0.5274	0.1103	-0.0402	-0.1065	-0.1068	-0.1017	-0.0812	-0.0402	0.0197	0.00745	0.0333
										1684.7	3.11
0.1620	0.0112	-0.1278	-0.2346	-0.3295	-0.4634	-0.5990	-0.7804	-0.9966	-1.0937	40	
-1.3279	-1.3517	-1.4331	-1.4839	-1.4300	-1.2602	-1.0940	-1.1110	0.7197	0.8384	0.601	0.2402
0.6248	0.3807	-0.0126	-0.1261	-0.1702	-0.1516	-0.1278	-0.0905	-0.0397	0.0298	0.00993	0.0215
										1699.0	3.49
0.1715	0.0129	-0.1286	-0.2291	-0.3195	-0.4436	-0.5616	-0.7184	-0.8906	-0.9605	48	
-1.0781	-1.1753	-1.2304	-1.2918	-1.4071	-1.1707	-0.9281	-0.6775	0.9131	0.6932	0.599	0.4013
0.4613	0.2175	-0.1473	-0.2323	-0.2377	-0.1967	-0.1592	-0.1098	-0.0335	0.0300	0.01241	0.0111
										1689.4	2.43
0.1704	0.0078	-0.1310	-0.2325	-0.3205	-0.4424	-0.5626	-0.7116	-0.8673	-0.9316	56	
-1.0332	-1.1077	-1.2075	-1.2312	-1.2312	-1.0516	-0.8131	-0.5998	0.9324	0.6697	0.601	0.3876
0.4395	0.1940	-0.1580	-0.2241	-0.2308	-0.1834	-0.1496	-0.1022	-0.0463	0.0349	0.01490	0.0080
										1701.4	7.67
0.1667	0.0045	-0.1443	-0.2525	-0.3556	-0.4908	-0.6345	-0.8086	-1.0081	-1.1078	64	
-1.2177	-1.3056	-1.3895	-1.6064	-1.6267	-1.4014	-1.1855	-1.0030	0.7888	0.8327	0.602	0.5433
0.6164	0.3679	-0.0141	-0.1105	-0.1460	-0.1189	-0.0970	-0.0632	-0.0226	0.0467	0.01738	0.0048
										1703.8	4.28

Table 3-10

ARA RUN 128 PSTEP 1		AGARD CASE 5		OSC PITCH		Damping +0.07790					
M=0.755	R=5.5*10 ⁶	$\omega c/2v=0.0814$	$\alpha_m=0.016$	$\alpha_0=2.51$							
0.2056	0.0453	-0.0990	-0.2050	-0.2999	-0.4158	-0.5256	-0.8831	-0.8399	-0.8005	4	
-0.7376	-0.6636	-0.5773	-0.4466	-0.2851	-0.0681	0.1784	0.3634	1.1623	0.2413	0.754	0.1008
-0.0003	-0.2284	-0.6316	-0.7290	-0.4183	-0.3517	-0.2555	-0.1594	-0.0718	0.0416	0.00000	-0.0074
										2336.0	1.09
0.2089	0.0551	-0.0803	-0.1751	-0.2600	-0.4778	-1.1719	-1.1411	-1.0537	-1.0242	8	
-0.9639	-0.8741	-0.7963	-0.6698	-0.5504	-0.3326	-0.0889	0.0944	1.1565	0.5129	0.755	0.3436
0.2729	0.0341	-0.3424	-0.4249	-0.3818	-0.2735	-0.2071	-0.1295	-0.0532	0.0514	0.00200	-0.0056
										2340.2	2.34
0.1996	0.0807	-0.0370	-0.1204	-0.3522	-0.5938	-1.2510	-1.1995	-1.1272	-1.0794	12	
-1.0303	-0.9616	-0.8967	-0.7470	-0.6563	-0.4184	-0.1609	0.0267	1.1426	0.5700	0.757	0.4001
0.3357	0.1015	-0.2786	-0.3779	-0.3595	-0.2713	-0.2124	-0.1388	-0.0567	0.0488	0.00399	-0.0013
										2348.6	2.01
0.2072	0.0713	-0.0460	-0.1152	-0.1794	-0.4018	-1.2010	-1.1442	-1.0602	-0.9984	16	
-0.9688	-0.9095	-0.8280	-0.7057	-0.5364	-0.2807	-0.0127	0.1899	1.1547	0.4308	0.753	0.2592
0.1825	-0.0399	-0.4265	-0.5167	-0.4697	-0.3986	-0.2746	-0.1831	-0.0831	0.0330	0.00599	0.0126
										2331.5	0.52
0.2139	0.0613	-0.0618	-0.1480	-0.2243	-0.3154	-0.3400	-0.8619	-0.8471	-0.7695	20	
-0.7412	-0.6982	-0.6108	-0.4434	-0.2403	0.0010	0.2730	0.4749	1.1617	0.1758	0.755	-0.0021
-0.0766	-0.2821	-0.6502	-0.7412	-0.6083	-0.4384	-0.3178	-0.2033	-0.0926	0.0404	0.00799	0.0138
										2339.8	-1.25
0.2057	0.0589	-0.0621	-0.1410	-0.2064	-0.2953	-0.3792	-0.4742	-0.4903	-0.4915	24	
-0.4606	-0.3989	-0.3187	-0.1472	0.0515	0.2933	0.5303	0.6981	1.1251	-0.1065	0.753	-0.2425
-0.3582	-0.5088	-0.8679	-1.0357	-1.0739	-0.4668	-0.3076	-0.2040	-0.0991	0.0391	0.00999	0.0044
										2333.9	-2.41
0.2138	0.0634	-0.0565	-0.1408	-0.2093	-0.2839	-0.3634	-0.4417	-0.4283	-0.4258	28	
-0.3793	-0.3072	-0.2301	-0.0711	0.1148	0.3422	0.5856	0.7410	1.1066	-0.1788	0.758	-0.2911
-0.4307	-0.5506	-0.9321	-1.0852	-1.1694	-0.5848	-0.2815	-0.1494	-0.0589	0.0573	0.01199	-0.0017
										2354.8	-2.00
0.2183	0.0562	-0.0763	-0.1709	-0.2519	-0.3488	-0.4458	-0.5624	-0.5600	-0.5428	32	
-0.5072	-0.4237	-0.3464	-0.1954	-0.0174	0.1937	0.4478	0.6111	1.1413	-0.0371	0.757	-0.1525
-0.2924	-0.4605	-0.8239	-1.0154	-1.0645	-0.3366	-0.2187	-0.1463	-0.0567	0.0538	0.01399	-0.0108
										2346.3	-0.54

Table 3.11

ARA RUN 218 M=0.3 R=2.7*10 ⁶			AGARD CASE 6 - RAMP α c/v=0.02545 Rad								
0.1542	0.0110	-0.1266	-0.1432	-0.1927	-0.2973	-0.3414	-0.4184	-0.4405	-0.4350	136	
-0.4515	-0.4790	-0.4680	-0.4129	-0.2973	-0.1597	-0.0165	0.1982	1.0186	0.0330	0.304	0.0232
-0.2478	-0.3524	-0.4460	-0.3799	-0.3469	-0.2698	-0.1982	-0.1542	-0.0661	-0.0165	0.00000	0.0009
										523.1	-0.03
0.1486	0.0057	-0.1486	-0.1772	-0.2344	-0.3430	-0.4001	-0.5087	-0.5430	-0.5316	145	
-0.5716	-0.6002	-0.6116	-0.5659	-0.4744	-0.3658	-0.2401	-0.0227	1.0632	0.2458	0.298	0.1331
-0.0629	-0.2001	-0.3544	-0.3087	-0.2915	-0.2286	-0.1601	-0.1315	-0.0457	-0.0114	0.00352	-0.0028
										503.8	1.08
0.1406	-0.0056	-0.1519	-0.1856	-0.2362	-0.3656	-0.4162	-0.5230	-0.5961	-0.5849	148	
-0.6355	-0.6805	-0.7086	-0.6974	-0.6468	-0.5680	-0.4724	-0.2643	1.0348	0.4218	0.300	0.2097
0.1125	-0.0450	-0.2475	-0.2418	-0.2475	-0.1856	-0.1350	-0.1012	-0.0394	-0.0056	0.00469	-0.0024
										512.1	1.86
0.1454	-0.0168	-0.1790	-0.2126	-0.2741	-0.4084	-0.4867	-0.5986	-0.6825	-0.6937	151	
-0.7664	-0.8279	-0.8671	-0.8950	-0.8894	-0.8615	-0.8279	-0.6265	0.9845	0.5986	0.301	0.3253
0.2853	0.1063	-0.1454	-0.1846	-0.1790	-0.1343	-0.1007	-0.0895	-0.0112	0.0056	0.00586	-0.0058
										514.8	2.94
0.1494	-0.0057	-0.1839	-0.2299	-0.2989	-0.4541	-0.5403	-0.6782	-0.7932	-0.8276	154	
-0.9139	-0.9828	-1.0748	-1.1495	-1.2012	-1.2185	-1.2587	-1.0805	0.9139	0.7932	0.297	0.4500
0.4943	0.2816	-0.0287	-0.0920	-0.1264	-0.0977	-0.0632	-0.0460	0.0172	0.0230	0.00703	-0.0051
										501.1	4.14
0.1352	-0.0353	-0.2057	-0.2703	-0.3826	-0.5172	-0.6053	-0.7640	-0.9050	-0.9438	156	
-1.0637	-1.1342	-1.2635	-1.3575	-1.4751	-1.5515	-1.6338	-1.4858	0.8463	0.8933	0.294	0.5494
0.5994	0.3702	0.0353	-0.0588	-0.1058	-0.0764	-0.0529	-0.0411	0.0118	0.0118	0.00782	-0.0061
										490.1	4.97
0.1463	-0.0054	-0.1843	-0.2331	-0.3252	-0.4770	-0.5637	-0.7318	-0.8781	-0.9486	158	
-1.0624	-1.1437	-1.2901	-1.4201	-1.5290	-1.7399	-1.8917	-1.7562	0.6938	0.9377	0.306	0.5959
0.6830	0.4824	0.1409	0.0325	-0.0217	-0.0054	-0.0000	-0.0000	0.0488	0.0434	0.00860	-0.0048
										531.1	5.84
0.1510	-0.0112	-0.1958	-0.2573	-0.3524	-0.5203	-0.6265	-0.8036	-0.9846	-1.0685	160	
-1.1971	-1.3146	-1.4768	-1.6670	-1.9244	-2.1313	-2.3495	-2.2600	0.5818	1.0797	0.301	0.7064
0.7832	0.5986	0.2294	0.0951	0.0224	0.0224	0.0336	0.0200	0.0615	0.0503	0.00938	-0.0045
										514.8	6.72
0.1258	-0.0229	-0.2058	-0.2801	-0.3944	-0.5773	-0.7145	-0.9089	-1.1375	-1.2404	163	
-1.4119	-1.5605	-1.7949	-2.0692	-2.4236	-2.7666	-3.1439	-3.1324	0.3087	1.0861	0.298	0.8499
0.9089	0.7259	0.3315	0.1715	0.0686	0.0372	0.0372	0.0400	0.0686	0.0457	0.01055	0.0005
										507.8	8.02
0.1086	-0.0343	-0.2172	-0.3029	-0.4230	-0.6116	-0.7602	-0.9717	-1.2347	-1.3604	165	
-1.5314	-1.7205	-1.9835	-2.3093	-2.7265	-3.1152	-3.6925	-3.6903	0.0915	1.0975	0.298	0.9454
0.9431	0.8060	0.4058	0.2206	0.1086	0.0857	0.0743	0.0572	0.0743	0.0457	0.01133	0.0013
										503.8	8.91
0.0966	-0.0398	-0.2388	-0.3184	-0.4377	-0.6424	-0.7959	-1.0347	-1.3189	-1.4553	167	
-1.6943	-1.8647	-2.1602	-2.5582	-3.0642	-3.5676	-4.2523	-4.3376	-0.1251	1.0574	0.290	1.0357
0.9664	0.8327	0.4718	0.2729	0.1470	0.1194	0.0966	0.0682	0.0910	0.0512	0.01212	0.0018
										506.6	9.85
0.0848	-0.0339	-0.2305	-0.3223	-0.4523	-0.6615	-0.8199	-1.0743	-1.3966	-1.5493	169	
-1.7698	-2.0129	-2.3352	-2.7873	-3.3812	-3.9104	-4.6004	-4.9531	-0.3675	1.0404	0.299	1.1270
0.9725	0.9103	0.5428	0.3506	0.2092	0.1640	0.1357	0.1018	0.1131	0.0622	0.01290	0.0034
										509.4	10.80
0.0747	-0.0460	-0.2414	-0.3448	-0.4770	-0.6954	-0.8736	-1.1552	-1.5058	-1.6783	171	
-1.9312	-2.2070	-2.5749	-3.0779	-3.8278	-4.4658	-5.4486	-5.7302	-0.6265	0.9943	0.297	1.2531
1.0460	0.9628	0.6322	0.4138	0.2701	0.2184	0.1782	0.1322	0.1322	0.0747	0.01369	0.0020
										501.1	11.76
0.0615	-0.0392	-0.2378	-0.3300	-0.4699	-0.6926	-0.8950	-1.1803	-1.5551	-1.7565	173	
-2.0138	-2.3158	-2.7242	-3.3115	-4.0947	-4.8610	-5.9374	-6.3042	-0.8838	0.8726	0.301	1.3046
0.9342	0.9789	0.6713	0.4331	0.2909	0.2349	0.2014	0.1510	0.1510	0.0783	0.01447	0.0066
										514.9	12.83
0.0455	-0.0312	-0.2445	-0.3411	-0.4832	-0.7277	-0.9380	-1.2507	-1.6771	-1.8988	175	
-2.1838	-2.5241	-2.9675	-3.6440	-4.5423	-5.4291	-6.6286	-7.6235	-1.1945	0.7959	0.298	1.4453
0.9437	1.0403	0.7618	0.5458	0.3638	0.3127	0.2558	0.1876	0.1705	0.0910	0.01525	0.0069
										506.6	13.88
-0.0234	-0.0935	-0.2630	-0.3857	-0.5610	-0.8240	-1.0577	-1.3908	-1.8700	-2.1272	178	
-2.4803	-2.8810	-3.4595	-4.3069	-5.2419	-6.2938	-8.0937	-9.7015	-1.7006	0.6194	0.294	1.6368
0.8707	1.0694	0.8932	0.6194	0.4324	0.3565	0.2863	0.2162	0.1928	0.0935	0.01642	0.0036
										492.8	15.54

Table 3-12

ARA RUN 227			AGARD CASE 7			- RAMP					
M=0.57			R=4.6*10 ⁶			$\alpha_c/v=0.0044$ Rad					
0.1899	0.0429	-0.0776	-0.1552	-0.2279	-0.3072	-0.3881	-0.4822	-0.5450	-0.5334	151	
-0.5979	-0.5648	-0.5599	-0.4806	-0.3501	-0.1354	0.0661	0.2874	1.1082	0.1107	0.613	0.0282
-0.1453	-0.3154	-0.5202	-0.4905	-0.4129	-0.3055	-0.2345	-0.1552	-0.0694	0.0347	0.00000	0.0018
										1743.8	-0.01
0.1933	0.0413	-0.0859	-0.1751	-0.2544	-0.3370	-0.4294	-0.5418	-0.6343	-0.6425	169	
-0.7235	-0.6871	-0.7069	-0.6557	-0.5434	-0.3551	-0.1553	0.0611	1.1133	0.3138	0.613	0.1363
0.0512	-0.1454	-0.3931	-0.3981	-0.3436	-0.2593	-0.1966	-0.1272	-0.0529	0.0429	0.00698	0.0014
										1743.6	0.98
0.1919	0.0410	-0.0935	-0.1854	-0.2723	-0.3707	-0.4790	-0.6184	-0.7382	-0.7693	180	
-0.8743	-0.8514	-0.9088	-0.8924	-0.8251	-0.6496	-0.4708	-0.2264	1.0826	0.5216	0.615	0.2540
0.2641	0.0377	-0.2575	-0.3035	-0.2789	-0.2116	-0.1624	-0.1066	-0.0344	0.0476	0.01126	0.0043
										1755.7	1.97
0.1885	0.0347	-0.1058	-0.2084	-0.3076	-0.4134	-0.5391	-0.7012	-0.8533	-0.9178	189	
-1.0468	-1.0501	-1.1327	-1.1725	-1.1510	-0.9823	-0.8136	-0.5689	1.0286	0.6946	0.612	0.3798
0.4432	0.2067	-0.1406	-0.2166	-0.2150	-0.1703	-0.1306	-0.0827	-0.0215	0.0496	0.01475	0.0059
										1741.5	2.93
0.1921	0.0331	-0.1143	-0.2219	-0.3295	-0.4488	-0.5945	-0.7733	-0.9737	-1.0664	197	
-1.2271	-1.2486	-1.4722	-1.4788	-1.5450	-1.3016	-1.1509	-0.9141	0.9356	0.8330	0.612	0.5050
0.5962	0.3511	-0.0265	-0.1292	-0.1507	-0.1225	-0.0927	-0.0546	-0.0050	0.0580	0.01786	0.0083
										1739.2	3.94
0.1805	0.0331	-0.1159	-0.2318	-0.3444	-0.4720	-0.6276	-0.8230	-1.0317	-1.1128	203	
-1.3496	-1.7586	-1.8216	-1.8696	-1.7901	-1.5699	-1.3993	-1.1724	0.8462	0.9191	0.612	0.6105
0.6988	0.4587	0.0696	-0.0530	-0.0977	-0.0828	-0.0629	-0.0348	0.0083	0.0613	0.02019	0.0129
										1739.2	4.79
0.1755	0.0315	-0.1176	-0.2335	-0.3544	-0.4852	-0.6376	-0.8214	-1.1377	-1.7603	210	
-2.1528	-2.1114	-2.1561	-2.1213	-2.0236	-1.8497	-1.6692	-1.4341	0.7203	0.9957	0.612	0.7425
0.7949	0.5746	0.1656	0.0199	-0.0364	-0.0391	-0.0315	-0.0116	0.0232	0.0662	0.02291	0.0212
										1739.2	5.79
0.1648	0.0250	-0.1232	-0.2398	-0.3580	-0.4845	-0.6211	-0.8925	-1.5152	-2.3228	216	
-2.4027	-2.3544	-2.3544	-2.3128	-2.2412	-2.0514	-1.8699	-1.6184	0.6074	1.0540	0.610	0.8628
0.8792	0.6694	0.2514	0.0899	0.0117	0.0017	-0.0017	0.0083	0.0366	0.0699	0.02523	0.0263
										1729.7	6.70
0.0747	-0.0000	-0.1279	-0.2408	-0.3753	-0.6027	-0.9083	-1.2254	-1.5575	-1.6854	223	
-1.7983	-2.3272	-2.5239	-2.4873	-2.4159	-2.2482	-2.0324	-1.9245	0.4666	1.0843	0.610	0.9573
0.9315	0.7356	0.3254	0.1461	0.0598	0.0349	0.0183	0.0199	0.0315	0.0465	0.02795	0.0153
										1734.5	7.75
-0.0616	-0.1083	-0.2664	-0.3912	-0.6026	-0.7075	-0.8224	-1.0421	-1.3784	-1.5898	229	
-1.7397	-2.0410	-2.6353	-2.6054	-2.5404	-2.3873	-2.1958	-2.1492	0.3446	1.1037	0.609	0.9878
0.9706	0.7774	0.3662	0.1798	0.0749	0.0383	0.0183	0.0017	0.0033	-0.0050	0.03028	-0.0102
										1730.0	8.73
-0.0789	-0.1527	-0.2467	-0.3256	-0.4163	-0.6143	-0.8325	-1.1749	-1.4704	-1.5912	235	
-1.6265	-1.7893	-2.1182	-2.6117	-2.6470	-2.3060	-2.3331	-2.3079	0.2383	1.1289	0.606	0.9587
0.9970	0.8107	0.3978	0.2031	0.0839	0.0436	0.0117	-0.0117	-0.0201	-0.0420	0.03261	0.0026
										1715.8	9.68
-0.1892	-0.2250	-0.3068	-0.3886	-0.5642	-0.7159	-0.9443	-1.1932	-1.4267	-1.4727	241	
-1.5512	-1.6483	-1.7847	-2.2671	-2.6063	-2.5245	-2.4716	-2.4563	0.1398	1.1386	0.601	0.9623
1.0176	0.8404	0.4261	0.2131	0.0938	0.0426	-0.0034	-0.0358	-0.0563	-0.0972	0.03493	-0.0147
										1689.6	10.63
-0.2864	-0.3000	-0.4330	-0.4892	-0.5455	-0.6529	-0.7654	-1.0466	-1.3018	-1.3944	248	
-1.3103	-1.6961	-2.0694	-2.7410	-2.8075	-2.6843	-2.4444	-2.5859	0.0324	1.1455	0.601	1.0090
1.0483	0.8847	0.4739	0.2506	0.1210	0.0545	0.0034	-0.0409	-0.0733	-0.1381	0.03765	-0.0170
										1689.5	11.74
-0.4212	-0.4505	-0.5644	-0.6506	-0.7783	-0.9388	-0.6389	-1.0132	-1.1030	-1.2221	254	
-1.4275	-1.6830	-1.9988	-2.3044	-2.8464	-2.8533	-2.6997	-2.6910	-0.0742	1.1479	0.595	0.9920
1.0501	0.8959	0.4799	0.2537	0.1033	0.0328	-0.0242	-0.0829	-0.1329	-0.2158	0.03949	-0.0340
										1668.5	12.70
-0.3785	-0.4944	-0.5791	-0.6050	-0.6655	-0.7917	-0.8418	-1.0440	-1.1391	-1.2463	260	
-1.5989	-1.7631	-1.9342	-2.2471	-2.8434	-2.8227	-2.7725	-2.9012	-0.1590	1.1443	0.595	1.0459
1.0665	0.9282	0.5237	0.2904	0.1383	0.0622	-0.0069	-0.0674	-0.1210	-0.2109	0.04232	-0.0466
										1666.2	13.72
-0.3402	-0.6507	-0.6410	-0.6682	-0.6349	-0.7822	-0.7857	-0.8910	-1.1909	-1.1347	266	
-1.2014	-1.4767	-1.6065	-1.8433	-2.2344	-2.6045	-2.8710	-2.4063	-0.2578	1.1610	0.590	1.0192
1.0979	0.9734	0.5682	0.3227	0.1649	0.0772	-0.0018	-0.0754	-0.1368	-0.2420	0.04464	-0.0725
										1642.1	14.80

Table 3.13

ARA RUN 230		AGARD CASE B		RAMP							
M=0.56	R=4.5*10 ⁶	$\alpha c/v=0.01492$ Rad									
0.1932	0.0446	-0.0710	-0.1486	-0.2246	-0.2773	-0.3745	-0.4724	-0.5351	-0.5285	64	
-0.5814	-0.5533	-0.5533	-0.4691	-0.3353	-0.1156	0.0826	0.2940	1.1099	0.1090	0.613	0.0250
-0.1470	-0.3122	-0.5170	-0.4905	-0.4113	-0.2973	-0.2246	-0.1486	-0.0528	0.0380	0.00000	0.0014
										1743.7	0.01
0.1896	0.0316	-0.0931	-0.1829	-0.2611	-0.3476	-0.4390	-0.5504	-0.6336	-0.6452	74	
-0.7018	-0.6668	-0.6889	-0.6253	-0.5105	-0.3226	-0.1231	0.0815	1.1125	0.2877	0.610	0.1305
0.0216	-0.1680	-0.4157	-0.4174	-0.3492	-0.2627	-0.1979	-0.1280	-0.0532	0.0349	0.00388	-0.0009
										1731.9	1.08
0.1805	0.0248	-0.1076	-0.1987	-0.2848	-0.3776	-0.4769	-0.6061	-0.7088	-0.7336	77	
-0.8065	-0.7767	-0.8131	-0.7717	-0.6806	-0.5084	-0.3213	-0.0927	1.1045	0.4372	0.612	0.2184
0.1755	-0.0397	-0.3179	-0.3428	-0.2997	-0.2236	-0.1722	-0.1093	-0.0431	0.0348	0.00505	-0.0013
										1739.1	1.90
0.1832	0.0266	-0.1132	-0.2148	-0.3147	-0.4196	-0.5345	-0.6894	-0.8293	-0.8859	80	
-0.9758	-0.9609	-1.0208	-1.0058	-0.9625	-0.7977	-0.6228	-0.4163	1.0924	0.6328	0.610	0.3458
0.3747	0.1365	-0.1865	-0.2498	-0.2331	-0.1732	-0.1349	-0.0799	-0.0200	0.0466	0.00621	-0.0006
										1729.5	2.96
0.1850	0.0330	-0.1140	-0.2213	-0.3270	-0.4393	-0.5731	-0.7333	-0.9017	-0.9827	82	
-1.0884	-1.0884	-1.1776	-1.1825	-1.1776	-1.0223	-0.8621	-0.6639	1.0553	0.7481	0.613	0.4342
0.5054	0.2626	-0.0941	-0.1767	-0.1784	-0.1321	-0.0974	-0.0545	-0.0050	0.0362	0.00699	0.0005
										1743.8	1.83
0.1794	0.0266	-0.1229	-0.2391	-0.3504	-0.4716	-0.6161	-0.8021	-1.0064	-1.1127	84	
-1.2423	-1.2638	-1.4099	-1.4548	-1.4797	-1.2704	-1.1127	-0.9283	1.0230	0.8602	0.611	0.5422
0.6277	0.3853	0.0017	-0.0996	-0.1529	-0.0915	-0.0681	-0.0332	0.0083	0.0648	0.00776	0.0011
										1734.2	4.70
0.1730	0.0266	-0.1281	-0.2478	-0.3675	-0.5006	-0.6569	-0.8581	-1.0727	-1.2124	86	
-1.4618	-1.6348	-1.7213	-1.8510	-1.7346	-1.5417	-1.3604	-1.1874	0.9762	0.9548	0.611	0.6592
0.7434	0.5106	0.1081	-0.0233	-0.0665	-0.0466	-0.0333	-0.0083	0.0249	0.0688	0.00834	0.0049
										1731.7	5.67
0.1671	0.0278	-0.1245	-0.2474	-0.3702	-0.5028	-0.6618	-0.8470	-1.1746	-1.6873	88	
-2.0281	-1.9380	-1.9839	-2.0232	-1.9187	-1.7512	-1.5914	-1.3826	0.9092	1.0079	0.616	0.7628
0.8198	0.6094	0.1933	0.0475	-0.0033	-0.0016	0.0033	0.0213	0.0426	0.0754	0.00731	0.0104
										1758.0	4.60
0.1613	0.0300	-0.1314	-0.2561	-0.3825	-0.5122	-0.6569	-0.9446	-1.5782	-2.3116	90	
-2.3066	-2.2234	-2.2284	-2.2484	-2.1586	-1.9823	-1.7777	-1.5847	0.9498	1.0776	0.611	0.9008
0.9063	0.7068	0.2827	0.1214	0.0499	0.0382	0.0303	0.0399	0.0365	0.0815	0.01009	0.0153
										1731.8	7.97
0.1678	0.0183	-0.1299	-0.2408	-0.3504	-0.5215	-0.6752	-1.0116	-1.6740	-2.1703	92	
-2.4246	-2.4030	-2.4014	-2.4279	-2.3316	-2.1722	-1.9213	-1.6527	0.7805	1.1143	0.611	1.0339
0.9715	0.7809	0.3620	0.1877	0.1030	0.0830	0.0681	0.0664	0.0731	0.0880	0.01086	0.0126
										1734.2	8.92
0.0743	-0.0000	-0.1602	-0.3220	-0.5631	-0.9049	-1.2314	-1.4366	-1.5906	-1.5753	94	
-1.7240	-2.2390	-2.3993	-2.5679	-2.4568	-2.3518	-2.1566	-2.1450	0.6932	1.1299	0.612	1.1209
1.0089	0.8356	0.4310	0.2444	0.1438	0.1122	0.0859	0.0710	0.0760	0.0710	0.01164	-0.0192
										1744.1	9.55
-0.0764	-0.2198	-0.4196	-0.5348	-0.6709	-1.0187	-1.3105	-1.3420	-1.3437	-1.2934	96	
-1.3570	-1.8435	-1.6933	-2.0046	-2.2195	-2.3206	-2.3610	-2.3993	0.6260	1.1472	0.609	1.1567
1.0306	0.8924	0.4912	0.2947	0.1818	0.1349	0.0932	0.0649	0.0516	0.0117	0.01241	-0.0758
										1729.7	10.56
-0.3721	-0.2038	-0.3272	-0.4160	-0.5376	-0.8414	-1.1136	-1.2688	-1.5027	-1.6745	98	
-1.7013	-1.6228	-1.6211	-1.6312	-1.6452	-2.6629	-2.3110	-2.3143	-0.5476	1.1637	0.608	1.0933
1.3832	0.9333	0.5309	0.3172	0.1853	0.1219	0.0668	0.0317	-0.0100	-0.0902	0.01319	-0.0403
										1725.0	11.63
-0.3463	-0.3117	-0.4410	-0.6231	-0.7605	-0.9435	-0.8602	-1.3886	-1.3637	-1.3770	100	
-1.8803	-1.9820	-1.9753	-1.9937	-1.6454	-2.7373	-2.6056	-2.6072	0.4668	1.1436	0.608	1.1169
1.0719	0.9385	0.5418	0.3217	0.1834	0.1167	0.0617	0.0132	-0.0300	-0.1050	0.01596	-0.0599
										1727.6	12.69
-0.5488	-0.5842	-0.7003	-0.6885	-0.7121	-0.7643	-0.8249	-1.0185	-1.4478	-1.4919	102	
-1.5239	-1.6705	-1.4111	-1.5993	-1.6582	-2.7541	-2.7070	-2.7121	0.4040	1.1717	0.609	1.1387
1.1111	0.9831	0.5926	0.3636	0.2172	0.1448	0.0758	0.0135	-0.0438	-0.1566	0.01674	-0.0917
										1710.8	13.77
-0.4878	-0.5932	-0.6578	-0.6765	-0.7071	-0.7581	-0.8703	-0.9693	-1.1524	-1.2391	104	
-1.3972	-1.6704	-1.6760	-1.6590	-1.6947	-2.5937	-2.6380	-2.7978	0.3230	1.1711	0.602	1.0878
1.1235	1.0063	0.6136	0.3773	0.2227	0.1343	0.0544	-0.0204	-0.0824	-0.2159	0.01552	-0.0775
										1874.3	14.97

Table 3-14

ARA RUN 6 QUASI-STATIC												
M=0.3	R=2	6×10^6	$\alpha_m = 10.75$	$\alpha_o = 11.16$	1.8 Hz							
0.1349	-0.0066	-0.1537	-0.1877	-0.2443	-0.3405	-0.3801	-0.4424	-0.4594	-0.4707	80		
-0.4933	-0.5046	-0.4877	-0.4367	-0.3179	-0.1764	0.0160	0.2254	1.0008	-0.0292	0.299	0.0140	
-0.2783	-0.3858	-0.5103	-0.4480	-0.3514	-0.3065	-0.2900	-0.1764	-0.1198	-0.0292	0.0000	-0.0013	
										308.9	-0.12	
0.1233	-0.0306	-0.1962	-0.2317	-0.2908	-0.3973	-0.4447	-0.5275	-0.5571	-0.5926	84		
-0.6221	-0.6517	-0.6376	-0.6340	-0.5334	-0.4328	-0.2554	-0.0483	1.0461	0.2002	0.293	0.1125	
-0.0779	-0.2435	-0.4328	-0.4032	-0.3559	-0.2968	-0.2554	-0.1784	-0.1252	-0.0424	0.01110	-0.0012	
										486.8	0.69	
0.1992	-0.0412	-0.2031	-0.2610	-0.3304	-0.4460	-0.5097	-0.6138	-0.6716	-0.7121	88		
-0.7699	-0.8335	-0.8740	-0.9029	-0.8798	-0.8220	-0.6947	-0.4981	0.9247	0.4851	0.296	0.2514	
0.1901	-0.0007	-0.2641	-0.3015	-0.2899	-0.2436	-0.2147	-0.1569	-0.1164	-0.0470	0.02220	0.0016	
										498.0	2.04	
0.1232	-0.0344	-0.1976	-0.2595	-0.3270	-0.4564	-0.5127	-0.6365	-0.7153	-0.7547	90		
-0.8371	-0.9179	-0.9686	-1.0361	-1.0473	-1.0473	-0.9573	-0.7941	0.7929	0.6128	0.300	0.3288	
0.3258	0.1232	-0.1807	-0.2201	-0.2370	-0.2088	-0.1694	-0.1073	-0.0794	-0.0287	0.02775	0.0010	
										311.8	2.84	
0.1259	-0.0351	-0.2077	-0.2824	-0.3515	-0.4952	-0.5758	-0.7023	-0.7943	-0.8806	92		
-0.9438	-1.0704	-1.1624	-1.2602	-1.3292	-1.3694	-1.3464	-1.2026	0.6435	0.7643	0.297	0.4340	
0.4767	0.2582	-0.0869	-0.1617	-0.1904	-0.1502	-0.1387	-0.0984	-0.0696	-0.0179	0.03330	0.0011	
										500.8	3.63	
0.0977	-0.0585	-0.2377	-0.3245	-0.3947	-0.5385	-0.6368	-0.7756	-0.9028	-0.9895	94		
-1.0763	-1.1572	-1.3654	-1.4985	-1.6488	-1.7413	-1.7934	-1.6719	0.3348	0.8668	0.296	0.5268	
0.4066	0.3753	-0.0064	-0.1163	-0.1626	-0.1510	-0.1452	-0.1047	-0.0758	-0.0353	0.03885	0.0034	
										498.0	4.62	
0.1025	-0.0405	-0.2349	-0.3093	-0.4065	-0.5552	-0.6639	-0.8210	-0.9784	-1.0814	96		
-1.1937	-1.3158	-1.4417	-1.5795	-1.6807	-2.1222	-2.2938	-2.1891	-0.0062	0.9546	0.298	0.6326	
0.7259	0.5085	0.1025	-0.0119	-0.0977	-0.0977	-0.0863	-0.0376	-0.0405	-0.0119	0.04441	0.0040	
										503.6	5.61	
0.0881	-0.0716	-0.2609	-0.3614	-0.4619	-0.6334	-0.7376	-0.9410	-1.1361	-1.2663	98		
-1.3964	-1.5560	-1.7512	-1.9878	-2.4491	-2.6975	-2.9518	-2.7577	-0.5388	1.0284	0.293	0.7745	
0.8392	0.6301	0.1886	0.0526	-0.0420	-0.0598	-0.0775	-0.0539	-0.0939	-0.0243	0.04995	0.0051	
										487.0	6.59	
0.1045	-0.0339	-0.2501	-0.3512	-0.4702	-0.6545	-0.7794	-0.9934	-1.2254	-1.3740	100		
-1.5946	-1.7427	-1.9865	-2.2957	-2.7833	-3.2412	-3.5861	-3.6634	-1.1243	1.0878	0.292	0.8889	
0.9273	0.7548	0.3029	0.1364	0.0234	-0.0063	-0.0301	-0.0063	-0.0123	0.0036	0.05951	0.0072	
										484.3	7.67	
0.0830	-0.0650	-0.2707	-0.3766	-0.5000	-0.6764	-0.8293	-1.0527	-1.3231	-1.4936	102		
-1.6738	-1.9051	-2.1932	-2.5871	-3.0692	-3.8217	-4.2391	-4.4155	-1.7523	1.0462	0.294	0.9937	
0.9580	0.8169	0.3877	0.1596	0.0762	0.0350	0.0056	0.0056	-0.0062	0.0036	0.06106	0.0075	
										489.9	8.72	
0.0899	-0.0394	-0.2307	-0.3488	-0.4613	-0.6535	-0.8100	-1.0519	-1.3388	-1.5188	104		
-1.7269	-1.9407	-2.2937	-2.7450	-3.3131	-3.8924	-4.7755	-5.0912	-2.4019	0.9043	0.291	1.0301	
0.9337	0.8549	0.4612	0.2643	0.1237	0.0787	0.0506	0.0449	0.0281	0.0225	0.06662	0.0124	
										512.0	9.74	
0.0302	-0.0381	-0.2441	-0.3719	-0.5056	-0.7090	-0.8892	-1.1449	-1.4878	-1.6971	106		
-1.8295	-2.1143	-2.5921	-3.1842	-3.9591	-4.4984	-5.7771	-6.2362	-3.2721	0.9474	0.296	1.1814	
0.9590	0.9358	0.5464	0.3313	0.1860	0.1221	0.0872	0.0840	0.0349	0.0175	0.07316	0.0140	
										495.5	10.83	
0.0624	-0.0450	-0.2147	-0.3391	-0.4804	-0.6896	-0.8818	-1.1332	-1.5151	-1.7469	108		
-1.8997	-2.3123	-2.7138	-3.3188	-4.1330	-4.8680	-6.6660	-7.3443	-3.9011	0.8709	0.300	1.2479	
0.9501	0.9614	0.6108	0.4016	0.2433	0.1755	0.1244	0.1076	0.0737	0.0398	0.07772	0.0192	
										509.4	11.93	
-0.0500	-0.1412	-0.2600	-0.3995	-0.4918	-0.7180	-0.9216	-1.2069	-1.6116	-1.8772	111		
-2.1406	-2.3048	-2.9372	-3.6357	-4.5494	-5.3094	-8.4364	-9.1262	-4.9871	0.6673	0.293	1.3407	
0.8539	0.9557	0.6617	0.4468	0.2659	0.1811	0.1302	0.0962	0.0367	0.0001	0.05003	0.0214	
										509.3	13.54	
-0.0764	-0.2586	-0.4114	-0.5466	-0.4819	-0.7523	-0.9932	-1.3694	-1.7844	-1.9101	113		
-2.1607	-2.8037	-3.7449	-4.6997	-4.4903	-5.2073	-6.9411	-8.1377	-3.3659	0.6877	0.294	1.4063	
0.8934	1.0168	0.7053	0.4761	0.2880	0.1940	0.1293	0.0941	0.0394	-0.0411	0.09159	0.0068	
										490.0	14.55	
-0.2378	-0.3739	-0.6077	-0.8356	-0.9934	-1.2555	-1.5836	-1.8371	-1.3382	-1.5836	115		
-1.5212	-1.6070	-1.8349	-2.3726	-3.1557	-3.7010	-4.3420	-5.1427	-4.8271	0.7540	0.295	1.3783	
0.8235	0.9936	0.6897	0.4501	0.2573	0.1696	0.0878	0.0469	-0.0408	-0.1109	0.07715	-0.0991	
										492.8	15.55	

Table 3.15

ARA RUN 11 QUASI-STATIC
 $M=0.58$ $R=4.6 \times 10^6$ $\alpha_m=8.99$ $\alpha_0=9.55$ 1.8 Hz

0.1774	0.0287	-0.0935	-0.1643	-0.2298	-0.3183	-0.3892	-0.4741	-0.5237	-0.5467	82	
-0.5680	-0.5680	-0.5503	-0.4741	-0.3396	-0.1448	0.0960	0.2872	1.0981	0.0730	0.585	0.0255
-0.1643	-0.3431	-0.5220	-0.4812	-0.4069	-0.3113	-0.2387	-0.1590	-0.0811	0.0198	0.00000	0.0009
										1626.6	-0.13
0.1730	0.0196	-0.1055	-0.1795	-0.2500	-0.3364	-0.4175	-0.5127	-0.5743	-0.6078	84	
-0.6413	-0.6396	-0.6308	-0.5743	-0.4545	-0.2589	-0.0156	0.1677	1.0860	0.1747	0.585	0.0747
-0.0632	-0.2589	-0.4686	-0.4510	-0.3910	-0.3012	-0.2342	-0.1637	-0.0826	0.0179	0.00537	0.0019
										1634.0	0.26
0.1804	0.0301	-0.1027	-0.1778	-0.2494	-0.3455	-0.4311	-0.5307	-0.6093	-0.6425	86	
-0.6932	-0.7054	-0.7106	-0.6687	-0.5691	-0.3927	-0.1481	0.0458	1.0836	0.3009	0.589	0.1350
0.0686	-0.1463	-0.3892	-0.3962	-0.3420	-0.2651	-0.2005	-0.1324	-0.0625	0.0336	0.01074	0.0014
										1648.5	0.76
0.1733	0.0197	-0.1162	-0.2009	-0.2751	-0.3757	-0.4745	-0.5840	-0.6881	-0.7340	88	
-0.7905	-0.8188	-0.8382	-0.8188	-0.7464	-0.5822	-0.3474	-0.1391	1.0665	0.4169	0.585	0.2044
0.1804	-0.0509	-0.3157	-0.3580	-0.3174	-0.2486	-0.1921	-0.1303	-0.0615	0.0215	0.01611	0.0036
										1631.5	1.34
0.1814	0.0268	-0.1121	-0.2017	-0.2843	-0.3915	-0.4969	-0.6252	-0.7553	-0.8063	90	
-0.8941	-0.9398	-0.9838	-0.9873	-0.9521	-0.8045	-0.5795	-0.3827	1.0285	0.3523	0.587	0.2881
0.3238	0.0830	-0.2193	-0.2878	-0.2614	-0.2052	-0.1613	-0.1068	-0.0435	0.0356	0.02148	0.0053
										1638.7	2.00
0.1740	0.0196	-0.1243	-0.2173	-0.3085	-0.4244	-0.5384	-0.6841	-0.8332	-0.8875	92	
-1.0140	-1.0894	-1.1631	-1.2017	-1.2070	-1.0578	-0.8332	-0.6349	0.9338	0.6776	0.587	0.3753
0.4460	0.1933	-0.1383	-0.2313	-0.2243	-0.1769	-0.1401	-0.0927	-0.0366	0.0371	0.02685	0.0063
										1641.3	2.71
0.1710	0.0197	-0.1317	-0.2285	-0.3271	-0.4503	-0.5787	-0.7495	-0.9219	-0.9976	94	
1.1085	-1.2634	-1.3813	-1.4622	-1.5291	-1.3707	-1.1472	-0.9290	0.8169	0.7976	0.586	0.4725
0.5740	0.3206	-0.0419	-0.1599	-0.1739	-0.1440	-0.1141	-0.0794	-0.0243	0.0373	0.03222	0.0096
										1636.4	3.49
0.1712	0.0179	-0.1354	-0.2394	-0.3470	-0.4809	-0.6184	-0.8088	-1.0132	-1.1137	96	
-1.2424	-1.2335	-1.7077	-1.8875	-1.9227	-1.6900	-1.4715	-1.2706	0.6683	0.8904	0.585	0.5795
0.6806	0.4374	0.0461	-0.0720	-0.1178	-0.0967	-0.0808	-0.0508	-0.0068	0.0461	0.03759	0.0113
										1634.0	4.32
0.1583	0.0214	-0.1313	-0.2418	-0.3559	-0.4998	-0.6402	-0.8420	-1.0543	-1.1227	98	
-1.1227	-2.1019	-2.2195	-2.2405	-2.1616	-1.9878	-1.7457	-1.5246	0.5065	0.7385	0.587	0.6808
0.7725	0.5391	0.1320	-0.0014	-0.0628	-0.0593	-0.0505	-0.0277	0.0056	0.0512	0.04296	0.0176
										1641.2	5.21
0.1502	0.0145	-0.1403	-0.2559	-0.3715	-0.5226	-0.6791	-0.8712	-1.0010	-1.1398	100	
-2.3847	-2.5110	-2.5626	-2.5128	-2.4541	-2.2673	-2.0415	-1.7925	0.3328	1.0264	0.583	0.7996
0.8593	0.6316	0.2137	0.0554	-0.0175	-0.0264	-0.0264	-0.0104	0.0145	0.0483	0.04832	0.0252
										1619.3	6.10
0.1342	0.0091	-0.1427	-0.2517	-0.3804	-0.5286	-0.6733	-0.8520	-1.1450	-1.9739	102	
-2.6742	-2.7457	-2.7743	-2.7350	-2.6707	-2.4956	-2.2223	-2.0865	0.1520	1.0739	0.581	0.9017
0.9345	0.7184	0.2932	0.1199	0.0288	0.0073	-0.0034	0.0037	0.0198	0.0466	0.05371	0.0327
										1612.1	7.01
0.0962	-0.0123	-0.1475	-0.2613	-0.3787	-0.5191	-0.6650	-0.8517	-1.3763	-1.9630	104	
-2.7262	-2.7884	-2.8898	-2.8489	-2.7848	-2.6195	-2.3989	-2.3474	0.0339	1.0779	0.582	0.9428
0.9552	0.7506	0.3363	0.1389	0.0499	0.0233	0.0037	0.0019	0.0108	0.0230	0.05908	0.0369
										1619.4	7.94
0.0393	-0.0499	-0.1765	-0.2782	-0.3870	-0.5350	-0.6760	-0.9221	-1.4465	-1.8514	106	
-2.1886	-2.8343	-2.9092	-2.9377	-2.8878	-2.7255	-2.5221	-2.4829	-0.0659	1.0899	0.581	0.9565
0.9811	0.7849	0.3693	0.1660	0.0607	0.0250	-0.0017	-0.0124	-0.0106	-0.0088	0.06445	0.0353
										1614.6	8.79
-0.1562	-0.2046	-0.2638	-0.3051	-0.3895	-0.5474	-0.7179	-1.0157	-1.5344	-1.8448	108	
-1.9381	-2.0907	-2.3850	-2.7833	-2.9430	-2.8390	-2.6649	-2.6416	-0.1544	1.0928	0.579	0.9632
0.9959	0.8057	0.3911	0.1812	0.0681	0.0287	-0.0090	-0.0306	-0.0431	-0.0663	0.06982	0.0150
										1604.9	9.74
-0.2378	-0.2612	-0.3242	-0.3476	-0.4322	-0.5870	-0.7868	-1.0477	-1.5463	-1.6867	110	
-1.7983	-1.8991	-1.9729	-1.9837	-2.2015	-2.8764	-2.7720	-2.7648	-0.2396	1.0995	0.577	0.9387
1.0059	0.8255	0.4138	0.1942	0.0682	0.0214	-0.0200	-0.0524	-0.0776	-0.1154	0.07520	0.0001
										1600.1	10.63
-0.3974	-0.4787	-0.5509	-0.5491	-0.5906	-0.6646	-0.8307	-1.0275	-1.2406	-1.2333	112	
-1.1387	-1.1358	-1.0943	-1.1792	-2.3892	-2.6686	-2.7715	-2.7625	-0.1754	1.1064	0.576	0.9087
1.0144	0.8447	0.4330	0.2110	0.0792	0.0160	-0.0364	-0.0797	-0.1176	-0.1916	0.08057	-0.0508
										1599.2	11.56

Table 3.16

ARA RUN 151 QUASI-STATIC

M=0.745 R=5.5*10⁶ $\alpha_m=0.09$ $\alpha_o=5$ 1.8 Hz

0.1715	0.0418	-0.0567	-0.1228	-0.1689	-0.2313	-0.2799	-0.3223	-0.2811	-0.2599	15	
-0.2151	-0.1427	-0.0604	0.0904	0.2949	0.5019	0.7239	0.8623	0.9994	-0.4644	0.746	-0.4703
-0.7250	-0.8061	-1.1777	-1.2787	-1.3560	-0.6964	-0.4146	-0.1689	-0.0592	0.0543	0.00000	-0.0020
										2309.7	-3.27
0.1906	0.0482	-0.0605	-0.1305	-0.1830	-0.2529	-0.3079	-0.3566	-0.3266	-0.3154	16	
-0.2654	-0.1980	-0.1180	0.0257	0.2331	0.4417	0.6741	0.8240	1.0327	-0.3866	0.745	-0.4168
-0.6477	-0.7514	-1.1313	-1.2425	-1.3187	-0.6340	-0.3179	-0.1642	-0.0743	0.0419	0.00555	-0.0029
										2305.1	-2.85
0.1968	0.0519	-0.0593	-0.1342	-0.1942	-0.2692	-0.3329	-0.3916	-0.3716	-0.3629	17	
-0.3167	-0.2492	-0.1717	-0.0268	0.1681	0.3843	0.6204	0.7766	1.0527	-0.3167	0.745	-0.3653
-0.5740	-0.6940	-1.0775	-1.1987	-1.2699	-0.5565	-0.2779	-0.1730	-0.0818	0.0407	0.01109	-0.0033
										2305.1	-2.40
0.2022	0.0530	-0.0639	-0.1435	-0.2082	-0.2928	-0.3587	-0.4370	-0.4271	-0.4096	18	
-0.3748	-0.3102	-0.2318	-0.0888	0.1089	0.3265	0.5665	0.7245	1.0801	-0.2306	0.747	-0.3010
-0.4867	-0.6310	-1.0003	-1.1421	-1.2117	-0.4159	-0.2729	-0.1871	-0.0913	0.0380	0.01663	-0.0040
										2315.9	-1.98
0.2095	0.0542	-0.0688	-0.1521	-0.2254	-0.3111	-0.3906	-0.4851	-0.4925	-0.4764	19	
-0.4515	-0.3844	-0.3136	-0.1682	0.0269	0.2592	0.5003	0.6680	1.1104	-0.1297	0.748	-0.2322
-0.3844	-0.5571	-0.9100	-1.0740	-1.0802	-0.3658	-0.2912	-0.1955	-0.0937	0.0356	0.02217	-0.0021
										2317.8	-1.54
0.2145	0.0530	-0.0713	-0.1620	-0.2427	-0.3384	-0.4291	-0.5360	-0.5596	-0.5532	20	
-0.5298	-0.4652	-0.3943	-0.2527	-0.0563	0.1698	0.4233	0.5998	1.1329	-0.0303	0.749	-0.1589
-0.2862	-0.4764	-0.8231	-0.9660	-0.9274	-0.3949	-0.3049	-0.1930	-0.0924	0.0406	0.02772	-0.0004
										2317.6	-1.06
0.2026	0.0454	-0.0834	-0.1775	-0.2592	-0.3607	-0.4622	-0.6008	-0.6627	-0.6565	21	
-0.6281	-0.5525	-0.4882	-0.3433	-0.1552	0.0726	0.3301	0.5009	1.1384	0.0590	0.750	-0.0338
-0.1911	-0.4003	-0.7556	-0.9152	-0.5166	-0.4077	-0.3012	-0.1960	-0.0933	0.0342	0.03327	-0.0022
										2326.6	-0.59
0.2095	0.0512	-0.0788	-0.1745	-0.2616	-0.3708	-0.4873	-0.6112	-0.7965	-0.7911	22	
-0.6971	-0.6296	-0.5695	-0.4272	-0.2444	-0.0187	0.2389	0.4192	1.1406	0.1678	0.755	0.0137
-0.0764	-0.2972	-0.6701	-0.7167	-0.5437	-0.3855	-0.2874	-0.1831	-0.0825	0.0414	0.03881	0.0018
										2347.7	-0.06
0.2091	0.0474	-0.0836	-0.1840	-0.2721	-0.3738	-0.4582	-0.5492	-0.8806	-0.8182	23	
-0.7558	-0.7178	-0.6517	-0.5097	-0.3334	-0.1105	0.1515	0.3413	1.1396	0.2593	0.755	0.0973
0.0144	-0.2085	-0.5880	-0.6345	-0.5121	-0.3750	-0.2734	-0.1766	-0.0811	0.0401	0.04436	0.0033
										2352.2	0.40
0.2049	0.0427	-0.0876	-0.1884	-0.2695	-0.3680	-0.4759	-1.0449	-0.9565	-0.8926	24	
-0.8994	-0.8151	-0.7303	-0.5951	-0.4219	-0.1970	0.0685	0.2553	1.1402	0.3401	0.754	0.1610
0.0968	-0.1355	-0.5079	-0.5706	-0.4636	-0.3432	-0.2584	-0.1673	-0.0753	0.0415	0.04990	0.0049
										2343.4	0.86
0.2115	0.0527	-0.0803	-0.1727	-0.2441	-0.3377	-0.4894	-1.1135	-1.0187	-0.9731	25	
-0.9364	-0.8820	-0.7958	-0.6652	-0.5089	-0.2774	-0.0101	0.1795	1.1486	0.4258	0.754	0.2535
0.1894	-0.0458	-0.4202	-0.5015	-0.4214	-0.3118	-0.2355	-0.1505	-0.0668	0.0465	0.05545	0.0034
										2338.8	1.31
0.2011	0.0516	-0.0794	-0.1635	-0.2364	-0.3317	-1.2239	-1.1732	-1.1015	-1.0570	26	
-1.0076	-0.9532	-0.8889	-0.7394	-0.6072	-0.3711	-0.1128	0.0812	1.1342	0.5002	0.752	0.3481
0.2654	0.0244	-0.3489	-0.4403	-0.3785	-0.2908	-0.2216	-0.1449	-0.0646	0.0464	0.06098	-0.0004
										2330.3	1.79
0.1925	0.0543	-0.0689	-0.1486	-0.2731	-0.3619	-1.3014	-1.2417	-1.1707	-1.1246	27	
-1.0761	-1.0325	-0.9703	-0.8047	-0.7051	-0.4598	-0.2021	-0.0092	1.1200	0.5598	0.748	0.4134
0.3257	0.0842	-0.2943	-0.3976	-0.3528	-0.2743	-0.2121	-0.1399	-0.0677	0.0406	0.06653	-0.0012
										2313.3	2.21
0.1847	0.0675	-0.0484	-0.1360	-0.2368	-0.3307	-1.3276	-1.2647	-1.2018	-1.1488	28	
-1.1155	-1.0760	-1.0032	-0.8404	-0.7762	-0.5160	-0.2705	-0.0855	1.1049	0.6189	0.752	0.4723
0.3956	0.1591	-0.2224	-0.3322	-0.3050	-0.2446	-0.1878	-0.1200	-0.0521	0.0453	0.07203	-0.0043
										2324.7	2.61
0.1596	0.0671	-0.0455	-0.2269	-0.4720	-0.6759	-1.3939	-1.3464	-1.2726	-1.2201	29	
-1.1876	-1.1450	-1.0687	-0.9324	-0.8636	-0.5921	-0.3457	-0.1593	1.0890	0.6637	0.746	0.5356
0.4461	0.1959	-0.1894	-0.3044	-0.2932	-0.2419	-0.1881	-0.1293	-0.0630	0.0258	0.07762	-0.0086
										2302.4	2.95
0.1177	0.0543	-0.0764	-0.2544	-0.4860	-0.6814	-1.1096	-1.3797	-1.3025	-1.2751	30	
-1.2191	-1.1755	-1.0996	-0.9863	-0.9092	-0.6304	-0.3889	-0.2047	1.0700	0.6978	0.747	0.5413
0.4837	0.2385	-0.1524	-0.2768	-0.2756	-0.2271	-0.1822	-0.1287	-0.0702	0.0132	0.08317	-0.0066
										2313.7	3.35

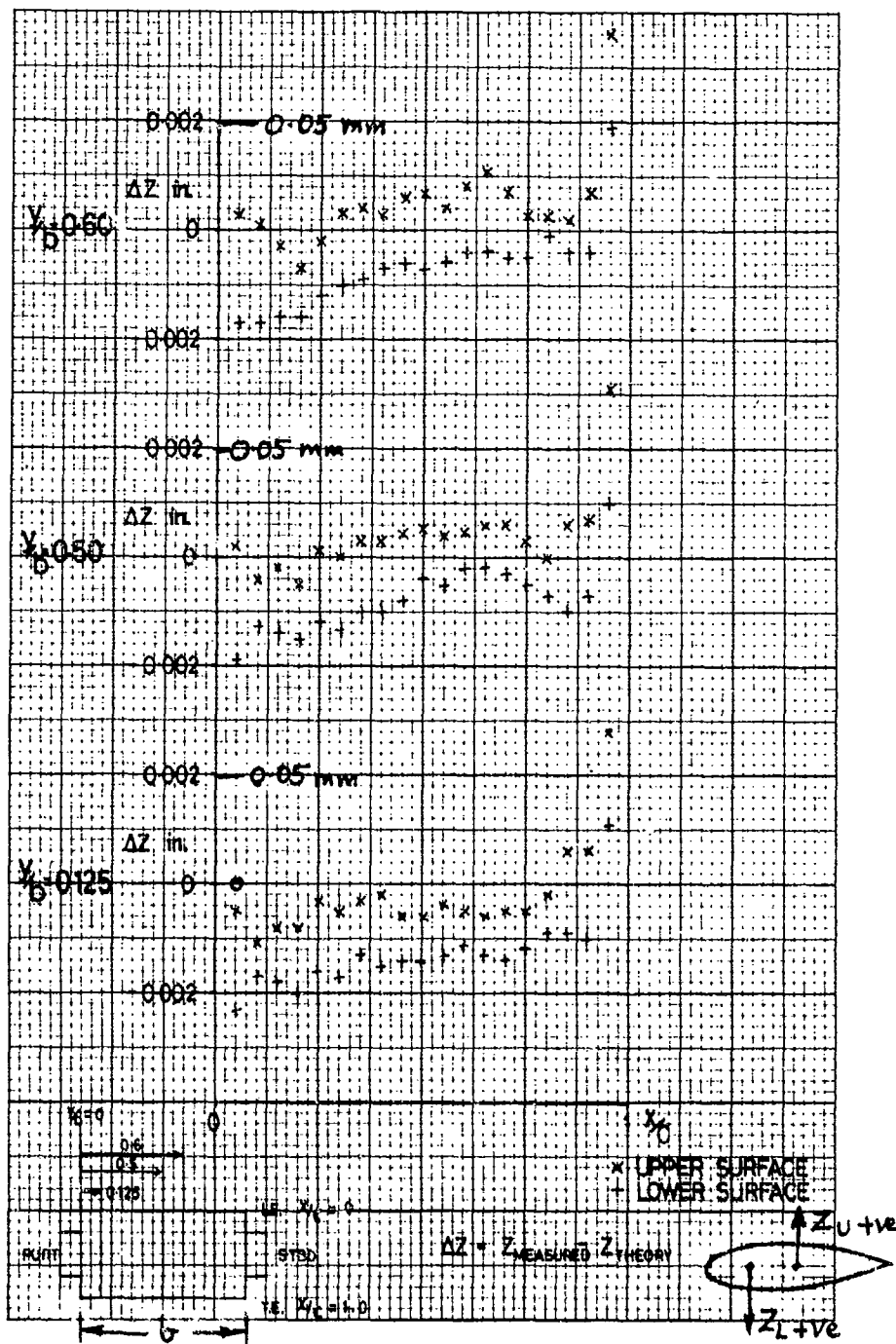


Fig 3.1 Profile inspection of NACA 0012 wing: $Z_m - Z_t$

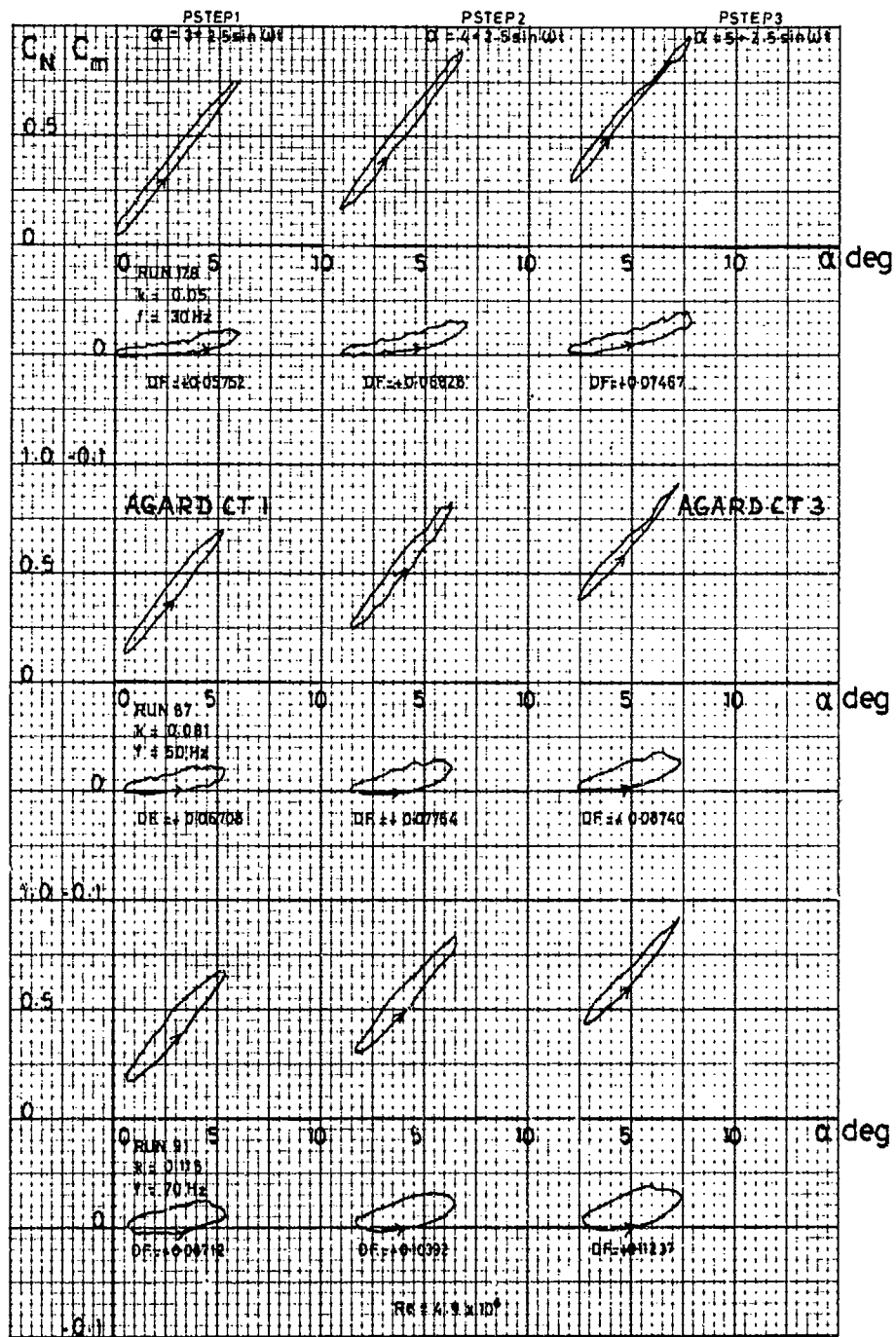


Fig 3.2 C_N, C_m v. incidence over range of $\alpha_m = 3^\circ, 4^\circ, 5^\circ$; $\alpha_0 = 2.5^\circ$.
Effect of frequency $k = 0.05, 0.08, 0.12$; $M = 0.6$

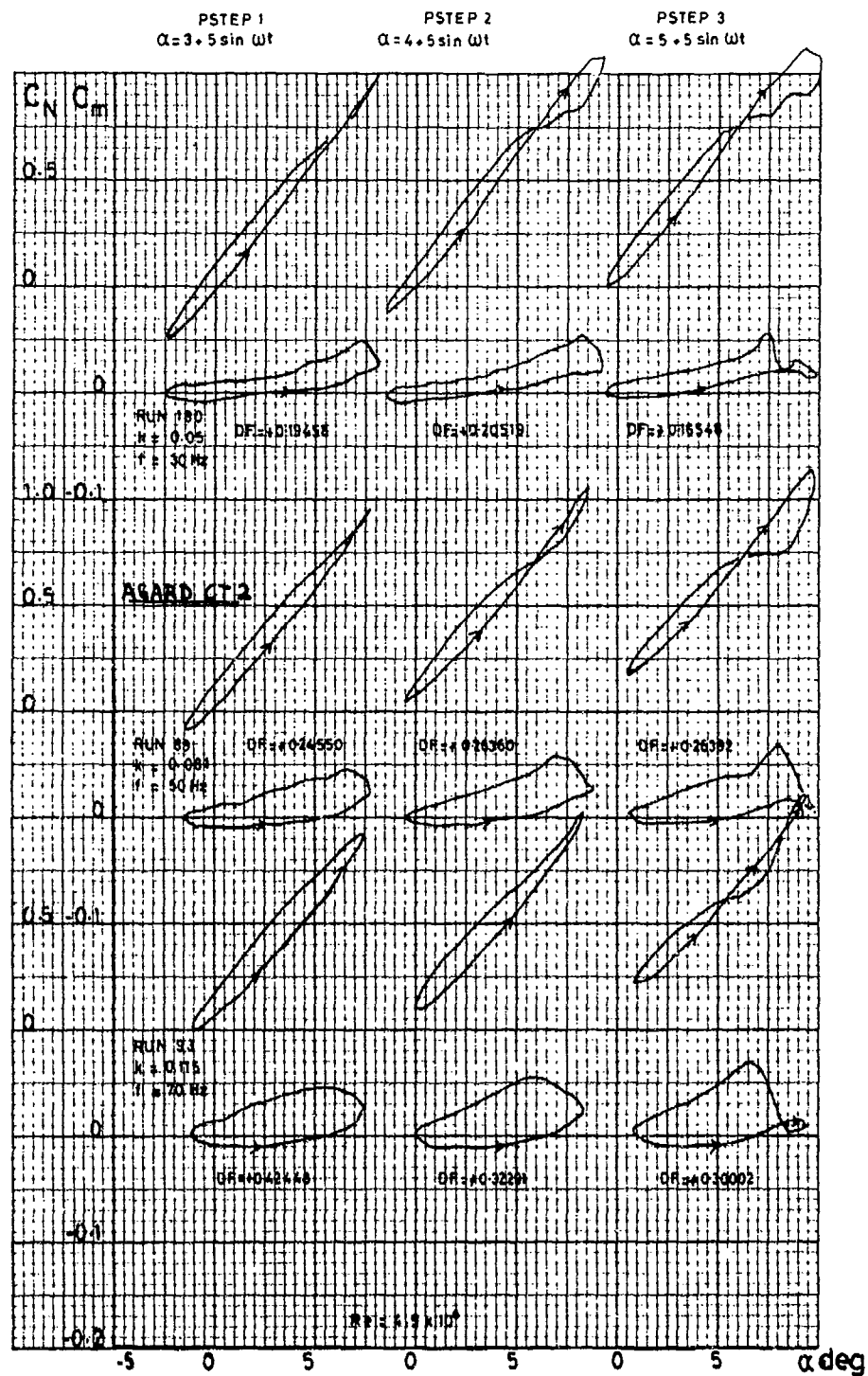


Fig 3.3 C_N, C_m v. incidence over range of $\alpha_m = 3^{\circ}, 4^{\circ}, 5^{\circ}$; $\alpha_0 = 5^{\circ}$.
 Effect of frequency $k = 0.05, 0.08, 0.12$; $M = 0.6$

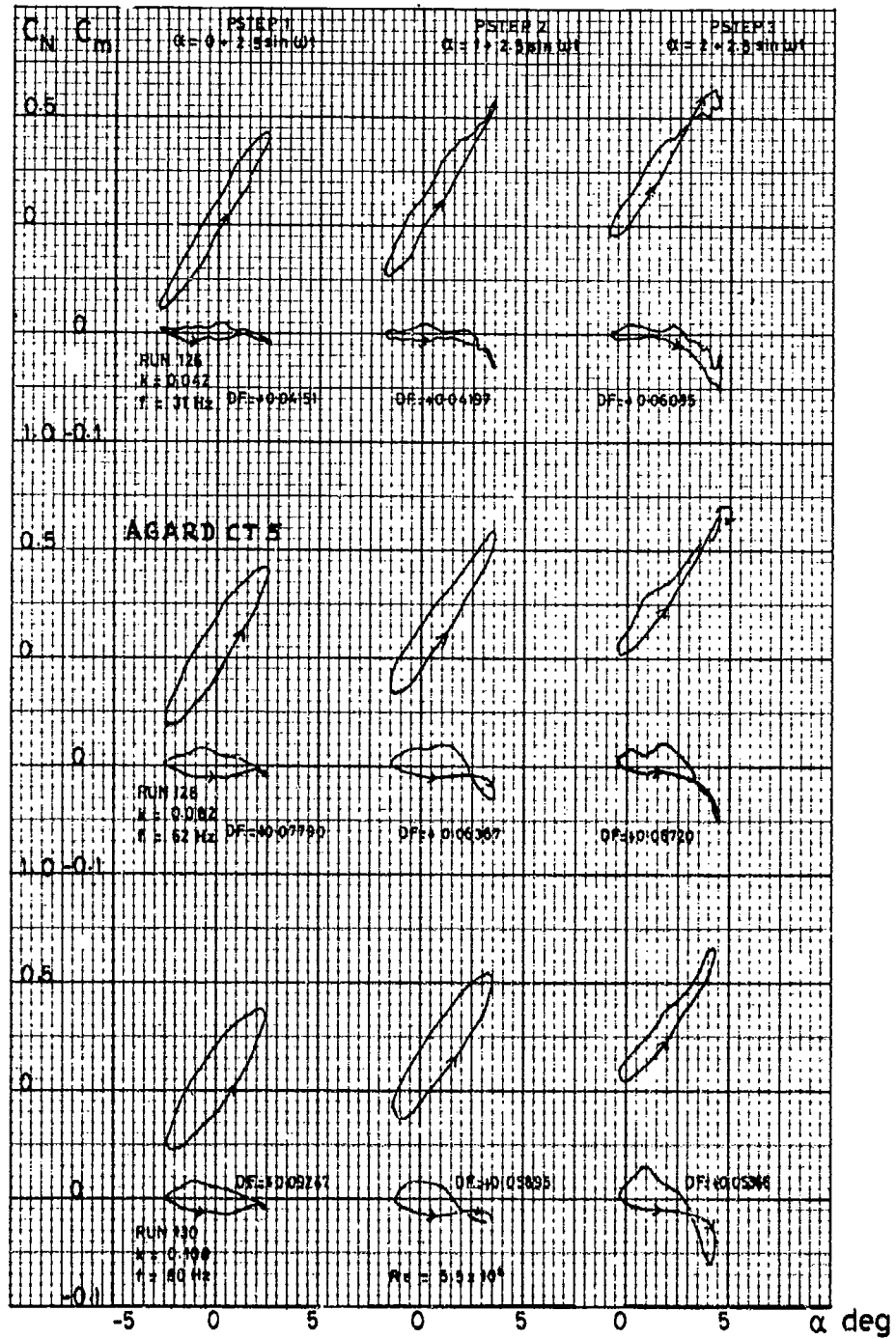


Fig 3.4 C_N, C_m v. incidence over range of $\alpha_m = 0^\circ, 1^\circ, 2^\circ$; $\alpha_0 = 2.5^\circ$.
Effect of frequency $k = 0.04, 0.08, 0.10$; $M = 0.75$

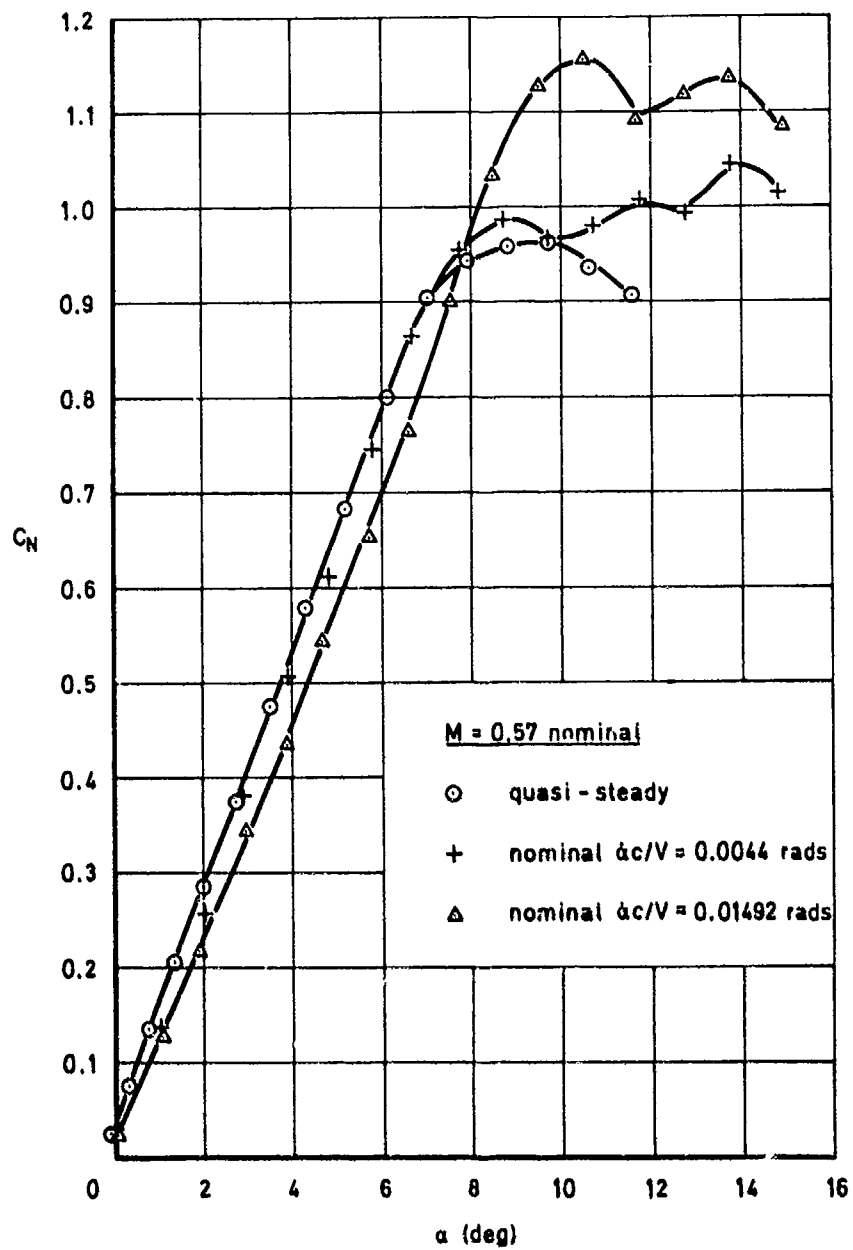


Fig 3.5 Lift ν . incidence for different rates of change

DATA SET 4

NLR 7301 SUPERCRITICAL AIRFOIL OSCILLATORY PITCHING AND OSCILLATING FLAP

by

R.J. Zwaan, NLR

INTRODUCTION

The supercritical airfoil NLR 7301 has a maximum thickness of 16.5 per cent of the chord. In the set of two-dimensional aeroelastic configurations this airfoil represents the category of thick and blunt-nosed airfoils.

The airfoil was investigated in two wind-tunnel tests with different models. In the first test the model could be driven harmonically in a pitching motion about an axis at 40 per cent of the chord. Information about this configuration is designated with the letter "A". In the second test harmonic rotation of a trailing-edge flap was considered. The flap axis was located at 75 per cent of the chord; the flap had no aerodynamic balance. Information about this configuration is designated with the letter "B".

In transonic flow the contribution of the shock to the aerodynamic loading can of course be very different. As an illustration, pressure distributions on the upper surface are compared for a flow with a strong shock and a shock-free flow. Also results of thin-airfoil theory have been added. In the strong shock cases (A: Fig. 4.1, B: Fig. 4.5) the pressure peak due to the moving shock dominates in the pressure distribution, with a strength which diminishes with frequency. Although the flow conditions are the same for both configurations, the mean pressure distributions differ slightly. The cause of these differences could not be traced. In the shock-free cases (A: Fig. 4.2, B: Fig. 4.6) the pressure distribution shows a wide bulge. The pressure distributions of configuration A show very clearly that with increasing frequency the bulge decreases while at the same time a weak shock develops. Also here the mean pressure distributions should be the same. For unexplained reasons, however, shock-free flow could only be realized at slightly different Mach numbers.

Lift and moment coefficients are presented in figures 4.3 and 4.4 for configuration A and in figures 4.7 and 4.8 for configuration B. The influence of fixing boundary layer transition is remarkable. Configuration A shows only minor differences. Forced transition at 0.3 c is obviously not so effective in this case. The differences are larger for configuration B, which includes also fixed transition at 0.07 c. Characteristic changes occur in particular in the lift coefficient at low frequencies. Transition fixing has obviously the effect of reducing both the lift magnitude and the phase lag.

An aspect that emerges especially in the present case of a supercritical airfoil is the difference in the specification of theoretical and experimental shock-free flow. In the General Review it was pointed out that this difference is mainly due to viscous effects and tunnel interference. It was further proposed to choose the CT specification such that theory would produce a flow similar to that observed in the experiment. This is illustrated in figure 4.9 where the theoretical design pressure distribution calculated with a hodograph theory is compared with a shock-free pressure distribution measured at free transition.

1	AIRFOIL	
1.1	Designation	NLR 7301 (also NLR HT 7310810)
1.2	Type of airfoil	Thick, aft-loaded, shock-free supercritical; designed by means of Boerstool hodograph method
1.3	Geometry	See Table 4.1
	Nose radius	0.05 c
	Maximum thickness	t/c = 16.5 %
	Base thickness	Zero
1.4	Design condition	
	Design condition	Potential flow (hodograph theory): M = 0.721 C _q = 0.595
	Design pressure distribution	Steady experiment (free transition, NLR Pilot Tunnel): M = 0.747, C _q = 0.455; see Fig. 4.9
1.5	Additional remarks	"Shock-free" pressure distributions for configuration A shown in Fig. 4.2 and for configuration B shown in Fig. 4.6
1.6	References on airfoil	
2	MODEL GEOMETRY	
2.1	Chord length	0.18 m
2.2	Span	0.42 m
2.3	Actual model coordinates and accuracy of measurements	See Table 4.2
2.4	Flap: hinge and gap details	A: not applicable B: hinge axis at 0.75 c; gap width 0.35 mm

2.5	Additional remarks	-
2.6	References on model	-
3	WIND TUNNEL	
3.1	Designation	NLR Pilot Tunnel
3.2	Type of tunnel	Continuous, closed circuit
3.3	Test section dimensions	Rectangular; see Fig. 4.10 height 0.55 m, width 0.42 m
3.4	Type of roof and floor	10 % slotted top and bottom walls, separate top and bottom plenums
3.5	Type of side walls	Solid side walls
3.6	Ventilation geometry	See Fig. 4.10
3.7	Thickness of side wall boundary layer	Thickness 10 % of test section semi-width, no special treatment
3.8	Thickness of boundary layers at roof and floor	Not measured; probably comparable with side wall boundary layers
3.9	Method of measuring Mach number	Derived from static pressure measured upstream of model and from total pressure measured in settling chamber
3.10	Uniformity of Mach number over test section	See Fig. 4.11 (empty test section)
3.11	Sources and levels of noise or turbulence in empty tunnel	Turbulence/noise level, see Fig. 4.12
3.12	Tunnel resonances	No evidence
3.13	Additional remarks	For two-dimensionality of the flow see Ref. 4.3
3.14	References on tunnel	Ref. 4.2
4	MODEL MOTION	
4.1	Mode of applied motion	A: pitching oscillation of airfoil B: oscillation of trailing-edge flap
4.2	Range of amplitude	A: $\alpha_0 = 0.1^\circ$ to 1.5° B: $\delta_0 = 0.1^\circ$ to 2.0°
4.3	Range of frequency	A: $f = 0$ to 80 Hz; $k = 0$ to 0.26 B: $f = 0$ to 200 Hz; $k = 0$ to 0.65
4.4	Method of application	A) hydraulic excitation at one side B) of the model
4.5	Purity of applied motion	Checked by spectral analysis; no data stored
4.6	Natural frequencies and normal modes of model	No interference with natural vibration modes
4.7	Static or dynamic elastic distortion during tests	Negligible
4.8	Additional remarks	-
5	TEST CONDITIONS	
5.1	Tunnel height/model chord ratio	3.1
5.2	Tunnel width/model chord ratio	2.3
5.3	Range of Mach number	A: $M = 0.5$ to 0.8 B: $M = 0.5$ to 0.82
5.4	Range of tunnel total pressure	Atmospheric
5.5	Range of tunnel total temperature	313 ± 1 K
5.6	Range of model steady mean incidence	A: $\alpha_m = 0^\circ$ to 3° B: $\alpha_m = 0^\circ$ to 3° ; $\delta_m = 0^\circ$
5.7	Definition of model incidence	Incidence datum line $\alpha = 0$ relates to the x-axis as used in Tables 4.1 and 4.2. Datum line is parallel to test section centre line for $\alpha_m = 0$
5.8	Position of transition, if free	A) part of the test performed with natural B) transition; position of transition not measured
5.9	Position and type of trip, if transition fixed	A: strip of carborundum grains at 0.3 c B: strip of carborundum grains at 0.07 c or 0.3 c
5.10	For mixed flow, position of sonic boundary in relation to roof and floor	Not measured
5.11	Flow instabilities during tests	No evidence

- 5.12 Additional remarks -
 5.13 References describing tests A: Ref. 4.4
 B: not available

6 MEASUREMENTS AND OBSERVATIONS

- | | | | |
|------|---|--|---|
| 6.1 | Steady pressures for the mean conditions | | ✓ |
| 6.2 | Steady pressures for small changes from the mean conditions | | ✓ |
| 6.3 | Quasi-steady pressures | | |
| 6.4 | Unsteady pressures | | ✓ |
| 6.5 | Steady forces for the mean conditions | measured directly
integrated press. | ✓ |
| 6.6 | Steady forces for small changes from the mean conditions | measured directly
integrated press. | ✓ |
| 6.7 | Quasi-steady forces | measured directly
integrated press. | |
| 6.8 | Unsteady forces | measured directly
integrated press. | ✓ |
| 6.9 | Measurement of actual motion at points on model | | ✓ |
| 6.10 | Observation or measurement of boundary layer properties | | |
| 6.11 | Visualization of surface flow | | |
| 6.12 | Visualization of shockwave movements | | ✓ |
| 6.13 | Additional remarks | | |

7 INSTRUMENTATION

- 7.1 Steady pressures
- 7.1.1 Position of orifices spanwise and chordwise See 7.2.1
- 7.1.2 Type of measuring system See 7.2.3
- 7.2 Unsteady pressures
- 7.2.1 Position of orifices spanwise and chordwise A: see Figs 4.13 and 4.14
B: see Figs 4.15 and 4.16
- 7.2.2 Diameter of orifices 0.8 mm
- 7.2.3 Type of measuring system A: 40 pressure tubes + 13 in situ pressure transducers
B: 46 pressure tubes + 12 in situ pressure transducers
- 7.2.4 Type of transducers ±7.5 psi Statham differential pressure transducers,
and ±5 psi Kulite miniature pressure transducers
- 7.2.5 Principle and accuracy of calibration Calibration uses transfer functions of pressure tubes, see Ref. 4.4; for accuracy see 9.10
- 7.3 Model motion
- 7.3.1 Method of measurement A: with accelerometers, see Fig. 4.13
B: with accelerometers, see Fig. 4.15
- 7.3.2 Accuracy See 9.10
- 7.4 Processing of unsteady measurements
- 7.4.1 Method of acquiring and processing measurements See Fig. 4.17
- 7.4.2 Type of analysis A: signal analysis of TFA over 20 cycles for $f = 30, 80$ Hz and 60 cycles for $f = 200$ Hz
B: signal length during TFA analysis was 1 s
- 7.4.3 Unsteady pressure quantities obtained and accuracies achieved A: Fundamental harmonics
B: Fundamental harmonics and occasionally second and third harmonics
For accuracy see 9.10
- 7.4.4 Method of integration to obtain forces Trapezoidal rule
- 7.5 Additional remarks -
- 7.6 References on techniques A: Refs 4.4, 4.5
B: Ref. 4.6

8 DATA PRESENTATION

- 8.1 Test cases for which data could be made available A: see Table 4.3
B: not available
- 8.2 Test cases for which data are included in this document A) : see Table 4.4
B) :
- 8.3 Steady pressures Mean pressures for:
A: Tables 4.5 to 4.14
B: Tables 4.15 to 4.23
- 8.4 Quasi-steady or steady perturbation pressures Steady pressure derivatives for:
A: Tables 4.5, 4.8, 4.12
B: Tables 4.15, 4.17, 4.19
- 8.5 Unsteady pressures A: Tables 4.6, 4.7, 4.9 to 4.11, 4.13, 4.14
B: Tables 4.16, 4.18, 4.20 to 4.23
- 8.6 Steady forces or moments See 8.3
- 8.7 Quasi-steady or steady perturbation forces See 8.4
- 8.8 Unsteady forces and moments See 8.5
- 8.9 Other forms in which data could be made available if required -
- 8.10 References giving other presentations of data -

9 COMMENTS ON DATA

- 9.1 Accuracy
- 9.1.1 Mach number ± 0.002 . No corrections made for Mach number nonuniformity
- 9.1.2 Steady incidence $\pm 0.02^\circ$
- 9.1.3 Reduced frequency ± 0.0005
- 9.1.4 Steady pressure coefficients Not known
- 9.1.5 Steady pressure derivatives Not applicable
- 9.1.6 Unsteady pressure coefficients Not known
- 9.2 Sensitivity to small changes of parameter No evidence
- 9.3 Spanwise variations No evidence
- 9.4 Non-linearities Part of analysis of experimental results; see Ref. 4.4
- 9.5 Influence of tunnel total pressure -
- 9.6 Wall interference corrections No corrections included, but under steady conditions it is normal to make the following corrections to measurements made in this tunnel:
steady corrections:
 $\Delta C_{L_1} = -1.4 C_{L_1} + 0.56 (C_{L_1} + 0.25 C_{L_2}) / \sqrt{1-M^2}$,
(deg) ($\pm 15\%$)
 $\Delta C_{L_2} = -0.015 C_{L_2} / (1-M^2)$, ($\pm 30\%$)
 $\Delta C_{M_2} = -0.25 \Delta C_{L_2}$, ($\pm 30\%$)
- 9.7 Other relevant tests on same model -
- 9.8 Relevant tests on other models of nominally the same airfoil See Data Set 5
- 9.9 Any remarks relevant to comparison between experiment and theory -
- 9.10 Additional remarks No systematic investigations of separate accuracies have been performed, accuracy of lift and moment coefficients is estimated to be 5 to 10 per cent in magnitude and 3 to 6 degrees in phase angle
- 9.11 References on discussion of data A: Ref. 4.4

10 PERSONAL CONTACT FOR FURTHER INFORMATION

R.J. Zwaan, National Aerospace Laboratory (NLR), Anthony Fokkerweg 2, 1059 CM Amsterdam, The Netherlands

11 LIST OF REFERENCES

- 4.1 J. Barche c.s. Experimental data base for computer program assessment
AGARD-AR-138, 1979
- 4.2 J. Zwaaneveld Principal data of the NLL Pilot Tunnel
NLL Report MP 185, 1959
- 4.3 H.A. Dambrink Investigation of the 2-dimensionality of the flow around a profile in the
NLR 0.55x0.42 m² transonic wind tunnel
NLR Memorandum AC-72-018, 1972
- 4.4 H. Tijdeman Investigations of the transonic flow around oscillating airfoils
NLR TR 77090 U, 1977
- 4.5 P.H. Fuykschot DYDRA-Data logger for dynamic measurements
L.J.M. Joosten
NLR MP 69012 U, 1969
- 4.6 P.H. Fuykschot PHAROS, processor for harmonic analysis of the response of oscillating
surfaces
NLR MP 77012 U, 1977
- 4.7 S.R. Bland AGARD Two-dimensional aeroelastic configurations
AGARD-AR-156, 1979

12 NOTATION AND LIST OF SYMBOLS

DATA SET	STANDARD
ALPHA	mean wing incidence, α_m , deg
AMPL.	flap amplitude, δ_0 , deg; see Note 2 below
C2	pitch amplitude, α_0 , deg; see Note 2 below
CL	mean wing lift coefficient, C_l
CLIM	k_a'' in Tables 4.5 to 4.14; k_c'' in Tables 4.15 to 4.23
CLRE	k_a' in Tables 4.5 to 4.14; k_c' in Tables 4.15 to 4.23
CM	mean wing moment coefficient (about 0.25 c), C_m
CMIN	m_a'' in Tables 4.5 to 4.14; m_c'' in Tables 4.15 to 4.23
CMRE	m_a' in Tables 4.5 to 4.14; m_c' in Tables 4.15 to 4.23
CP	mean pressure coefficient, C_p
CPIM	imaginary component of oscillatory pressure coefficient, rad^{-1} . In Tables 4.5 to 4.14 it represents C_p''/α_0 , in Tables 4.15 to 4.23 it represents C_p''/δ_0
CPRE	real component of oscillatory pressure coefficient, rad^{-1} . In Tables 4.5 to 4.14 it represents C_p'/α_0 , in Tables 4.15 to 4.23 it represents C_p'/δ_0 . If $k = 0$, then $CPRE = [C_p(+\delta_0) - C_p(-\delta_0)]/2\alpha_0$ and $CPRE = [C_p(+\delta_0) - C_p(-\delta_0)]/2\delta_0$, resp.
DELTA	mean flap angle, δ_m , deg
FREQ.	frequency, f , Hz
HARM	order of harmonic
k_a	oscillatory wing lift coefficient, \tilde{C}_l/α_0 , rad^{-1}
k_c	oscillatory wing lift coefficient, \tilde{C}_l/δ_0 , rad^{-1}
M	mean local Mach number, M_t
MACH	free-stream Mach number, M
e_a	oscillatory wing moment coefficient, $-2 \tilde{C}_m/\alpha_0$, rad^{-1}
e_c	oscillatory wing moment coefficient, $-2 \tilde{C}_m/\delta_0$, rad^{-1}
NUMBER.	run number
NCHE, NCIM	real and imaginary components of oscillatory flap moment coefficient, $-2 \tilde{C}_h/\alpha_0$, rad^{-1}
PO	total pressure, p_t , Pa
Q	dynamic pressure, q , Pa
RCRE, RCIM	real and imaginary components of oscillatory flap lift coefficient, \tilde{C}_{lf}/α_0 , rad^{-1}
RE	Reynolds number based on wing chord, Re
RFREQ	reduced frequency, $k = \pi fc/V$
•	(suffix) upper side
-	(suffix) lower side
•	(superscript) critical value

Note 1: Symbols not mentioned here conform to the notation in the General Review.

Note 2: The oscillatory motions are defined as $\alpha = \alpha_0 \sin \omega t$ and $\delta = \delta_0 \sin \omega t$. The equation for a corresponding oscillatory pressure (including higher harmonics, if available) reads:

$$p(t) = p_m + p' \sin \omega t + p'' \cos \omega t + p_1' \sin 2\omega t + p_1'' \cos 2\omega t + \text{etc.}$$

Similar expressions hold for the aerodynamic coefficients.

TABLE 4.1

Contour data of the NLR 7301 airfoil

UPPER PART				LOWER PART			
X	Z	X	Z	X	Z	X	Z
0.0000012	-.0004167	0.4297467	+.0000016	0.0000016	-.0004167	0.4297467	-.0004167
0.0002895	+.0052171	0.4374629	+.0077357	0.0002895	+.0052171	0.4374629	+.0077357
0.0008870	+.0097478	0.4452811	+.0074934	0.0008870	+.0097478	0.4452811	+.0074934
0.0017458	+.0122177	0.4531000	+.0072374	0.0017458	+.0122177	0.4531000	+.0072374
0.0028947	+.0129337	0.4609190	+.0069790	0.0028947	+.0129337	0.4609190	+.0069790
0.0043436	+.0128177	0.4687380	+.0067206	0.0043436	+.0128177	0.4687380	+.0067206
0.0060925	+.0118737	0.4765570	+.0064622	0.0060925	+.0118737	0.4765570	+.0064622
0.0081414	+.0101197	0.4843760	+.0062038	0.0081414	+.0101197	0.4843760	+.0062038
0.0104903	+.0075657	0.4921950	+.0059454	0.0104903	+.0075657	0.4921950	+.0059454
0.0131392	+.0043117	0.5000140	+.0056870	0.0131392	+.0043117	0.5000140	+.0056870
0.0160881	+.0003577	0.5078330	+.0054286	0.0160881	+.0003577	0.5078330	+.0054286
0.0193370	-.0031963	0.5156520	+.0051702	0.0193370	-.0031963	0.5156520	+.0051702
0.0228859	-.0061423	0.5234710	+.0049118	0.0228859	-.0061423	0.5234710	+.0049118
0.0267348	-.0085883	0.5312900	+.0046534	0.0267348	-.0085883	0.5312900	+.0046534
0.0308837	-.0105343	0.5391090	+.0043950	0.0308837	-.0105343	0.5391090	+.0043950
0.0353326	-.0119803	0.5469280	+.0041366	0.0353326	-.0119803	0.5469280	+.0041366
0.0400815	-.0129263	0.5547470	+.0038782	0.0400815	-.0129263	0.5547470	+.0038782
0.0451304	-.0133723	0.5625660	+.0036198	0.0451304	-.0133723	0.5625660	+.0036198
0.0504793	-.0134183	0.5703850	+.0033614	0.0504793	-.0134183	0.5703850	+.0033614
0.0561282	-.0130643	0.5782040	+.0031030	0.0561282	-.0130643	0.5782040	+.0031030
0.0620771	-.0123103	0.5860230	+.0028446	0.0620771	-.0123103	0.5860230	+.0028446
0.0683260	-.0111563	0.5938420	+.0025862	0.0683260	-.0111563	0.5938420	+.0025862
0.0748749	-.0096023	0.6016610	+.0023278	0.0748749	-.0096023	0.6016610	+.0023278
0.0817238	-.0076483	0.6094800	+.0020694	0.0817238	-.0076483	0.6094800	+.0020694
0.0888727	-.0052943	0.6173000	+.0018110	0.0888727	-.0052943	0.6173000	+.0018110
0.0963216	-.0025403	0.6251190	+.0015526	0.0963216	-.0025403	0.6251190	+.0015526
0.1040705	+.0005137	0.6329380	+.0012942	0.1040705	+.0005137	0.6329380	+.0012942
0.1121194	+.0034597	0.6407570	+.0010358	0.1121194	+.0034597	0.6407570	+.0010358
0.1204683	+.0061057	0.6485760	+.0007774	0.1204683	+.0061057	0.6485760	+.0007774
0.1291172	+.0084517	0.6563950	+.0005190	0.1291172	+.0084517	0.6563950	+.0005190
0.1380661	+.0104977	0.6642140	+.0002606	0.1380661	+.0104977	0.6642140	+.0002606
0.1473150	+.0122437	0.6720330	+.0000022	0.1473150	+.0122437	0.6720330	+.0000022
0.1568639	+.0136897	0.6798520	-.0002562	0.1568639	+.0136897	0.6798520	-.0002562
0.1667128	+.0148357	0.6876710	-.0005146	0.1667128	+.0148357	0.6876710	-.0005146
0.1768617	+.0156817	0.6954900	-.0007730	0.1768617	+.0156817	0.6954900	-.0007730
0.1873106	+.0162277	0.7033090	-.0010314	0.1873106	+.0162277	0.7033090	-.0010314
0.1980595	+.0164737	0.7111280	-.0012900	0.1980595	+.0164737	0.7111280	-.0012900
0.2091084	+.0164197	0.7189470	-.0015486	0.2091084	+.0164197	0.7189470	-.0015486
0.2204573	+.0160657	0.7267660	-.0018072	0.2204573	+.0160657	0.7267660	-.0018072
0.2321062	+.0154117	0.7345850	-.0020658	0.2321062	+.0154117	0.7345850	-.0020658
0.2440551	+.0144577	0.7424040	-.0023244	0.2440551	+.0144577	0.7424040	-.0023244
0.2563040	+.0132037	0.7502230	-.0025830	0.2563040	+.0132037	0.7502230	-.0025830
0.2688529	+.0117497	0.7580420	-.0028416	0.2688529	+.0117497	0.7580420	-.0028416
0.2817018	+.0100957	0.7658610	-.0031002	0.2817018	+.0100957	0.7658610	-.0031002
0.2948507	+.0082417	0.7736800	-.0033588	0.2948507	+.0082417	0.7736800	-.0033588
0.3083000	+.0061877	0.7815000	-.0036174	0.3083000	+.0061877	0.7815000	-.0036174
0.3220493	+.0039337	0.7893190	-.0038760	0.3220493	+.0039337	0.7893190	-.0038760
0.3361000	+.0014797	0.7971380	-.0041346	0.3361000	+.0014797	0.7971380	-.0041346
0.3504507	-.0011743	0.8049570	-.0043932	0.3504507	-.0011743	0.8049570	-.0043932
0.3651000	-.0039183	0.8127760	-.0046518	0.3651000	-.0039183	0.8127760	-.0046518
0.3800500	-.0067123	0.8205950	-.0049104	0.3800500	-.0067123	0.8205950	-.0049104
0.3953000	-.0095563	0.8284140	-.0051690	0.3953000	-.0095563	0.8284140	-.0051690
0.4108500	-.0124503	0.8362330	-.0054276	0.4108500	-.0124503	0.8362330	-.0054276
0.4267000	-.0153943	0.8440520	-.0056862	0.4267000	-.0153943	0.8440520	-.0056862
0.4428500	-.0183883	0.8518710	-.0059448	0.4428500	-.0183883	0.8518710	-.0059448
0.4593000	-.0214323	0.8596900	-.0062034	0.4593000	-.0214323	0.8596900	-.0062034
0.4760500	-.0245263	0.8675090	-.0064620	0.4760500	-.0245263	0.8675090	-.0064620
0.4931000	-.0276703	0.8753280	-.0067206	0.4931000	-.0276703	0.8753280	-.0067206
0.5104500	-.0308643	0.8831470	-.0069792	0.5104500	-.0308643	0.8831470	-.0069792
0.5281000	-.0341083	0.8909660	-.0072378	0.5281000	-.0341083	0.8909660	-.0072378
0.5460500	-.0374023	0.8987850	-.0074964	0.5460500	-.0374023	0.8987850	-.0074964
0.5643000	-.0407463	0.9066040	-.0077550	0.5643000	-.0407463	0.9066040	-.0077550
0.5828500	-.0441403	0.9144230	-.0080136	0.5828500	-.0441403	0.9144230	-.0080136
0.6017000	-.0475843	0.9222420	-.0082722	0.6017000	-.0475843	0.9222420	-.0082722
0.6208500	-.0510783	0.9300610	-.0085308	0.6208500	-.0510783	0.9300610	-.0085308
0.6403000	-.0546223	0.9378800	-.0087894	0.6403000	-.0546223	0.9378800	-.0087894
0.6600500	-.0582163	0.9457000	-.0090480	0.6600500	-.0582163	0.9457000	-.0090480
0.6801000	-.0618603	0.9535190	-.0093066	0.6801000	-.0618603	0.9535190	-.0093066
0.7004500	-.0655543	0.9613380	-.0095652	0.7004500	-.0655543	0.9613380	-.0095652
0.7211000	-.0693083	0.9691570	-.0098238	0.7211000	-.0693083	0.9691570	-.0098238
0.7420500	-.0731223	0.9769760	-.0100824	0.7420500	-.0731223	0.9769760	-.0100824
0.7633000	-.0769963	0.9847950	-.0103410	0.7633000	-.0769963	0.9847950	-.0103410
0.7848500	-.0809303	0.9926140	-.0106000	0.7848500	-.0809303	0.9926140	-.0106000
0.8067000	-.0849243	1.0004330	-.0108590	0.8067000	-.0849243	1.0004330	-.0108590
0.8288500	-.0889783	1.0082520	-.0111180	0.8288500	-.0889783	1.0082520	-.0111180
0.8513000	-.0930923	1.0160710	-.0113770	0.8513000	-.0930923	1.0160710	-.0113770
0.8740500	-.0972663	1.0238900	-.0116360	0.8740500	-.0972663	1.0238900	-.0116360
0.8971000	-.1015003	1.0317090	-.0118950	0.8971000	-.1015003	1.0317090	-.0118950
0.9204500	-.1057943	1.0395280	-.0121540	0.9204500	-.1057943	1.0395280	-.0121540
0.9441000	-.1101483	1.0473470	-.0124130	0.9441000	-.1101483	1.0473470	-.0124130
0.9680500	-.1145623	1.0551660	-.0126720	0.9680500	-.1145623	1.0551660	-.0126720
0.9923000	-.1190363	1.0629850	-.0129310	0.9923000	-.1190363	1.0629850	-.0129310
1.0168500	-.1235703	1.0708040	-.0131900	1.0168500	-.1235703	1.0708040	-.0131900
1.0417000	-.1281643	1.0786230	-.0134490	1.0417000	-.1281643	1.0786230	-.0134490
1.0668500	-.1328183	1.0864420	-.0137080	1.0668500	-.1328183	1.0864420	-.0137080
1.0923000	-.1375323	1.0942610	-.0139670	1.0923000	-.1375323	1.0942610	-.0139670
1.1180500	-.1423063	1.1020800	-.0142260	1.1180500	-.1423063	1.1020800	-.0142260
1.1441000	-.1471403	1.1099000	-.0144850	1.1441000	-.1471403	1.1099000	-.0144850
1.1704500	-.1520343	1.1177190	-.0147440	1.1704500	-.1520343	1.1177190	-.0147440
1.1971000	-.1569883	1.1255380	-.0150030	1.1971000	-.1569883	1.1255380	-.0150030
1.2240500	-.1619923	1.1333570	-.0152620	1.2240500	-.1619923	1.1333570	-.0152620
1.2513000	-.1670463	1.1411760	-.0155210	1.2513000	-.1670463	1.1411760	-.0155210
1.2788500	-.1721503	1.1490000	-.0157800	1.2788500	-.1721503	1.1490000	-.0157800
1.3067000	-.1773043	1.1568190	-.0160390	1.3067000	-.1773043	1.1568190	-.0160390
1.3348500	-.1825083	1.1646380	-.0162980	1.3348500	-.1825083	1.1646380	-.0162980
1.3633000	-.1877623	1.1724570	-.0165570	1.3633000	-.1877623	1.1724570	-.0165570
1.3920500	-.1930663	1.1802760	-.0168160	1.3920500	-.1930663	1.1802760	-.0168160
1.4211000	-.1984203	1.1880950	-.0170750	1.4211000	-.1984203	1.1880950	-.0170750
1.4504500	-.2038243	1.1959140	-.0173340	1.4504500	-.2038243	1.1959140	-.0173340
1.4801000	-.2092783	1.2037330	-.0175930	1.4801000	-.2092783	1.2037330	-.0175930
1.5100500	-.2147823	1.2115520	-.0178520	1.5100500	-.2147823	1.2115520	-.0178520
1.5403000	-.2203363	1.2193710	-.0181110	1.5403000	-.2203363	1.2193710	-.0181110
1.5708500	-.2259403	1.2271900	-.0183700	1.5708500	-.2259403	1.2271900	-.0183700
1.6017000	-.2315943	1.2350090	-.0186290	1.6017000	-.2315943	1.2350090	-.0186290
1.6328500	-.2372983	1.2428280	-.0188880	1.6328500	-.2372983	1.2428280	-.0188880
1.6643000	-.2430523	1.2506470	-.0191470	1.6643000	-.2430523	1.2506470	-.0191470

TABLE 4.2

Actual contour data of the
NLR 7301 airfoil (conf. B)
(measures in mm)

x	z _{upper}	z _{lower}
000.000	000.000	-000.000
000.500	003.250	-002.820
001.000	004.595	-003.780
002.000	006.360	-005.025
003.000	007.750	-005.880
004.000	008.415	-006.525
005.000	009.030	-007.065
006.000	009.520	-007.520
007.000	009.940	-007.930
008.000	010.315	-008.290
009.000	010.640	-008.620
010.000	010.935	-008.920
015.000	012.045	-010.110
020.000	013.080	-010.990
025.000	013.545	-011.695
030.000	014.105	-012.375
040.000	014.945	-013.125
050.000	015.400	-013.620
060.000	015.815	-013.795
070.000	015.910	-013.665
080.000	015.800	-013.190
090.000	015.400	-012.245
100.000	014.910	-010.810
110.000	014.055	-009.030
120.000	012.835	-006.945
130.000	011.240	-004.760
134.500	010.410	-003.785
137.500	009.940	-003.165
140.500	009.450	-002.645
150.000	007.335	-000.780
160.000	005.135	000.495
170.000	002.935	000.975
175.000	001.855	000.860
180.000	000.775	000.465

TABLE 4.3

Test program for the NLR 7301 airfoil (conf. A)

Basic program: amplitude of oscillation: $\alpha_0 = 0.5$ degree
frequencies: 0, 10 and 80 Hz
transition strip at $x/c = 0.3$

Incidence	MACH NUMBER										
	.5	.6	.65	.675	.70	.725	.74	.75	.76	.775	.80
$\alpha_m = 0^\circ$	x				x			x			
0.85	x	x	x	x	x	x	x	x	x	x	x
1.50	x				x			x			
3.00	x	x	x	x	x	x		x			

Influence of amplitude and frequency transition strip at $x/c = 0.3$

Incidence	amplitude α_0	freq.	MACH NUMBER		
			.5	.7	.75
$\alpha_m = 0.85^\circ$	0.1; 0.25; 0.75; 1.0; 1.5	10; 80 Hz	x	x	x
3.00	0.1; 0.25; 0.75; 1.0	10; 80			x
0.85°	0.5; 1.0	10; 30; 60; 80 Hz	x	x	x
3.00	2.5; 1.0	10; 30; 60; 80			x

Additional tests with natural transition

Incidence	amplitude α_0	freq.	MACH NUMBER		
			.5	.7	.75
$\alpha_m = 0.85^\circ$	0.5; 1.0	10 Hz	x	x	x
	0.5; 0.75	80	x	x	x
3.00	0.5; 1.0	10			x
	0.5; 0.75	80			x
0.85	0.5	30; 60	x		x

Note regarding Tables 4.1 and 4.2: In Ref. 4.7 the contour coordinates have been transformed to unit chord. The model was designed to shape given by Table 4.1, but the trailing edge was cut off at $x/c = 1.0$. The actual measured shape of the model is given in the table above.

TABLE 4.4
Test cases for the NLE 730 airfoil (conf's A and B) included in Data Set 4

Mission	Flow	CF Case				Data Set 4				Re*10 ⁻⁶	Trans.	Harm.	Table			
		Mo	M	α , °	α , °	Run No	M	σ_m	δ_m					α , °	k	
Pitching about 0.4 c (conf. A)	Subsonic	z1	0.500	0.40	0.5	0	12201	0.499	0.85		0.50	0	1.70	0.3 c	1	4.5
		1	0.500	0.40	0.5	0.098	1601	0.499	0.85		0.55	0.098	1.70	0.3 c	1	4.6
		2	0.500	0.40	0.5	0.262	1301	0.498	0.85		0.44	0.262	1.70	0.3 c	1	4.7
		12	0.700	2.00	0.5	0	14495	0.696	3.00		0.50	0	2.11	0.3 c	1	4.8
		3	0.700	2.00	0.5	0.072	3805	0.696	3.00		0.42	0.072	2.11	0.3 c	1	4.9
Transonic with shock	Subsonic	4	0.700	2.00	1.0	0.072	3905	0.696	3.00		0.98	0.072	2.11	0.3 c	1	4.10
		5	0.700	2.00	0.5	0.192	52705	0.695	3.00		0.55	0.192	2.12	0.3 c	1	4.11
		43	0.721	-0.19	0.5	0	16808	0.744	0.85		0.50	0	2.22	free	1	4.12
		6	0.721	-0.19	0.5	0.068	9608	0.744	0.85	no measurement	0.46	0.068	2.23	free	1	4.13
		7	0.721	-0.19	1.0	0.068										
Flap rotation (conf. B)	Subsonic	8*	0.721	-0.19	0.5	0.181	6708	0.744	0.85		0.61	0.181	2.22	free	1	4.14
		9	0.721	-0.19	0.5	0.453				no measurement						
		z4	0.500	0.40	1.0	0	250	0.503	0		0.95	0	1.69	0.07 c	1	4.15
		10	0.500	0.40	1.0	0.098	253	0.502	0		0.97	0.098	1.69	0.07 c	1	4.16
		z5	0.700	2.00	1.0	0	129	0.702	3.00		0.95	0	2.14	0.3 c	1	4.17
Supercritical design	Transonic with shock	11	0.700	2.00	1.0	0.071	120	0.701	3.00		0.97	0.071	2.14	0.3 c	1	4.18
		z6	0.721	-0.19	1.0	0	160	0.754	0.85		0.96	0	2.23	free	1	4.19
		12	0.721	-0.19	1.0	0.067	148-150	0.755	0.85	0.01	0.95	0.067	2.23	free	1,2,3	4.20-4.22
		13*	0.721	-0.19	1.0	0.161				no measurement						
		14	0.721	-0.19	1.0	0.445	162	0.756	0.85	-0.01	0.90	0.445	2.23	free	1	4.23

Remarks on Table 4.4

Cases z1 to z6 are extra to the computational cases identified in Ref. 4.7. They correspond to zero-frequency ($k = 0$) experimental data that are closely related to the CF Cases for which $k \neq 0$. The asterisks denote Priority Cases.

TABLE 4.5

RUN 12201

M	.499	C2	.50	STAT.		QUASI-INSTAT.	
ALPHA	.85	FREQ	0.	CL	.303	RE	1.835
PO	10376.	K	0.000	CM	.068	IM	0.000
RE	1.70E6						
Q	1524.						

X/C	UPPERSIDE				LOWERSIDE			
	CP+	M+	CPRE+	CPIM+	CP-	M-	CPRE-	CPIM-
.01	-.068	.516	-12.204	0.000	.284	.420	11.230	0.000
.05	-1.148	.771	-12.834	0.000	-.369	.591	9.511	0.000
.10	-.859	.705	-9.225	0.000	-.372	.591	6.417	0.000
.15	-.683	.665	-5.214	0.000	-.386	.595	5.099	0.000
.20	-.647	.657	-5.099	0.000	-.403	.599	4.469	0.000
.25	-.626	.652	-4.183	0.000	-.421	.603	3.953	0.000
.30	-.635	.654	-3.495	0.000	-.417	.602	3.151	0.000
.35	-.594	.644	-2.979	0.000	-.429	.605	2.922	0.000
.40	-.587	.643	-2.636	0.000	-.444	.609	2.693	0.000
.45	-.579	.641	-2.235	0.000	-.445	.609	2.177	0.000
.50	-.570	.639	-2.063	0.000	-.397	.597	1.833	0.000
.55	-.556	.635	-1.776	0.000	-.300	.574	1.318	0.000
.60	-.539	.631	-1.261	0.000	-.203	.550	1.089	0.000
.65	-.491	.620	-.859	0.000	-.086	.521	.688	0.000
.70	-.408	.600	-.458	0.000	.029	.491	.630	0.000
.75	-.307	.576	-.286	0.000	.129	.464	.458	0.000
.80	-.193	.548	-.115	0.000	.208	.442	.401	0.000
.85	-.086	.521	.057	0.000	.269	.425	.458	0.000
.90	.012	.496	-.057	0.000	.298	.416	.286	0.000
.95	.089	.475	-.516	0.000	.301	.415	.115	0.000

TABLE 4.6

RUN 1601

M	.499	C2	.55	STAT.		INSTAT.	
ALPHA	.85	FREQ	30.	CL	.311	RE	1.481
PO	10398.	K	.098	CM	.069	IM	-.170
RE	1.70E6						.151
Q	1529.						

X/C	UPPERSIDE				LOWERSIDE			
	CP+	M+	CPRE+	CPIM+	CP-	M-	CPRE-	CPIM-
.01	-.070	.518	-10.360	2.296	.296	.417	6.804	-3.146
.05	-1.163	.776	-11.456	2.389	-.351	.586	7.090	-2.048
.10	-.846	.703	-8.108	1.833	-.373	.592	4.808	-1.920
.15	-.707	.672	-3.138	.352	-.363	.594	4.104	-1.096
.20	-.654	.659	-4.080	.853	-.400	.598	3.403	-.864
.25	-.633	.655	-3.339	.514	-.415	.602	2.854	-.738
.30	-.642	.657	-2.972	.213	-.413	.601	2.725	-.614
.35	-.599	.647	-2.920	.004	-.426	.604	2.671	.011
.40	-.594	.645	-2.413	.024	-.440	.608	2.356	.164
.45	-.582	.643	-2.059	-.054	-.440	.608	1.963	.091
.50	-.571	.640	-1.804	-.181	-.393	.597	1.688	.237
.55	-.562	.638	-1.398	-.139	-.297	.573	1.492	.258
.60	-.542	.633	-1.045	-.155	-.201	.550	1.089	.164
.65	-.494	.622	-.705	-.200	-.084	.520	.852	.296
.70	-.410	.602	-.412	-.227	.030	.491	.259	-.067
.75	-.307	.577	-.191	-.277	.130	.464	.547	.422
.80	-.195	.549	.054	-.279	.212	.441	.571	.457
.85	-.085	.522	.091	-.256	.269	.425	.562	.533
.90	.011	.497	-.090	-.152	.300	.416	.440	.431
.95	.086	.477	-.466	-.092	.302	.415	.250	.284

TABLE 4.7

RUN 1301

M	.498	C2	.44	STAT.	INSTAT.				
ALPHA	.85	FREQ	30.	CL	.290	RE	1.355	IM	.015
P0	10398.	K	.262	CM	.071		.096		.310
RE	1.70E6								
Q	1524.								

X/C	UPPERSIDE				LOWERSIDE			
	CP+	M+	CPRE+	CPIM+	CP-	M-	CPRE-	CPIM-
.01	-.014	.502	-9.118	4.392	.248	.431	5.363	-3.002
.05	-1.106	.760	-8.298	3.528	-.400	.598	5.742	-2.356
.10	-.806	.692	-6.065	1.829	-.402	.598	3.390	-1.596
.15	-.693	.666	-2.099	-.165	-.408	.600	3.630	-1.041
.20	-.637	.653	-3.772	.745	-.418	.602	3.043	-.636
.25	-.620	.649	-3.161	.289	-.436	.606	2.558	-.359
.30	-.635	.653	-2.886	-.023	-.431	.605	2.217	-.317
.35	-.594	.643	-2.839	-.250	-.441	.608	2.911	.124
.40	-.508	.642	-2.251	-.357	-.452	.610	2.829	.443
.45	-.576	.639	-1.996	-.462	-.451	.610	2.216	.503
.50	-.570	.638	-1.819	-.556	-.402	.598	2.062	.727
.55	-.562	.636	-1.352	-.610	-.304	.575	1.573	.807
.60	-.544	.631	-1.034	-.643	-.206	.551	1.132	.821
.65	-.499	.621	-.663	-.645	-.089	.521	1.005	1.079
.70	-.415	.601	-.526	-.690	.026	.491	.177	.151
.75	-.313	.577	-.321	-.748	.128	.464	.999	1.244
.80	-.200	.549	-.102	-.749	.209	.442	1.125	1.202
.85	-.091	.521	-.057	-.714	.266	.425	1.367	1.166
.90	.007	.496	-.158	-.561	.299	.416	.932	.836
.95	.085	.475	-.481	-.048	.301	.415	.488	.450

TABLE 4.8

RUN 14405

M	.696	C2	.50	STAT.	QUAST-INSTAT.				
ALPHA	3.00	FREQ	0.	CL	.715	RE	3.250	IM	0.000
P0	10220.	K	0.000	CM	.074		.373		0.000
RF	2.11FA								
Q	2509.								

X/C	UPPERSIDE				LOWERSIDE			
	CP+	M+	CPRE+	CPIM+	CP-	M-	CPRE-	CPIM-
.01	.004	.695	-5.500	0.000	.601	.449	6.474	0.000
.05	-1.661	1.398	-7.219	0.000	-.092	.731	7.907	0.000
.10	-1.671	1.403	-7.850	0.000	-.201	.773	6.704	0.000
.15	-1.607	1.368	-8.021	0.000	-.258	.794	5.844	0.000
.20	-1.562	1.344	-8.308	0.000	-.312	.814	5.386	0.000
.25	-1.536	1.331	-9.969	0.000	-.356	.831	5.042	0.000
.30	-1.508	1.316	-11.803	0.000	-.373	.837	4.813	0.000
.35	-1.518	1.321	-22.746	0.000	-.409	.851	4.183	0.000
.40	-1.406	1.266	-57.640	0.000	-.453	.868	3.896	0.000
.45	-.585	.918	-49.790	0.000	-.465	.872	3.323	0.000
.50	-.576	.915	1.318	0.000	-.412	.852	2.922	0.000
.55	-.631	.936	9.626	0.000	-.290	.806	2.177	0.000
.60	-.648	.941	8.652	0.000	-.169	.760	1.604	0.000
.65	-.589	.920	5.214	0.000	-.044	.713	1.261	0.000
.70	-.471	.875	2.693	0.000	.079	.666	1.089	0.000
.75	-.337	.824	1.318	0.000	.184	.625	.974	0.000
.80	-.200	.770	.458	0.000	.267	.592	.917	0.000
.85	-.075	.725	-.057	0.000	.324	.569	.859	0.000
.90	.032	.684	-.286	0.000	.356	.556	.745	0.000
.95	.114	.653	-.286	0.000	.354	.557	.630	0.000

TABLE 4.9

RUN 3805

M	.696	C2	.42	STAT.	INSTAT.	
ALPHA	3.00	FREQ	30.	CL	RE	IM
PO	10220.	K	.072	CM	.296	-.90
NE	2.11E6					.106
W	2505.					

X/C	UPPERSIDE				LOWERSIDE			
	CP+	M+	CPRE+	CPIM+	CP-	M-	CPRE-	CPIM-
.01	.001	.695	-4.068	1.563	.605	.447	4.478	-2.328
.05	-1.669	1.398	-6.156	1.863	-.084	.728	6.187	-2.665
.10	-1.682	1.405	-9.320	1.586	-.200	.772	4.633	-2.476
.15	-1.622	1.372	-9.811	1.036	-.259	.794	4.308	-2.078
.20	-1.572	1.346	-9.316	2.170	-.315	.815	3.680	-2.034
.25	-1.554	1.326	-8.715	2.920	-.364	.833	3.458	-1.909
.30	-1.478	1.298	-10.091	5.812	-.385	.841	2.353	-2.017
.35	-1.463	1.290	-19.295	8.129	-.413	.852	3.845	-1.367
.40	-1.122	1.134	-74.021	40.662	-.448	.865	4.448	-1.226
.45	-.720	.969	-34.136	3.267	-.466	.872	3.831	-1.196
.50	-.620	.930	-.667	-6.649	-.410	.851	3.454	-.855
.55	-.622	.931	10.303	-6.919	-.289	.805	2.630	-.647
.60	-.631	.934	8.852	-5.420	-.170	.760	2.305	-.552
.65	-.574	.914	5.066	-3.002	-.044	.713	1.858	-.322
.70	-.464	.871	2.838	-1.691	.079	.666	.353	-.393
.75	-.333	.821	1.978	-1.062	.183	.625	1.575	.065
.80	-.198	.770	1.026	-.487	.264	.593	1.795	.192
.85	-.073	.725	.435	-.362	.323	.569	1.826	.310
.90	.033	.683	.022	-.473	.354	.556	1.565	.068
.95	.112	.652	-.369	-.596	.353	.557	1.153	-.261

TABLE 4.10

RUN 3905

M	.696	C2	.48	STAT.	INSTAT.	
ALPHA	4.00	FREQ	30.	CL	RE	IM
PO	10220.	K	.072	CM	.306	-.988
NE	2.11E6					.003
W	2509.					

X/C	UPPERSIDE				LOWERSIDE			
	CP+	M+	CPRE+	CPIM+	CP-	M-	CPRE-	CPIM-
.01	.013	.691	-4.005	1.351	.604	.447	3.921	-2.109
.05	-1.666	1.399	-5.628	1.316	-.084	.728	5.863	-2.194
.10	-1.686	1.411	-8.972	1.172	-.202	.774	4.267	-2.127
.15	-1.622	1.375	-7.543	1.655	-.263	.796	4.523	-1.770
.20	-1.554	1.339	-6.781	2.275	-.319	.817	3.697	-1.785
.25	-1.412	1.317	-8.630	2.748	-.367	.835	3.240	-1.686
.30	-1.453	1.288	-9.320	3.526	-.384	.841	3.835	-1.784
.35	-1.229	1.185	-31.991	17.920	-.416	.854	3.633	-1.288
.40	-1.110	1.130	-34.780	18.621	-.452	.867	4.728	-1.081
.45	-.931	1.055	-23.743	10.023	-.468	.873	3.495	-1.059
.50	-.746	.981	-7.757	-1.004	-.413	.853	3.030	-.752
.55	-.659	.950	2.002	-3.133	-.292	.807	2.511	-.556
.60	-.610	.927	6.594	-4.290	-.172	.762	1.798	-.410
.65	-.552	.905	5.093	-2.865	-.046	.714	1.468	-.248
.70	-.446	.865	3.157	-1.810	.077	.667	.512	-.349
.75	-.320	.817	1.574	-.900	.182	.626	1.273	-.002
.80	-.190	.768	.796	-.447	.262	.594	1.331	.130
.85	-.070	.723	.141	-.279	.320	.571	1.368	.171
.90	.031	.684	-.086	-.333	.351	.558	1.191	.037
.95	.107	.655	-.114	-.558	.351	.558	1.028	-.280

TABLE 4.11

RUN 52705

M	.695	O2	.55	STAT.		INSTAT.	
ALPHA	3.00	FREQ	80.	CL	.694	RE	1.541
PO	10265.	K	.192	CM	.072	IM	-.989
MC	2.12E6						.087
W	2511.						

X/C	UPPERSIDE				LOWERSIDE			
	CP+	M+	CPRE+	CPIM+	CP-	M-	CPRE-	CPIM-
.01	.010	.691	-2.639	1.667	.599	.443	2.724	-1.662
.05	-1.657	1.389	-4.196	2.153	-.095	.730	3.438	-1.706
.10	-1.667	1.395	-3.680	1.892	-.206	.772	2.436	-.983
.15	-1.604	1.361	-6.745	3.486	-.267	.795	2.347	-.805
.20	-1.597	1.346	-5.944	3.449	-.323	.816	2.223	-.693
.25	-1.520	1.317	-5.168	3.809	-.368	.833	1.997	-.502
.30	-1.458	1.291	-3.517	3.595	-.390	.841	1.267	.136
.35	-1.454	1.284	-6.493	12.094	-.417	.852	2.171	-.180
.40	-1.098	1.122	-14.141	42.695	-.453	.863	2.266	-.372
.45	-.687	.955	-12.598	9.450	-.473	.872	2.020	-.199
.50	-.608	.924	-2.708	-5.711	-.415	.851	1.870	-.002
.55	-.626	.931	1.611	-7.332	-.294	.805	1.507	.163
.60	-.639	.936	1.749	-9.694	-.173	.760	1.210	.254
.65	-.585	.916	1.457	-3.256	-.044	.711	1.104	.418
.70	-.466	.871	.874	-2.002	.078	.665	.225	.067
.75	-.334	.821	.739	-1.362	.182	.624	1.358	.411
.80	-.199	.770	.690	-.849	.264	.592	1.582	.293
.85	-.074	.723	.585	-.510	.324	.567	1.870	.247
.90	.032	.682	.125	-.354	.355	.555	1.404	.036
.95	.112	.652	-.284	-.290	.354	.555	.788	-.166

TABLE 4.12

RUN 14400

M	.744	O2	.90	STAT.		QUASI-INSTAT.	
ALPHA	.85	FREQ	n.	CL	.481	RE	3.522
PO	10335.	K	0.000	CM	.108	IM	0.000
RE	2.22E6						0.000
Q	2772.						

X/C	UPPERSIDE				LOWERSIDE			
	CP+	M+	CPRE+	CPIM+	CP-	M-	CPRE-	CPIM-
.01	.328	.607	-5.214	0.000	.742	.604	8.193	0.000
.05	-1.101	1.229	-11.250	0.000	-.440	.424	11.001	0.000
.10	-1.140	1.259	-8.652	0.000	-.484	.464	9.683	0.000
.15	-1.113	1.234	-10.943	0.000	-.516	.459	7.964	0.000
.20	-1.074	1.217	-14.897	0.000	-.464	.470	7.735	0.000
.25	-1.060	1.208	-10.022	0.000	-.612	1.000	5.652	0.000
.30	-1.047	1.201	-21.944	0.000	-.624	1.005	7.047	0.000
.35	-1.037	1.197	-18.335	0.000	-.681	1.017	7.907	0.000
.40	-1.039	1.197	-18.792	0.000	-.676	1.028	7.047	0.000
.45	-1.046	1.201	-18.194	0.000	-.660	1.021	5.157	0.000
.50	-1.062	1.209	-17.762	0.000	-.857	.477	4.123	0.000
.55	-1.043	1.201	-16.157	0.000	-.348	.892	2.235	0.000
.60	-1.001	1.179	-12.777	0.000	-.184	.820	2.003	0.000
.65	-.785	1.078	-14.610	0.000	-.034	.798	1.662	0.000
.70	-.443	.997	2.749	0.000	.044	.783	1.662	0.000
.75	-.307	.871	1.375	0.000	.205	.648	2.005	0.000
.80	-.178	.817	-.286	0.000	.281	.626	1.891	0.000
.85	-.056	.766	-.816	0.000	.342	.600	1.891	0.000
.90	.063	.718	.401	0.000	.385	.581	2.120	0.000
.95	.162	.677	2.005	0.000	.394	.576	2.177	0.000

TABLE 4.13

RUN 9604

M	.744	C2	.46	STAT.	INSTAT.		
ALPHA	.85	FREQ	30.	CL	RE	IM	
P0	10380.	K	.068	CM	2.710	-.914	
RE	2.23E6				.157	.074	
U	2785.						

X/C	UPPERSIDE				LOWERSIDE			
	CP+	M+	CPRE+	CPIM+	CP-	M-	CPRE-	CPIM-
.01	.329	.605	-3.845	1.210	.332	.604	4.500	-2.394
.05	-1.093	1.225	-8.934	2.739	-.435	.924	7.494	-2.975
.10	-1.153	1.257	-8.638	1.809	-.486	.945	6.085	-2.661
.15	-1.111	1.234	-8.954	1.699	-.517	.959	6.092	-2.130
.20	-1.062	1.210	-7.623	3.184	-.566	.980	5.631	-2.170
.25	-1.041	1.199	-4.752	3.917	-.619	1.003	5.684	-2.346
.30	-1.023	1.190	-10.687	4.692	-.627	1.006	6.345	-1.730
.35	-1.009	1.184	-12.728	6.138	-.652	1.017	6.361	-1.423
.40	-1.012	1.185	-12.752	7.085	-.687	1.032	5.064	-1.614
.45	-1.011	1.185	-14.213	8.315	-.665	1.023	3.797	-1.090
.50	-1.007	1.182	-18.586	11.621	-.564	.979	2.687	-.537
.55	-1.030	1.194	-13.956	8.002	-.360	.892	.816	.038
.60	-1.030	1.194	-9.447	1.031	-.187	.821	.393	.102
.65	-.722	1.049	20.134	-12.438	-.035	.758	.049	.119
.70	-.449	.931	6.371	-4.040	.096	.704	.111	-.043
.75	-.297	.867	3.074	-1.595	.200	.660	1.217	.352
.80	-.168	.813	1.813	-.455	.276	.628	1.495	.433
.85	-.048	.764	.563	-.076	.337	.602	1.636	.497
.90	.061	.719	-.646	-.127	.373	.585	1.032	.167
.95	.150	.682	-1.429	-.302	.387	.560	.319	-.168

TABLE 4.14

RUN 6706

M	.744	C2	.61	STAT.	INSTAT.		
ALPHA	.85	FREQ	80.	CL	RE	IM	
P0	10333.	K	.181	CM	1.498	-.586	
RE	2.22E6				.239	.255	
U	2770.						

X/C	UPPERSIDE				LOWERSIDE			
	CP+	M+	CPRE+	CPIM+	CP-	M-	CPRE-	CPIM-
.01	.323	.604	-2.485	1.472	.338	.601	2.747	-1.772
.05	-1.107	1.231	-6.763	3.710	-.428	.921	3.809	-2.291
.10	-1.167	1.263	-3.525	1.841	-.484	.944	3.170	-1.987
.15	-1.125	1.240	-5.486	2.970	-.511	.956	3.285	-1.459
.20	-1.077	1.216	-4.085	3.026	-.563	.978	3.051	-1.256
.25	-1.059	1.207	-4.067	3.493	-.607	.997	2.934	-1.079
.30	-1.041	1.198	-4.510	4.794	-.622	1.003	3.645	-.763
.35	-1.032	1.193	-4.300	6.034	-.642	1.012	3.599	-.252
.40	-1.032	1.193	-3.802	6.416	-.677	1.028	2.839	.183
.45	-1.031	1.193	-3.531	7.356	-.657	1.019	2.138	.471
.50	-1.015	1.185	-2.966	10.747	-.558	.976	1.385	1.233
.55	-1.014	1.184	-3.064	9.904	-.359	.892	.357	1.266
.60	-.934	1.175	-6.754	1.791	-.187	.828	.239	1.134
.65	-.673	1.027	-4.213	-14.659	-.035	.758	.135	1.316
.70	-.430	.930	.572	-6.041	.096	.704	.092	.222
.75	-.303	.869	1.383	-2.949	.202	.659	1.319	.944
.80	-.171	.814	1.351	-1.649	.276	.627	1.716	.483
.85	-.050	.764	.889	-1.202	.339	.601	1.907	.359
.90	.060	.719	-.004	-.403	.380	.583	1.053	.293
.95	.149	.682	-.771	-.330	.388	.579	.302	.269

TABLE 4.15

Pressure distributions for NLR 7301 with control surface and transition strip at $x/c = .07$
ZERO FREQUENCY TEST DATA NLR 7301 WITH OSCILLATING FLAP

X/C	UPPERSIDE				LOWERSIDE			
	CP+	M+	CPRE+	CPIM+	CP-	M-	CPRE-	CPIM-
.010	.121	.470	-2.816	.000	.067	.485	3.157	.000
.030	-.940	.730	-4.084	.000	-.467	.619	3.189	.000
.050	-.873	.715	-3.457	.000	-.535	.636	2.607	.000
.100	-.627	.657	-2.129	.000	-.465	.619	2.207	.000
.150	-.568	.644	-1.839	.000	-.468	.620	1.846	.000
.200	-.544	.638	-1.718	.000	-.474	.621	1.706	.000
.250	-.533	.635	-1.670	.000	-.481	.623	1.646	.000
.300	-.523	.633	-1.622	.000	-.489	.625	1.645	.000
.350	-.511	.630	-1.597	.000	-.485	.624	1.645	.000
.400	-.509	.630	-1.621	.000	-.496	.626	1.685	.000
.450	-.504	.628	-1.597	.000	-.483	.623	1.786	.000
.500	-.500	.627	-1.693	.000	-.430	.611	1.807	.000
.550	-.489	.625	-1.766	.000	-.328	.586	1.768	.000
.600	-.469	.620	-1.958	.000	-.222	.560	1.770	.000
.650	-.421	.608	-2.102	.000	-.109	.531	1.812	.000
.700	-.340	.589	-2.389	.000	.008	.501	1.854	.000
.725	-.286	.576	-2.509	.000	.053	.489	1.854	.000
.760	-.271	.572	-3.496	.000	.115	.472	1.975	.000
.775	-.235	.563	-2.580	.000	.138	.465	1.635	.000
.800	-.171	.547	-1.761	.000	.174	.455	1.355	.000
.850	-.067	.520	-1.013	.000	.227	.440	.955	.000
.900	.020	.498	-.361	.000	.259	.431	1.016	.000
.950	.097	.477	-.408	.000	.269	.428	.575	.000

TEST DATA	MODEL DATA	OVERALL DATA	STEADY	UNSTEADY
MEETRUNNR. 250	ALPHA .00 DEG.			RE IM
MACH .503	DELTA .02 DEG.	NORMAL FORCE CL .173		1.090 .000
Q [PA] 15004	AMPL. .95 DEG.	MOMENT(1/4C) CM .058		.393 .000
RE 1.69E6	FREQ. .0 HZ	FLAP FORCE RC .0625		.1634 .0000
HARM 1	RFREQ .000	HINGE MOMENT NC .0059		.0246 .0000
IDENTNR. 10				

TABLE 4.16

FUNDAMENTAL FREQUENCY TEST DATA NLR 7301 WITH OSCILLATING FLAP

X/C	UPPERSIDE				LOWERSIDE			
	CP+	M+	CPRE+	CPIM+	CP-	M-	CPRE-	CPIM-
.010	.126	.469	-2.159	1.234	.069	.484	2.243	-1.519
.030	-.935	.728	-3.015	1.557	-.464	.618	2.675	-1.422
.050	-.867	.713	-2.803	1.411	-.531	.634	.973	-1.323
.100	-.629	.658	-1.950	.987	-.477	.620	1.900	-.860
.150	-.570	.643	-1.384	.755	-.471	.620	1.389	-.839
.200	-.545	.638	-1.238	.629	-.474	.621	1.321	-.675
.250	-.534	.635	-1.237	.629	-.483	.623	1.291	-.568
.300	-.522	.632	-1.363	.483	-.488	.624	.976	-.584
.350	-.512	.630	-1.362	.484	-.488	.624	1.306	-.447
.400	-.509	.629	-1.290	.421	-.497	.626	1.419	-.439
.450	-.503	.628	-1.425	.411	-.483	.623	1.418	-.439
.500	-.501	.627	-1.551	.266	-.437	.610	1.521	-.320
.550	-.487	.624	-1.550	.266	-.326	.585	1.622	-.201
.600	-.470	.620	-1.820	.247	-.222	.559	1.776	-.024
.650	-.421	.608	-1.954	.239	-.107	.530	1.929	.152
.700	-.340	.588	-2.347	.078	.009	.500	1.970	.319
.725	-.283	.574	-2.416	.144	.057	.487	1.975	.205
.760	-.269	.571	-3.494	.072	.117	.471	2.123	.492
.775	-.233	.562	-2.728	-.215	.140	.465	1.788	.471
.800	-.172	.547	-1.711	-.213	.174	.455	1.565	.454
.850	-.067	.520	-.901	-.159	.228	.440	1.119	.429
.900	.022	.497	-.368	-.069	.261	.430	.955	.362
.950	.097	.476	-.425	-.194	.270	.428	.517	.225

TEST DATA	MODEL DATA	OVERALL DATA	STEADY	UNSTEADY
MEETRUNNR. 253	ALPHA .00 DEG.			RE IM
MACH .502	DELTA .02 DEG.	NORMAL FORCE CL .172		.927 -.197
Q [PA] 15024	AMPL. .97 DEG.	MOMENT(1/4C) CM .058		.418 .065
RE 1.69E6	FREQ. 30.0 HZ	FLAP FORCE RC .0625		.1705 .0376
HARM 1	RFREQ .000	HINGE MOMENT NC .0059		.0255 .0077
IDENTNR. 10				

TABLE 4.17

ZERO FREQUENCY TEST DATA NLR 7301 WITH OSCILLATING FLAP

X/C	UPPERSIDE				LOWERSIDE			
	CP+	H+	CPRE+	CPIN+	CP-	H-	CPRE-	CPIN-
.010	.009	.699	-.832	.000	.583	.461	1.305	.000
.030	-1.467	1.312	-.984	.000	.055	.681	1.750	.000
.050	-1.597	1.381	-1.214	.000	-.107	.743	1.775	.000
.100	-1.562	1.361	-1.078	.000	-.208	.782	1.574	.000
.150	-1.501	1.329	-1.345	.000	-.259	.801	1.550	.000
.200	-1.459	1.307	-1.522	.000	-.312	.821	1.614	.000
.250	-1.430	1.293	-2.411	.000	-.356	.838	1.644	.000
.300	-1.302	1.230	-10.641	.000	-.380	.847	1.683	.000
.350	-.857	1.035	-23.199	.000	-.424	.864	1.890	.000
.400	-.633	.945	-3.794	.000	-.466	.880	2.258	.000
.450	-.616	.939	.741	.000	-.476	.884	2.263	.000
.500	-.641	.949	.823	.000	-.423	.864	2.263	.000
.550	-.638	.947	-.449	.000	-.304	.818	1.914	.000
.600	-.605	.934	-1.202	.000	-.188	.774	1.957	.000
.650	-.506	.896	-1.699	.000	-.062	.726	1.971	.000
.700	-.381	.848	-1.984	.000	.063	.678	2.034	.000
.725	-.307	.819	-2.121	.000	.117	.657	2.063	.000
.760	-.252	.799	-2.488	.000	.178	.633	2.235	.000
.775	-.217	.785	-1.813	.000	.205	.622	1.847	.000
.800	-.152	.760	-1.168	.000	.245	.606	1.503	.000
.850	-.042	.718	-.743	.000	.305	.582	1.110	.000
.900	.044	.685	-.785	.000	.338	.568	.874	.000
.950	.166	.661	-1.093	.000	.337	.568	.423	.000

TEST DATA	MODEL DATA	OVERALL DATA	STEADY	UNSTEADY
MEETRNNR. 129	ALPHA 3.00 DEG.			RE IN
MACH .702	DELTA -.08 DEG.	NORMAL FORCE CL	.593	1.410 .000
Q [PA] 25035	AMPL. .95 DEG.	MOMENT(1/4C) CM	.052	.484 .000
RE 2.1486	FREQ. .0 HZ	FLAP FORCE RC	.0743	.1615 .0000
HARM 1	HFREQ .000	HINGE MOMENT NC	.0073	.0282 .0000
IDENTNR. 5				

TABLE 4.18

FUNDAMENTAL FREQUENCY TEST DATA NLR 7301 WITH OSCILLATING FLAP

X/C	UPPERSIDE				LOWERSIDE			
	CP+	H+	CPRE+	CPIN+	CP-	H-	CPRE-	CPIN-
.010	.006	.699	-.709	.568	.584	.460	.940	-.829
.030	-1.477	1.312	-.982	.945	.659	.679	1.855	-.694
.050	-1.600	1.380	-1.121	.835	-.105	.742	.844	-1.057
.100	-1.559	1.358	-.887	.705	-.207	.781	.762	-.933
.150	-1.500	1.326	-1.116	.942	-.258	.800	.983	-.926
.200	-1.437	1.305	-1.220	1.009	-.310	.820	1.000	-.886
.250	-1.426	1.289	-1.726	1.507	-.356	.837	1.097	-.854
.300	-1.277	1.215	-5.784	4.585	-.379	.846	1.193	-.853
.350	-.880	1.043	-17.495	10.740	-.422	.863	1.421	-.861
.400	-.652	.952	-5.238	.628	-.462	.878	1.519	-.865
.450	-.622	.940	-.373	-1.670	-.476	.883	1.744	-.846
.500	-.640	.947	-.030	-1.932	-.422	.863	1.871	-.879
.550	-.636	.946	-.898	-1.355	-.361	.816	1.933	-.495
.600	-.599	.931	-1.503	-.841	-.181	.771	1.990	-.339
.650	-.568	.894	-1.768	-.536	-.098	.724	2.058	-.186
.700	-.379	.846	-2.032	-.540	.066	.676	2.186	-.630
.725	-.317	.819	-2.166	-.619	.118	.656	2.181	-.070
.760	-.235	.799	-2.621	-.252	.173	.634	2.408	.059
.775	-.217	.784	-1.908	-.640	.202	.622	2.150	.254
.800	-.151	.759	-1.136	-.595	.243	.606	1.763	.289
.850	-.042	.718	-.629	-.342	.304	.582	1.381	.284
.900	.040	.686	-.824	-.189	.337	.568	1.025	.219
.950	.098	.663	-1.304	-.154	.334	.569	.451	.078

TEST DATA	MODEL DATA	OVERALL DATA	STEADY	UNSTEADY
MEETRNNR. 120	ALPHA 3.00 DEG.			RE IN
MACH .702	DELTA .03 DEG.	NORMAL FORCE CL	.595	1.213 -.350
Q [PA] 25006	AMPL. .97 DEG.	MOMENT(1/4C) CM	.053	.516 .069
RE 2.1486	FREQ. 30.0 HZ	FLAP FORCE RC	.0746	-.1783 .0384
HARM 1	HFREQ .071	HINGE MOMENT NC	.0073	.0316 .6068
IDENTNR. 5				

TABLE 4.19

ZERO FREQUENCY TEST DATA NLR 7301 WITH OSCILLATING FLAP

X/C	UPPERSIDE			LOWERSIDE				
	CP+	M+	CPRE+	CPIN+	CP-	M-	CPRE-	CPIN-
.010	.329	.613	-.993	.000	.312	.621	1.591	.000
.030	-.958	1.178	-1.801	.000	-.287	.874	2.148	.000
.050	-1.016	1.207	-1.983	.000	-.451	.945	2.308	.000
.100	-1.092	1.246	-1.542	.000	-.512	.971	2.319	.000
.150	-1.034	1.216	-2.036	.000	-.531	.979	2.167	.000
.200	-1.008	1.203	-2.465	.000	-.582	1.002	2.383	.000
.250	-.976	1.186	-3.181	.000	-.623	1.020	2.458	.000
.300	-.956	1.177	-4.652	.000	-.671	1.042	3.444	.000
.350	-.937	1.167	-8.831	.000	-.690	1.051	3.920	.000
.400	-.918	1.158	-8.427	.000	-.732	1.070	4.483	.000
.450	-.872	1.136	-8.701	.000	-.701	1.055	7.333	.000
.500	-.748	1.077	-9.521	.000	-.584	1.003	3.770	.000
.550	-.762	1.083	-7.920	.000	-.376	.912	2.504	.000
.600	-.626	1.022	-5.886	.000	-.204	.839	2.268	.000
.650	-.519	.974	-1.835	.000	-.058	.778	2.313	.000
.700	-.380	.914	-2.003	.000	.077	.721	2.401	.000
.725	-.299	.880	-2.145	.000	.132	.698	2.607	.000
.760	-.249	.859	-2.340	.000	.201	.669	2.467	.000
.775	-.214	.844	-1.779	.000	.228	.657	2.142	.000
.800	-.143	.814	-1.193	.000	.268	.640	1.850	.000
.850	-.024	.764	-.710	.000	.330	.613	1.482	.000
.900	.073	.723	-.917	.000	.369	.596	1.169	.000
.950	.142	.694	-1.268	.000	.372	.594	.670	.000

TEST DATA	MODEL DATA	OVERALL DATA	STEADY	UNSTEADY
HEETRNNR. 160	ALPHA .85 DEG.			RE IM
MACH .754	DELTA .01 DEG.	NORMAL FORCE CL	.352	2.043 .000
Q [PA] 27504	AMPL. .96 DEG.	MOMENT(1/4C) CN	.076	.814 .000
RE 2.23E6	FREQ. 0 HZ	FLAP FORCE RC	.0761	.1870 .0000
HARM 1	HFREQ .060	HINGE MOMENT HC	.0073	.0345 .0000
IDENTNR. 6				

TABLE 4.20

FUNDAMENTAL FREQUENCY TEST DATA NLR 7301 WITH OSCILLATING FLAP

X/C	UPPERSIDE			LOWERSIDE				
	CP+	M+	CPRE+	CPIN+	CP-	M-	CPRE-	CPIN-
.010	.329	.614	-.452	.624	.314	.621	.938	-1.128
.030	-.958	1.178	-.579	1.044	-.287	.875	1.420	-1.588
.050	-1.017	1.209	-.284	.925	-.452	.946	.265	-1.187
.100	-1.090	1.247	-.330	.919	-.512	.972	.404	-1.298
.150	-1.033	1.217	-.479	1.215	-.530	.980	.385	-1.323
.200	-1.001	1.201	-.534	1.459	-.575	1.000	.480	-1.378
.250	-.975	1.188	-.699	1.853	-.621	1.020	.858	-1.567
.300	-.951	1.176	-.877	2.524	-.672	1.044	.939	-1.619
.350	-.928	1.165	-1.392	4.194	-.689	1.051	1.909	-2.222
.400	-.871	1.137	-3.247	8.478	-.728	1.069	2.414	-2.168
.450	-.834	1.119	-4.606	5.156	-.720	1.065	3.145	-2.934
.500	-.800	1.103	-7.824	8.778	-.583	1.004	3.172	-1.336
.550	-.763	1.085	-10.508	1.371	-.377	.914	2.132	-.490
.600	-.679	1.047	-8.004	-3.403	-.207	.862	1.983	-.359
.650	-.513	.972	-2.092	-1.180	-.059	.779	2.122	-.282
.700	-.371	.911	-2.063	-.568	.076	.722	2.323	-.229
.725	-.295	.879	-2.294	-.345	.131	.700	2.299	-.277
.760	-.238	.853	-2.377	-.176	.201	.669	2.342	-.176
.775	-.205	.841	-1.704	-.615	.227	.658	2.177	-.026
.800	-.137	.812	-.909	-.563	.267	.641	1.921	-.000
.850	-.022	.764	-.514	-.298	.330	.614	1.551	.026
.900	.068	.724	-1.078	-.251	.369	.596	1.122	-.073
.950	.136	.698	-1.604	-.264	.372	.595	.647	-.195

TEST DATA	MODEL DATA	OVERALL DATA	STEADY	UNSTEADY
HEETRNNR. 148	ALPHA .85 DEG.			RE IM
MACH .753	DELTA .01 DEG.	NORMAL FORCE CL	.350	1.325 -.826
Q [PA] 27538	AMPL. .95 DEG.	MOMENT(1/4C) CN	.076	.781 -.120
RE 2.23E6	FREQ. 30.0 HZ	FLAP FORCE RC	.0759	.1877 .0195
HARM 1	HFREQ .067	HINGE MOMENT HC	.0074	.0362 .0032
IDENTNR. 6				

TABLE 4.21

FIRST HARMONIC TEST DATA NLR 7301 WITH OSCILLATING FLAP

X/C	UPPERSIDE				LOWERSIDE			
	CP+	M+	CPRE+	CPIN+	CP-	M-	CPRE-	CPIN-
.010	.329	.614	-.015	.015	.313	.621	-.047	-.066
.030	-.956	1.178	-.048	.042	-.288	.875	-.045	-.018
.050	-1.014	1.207	-.007	-.005	-.452	.946	.016	.011
.100	-1.090	1.247	.008	.005	-.512	.972	-.043	.001
.150	-1.033	1.217	-.027	.026	-.531	.980	-.033	-.010
.200	-.999	1.199	-.030	.063	-.574	.999	-.058	-.012
.250	-.974	1.186	-.105	.153	-.621	1.020	-.111	-.015
.300	-.954	1.177	-.139	.242	-.674	1.044	-.039	-.088
.350	-.930	1.165	-.507	.848	-.690	1.051	-.149	-.191
.400	-.873	1.137	-2.026	2.922	-.727	1.068	-.182	-.189
.450	-.830	1.117	-2.427	-6.32	-.719	1.064	.968	-.052
.500	-.795	1.100	-1.356	-4.594	-.582	1.003	.159	.015
.550	-.761	1.084	2.920	-3.489	-.374	.912	.012	.044
.600	-.674	1.044	2.237	2.641	-.202	.839	.031	.001
.650	-.510	.971	.267	.514	-.056	.778	.067	.029
.700	-.371	.911	-.110	.211	.078	.721	.105	.012
.725	-.295	.879	-.182	.029	.131	.699	-.016	-.010
.760	-.239	.855	-.202	-.082	.202	.669	.092	.003
.775	-.206	.841	-.339	-.126	.227	.658	.076	-.015
.800	-.137	.812	-.250	-.159	.267	.641	.058	-.009
.850	-.021	.763	-.062	-.020	.330	.613	.008	.000
.900	.069	.725	.142	.196	.369	.596	-.001	.020
.950	.135	.697	-.237	.257	.372	.595	.040	.014

TEST DATA	MODEL DATA	OVERALL DATA	STEADY	UNSTEADY	
MEETRNHR. 149	ALPHA .85 DEG.			RZ	IM
MACH .754	DELTA .02 DEG.	NORMAL FORCE CL	.350	.037	.007
Q (PA) 27528	AMPL. .95 DEG.	MOMENT(1/4C) CM	.076	-.004	.013
RE 2.2386	FREQ. 30.0 HZ	FLAP FORCE RC	.0759	.0033	-.0034
NARM 2	BFREQ .067	HINGE MOMENT MC	.0074	-.0013	-.0021
IDENTNR. 6					

TABLE 4.22

SECOND HARMONIC TEST DATA NLR 7301 WITH OSCILLATING FLAP

X/C	UPPERSIDE				LOWERSIDE			
	CP+	M+	CPRE+	CPIN+	CP-	M-	CPRE-	CPIN-
.010	.329	.614	.021	-.026	.313	.621	.025	-.037
.030	-.955	1.178	-.032	.091	-.288	.875	.048	-.031
.050	-1.014	1.207	-.008	.046	-.452	.946	.025	-.030
.100	-1.091	1.247	-.000	.024	-.511	.972	.025	.005
.150	-1.034	1.217	-.017	.030	-.530	.980	.038	-.003
.200	-1.001	1.201	.001	.062	-.575	1.000	.023	-.001
.250	-.972	1.186	-.007	.043	-.620	1.020	.026	.018
.300	-.953	1.175	-.005	.118	-.671	1.043	.031	.007
.350	-.928	1.164	-.139	.217	-.689	1.051	.087	.060
.400	-.870	1.136	-1.110	1.159	-.727	1.068	.152	.107
.450	-.829	1.116	.302	-2.189	-.719	1.065	.330	-.033
.500	-.805	1.103	1.079	-.719	-.582	1.003	.047	.135
.550	-.735	1.082	-.963	2.435	-.373	.912	.004	.108
.600	-.671	1.043	-.322	-1.877	-.201	.839	.021	.104
.650	-.511	.972	-.117	-.489	-.057	.779	.006	.111
.700	-.371	.911	.001	-.211	.078	.722	.020	.112
.725	-.295	.879	-.004	-.119	.132	.699	.017	.113
.760	-.239	.855	-.060	-.062	.201	.669	.011	.102
.775	-.206	.841	.043	-.015	.228	.658	.011	.114
.800	-.136	.812	.034	-.009	.248	.641	.026	.100
.850	-.022	.764	.022	-.036	.330	.613	.011	.093
.900	.069	.725	-.013	-.155	.369	.596	-.006	.054
.950	.136	.697	-.078	-.150	.372	.595	-.028	.037

TEST DATA	MODEL DATA	OVERALL DATA	STEADY	UNSTEADY	
MEETRNHR. 150	ALPHA .85 DEG.			RZ	IM
MACH .755	DELTA .02 DEG.	NORMAL FORCE CL	.350	.031	.043
Q (PA) 27537	AMPL. .95 DEG.	MOMENT(1/4C) CM	.076	.011	.044
RE 2.2386	FREQ. 30.0 HZ	FLAP FORCE RC	.0759	-.0005	.0117
NARM 3	BFREQ .067	HINGE MOMENT MC	.0074	.0001	.0029
IDENTNR. 4					

TABLE 4.23

FUNDAMENTAL FREQUENCY TEST DATA NLR 7301 WITH OSCILLATING FLAP

X/C	UPPERSIDE				LOWERSIDE			
	CP+	M+	CPRE+	CPIN+	CP-	M-	CPRE-	CPIN-
.010	.334	.613	.154	-.688	.316	.621	-1.050	1.042
.030	-.946	1.177	.465	-1.072	-.285	.877	-1.841	1.397
.050	-1.006	1.207	.190	-.692	-.452	.948	-.922	.636
.100	-1.083	1.247	.122	-.703	-.511	.974	-1.242	.505
.150	-1.026	1.217	.099	-.509	-.530	.982	-1.559	.244
.200	-.993	1.200	-.103	-.925	-.573	1.001	-1.835	-.147
.250	-.966	1.187	-.332	-1.094	-.616	1.021	-2.146	-.784
.300	-.945	1.176	-.560	-1.161	-.670	1.045	-2.015	-1.425
.350	-.925	1.166	-.959	-1.320	-.680	1.050	-1.886	-3.774
.400	-.896	1.152	-1.049	-1.833	-.712	1.065	.422	-5.230
.450	-.788	1.100	-.505	-5.948	-.733	1.074	5.262	-6.610
.500	-.695	1.057	7.227	-1.821	-.972	1.001	6.297	-1.647
.550	-.687	1.053	7.596	3.866	-.365	.911	4.839	-.422
.600	-.661	1.041	.002	10.300	-.199	.840	3.657	.954
.650	-.545	.989	-7.826	7.013	-.057	.781	3.378	.856
.700	-.369	.913	-6.432	.319	.070	.727	3.207	.975
.725	-.299	.883	-5.431	-.581	.122	.705	2.887	1.038
.760	-.229	.853	-5.075	-1.432	.196	.673	2.809	1.223
.775	-.198	.840	-4.991	-1.792	.222	.662	2.675	1.415
.800	-.132	.812	-3.286	-2.022	.263	.644	2.336	1.535
.850	-.020	.765	-1.446	-1.301	.326	.617	1.637	1.782
.900	.070	.727	-1.047	-.845	.364	.600	1.301	1.543
.950	.135	.699	-1.397	-.102	.367	.598	.711	1.049

TEST DATA

NERTUNNR. 162
 MACH .754
 Q (PA) 27637
 RE 2.23E6
 NARN 1
 IDENTNR. 6

MODEL DATA

ALPHA .85 DEG.
 DELTA -.01 DEG.
 ANPL. .90 DEG.
 FREQ. 200.0 HZ
 RFREQ .443

OVERALL DATA

NORMAL FORCE CL .339
 MOMENT(I/4C) CM .073
 FLAP FORCE RC .0743
 HINGE MOMENT NC .0073

STEADY

RE .611
 IM -.102
 RE .740
 IM -.024
 RE .2801
 IM .1832
 RE .0443
 IM .0340

UNSTEADY

RE .611
 IM -.102
 RE .740
 IM -.024
 RE .2801
 IM .1832
 RE .0443
 IM .0340

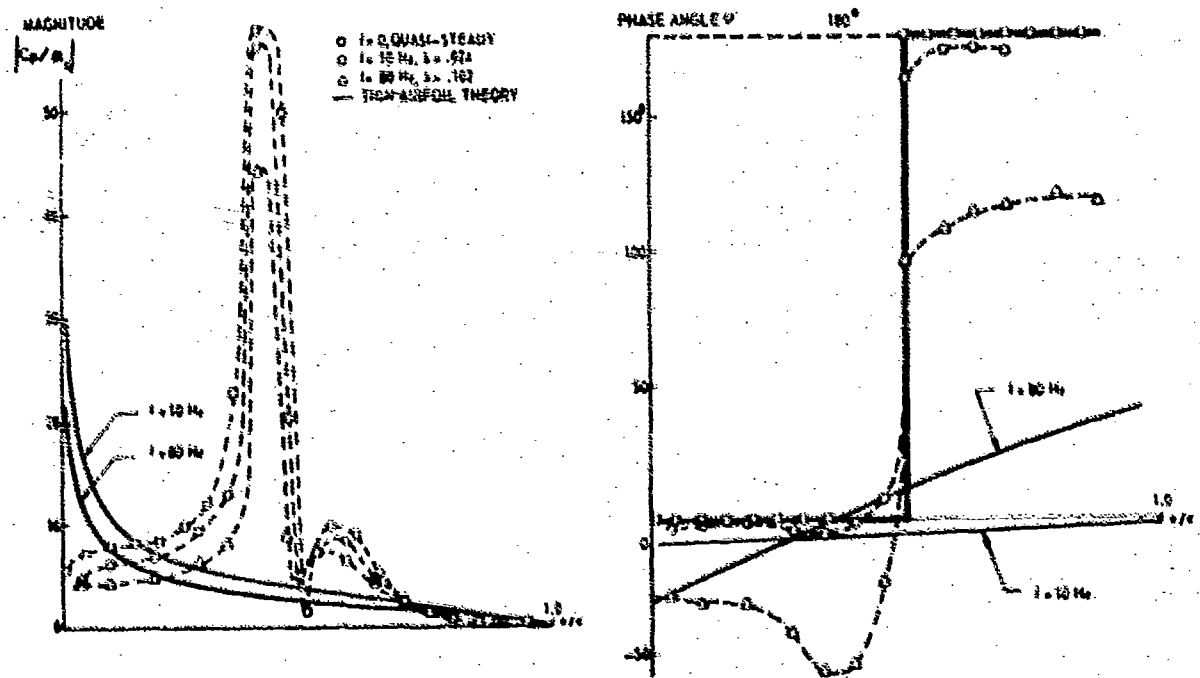
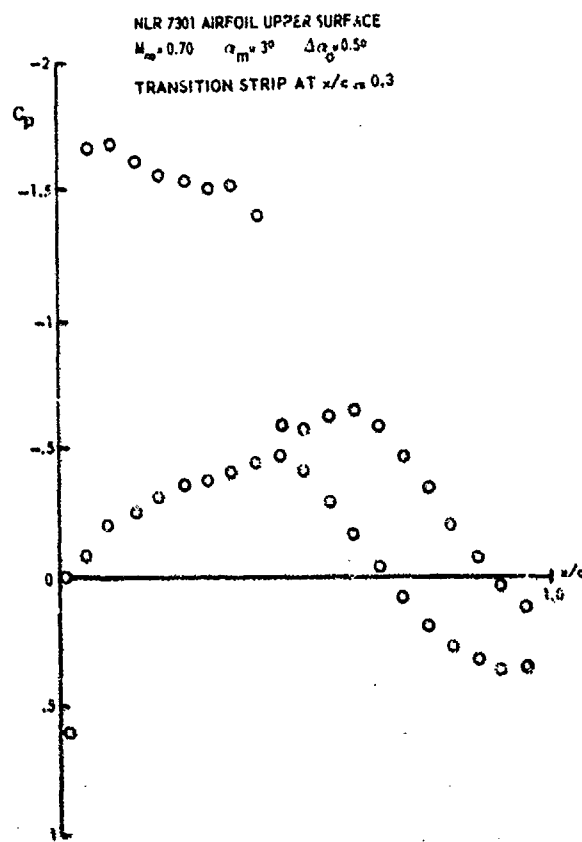
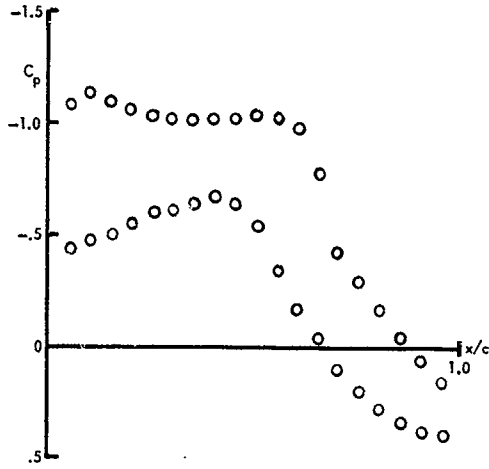
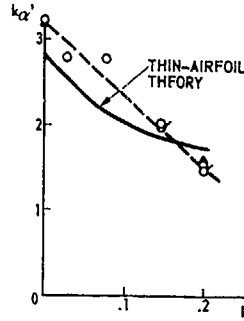


Fig. 4.1 Effect of shock wave on the unsteady pressure distributions; pitching oscillation

NLR 7301 AIRFOIL, UPPER SURFACE
 $M_\infty = 0.745$ $\alpha_m = 0.85^\circ$ $\Delta\alpha_0 = 0.5^\circ$



NLR 7301 AIRFOIL
 $M = 0.70$ $\alpha_m = 0.3^\circ$ $\Delta\alpha_0 = 0.5^\circ$



○ TRANSITION STRIP AT $x/c = 0.3$
 ◊ REPEATED TESTS
 △ NATURAL TRANSITION
 $Re = 2.1 \times 10^6$

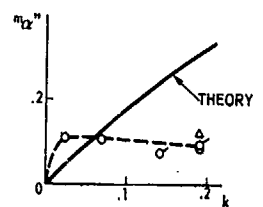
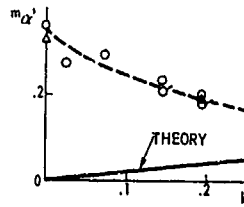
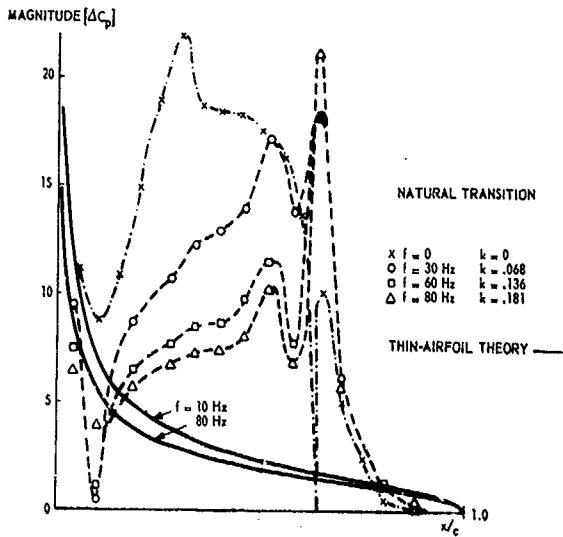
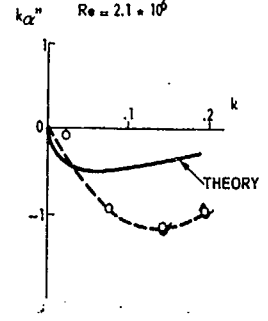


Fig. 4.3 Unsteady normal-force and moment coefficients as a function of frequency in transonic flow with a well-developed shock wave; pitching oscillation

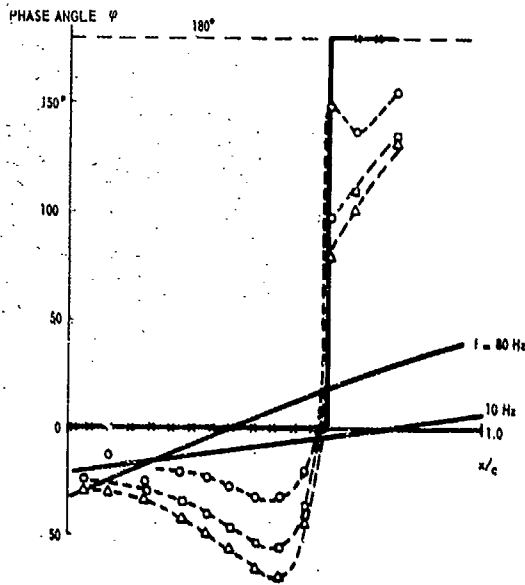
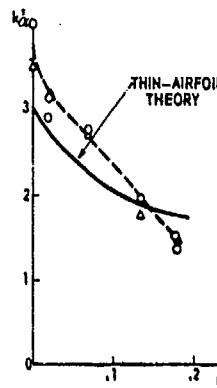


Fig. 4.2 Unsteady pressure distributions for the "shock-free" design point; pitching oscillation

NLR 7301 AIRFOIL
 $M = 0.745$ $\alpha = 0.85^\circ$ $\Delta\alpha_0 = 0.5^\circ$



○ TRANSITION STRIP AT $x/c = .3$
 △ NATURAL TRANSITION
 $Re = 2.2 \times 10^6$

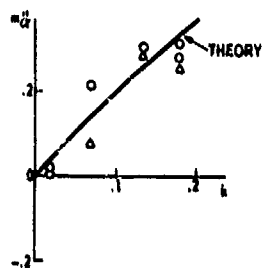
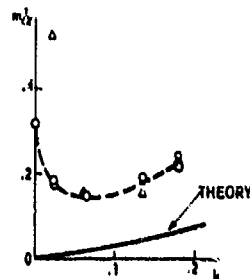
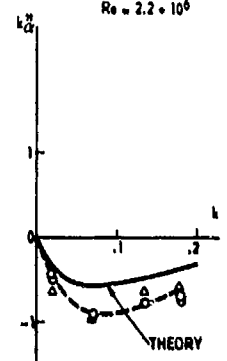


Fig. 4.4 Unsteady normal-force and moment coefficients as a function of frequency for the "shock-free" design point; pitching oscillation

NLR 7301 AIRFOIL UPPER SURFACE
 $M=0.7, \alpha_m=3^\circ, \delta_m=0^\circ, \delta_o=1^\circ$
 TRANSITION STRIP AT $x/c=0.3$

NLR 7301 AIRFOIL UPPER SURFACE
 $M=0.754, \alpha_m=0.85^\circ, \delta_m=0^\circ, \delta_o=1^\circ$
 NATURAL TRANSITION

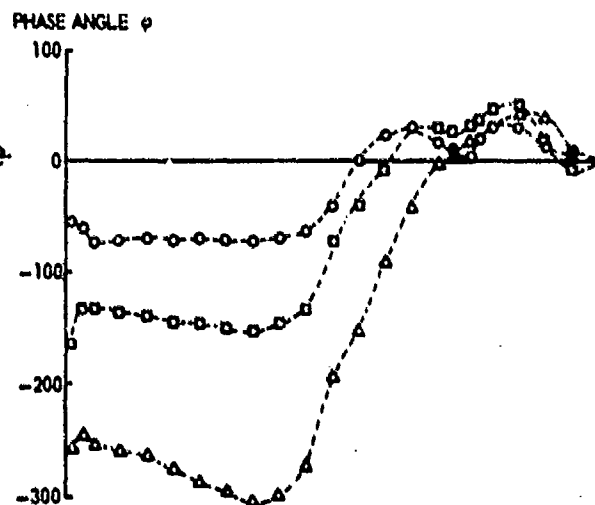
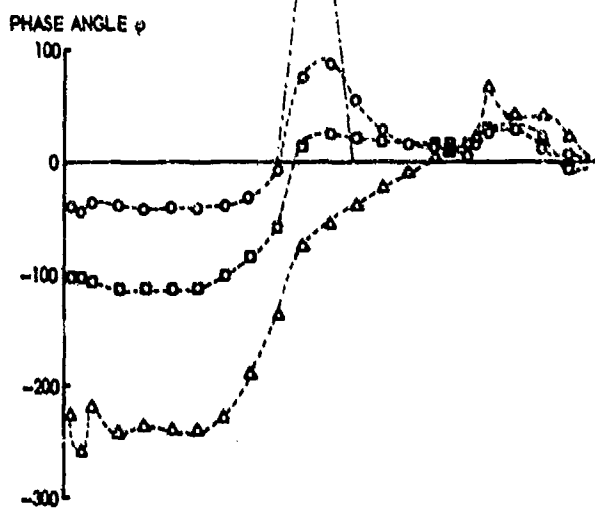
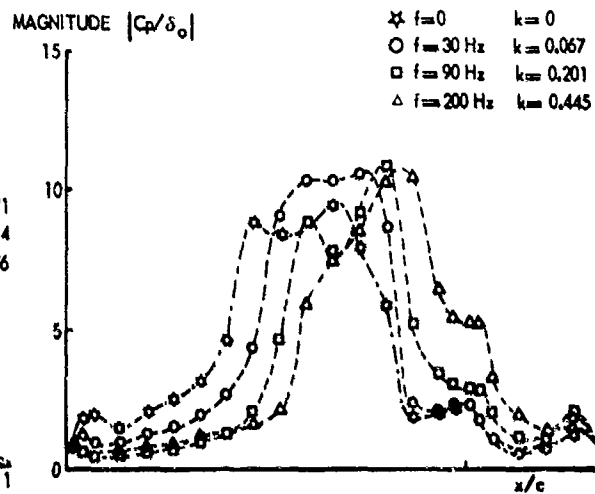
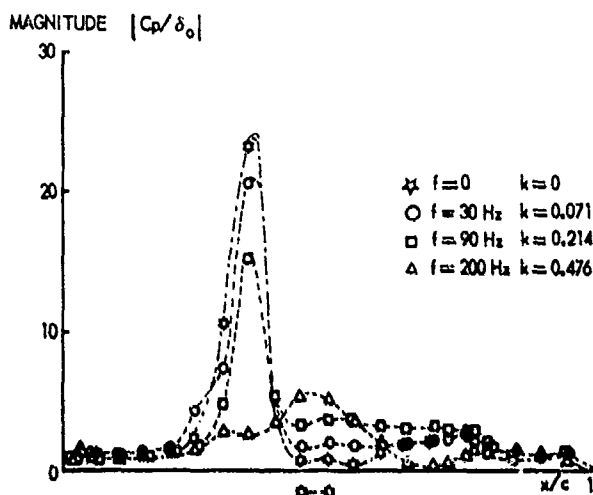
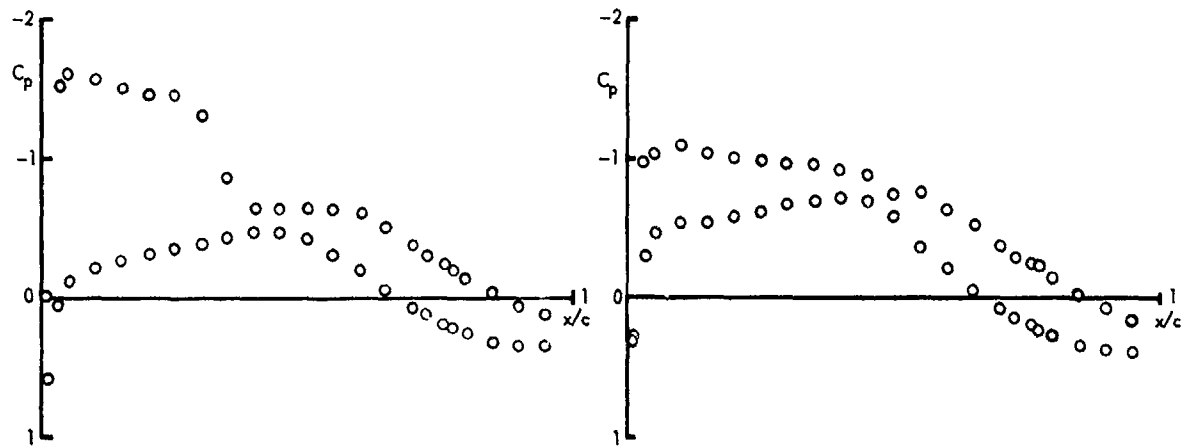


Fig. 4.5 Effect of shock wave on the unsteady pressure distributions; flap oscillation

Fig. 4.6 Unsteady pressure distributions for the "shock-fren" design point; flap oscillation

NLR 7301 AIRFOIL
 $\delta_m = 0^\circ$ $\delta_o = 1^\circ$ $Re = 2.2 \cdot 10^6$

O TRANSITION STRIP AT $X/C = 0.3$; $M = 0.754$, $\alpha_m = 1^\circ$
 V TRANSITION STRIP AT $X/C = 0.07$; $M = 0.756$, $\alpha_m = 1.2^\circ$
 Δ NATURAL TRANSITION ; $M = 0.754$, $\alpha_m = 0.85^\circ$

NLR 7301 AIRFOIL
 $M = 0.70$, $\alpha_m = 3^\circ$ $\delta_m = 0^\circ$ $\delta_o = 1^\circ$ $Re = 2.1 \cdot 10^6$

O TRANSITION STRIP AT $X/C = 0.3$
 V TRANSITION STRIP AT $X/C = 0.07$
 Δ NATURAL TRANSITION

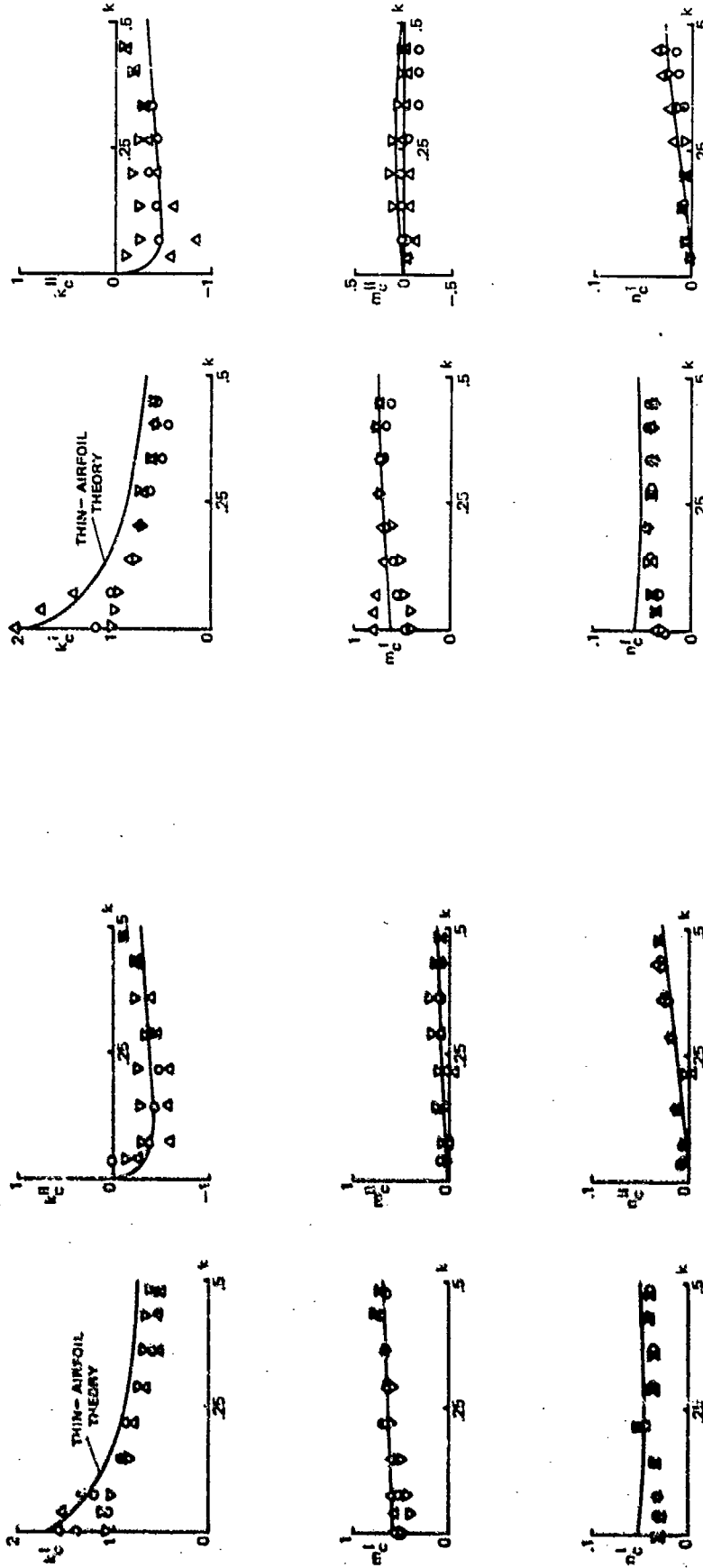


Fig. 4.8 Unsteady aerodynamic coefficients as functions of frequency for best "stuck-free" steady flow; flap oscillation

Fig. 4.7 Unsteady aerodynamic coefficients as functions of frequency in transonic flow with a well-developed shock wave; flap oscillation

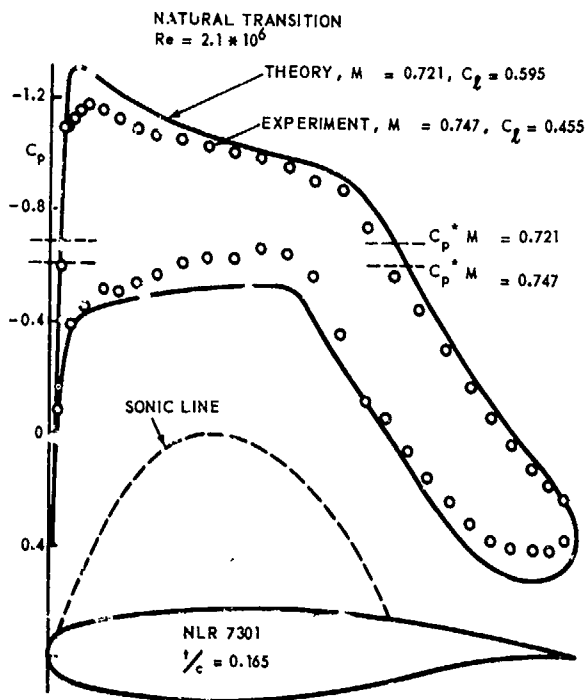


Fig. 4.9 Theoretical and experimental "shock-free" pressure distributions of the NLR 7301 airfoil (free transition)

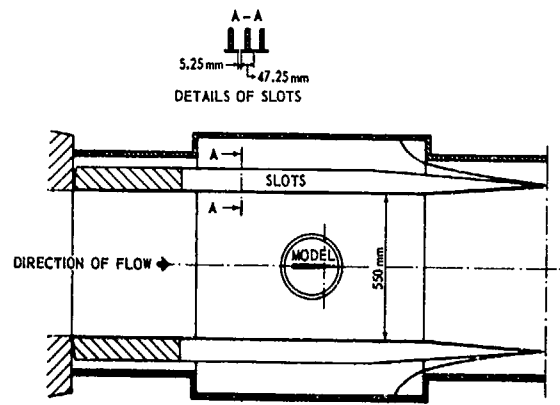


Fig. 4.10 Transonic test section of the NLR Pilot Tunnel

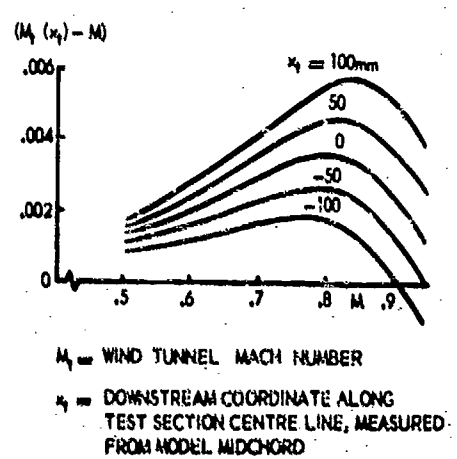


Fig. 4.11 Mach number distribution in NLR Pilot Tunnel test section

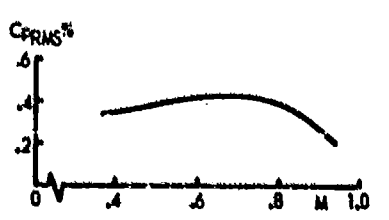


Fig. 4.12 Noise level in NLR Pilot Tunnel test section

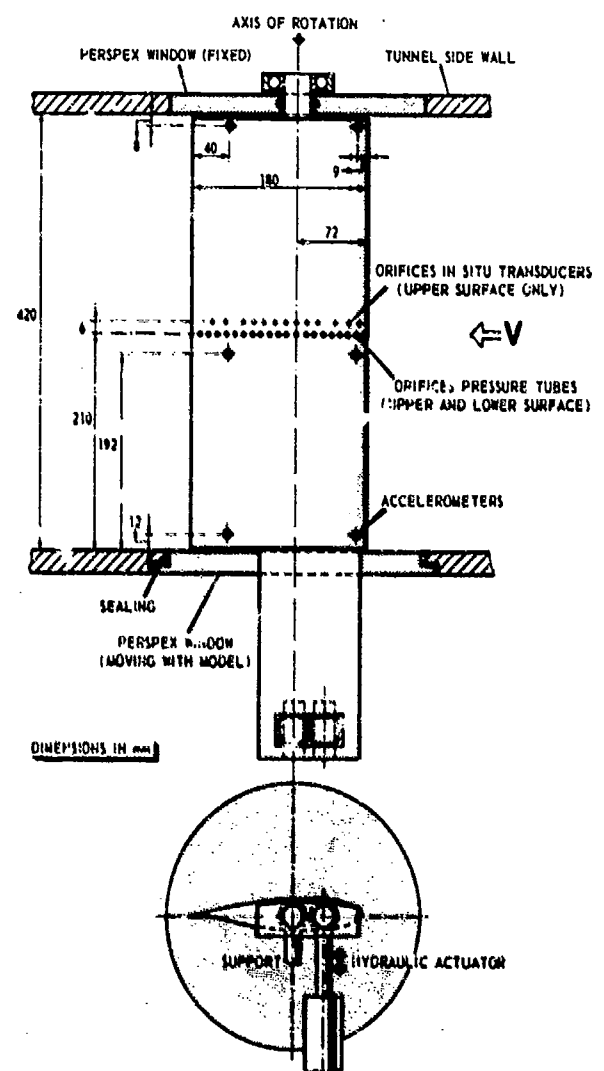
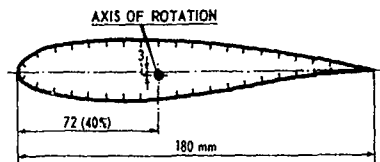


Fig. 4.13 Test set-up and instrumentation of the NLR 7301 airfoil (Conf. A)



PRESSURE ORIFICES TUBING SYSTEM (BOTH UPPER AND LOWER SURFACE)				IN SITU TRANSDUCERS (UPPER SURFACE ONLY)			
No. 1	$x/c = .01$	No. 11	$x/c = .50$	No. 1	$x/c = .04$	No. 11	$x/c = .70$
2	.05	12	.55	2	.10	12	.80
3	.10	13	.60	3	.19	13	.88
4	.15	14	.65	4	.28		
5	.20	15	.70	5	.34		
6	.25	16	.75	6	.40		
7	.30	17	.80	7	.46		
8	.35	18	.85	8	.52		
9	.40	19	.90	9	.58		
10	.45	20	.95	10	.64		

Fig. 4.14 Location of pressure orifices of the NLR 7301 airfoil (Conf. A)

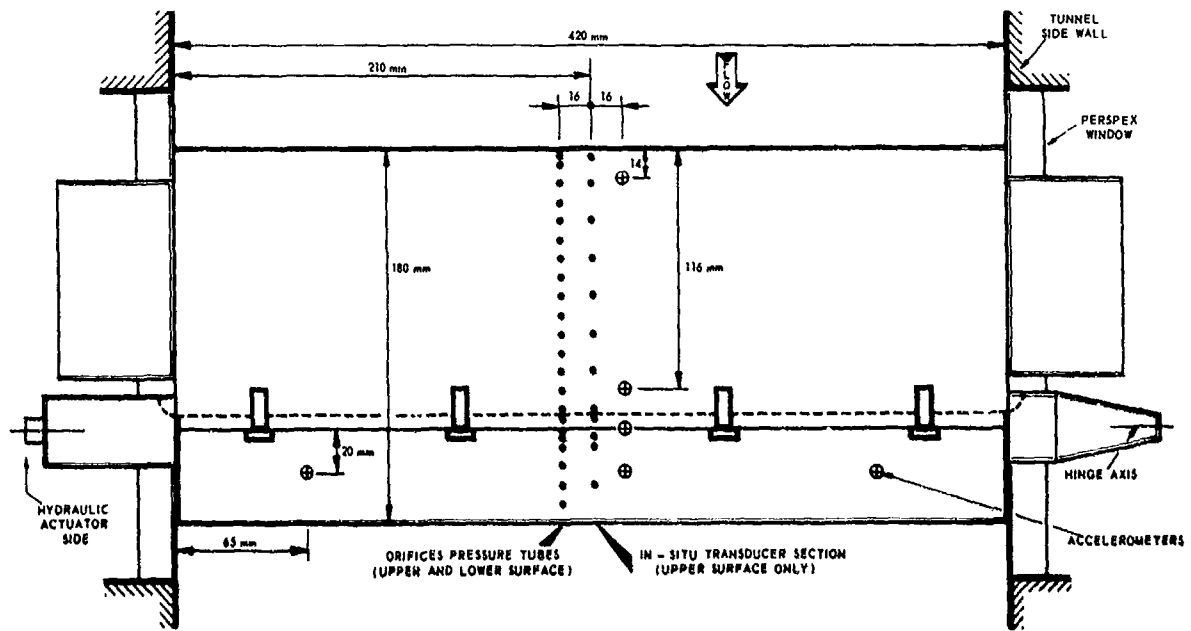
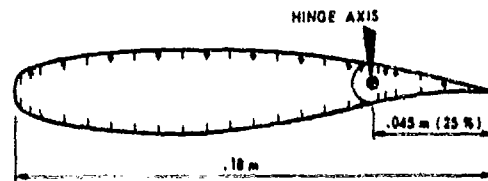


Fig. 4.15 Test set-up and instrumentation of the NLR 7301 airfoil with control surface (Conf. B)



PRESSURE ORIFICES TUBING SYSTEM (both upper and lower surface)				IN SITU TRANSDUCERS (upper surface only)	
no. 1	$x/c = .01$	no. 13	$x/c = .55$	no. 1	$x/c = .03$
2	.03	14	.60	2	.10
3	.05	15	.65	3	.20
4	.10	16	.70	4	.30
5	.15	17	.725	5	.40
6	.20	18	.76	6	.50
7	.25	19	.775	7	.60
8	.30	20	.8	8	.70
9	.35	21	.85	9	.725
10	.40	22	.90	10	.775
11	.45	23	.95	11	.80
12	.50			12	.90

Fig. 4.16 Location of pressure orifices of the NLR 7301 airfoil with control surface (Conf. B)

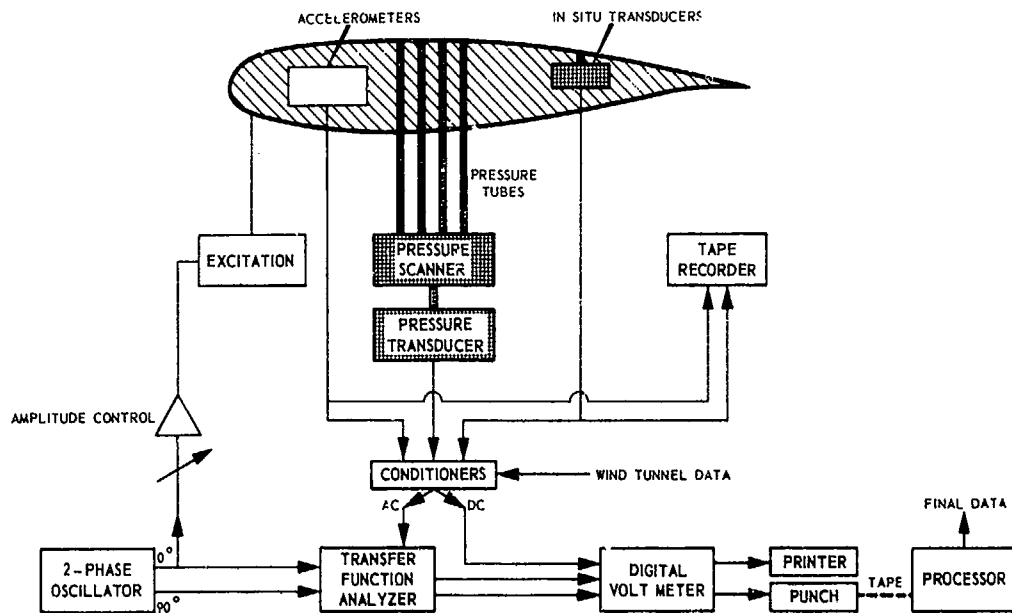


Fig. 4.17 Block diagram of measuring equipment (Conf. A). Similar equipment essentially for Conf. B

DATA SET 5

NLR 7301 SUPERCRITICAL AIRFOIL OSCILLATORY PITCHING

by

Sanford S. Davis, NASA Ames

INTRODUCTION AND DISCUSSION

Test data on the NLR 7301 supercritical airfoil were acquired concurrently with the NACA 64A010 data previously described in Data Set 2. The purpose of this Data Set is to tabulate numerical data from those tests that can be associated with the AGARD CT Cases and to present an overview of certain parametric data trends. The test arrangement for this airfoil is the same as that described in Data Set 2 and is reproduced in Fig. 5-1.

Users of these data should be aware of some differences in the methods of specifying the geometry of the NLR supercritical airfoil whose general properties are described in Ref. 5.1. The differences between the original coordinates which, as given by Table 4.1 of Data Set 4, locate the sharp trailing edge at $x/C \cong 1.015$, and the transformed coordinates given by Table 5 of Ref. 5.2 are explained in Data Set 4. However, the coordinates used to construct the model of the present tests were derived from the original specification in yet another manner. As for the model of Data Set 4, the physical model of the present tests was obtained by truncating the trailing edge of the original design at $x/C = 1.0$. But unlike the model of Data Set 4, the chord was redefined as the line connecting the nose of the airfoil with the bisection point of the truncated trailing edge. In effect, the design shape of the present model is the same as that of the NLR model of Data Set 4 and, apart from the trailing-edge truncation, is the same shape as that defined in Ref. 5.2 for the AGARD Computation Tests. However, because of the method of defining the chord line, there is a slight difference in the definitions of incidence. The sensitivity of the computed flow to the minor variations listed above is not expected to be a major problem, but the analyst should be aware of their existence.

The data base for this airfoil is presented in Table 5.1 and consists of 95 parametric combinations. The data subset corresponding to a pitching axis at $0.40c$ is listed in Table 5.2. The AGARD CT Cases advocated in Ref. 5.2 do not precisely match the current data set. In Table 5.3 tests from the current series are correlated with the AGARD CT Cases by matching similar mean flow conditions. The three flow regimes selected are: (1) a subcritical Mach number, (2) an off-design flow condition with a strong shock wave, and (3) the supercritical design point.

In these tests lower surface unsteady pressure data were sacrificed for the sake of increased upper surface resolution. For this reason lift and moment data are not available. In Tables 5.4 to 5.23 first harmonic upper surface and steady pressure data for the 20 runs identified in Table 5.3 are reproduced from Ref. 5.3. Complete instantaneous pressure distributions are presented in Tables 5.24 and 5.25 for the high Reynolds number data associated with AGARD CT Cases 6 and 8.

In Figs. 5.2 to 5.10 the steady pressure distributions are shown, and certain parametric trends are presented concerning the upper surface fundamental frequency pressure distribution. The picture that emerges is one of a complex dynamic flow pattern that is sensitive to many parameters. More coordinated research needs to be done before definitive data suitable for aeroelastic applications become available. Other supercritical airfoil data may be found in Data Set 4 and the references cited herein.

The effect of varying the frequency parameter alone is shown in Figs. 5.2 to 5.4. Figure 5.2 depicts a subsonic flow condition where the classical thin airfoil theory should remain valid. The general trend confirms the flat plate theory -- decreasing real portion and increasing imaginary portion as frequency increases -- except for the curious dip just upstream of the $0.2c$ station. This phenomenon is consistent with the full time-histories and comparison with other data (see Fig. 5.8) will show that it is really a viscous effect. (The dip in the mean pressure distribution at approximately $0.4c$ was traced to a surface wave in the airfoil contour.) In Fig. 5.3 the Mach number and mean angle of attack are increased enough to induce a strong shock wave with possible separation at the trailing edge. The pressure distributions are dramatically different at the two frequencies shown. An especially important point, one that cannot be stressed too strongly, is that the variation of unsteady lift and moment (not shown) may show erratic trends with frequency because of the balancing of positive and negative lobes in the pressure distributions. More examples of this phenomenon are described in Refs. 5.4, 5.5 and 5.6. Figure 5.4 completes this series by showing the variation of unsteady pressure distributions with frequency at the supercritical design point. Unlike conventional airfoils, a broad, high level of unsteady loading persists over the forward portion of the airfoil at low frequencies. The net effect is larger unsteady loads on supercritical airfoils than that usually found on conventional airfoils.

The next series of three figures shows data trends with varying oscillation amplitude. Figure 5.5 indicates that the normalized oscillatory pressure distribution remains relatively invariant in subsonic flow. This is a good indication of a linear response over the range indicated. Figure 5.6 shows only minor departures from linearity up to $\alpha_0 = 1^\circ$, even with a strong shock wave present. Figure 5.7 shows progressive changes with amplitude α_0 at the supercritical design point that cast doubt on the linearity assumption. Whether or not the response curves are "sufficiently linear" must await aeroelastic sensitivity calculations.

The next series of figures shows the scale effect on the steady and oscillatory pressures. In this connection, it should be noted that the model did not have a boundary layer transition trip. The trends on the unsteady pressures are disconcerting because the Reynolds number seems to be an important parameter, especially at and near the supercritical design point. In Fig. 5.8 the major effect of increasing Reynolds number is to induce the leading edge dip in the unsteady pressure distribution. In Fig. 5.9 the first harmonic pressures aft of the shock wave seem to be most affected. This may cause major changes in the unsteady moment as well as the lift. In Fig. 5.10 the unsteady loading at the design point seems to be significantly affected by changing the Reynolds number. At this stage it is impossible to trace the root causes of the relatively severe scale effects on a supercritical airfoil (see Ref. 5.3 for other data). A computational model that includes all of the significant physical effects is surely necessary.

The higher harmonic content of the unsteady pressure distributions is also significantly affected by flow condition. Figure 5.11 shows the complete space-time pressure distributions at the supercritical design point (CF Cases 6 and 8) when $Re = 11.5 \times 10^6$. The harmonic distortion is significantly affected by the frequency parameter, but is concentrated near the end of the region where the steady flow is supersonic. General trends should not be deduced from this special choice of parameters, just as harmonic distortion in the overall loads cannot be inferred from the harmonic content of the pressure distributions themselves (Ref. 5.4).

1 AIRFOIL

1.1	Designation	NLR
1.2	Type of airfoil	Supercritical - $t/c = 16.5\%$
1.3	Geometry	Table 2 of Ref. 5.3
1.4	Design condition	$M = 0.721$, $\alpha_m = -0.19^\circ$ (theoretical, quoted in Ref. 5.2)
1.5	Additional remarks	
1.6	References on airfoil	See Introduction of this Data Set.

2 MODEL GEOMETRY

2.1	Chord length	0.50 m (19.685 in.)
2.2	Span	1.35 m (53.2 in.)
2.3	Actual model coordinates and accuracy of measurement	Ref. 5.3
2.4	Flap: hinge and gap details	None
2.5	Additional remarks	Model mounted between splitter plates - see Fig. 5.1
2.6	References on model	Ref. 5.3

3 WIND TUNNEL

3.1	Designation	NASA Ames 11- X 11-Foot Transonic Wind Tunnel
3.2	Type of tunnel	Closed return, variable density
3.3	Test section dimensions	3.35 X 3.35 X 6.7 m (11 X 11 X 22 ft.)
3.4	Type of roof and floor	Baffled slat
3.5	Type of side walls	Same as 3.4
3.6	Ventilation geometry	1.78 cm (0.7 in.) slots, 24.4 cm (9.63 in.) slats. Open area ratio ~ 8% between splitters.
3.7	Thickness of side wall boundary layer	Very thin due to splitters
3.8	Thickness of boundary layers at roof and floor	Approx. 7.6 cm (3 in.)
3.9	Method of measuring Mach number	Static taps and splitters, see Ref. 5.6.
3.10	Uniformity of Mach number over test section	± 0.002
3.11	Sources and levels of noise or turbulence in empty tunnel	Not investigated
3.12	Tunnel resonances	None noted
3.13	Additional remarks	
3.14	References on tunnel	Ref. 5.3

4 MODEL MOTION

4.1	Mode of applied motion	Pitching about nominal 0.40c, also plunging
4.2	Range of amplitude	$\pm 0-2$ deg, ± 1 cm
4.3	Range of frequency	0-60 Hz
4.4	Method of application	Four graphite epoxy push-pull rods with differential motion of forward and aft pair, see Fig. 5.1.

4	MODEL MOTION (Continued)		
4.5	Purity of applied motion	Pure sinusoids	
4.6	Natural frequencies and normal modes of model	Lowest mode: torsion at 60 Hz	
4.7	Static or dynamic elastic distortion during tests	Not measured	
4.8	Additional remarks		
5	TEST CONDITIONS		
5.1	Tunnel height/model chord ratio	3.35 m/0.50 m = 6.7	
5.2	Tunnel width/model chord ratio	1.35 m/0.50 m = 2.7 (between splitter plates)	
5.3	Range of Mach number	0.40 - 0.85	
5.4	Range of tunnel total pressure	50 kN/m ² - 225 kN/m ² (0.5-2.25 ATM)	
5.5	Range of tunnel total temperature	290 K - 320 K	
5.6	Range of model steady, or mean, incidence	0 - 2.5 deg.	
5.7	Definition of model incidence	Chord line relative to wind tunnel.	
5.8	Position of transition, if free	Transition was observed using a sublimating material at two flow conditions. At M = 0.453, $\alpha_m = 0.57^\circ$, $Re = 4.5 \times 10^6$ a definite transition point was not observed. At M = 0.708, $\alpha_m = 0.58^\circ$, $Re = 6.2 \times 10^6$, transition occurred at $x/c \sim 0.10$.	
5.9	Position and type of trip, if transition fixed		
5.10	For mixed flow, position of sonic boundary in relation to roof and floor	Not measured	
5.11	Flow instabilities during tests	--	
5.12	Additional remarks	--	
5.13	References describing tests	--	
6	MEASUREMENTS AND OBSERVATIONS		
6.1	Steady pressures for the mean conditions		✓
6.2	Steady pressures for small changes from the mean conditions		-
6.3	Quasi-steady pressures		-
6.4	Unsteady pressures		✓
6.5	Steady forces for the mean conditions	measured directly	-
		integrated pressures	✓
6.6	Steady forces for small changes from the mean conditions	measured directly	-
		integrated pressures	-
6.7	Quasi-steady forces	measured directly	--
		integrated pressures	-
6.8	Unsteady forces	measured directly	-
		integrated pressure	-
6.9	Measurement of actual motion at points on model		✓
6.10	Observation or measurement of boundary layer properties		✓
6.11	Visualization of surface flow		✓
6.12	Visualization of shockwave movements		-
6.13	Additional remarks		-
7	INSTRUMENTATION		
7.1	Steady pressures		
7.1.1	Position of orifices spanwise and chordwise	Mid-span 29 upper, 12 lower. (May vary with data, see Table 5.4 for locations.)	
7.1.2	Type of measuring system	Pneumatic	
7.2	Unsteady pressures		
7.2.1	Position of orifices spanwise and chordwise	Mid-span, 29 upper, none on lower. (May vary with data, see Table 5.4 for locations.)	
7.2.2	Diameter of orifices	0.102 cm (0.040 in.)	

7 INSTRUMENTATION (Continued)

7.2.3	Type of measuring system	Strain-gauge-type miniature pressure transducers installed close to orifice with minimum cavities.
7.2.4	Type of transducers	Kulite model XCQL-7A-093.
7.2.5	Principle and accuracy of calibration	On-line calibrations. Up to 2% change in static sensitivity before and after run allowed.
7.3	Model motion	
7.3.1	Method of measurement	Motion of four push-pull rods with LVDT (reactive-type) transducers. Phase synchronism checked with wing-mounted accelerometers.
7.3.2	Accuracy	~ 1%
7.4	Processing of unsteady measurements	
7.4.1	Method of acquiring and processing measurements	Real-time digitization with on-line calibration and diagnostics. Signal averaging over approx. 100 cycles to suppress random noise (if present). Variable sampling time adjusted to yield 60 data points per cycle.
7.4.2	Type of analysis	On-line processing for frequency content of pressure distributions and comparisons with linear theory and other data.
7.4.3	Unsteady pressure quantities obtained and accuracies achieved	Signal averaged (essentially instantaneous) pressured distributions. Harmonic analysis of pressure distributions.
7.4.4	Method of integration to obtain forces	Numerical quadratures (see Appendix A of Ref. 5.3).
7.5	Additional remarks	
7.6	References on techniques	Ref. 5.6

8 DATA PRESENTATION

8.1	Test cases for which data could be made available	Table 5.1
8.2	Test cases for which data are included in this document	Table 5.3
8.3	Steady pressures	Tables 5.4 to 5.23
8.4	Quasi-steady or steady perturbation pressures	Not available
8.5	Unsteady pressures	Tables 5.4 to 5.25
8.6	Steady forces or moments	Not available
8.7	Quasi-steady or steady perturbation forces	Not available
8.8	Unsteady forces and moments	Not available
8.9	Other forms in which data could be made available if required	Magnetic tape
8.10	References giving other presentations of data	Refs. 5.3 to 5.5

9 COMMENTS ON DATA

9.1	Accuracy	
9.1.1	Mach number	±0.002
9.1.2	Steady incidence	±0.05 deg
9.1.3	Reduced frequency	±0.005
9.1.4	Steady pressure coefficients	1%
9.1.5	Steady pressure derivatives	N/A
9.1.6	Unsteady pressure coefficients	2%
9.2	Sensitivity to small changes of parameter	No evidence of undue sensitivity
9.3	Spanwise variations	Probably small
9.4	Nonlinearities	Depends on parametric conditions
9.5	Influence of tunnel total pressure	Minimal on model distortion, probably all Reynolds number effect.
9.6	Wall interference corrections	No corrections made
9.7	Other relevant tests on same model	None

9 COMMENTS ON DATA (Continued)

- 9.8 Relevant tests on other models of nominally the *same* aerofoil. See Data Set 4 of this Compendium
- 9.9 Any remarks relevant to comparison between experiment and theory
- 9.10 Additional remarks
- 9.11 References on discussion of data Refs. 5.4 and 5.5

10 PERSONAL CONTACT FOR FURTHER INFORMATION

Sanford Davis, Aerodynamics Division, NASA Ames Research Center, Moffett Field, CA 94035

11 REFERENCES

- 5.1 H. Tijdeman Investigations of the Transonic Flow Around Oscillating Airfoils. NLR TR 77090U, 1977.
- 5.2 S. R. Bland AGARD Two-Dimensional Aeroelastic Configurations. AGARD-AR-156, August 1979.
- 5.3 S. Davis and G. Malcolm Experimental Unsteady Aerodynamics of Conventional and Supercritical Airfoils. NASA TM-81221, August 1980.
- 5.4 S. Davis and G. Malcolm Unsteady Aerodynamics of Conventional and Supercritical Airfoils. AIAA Paper 80-734, Seattle, WA, May 1980.
- 5.5 S. Davis Experimental Studies of Scale Effects on Oscillating Airfoils at Transonic Speeds. AGARD-CP-296, February 1981, pp. 9-1 to 9-5.
- 5.6 S. Davis Computer/Experiment Integration for Unsteady Aerodynamic Research. Intl. Congress on Instrumentation in Aerospace Simulation Facilities. ICIASP '79 Record, September 1979, pp. 237-250.

12 NOTATION AND EXPLANATION OF TABLES*

GENERAL NOTATION

C, c	chord of airfoil, m
DI	dynamic index, data identification number
f, FREQ	frequency, Hz
k, K	reduced (nondimensional) frequency, $\frac{\omega c}{2V}$
M	free-stream Mach number
Re, RE	Reynolds number (based on chord)
t	time, s
V	free-stream velocity, m/s
x, x	distance along airfoil, m
x_0/a	pitch axis position relative to leading edge
$\alpha(t)$	instantaneous incidence, $\text{deg}(\alpha_m + \alpha_0 \cos \omega t)$
α_m	mean incidence, deg
α_0	oscillatory pitch amplitude, deg
ω	radian frequency, $\text{rad/s} (=2\pi f)$

TABLES 5.4 to 5.23

ALPHA	mean incidence, $\text{deg}(\alpha_m)$
PTOT	total pressure, $\text{N/m}^2 [P_t]$
PIRP	static pressure, $\text{N/m}^2 [P_s]$
QIMP	dynamic pressure, $\text{N/m}^2 [q]$
CPU(CPL)	steady upper (lower) surface pressure coefficient $[c_p]$
CPU,A	normalized complex amplitude of upper surface fundamental frequency pressure coefficient, per radian $[c_p'/\alpha_0 + ic_p''/\alpha_0]$

TABLES 5.24 and 5.25

PHASE	phase angle re $\alpha(t)_{\max}$ $[\omega t]$
ALPHA	oscillatory incidence $[\alpha_0 \cos(\omega t)]$
CP	instantaneous pressure coefficient $[c_p(t)]$

* Square-bracketed quantities indicate standard AGARD notation

TABLE 5.1. DATA BASE FOR NLR 7301 AIRFOIL

DI	M	α_m , deg	$Re \times 10^{-6}$	Motion	f , Hz	k
115	0.453	0.57	4.47	Pitching 0.52 deg about $x_{\alpha}/c = 0.394$	2.7	0.028
116	.453	.57	4.47	Pitching .50 deg about $x_{\alpha}/c = .404$	5.4	.055
117	.453	.57	4.47	Pitching .48 deg about $x_{\alpha}/c = .400$	10.7	.110
118	.453	.57	4.47	Pitching .49 deg about $x_{\alpha}/c = .391$	21.5	.221
119	.453	.57	4.47	Pitching .49 deg about $x_{\alpha}/c = .394$	32.2	.331
120	.453	.57	4.47	Pitching 1.04 deg about $x_{\alpha}/c = .384$	5.4	.055
121	.453	.57	4.47	Pitching 1. deg about $x_{\alpha}/c = .389$	21.5	.221
122	.453	.57	4.47	Pitching 2. deg about $x_{\alpha}/c = .393$	5.4	.055
123	.453	.57	4.47	Pitching 2.00 deg about $x_{\alpha}/c = .403$	21.5	.221
124	.708	.58	6.15	Pitching .52 deg about $x_{\alpha}/c = .394$	3.7	.025
125	.708	.58	6.15	Pitching .50 deg about $x_{\alpha}/c = .401$	7.5	.050
126	.708	.58	6.15	Pitching .49 deg about $x_{\alpha}/c = .402$	29.9	.200
127	.708	.58	6.15	Pitching 1.01 deg about $x_{\alpha}/c = .397$	7.5	.050
128	.708	.58	6.15	Pitching 1.00 deg about $x_{\alpha}/c = .398$	29.9	.200
129	.708	.58	6.15	Pitching 2.02 deg about $x_{\alpha}/c = .401$	7.5	.050
130	.708	.58	6.15	Pitching 2.00 deg about $x_{\alpha}/c = .399$	29.9	.200
131	.752	.37	6.21	Pitching .51 deg about $x_{\alpha}/c = .401$	4.0	.025
132	.752	.37	6.21	Pitching .50 deg about $x_{\alpha}/c = .401$	8.0	.050
133	.752	.37	6.21	Pitching 0.50 deg about $x_{\alpha}/c = .402$	16.0	0.100
134	.752	.37	6.21	Pitching .49 deg about $x_{\alpha}/c = .403$	32.0	.200
135	.752	.37	6.21	Pitching .50 deg about $x_{\alpha}/c = .403$	48.0	.300
136	.752	.37	6.21	Pitching 1.01 deg about $x_{\alpha}/c = .398$	8.0	.050
137	.752	.37	6.21	Pitching 1.00 deg about $x_{\alpha}/c = .397$	32.0	.200
138	.752	.37	6.21	Pitching 2.02 deg about $x_{\alpha}/c = .400$	8.0	.050
139	.752	.37	6.21	Pitching 2.01 deg about $x_{\alpha}/c = .399$	32.0	.200
140	.808	.36	6.26	Pitching .50 deg about $x_{\alpha}/c = .402$	8.5	.050
141	.808	.36	6.26	Pitching .50 deg about $x_{\alpha}/c = .407$	34.0	.199
142	.807	.36	11.78	Pitching .49 deg about $x_{\alpha}/c = .404$	8.7	.050
143	.807	.36	11.78	Pitching .49 deg about $x_{\alpha}/c = .398$	35.0	.200
144	.751	.37	11.48	Pitching .50 deg about $x_{\alpha}/c = .403$	8.2	.050
145	.751	.37	11.48	Pitching .51 deg about $x_{\alpha}/c = .399$	4.1	.025
146	.751	.37	11.48	Pitching .49 deg about $x_{\alpha}/c = .400$	16.5	.100
147	.751	.37	11.48	Pitching .49 deg about $x_{\alpha}/c = .401$	24.7	.150
148	.751	.37	11.48	Pitching .50 deg about $x_{\alpha}/c = .403$	33.0	.201
149	.751	.37	11.48	Pitching .50 deg about $x_{\alpha}/c = .400$	49.5	.301
150	.751	.37	11.48	Pitching 1.00 deg about $x_{\alpha}/c = .398$	8.2	.050
151	.751	.37	11.48	Pitching 1.00 deg about $x_{\alpha}/c = .400$	32.8	.200
152	.751	.37	11.48	Pitching 2.02 deg about $x_{\alpha}/c = .399$	8.2	.050
153	.751	.37	11.48	Pitching 2.00 deg about $x_{\alpha}/c = .402$	32.8	.200
154	.751	.37	11.48	Plunging 1.00 cm (0.395 in.)	8.2	.050
155	.751	.37	11.48	Plunging .90 cm (0.356 in.)	32.8	.200
156	.706	.59	11.22	Pitching .51 deg about $x_{\alpha}/c = .400$	3.9	.025
157	.706	.59	11.22	Pitching .50 deg about $x_{\alpha}/c = .402$	7.7	.050
158	.706	.59	11.22	Pitching .50 deg about $x_{\alpha}/c = .399$	15.4	.099
159	.706	.59	11.22	Pitching .49 deg about $x_{\alpha}/c = .401$	30.8	.199
160	.706	.59	11.22	Pitching .49 deg about $x_{\alpha}/c = .404$	46.2	.298
161	.706	.59	11.22	Pitching 1.01 deg about $x_{\alpha}/c = .398$	7.7	.050
162	.706	.59	11.22	Pitching 1.00 deg about $x_{\alpha}/c = .398$	30.8	.199
163	.706	.59	11.22	Pitching 2.01 deg about $x_{\alpha}/c = .401$	7.7	.050
164	.706	.59	11.22	Pitching 2.00 deg about $x_{\alpha}/c = .402$	30.8	.199
165	.706	.59	11.22	Plunging 1.00 cm (0.393 in.)	7.7	.050
166	.706	.59	11.22	Plunging 1.00 cm (0.392 in.)	30.8	0.199
167	.505	.58	9.34	Pitching .51 deg about $x_{\alpha}/c = .396$	2.8	.025
168	.505	.58	9.34	Pitching .51 deg about $x_{\alpha}/c = .401$	5.5	.049
169	.505	.58	9.34	Pitching .50 deg about $x_{\alpha}/c = .403$	11.0	.099
170	.505	.58	9.34	Pitching .50 deg about $x_{\alpha}/c = .404$	22.0	.198
171	.505	.58	9.34	Pitching .40 deg about $x_{\alpha}/c = .404$	33.0	.297
172	.505	.58	9.34	Pitching 1.02 deg about $x_{\alpha}/c = .399$	5.5	.049
173	.505	.58	9.34	Pitching 1.01 deg about $x_{\alpha}/c = .399$	32.0	.198
174	.505	.58	9.34	Pitching 2.04 deg about $x_{\alpha}/c = .400$	5.5	.049
175	.505	.58	9.34	Pitching 2.01 deg about $x_{\alpha}/c = .402$	22.0	.198
176	.505	.58	9.34	Plunging 1.01 cm (0.396 in.)	5.5	.049
177	.505	.58	9.34	Plunging .99 cm (0.389 in.)	22.0	.198
178	.712	.58	3.09	Pitching .50 deg about $x_{\alpha}/c = .403$	7.4	.049
179	.712	.58	3.09	Pitching .49 deg about $x_{\alpha}/c = .403$	29.7	.197
180	.712	.58	3.09	Pitching 2.02 deg about $x_{\alpha}/c = .402$	7.4	.049
181	.712	.58	3.09	Pitching 2.00 deg about $x_{\alpha}/c = .402$	29.7	.197
182	.712	.58	3.09	Plunging 1.00 cm (0.394 in.)	7.4	.049
183	.712	.58	3.09	Plunging .98 cm (0.388 in.)	29.7	.197
184	.508	.58	2.54	Pitching .50 deg about $x_{\alpha}/c = .402$	5.4	.050
185	.508	.58	2.54	Pitching .50 deg about $x_{\alpha}/c = .405$	21.4	.197
186	.508	.58	2.54	Pitching 2.03 deg about $x_{\alpha}/c = .400$	5.4	.050
187	.508	.58	2.54	Pitching 2.00 deg about $x_{\alpha}/c = .401$	21.4	.197
188	.508	.58	2.54	Plunging 1.01 cm (0.396 in.)	5.4	.050
189	.508	.58	2.54	Plunging .99 cm (0.389 in.)	21.4	.197
190	.752	.37	3.25	Pitching .50 deg about $x_{\alpha}/c = .403$	7.8	.050
191	.752	.37	3.25	Pitching .50 deg about $x_{\alpha}/c = .401$	31.4	.200

TABLE 5.1. CONCLUDED

DI	M	α_m , deg	$Re \times 10^{-6}$	Motion	f , Hz	k
192	0.752	0.37	3.25	Pitching 2.02 deg about $x_a/c = 0.401$	7.8	0.050
193	.752	.37	3.25	Pitching 2.00 deg about $x_a/c = .401$	31.4	.200
194	.752	.37	3.25	Plunging 1.00 cm (0.394 in.)	7.8	.050
195	.812	.35	3.29	Pitching .50 deg about $x_a/c = .403$	8.4	.050
196	.812	.35	3.29	Pitching .50 deg about $x_a/c = .404$	33.4	.198
197	.700	2.53	11.80	Pitching .49 deg about $x_a/c = .406$	7.5	.050
198	.700	2.53	11.80	Pitching .49 deg about $x_a/c = .405$	30.2	.201
199	.700	2.53	11.80	Pitching 1.01 deg about $x_a/c = 0.398$	7.5	0.050
200	.700	2.53	11.80	Pitching 1.00 deg about $x_a/c = .399$	30.2	.201
201	.700	2.53	11.80	Pitching 1.31 deg about $x_a/c = .403$	7.5	.050
202	.700	2.54	11.69	Plunging 1.00 cm (0.395 in.)	7.5	.050
203	.700	2.54	11.69	Plunging .86 cm (0.339 in.)	30.2	.201
204	.710	2.53	3.15	Pitching .50 deg about $x_a/c = .403$	7.4	.050
205	.710	2.53	3.15	Pitching .50 deg about $x_a/c = .403$	29.5	.199
206	.710	2.53	3.15	Pitching 1.01 deg about $x_a/c = .400$	7.4	.050
207	.710	2.53	3.15	Pitching 1.00 deg about $x_a/c = .399$	29.5	.199
208	.710	2.53	3.15	Plunging 1.01 cm (0.398 in.)	7.4	.050
209	.710	2.53	3.15	Plunging .87 cm (0.341 in.)	29.5	.199

TABLE 5.2. DATA BASE FOR NLR 7301 AIRFOIL, PITCHING OSCILLATION ABOUT 0.40c, ARRANGED IN FREQUENCY SWEEPS

M	α_m , deg	$Re \times 10^{-6}$	α_0 deg	k = 0.025	k = 0.05	k = 0.10	k = 0.15	k = 0.20	k = 0.25	k = 0.30
0.75	0.37	3.3	± 0.50			190		191		
.75	.37	6.2	± 0.50	131		132	133	134		135
.75	.37	11.5	± 0.50	145		144	146	147		149
.75	.37	6.2	± 1			136		137		
.75	.37	11.5	± 1			150		151		
.75	.37	3.3	± 2			192		193		
.75	.37	6.2	± 2			138		139		
.75	.37	11.5	± 2			152		153		
.80	.37	3.3	± 0.50			195		196		
.80	.37	6.2	± 0.50			140		141		
.80	.37	11.7	± 0.50			143		143		
.50	.57	2.5	± 0.50			184		185		
.45	.57	4.5	± 0.50	115		116	117	118		119
.50	.57	9.3	± 0.50	167		168	169	170		171
.45	.57	4.5	± 1			120		121		
.50	.57	9.5	± 1			172		173		
.50	.57	2.5	± 2			186		187		
.45	.57	4.5	± 2			122		123		
.50	.57	9.3	± 2			174		175		
.71	.57	3.1	± 0.50			178		179		
.70	.57	6.2	± 0.50	124		125		126		
.70	.57	11.2	± 0.50	156		157	158	159		160
.70	.57	6.2	± 1			127		128		
.70	.57	11.2	± 1			161		162		
.71	.57	3.1	± 2			180		181		
.70	.57	6.2	± 2			129		130		
.70	.57	11.2	± 2			163		164		
.70	2.5	3.2	± 0.5			204		205		
.70	2.5	11.8	± 0.5			197		198		
.70	2.5	3.2	± 1			206		207		
.70	2.5	11.8	± 1			199		200		

TABLE 5.23. MEAN AND FUNDAMENTAL FREQUENCY PRESSURE FOR AGARD CT CASE NO. 9; DYNAMIC INDEX 149

WING MODEL: NLR 7301 SUPERCRITICAL, CHORD= 500 METERS

WING MOTION: PITCHING 50 DEG ABOUT X/C= 400

DYNAMIC INDEX 149 STATIC INDEX 76

M 751 PTOT 293236 K 301
 ALPHA 37 QINF 55173 FREQ 49.5
 RE 1.14E 07 PINF 139946

-----UPPER SURFACE-----					-----LOWER SURFACE-----						
STEADY DATA		UNSTEADY DATA			STEADY DATA		UNSTEADY DATA				
-----CPU-----					-----CPL-----						
X/C	CPU	X/C	REAL	IMAG	PHASE	X/C	CPL	X/C	REAL	IMAG	PHASE
023	- 562	018	-2.473	.918	2.638	159.68	033	- 434			
045	-1.048	.067	-4.268	2.360	4.877	151.07	053	- 474			
.070	-1.036	.092	-3.426	2.121	4.030	148.25	106	- 531			
094	-1.131	.117	-3.423	2.076	4.003	148.77	209	- 516			
122	-1.097	.142	-3.770	2.815	4.705	143.26	309	- 750			
147	-1.043	.164	-3.641	2.704	4.535	143.41	381	- 627			
168	-1.059	.191	-2.727	2.056	2.415	143.00	460	- 628			
195	-1.021	.245	-3.196	3.397	4.777	133.27	532	- 440			
245	- 956	.294	-2.441	2.774	3.695	131.36	614	- 133			
297	- 991	.319	-1.867	2.535	3.148	126.39	684	066			
321	-1.000	.343	-1.420	2.837	3.145	116.85	779	238			
348	-1.009	.393	1.182	3.937	4.110	73.29	874	348			
369	-1.052	.424	3.147	10.268	10.739	72.97					
396	-1.052	.470	3.626	7.643	9.460	64.02					
420	- 973	.497	1.944	3.175	3.723	58.52					
450	- 920	.547	5.093	2.705	5.768	28.00					
473	- 856	.595	-0.421	.072	0.422	179.59					
499	- 905	.618	-4.367	-2.372	4.970	-151.51					
524	- 949	.647	-2.029	-2.051	2.005	-134.70					
550	- 999	.697	-1.378	-2.142	2.547	-122.76					
578	- 784	.746	- 289	-1.095	1.132	-104.75					
600	- 633	.796	- 065	- 575	578	-95.49					
624	- 625	.841	- 170	- 648	659	-104.69					
652	- 440	.916	- 358	- 173	396	-154.12					
700	- 353										
749	- 334										
797	- 110										
842	- 006										
914	122										

TABLE 5.24. INSTANTANEOUS PRESSURES AT THE UPPER SURFACE, HIGH REYNOLDS NUMBER DATA; CT CASE 6; DYNAMIC INDEX 144

	1	2	3	4	5	6	7	8	9	10	11	12	13
PHASE, DEGS	34.7	44.7	50.7	56.7	64.7	68.7	74.7	80.7	86.7	92.7	98.7	104.7	110.7
ALPHA, DEGS	.340	.365	.387	.402	.433	.461	.484	.506	.528	.549	.568	.584	.600
X/C													
1	.016	-.267	-.266	-.263	-.260	-.257	-.254	-.249	-.246	-.242	-.237	-.232	-.228
2	.067	-1.100	-1.102	-1.098	-1.095	-1.089	-1.085	-1.079	-1.073	-1.068	-1.062	-1.056	-1.051
3	.092	-1.100	-1.100	-1.100	-1.100	-1.100	-1.100	-1.100	-1.100	-1.100	-1.100	-1.100	-1.100
4	.117	-1.172	-1.170	-1.167	-1.163	-1.159	-1.154	-1.148	-1.142	-1.136	-1.130	-1.124	-1.118
5	.142	-1.128	-1.125	-1.122	-1.118	-1.113	-1.107	-1.100	-1.093	-1.086	-1.077	-1.069	-1.062
6	.168	-1.137	-1.134	-1.131	-1.127	-1.122	-1.116	-1.109	-1.103	-1.096	-1.088	-1.079	-1.071
7	.191	-1.102	-1.098	-1.095	-1.092	-1.087	-1.081	-1.074	-1.068	-1.062	-1.056	-1.049	-1.042
8	.245	-1.087	-1.085	-1.083	-1.080	-1.076	-1.071	-1.065	-1.059	-1.053	-1.047	-1.040	-1.033
9	.294	-1.101	-1.098	-1.095	-1.091	-1.086	-1.080	-1.074	-1.068	-1.062	-1.056	-1.049	-1.042
10	.319	-1.111	-1.108	-1.105	-1.101	-1.096	-1.091	-1.085	-1.079	-1.073	-1.067	-1.060	-1.053
11	.343	-1.131	-1.128	-1.125	-1.121	-1.116	-1.111	-1.105	-1.099	-1.093	-1.087	-1.080	-1.073
12	.393	-1.100	-1.107	-1.104	-1.102	-1.100	-1.100	-1.100	-1.100	-1.100	-1.100	-1.100	-1.100
13	.424	-1.113	-1.111	-1.108	-1.105	-1.100	-1.095	-1.087	-1.080	-1.073	-1.067	-1.060	-1.053
14	.470	-1.073	-1.077	-1.075	-1.072	-1.068	-1.063	-1.057	-1.051	-1.045	-1.039	-1.033	-1.027
15	.497	-1.073	-1.070	-1.067	-1.062	-1.056	-1.050	-1.044	-1.038	-1.032	-1.026	-1.020	-1.014
16	.547	-1.107	-1.102	-1.100	-1.097	-1.093	-1.088	-1.082	-1.076	-1.070	-1.064	-1.058	-1.052
17	.595	-.514	-.518	-.516	-.513	-.505	-.495	-.485	-.475	-.465	-.455	-.445	-.435
18	.618	-.424	-.423	-.422	-.417	-.412	-.406	-.400	-.394	-.388	-.382	-.376	-.370
19	.647	-.420	-.420	-.417	-.415	-.412	-.408	-.403	-.397	-.391	-.385	-.379	-.373
20	.697	-.382	-.382	-.380	-.378	-.376	-.373	-.369	-.364	-.358	-.352	-.346	-.340
21	.746	-.324	-.326	-.324	-.321	-.316	-.310	-.304	-.298	-.292	-.286	-.280	-.274
22	.796	-.180	-.180	-.180	-.187	-.187	-.188	-.188	-.188	-.188	-.188	-.188	-.188
23	.841	-.087	-.086	-.086	-.085	-.085	-.085	-.085	-.085	-.085	-.085	-.085	-.085
24	.916	-.135	-.137	-.140	-.138	-.135	-.137	-.136	-.135	-.135	-.135	-.135	-.135

TABLE 5.24. CONTINUED.

	J#	14	15	16	17	18	19	20	21	22	23	24	25	26
	PHASE,DEG#	116.7	122.7	128.7	134.7	140.7	146.7	152.7	158.7	164.7	170.7	176.7	182.7	188.7
	ALPHA,DEG#	-232	-276	-315	-349	-382	-413	-439	-460	-478	-475	-467	-467	-463
1	Z/C	*	*	*	*	*	*	*	*	*	*	*	*	*
1		.016	-.217	-.213	-.208	-.204	-.199	-.194	-.190	-.187	-.184	-.181	-.178	-.176
2		.067	-1.023	-1.013	-1.008	-1.001	-.995	-.988	-.982	-.976	-.971	-.964	-.959	-.957
3		.092	-1.123	-1.117	-1.111	-1.105	-1.099	-1.091	-1.084	-1.078	-1.073	-1.067	-1.064	-1.059
4		.117	-1.096	-1.091	-1.085	-1.079	-1.074	-1.068	-1.062	-1.057	-1.052	-1.047	-1.043	-1.038
5		.142	-1.045	-1.037	-1.028	-1.018	-1.010	-1.001	-.993	-.986	-.980	-.973	-.968	-.964
6		.164	-1.052	-1.044	-1.035	-1.025	-1.016	-1.007	-.998	-.990	-.984	-.978	-.973	-.969
7		.191	-1.027	-1.020	-1.013	-1.007	-1.001	-.993	-.987	-.980	-.975	-.968	-.963	-.959
8		.245	-.961	-.950	-.939	-.929	-.919	-.908	-.899	-.891	-.884	-.876	-.869	-.864
9		.294	-1.011	-1.002	-.992	-.983	-.976	-.965	-.953	-.944	-.934	-.922	-.914	-.901
10		.319	-1.030	-1.022	-1.013	-1.004	-.997	-.986	-.976	-.968	-.954	-.942	-.932	-.922
11		.343	-1.055	-1.044	-1.033	-1.021	-1.011	-.997	-.980	-.962	-.944	-.927	-.912	-.901
12		.393	-1.114	-1.101	-1.087	-1.069	-1.050	-1.024	-.992	-.926	-.906	-.900	-.901	-.897
13		.424	-1.006	-.984	-.955	-.899	-.846	-.830	-.809	-.806	-.833	-.815	-.790	-.750
14		.470	-.834	-.804	-.787	-.796	-.792	-.787	-.787	-.752	-.710	-.682	-.659	-.646
15		.497	-.807	-.800	-.839	-.839	-.834	-.838	-.813	-.739	-.686	-.663	-.671	-.687
16		.547	-1.055	-.997	-.984	-.948	-.858	-.797	-.798	-.801	-.819	-.841	-.860	-.893
17		.595	-.885	-.899	-.813	-.552	-.608	-.682	-.752	-.794	-.835	-.857	-.887	-.899
18		.618	-.814	-.832	-.841	-.859	-.871	-.877	-.855	-.860	-.858	-.858	-.858	-.858
19		.647	-.825	-.836	-.841	-.850	-.860	-.861	-.870	-.861	-.868	-.851	-.831	-.825
20		.687	-.348	-.371	-.374	-.376	-.381	-.381	-.378	-.380	-.374	-.374	-.372	-.370
21		.746	-.248	-.249	-.251	-.251	-.252	-.253	-.254	-.254	-.251	-.248	-.248	-.247
22		.796	-.112	-.113	-.113	-.113	-.113	-.115	-.114	-.115	-.115	-.116	-.116	-.116
23		.841	-.006	-.006	-.007	-.006	-.008	-.007	-.007	-.008	-.008	-.010	-.010	-.012
24		.916	.129	.108	.131	.119	.120	.139	.049	.106	.110	.113	.124	.093

	J#	27	28	29	30	31	32	33	34	35	36	37	38	39
	PHASE,DEG#	194.7	200.7	206.7	212.7	218.7	224.7	230.7	236.7	242.7	248.7	254.7	260.7	266.7
	ALPHA,DEG#	-475	-464	-440	-426	-397	-362	-321	-278	-229	-183	-134	-84	-33
1	Z/C	*	*	*	*	*	*	*	*	*	*	*	*	*
1		.016	-.173	-.173	-.172	-.173	-.174	-.176	-.178	-.182	-.186	-.189	-.194	-.203
2		.067	-.931	-.930	-.940	-.950	-.952	-.955	-.959	-.965	-.972	-.979	-.986	-.993
3		.092	-1.036	-1.056	-1.055	-1.055	-1.056	-1.059	-1.062	-1.066	-1.071	-1.078	-1.085	-1.090
4		.117	-1.029	-1.028	-1.027	-1.027	-1.029	-1.032	-1.035	-1.041	-1.046	-1.054	-1.062	-1.070
5		.142	-.957	-.956	-.955	-.954	-.956	-.960	-.964	-.970	-.977	-.984	-.993	-1.003
6		.164	-.977	-.976	-.975	-.975	-.976	-.979	-.982	-.987	-.993	-1.000	-1.007	-1.015
7		.191	-.952	-.950	-.949	-.949	-.949	-.953	-.956	-.962	-.968	-.974	-.980	-.987
8		.245	-.883	-.888	-.880	-.881	-.880	-.883	-.880	-.880	-.870	-.870	-.868	-.900
9		.294	-.867	-.860	-.796	-.759	-.766	-.742	-.751	-.769	-.811	-.878	-.925	-.947
10		.319	-.826	-.798	-.781	-.776	-.776	-.776	-.776	-.793	-.803	-.831	-.856	-.932
11		.343	-.777	-.769	-.772	-.760	-.742	-.745	-.740	-.740	-.746	-.760	-.810	-.897
12		.393	-.685	-.683	-.691	-.691	-.692	-.694	-.692	-.692	-.692	-.694	-.690	-.691
13		.424	-.754	-.749	-.687	-.640	-.648	-.654	-.653	-.652	-.652	-.651	-.653	-.651
14		.470	-.666	-.660	-.643	-.641	-.642	-.643	-.643	-.643	-.643	-.643	-.643	-.643
15		.507	-.713	-.713	-.711	-.712	-.685	-.686	-.686	-.689	-.684	-.683	-.681	-.686
16		.547	-.914	-.909	-.905	-.899	-.891	-.892	-.890	-.896	-.904	-.904	-.904	-.895
17		.595	-.804	-.809	-.806	-.802	-.801	-.807	-.808	-.805	-.804	-.804	-.801	-.802
18		.618	-.804	-.804	-.812	-.791	-.790	-.797	-.799	-.795	-.795	-.795	-.794	-.796
19		.647	-.530	-.538	-.532	-.519	-.508	-.502	-.500	-.507	-.505	-.507	-.509	-.503
20		.687	-.370	-.372	-.369	-.360	-.360	-.367	-.366	-.366	-.366	-.366	-.366	-.366
21		.736	-.247	-.246	-.245	-.246	-.244	-.244	-.244	-.244	-.244	-.244	-.244	-.244
22		.796	-.116	-.117	-.117	-.117	-.116	-.116	-.116	-.115	-.115	-.115	-.115	-.116
23		.841	-.013	-.013	-.013	-.013	-.013	-.013	-.013	-.011	-.013	-.011	-.012	-.012
24		.916	.104	.115	.129	.110	.120	.122	.113	.123	.110	.123	.127	.127

	J#	40	41	42	43	44	45	46	47	48	49	50	51	52
	PHASE,DEG#	272.7	278.7	284.7	290.7	296.7	302.7	308.7	314.7	320.7	326.7	332.7	338.7	344.7
	ALPHA,DEG#	424	476	431	401	324	274	215	153	106	60	16	-39	-93
1	Z/C	*	*	*	*	*	*	*	*	*	*	*	*	*
1		.016	-.208	-.213	-.214	-.224	-.236	-.250	-.263	-.277	-.291	-.305	-.320	-.326
2		.067	-1.008	-1.016	-1.023	-1.030	-1.043	-1.054	-1.063	-1.070	-1.076	-1.082	-1.086	-1.091
3		.092	-1.104	-1.111	-1.122	-1.131	-1.138	-1.145	-1.152	-1.159	-1.165	-1.171	-1.175	-1.179
4		.117	-1.089	-1.093	-1.099	-1.107	-1.116	-1.123	-1.131	-1.139	-1.145	-1.151	-1.153	-1.156
5		.142	-1.023	-1.023	-1.023	-1.023	-1.022	-1.020	-1.019	-1.017	-1.014	-1.012	-1.010	-1.008
6		.164	-1.032	-1.032	-1.031	-1.031	-1.031	-1.031	-1.030	-1.029	-1.028	-1.027	-1.026	-1.025
7		.191	-1.038	-1.038	-1.038	-1.038	-1.038	-1.038	-1.038	-1.038	-1.038	-1.038	-1.038	-1.038
8		.245	-.940	-.940	-.940	-.940	-.940	-.940	-.940	-.940	-.940	-.940	-.940	-.940
9		.294	-.877	-.877	-.877	-.877	-.877	-.877	-.877	-.877	-.877	-.877	-.877	-.877
10		.319	-.908	-.908	-.908	-.908	-.908	-.908	-.908	-.908	-.908	-.908	-.908	-.908
11		.343	-.903	-.903	-.903	-.903	-.903	-.903	-.903	-.903	-.903	-.903	-.903	-.903
12		.393	-.859	-.859	-.859	-.859	-.859	-.859	-.859	-.859	-.859	-.859	-.859	-.859
13		.424	-.859	-.859	-.859	-.859	-.859	-.859	-.859	-.859	-.859	-.859	-.859	-.859
14		.470	-.859	-.859	-.859	-.859	-.859	-.859	-.859	-.859	-.859	-.859	-.859	-.859
15		.507	-.859	-.859	-.859	-.859	-.859	-.859	-.859	-.859	-.859	-.859	-.859	-.859
16		.547	-.859	-.859	-.859	-.859	-.859	-.859	-.859	-.859	-.859	-.859	-.859	-.859
17		.595	-.859	-.859	-.859	-.859	-.859	-.859	-.859	-.859	-.859	-.859	-.859	-.859
18		.618	-.859	-.859	-.859	-.859	-.859	-.859	-.859	-.859	-.859	-.859	-.859	-.859
19		.647	-.859	-.859	-.859	-.859	-.859	-.859	-.859	-.859	-.859	-.859	-.859	-.859
20		.687	-.859	-.859	-.859	-.859	-.859	-.859	-.859	-.859	-.859	-.859	-.859	-.859
21		.736	-.859	-.859	-.859	-.859	-.859	-.859	-.859	-.859	-.859	-.859	-.859	-.859
22		.796	-.859	-.859	-.859	-.859	-.859	-.859	-.859	-.859	-.859	-.859	-.859	-.859
23		.841	-.859	-.859	-.859	-.85								

TABLE 5.24. CONCLUDED

	J=	53	54	55	56	57	58	59	60	61	62	63	64	65
PHASE, DEG	350.7	356.7	362.7	368.7	374.7	380.7	386.7	392.7	398.7	404.7	410.7	416.7	422.7	
ALPHA, DEGR	.482	.486	.487	.483	.478	.465	.448	.427	.403	.372	.335	.291	.242	
1	X/C	*	*	*	*	*	*	*	*	*	*	*	*	*
1	.016	-.264	-.266	-.267	-.268	-.269	-.269	-.270	-.268	-.267	-.265	-.264	-.262	-.258
2	.067	-1.099	-1.102	-1.104	-1.106	-1.108	-1.108	-1.108	-1.107	-1.105	-1.102	-1.099	-1.096	-1.091
3	.092	-1.186	-1.188	-1.190	-1.191	-1.192	-1.193	-1.193	-1.192	-1.191	-1.190	-1.187	-1.185	-1.181
4	.117	-1.168	-1.171	-1.172	-1.174	-1.175	-1.175	-1.174	-1.174	-1.173	-1.171	-1.168	-1.165	-1.161
5	.142	-1.122	-1.125	-1.127	-1.129	-1.130	-1.131	-1.130	-1.129	-1.128	-1.126	-1.123	-1.120	-1.115
6	.164	-1.131	-1.134	-1.136	-1.138	-1.139	-1.140	-1.139	-1.138	-1.137	-1.135	-1.132	-1.128	-1.123
7	.191	-1.095	-1.098	-1.101	-1.103	-1.104	-1.105	-1.104	-1.103	-1.101	-1.099	-1.097	-1.093	-1.088
8	.245	-1.039	-1.043	-1.045	-1.047	-1.048	-1.049	-1.049	-1.048	-1.046	-1.044	-1.043	-1.039	-1.034
9	.294	-1.092	-1.096	-1.099	-1.101	-1.102	-1.103	-1.104	-1.102	-1.100	-1.098	-1.095	-1.091	-1.086
10	.319	-1.101	-1.105	-1.108	-1.110	-1.112	-1.113	-1.113	-1.112	-1.110	-1.098	-1.095	-1.091	-1.086
11	.345	-1.120	-1.125	-1.128	-1.130	-1.132	-1.133	-1.133	-1.132	-1.130	-1.129	-1.126	-1.121	-1.117
12	.395	-1.174	-1.178	-1.181	-1.184	-1.186	-1.188	-1.189	-1.188	-1.187	-1.186	-1.182	-1.177	-1.172
13	.424	-1.194	-1.197	-1.110	-1.113	-1.114	-1.114	-1.114	-1.113	-1.112	-1.111	-1.108	-1.103	-1.101
14	.470	-1.018	-1.021	-1.026	-1.029	-1.031	-1.032	-1.032	-1.032	-1.030	-1.028	-1.025	-1.021	-1.017
15	.497	-1.053	-1.061	-1.066	-1.070	-1.073	-1.074	-1.074	-1.073	-1.071	-1.068	-1.065	-1.061	-1.056
16	.547	-1.147	-1.165	-1.174	-1.180	-1.184	-1.186	-1.189	-1.187	-1.186	-1.183	-1.180	-1.174	-1.165
17	.595	-.541	-.529	-.532	-.530	-.529	-.529	-.528	-.528	-.525	-.519	-.514	-.508	-.499
18	.618	-.422	-.424	-.428	-.434	-.430	-.429	-.428	-.428	-.425	-.424	-.420	-.415	-.408
19	.647	-.417	-.421	-.423	-.426	-.425	-.425	-.425	-.424	-.420	-.420	-.417	-.412	-.410
20	.697	-.344	-.343	-.344	-.347	-.345	-.344	-.343	-.343	-.342	-.343	-.340	-.339	-.340
21	.746	-.232	-.230	-.232	-.233	-.231	-.232	-.230	-.232	-.231	-.230	-.228	-.229	-.229
22	.796	-.109	-.109	-.109	-.110	-.110	-.109	-.108	-.108	-.109	-.107	-.106	-.107	-.106
23	.841	-.006	-.007	-.008	-.006	-.006	-.007	-.007	-.004	-.007	-.006	-.004	-.005	-.005
24	.916	.124	.138	.124	.117	.132	.137	.136	.125	.138	.138	.133	.137	.140

TABLE 5.25. INSTANTANEOUS PRESSURES AT THE UPPER SURFACE, HIGH REYNOLDS NUMBER DATA; CT CASE 8; DYNAMIC INDEX 148

	J=	1	2	3	4	5	6	7	8	9	10	11	12	13
PHASE, DEG	1.5	7.5	13.5	19.5	25.5	31.5	37.5	43.5	49.5	55.5	61.5	67.5	73.5	
ALPHA, DEGR	.490	.483	.471	.456	.437	.414	.388	.358	.323	.285	.244	.199	.151	
1	X/C	*	*	*	*	*	*	*	*	*	*	*	*	*
1	.016	-.266	-.247	-.248	-.249	-.249	-.249	-.250	-.249	-.248	-.247	-.246	-.244	-.244
2	.067	-1.078	-1.075	-1.077	-1.078	-1.078	-1.078	-1.078	-1.078	-1.078	-1.077	-1.075	-1.073	-1.070
3	.092	-1.161	-1.163	-1.165	-1.166	-1.167	-1.167	-1.167	-1.167	-1.167	-1.167	-1.165	-1.163	-1.161
4	.117	-1.140	-1.142	-1.143	-1.143	-1.143	-1.143	-1.143	-1.143	-1.143	-1.143	-1.143	-1.141	-1.138
5	.142	-1.067	-1.069	-1.069	-1.069	-1.069	-1.069	-1.069	-1.069	-1.069	-1.069	-1.069	-1.067	-1.060
6	.164	-1.096	-1.100	-1.101	-1.105	-1.106	-1.107	-1.107	-1.107	-1.107	-1.107	-1.106	-1.105	-1.103
7	.191	-1.061	-1.064	-1.065	-1.067	-1.068	-1.068	-1.068	-1.068	-1.068	-1.068	-1.067	-1.066	-1.064
8	.245	-.495	-.499	-.499	-.499	-.499	-.499	-.499	-.499	-.499	-.499	-.499	-.497	-.495
9	.294	-1.021	-1.025	-1.029	-1.031	-1.033	-1.033	-1.033	-1.033	-1.033	-1.033	-1.033	-1.033	-1.031
10	.319	-1.027	-1.030	-1.033	-1.037	-1.040	-1.042	-1.044	-1.044	-1.044	-1.044	-1.044	-1.044	-1.043
11	.345	-1.038	-1.038	-1.041	-1.042	-1.044	-1.044	-1.044	-1.044	-1.044	-1.044	-1.044	-1.044	-1.043
12	.395	-1.074	-1.080	-1.087	-1.104	-1.110	-1.116	-1.120	-1.124	-1.127	-1.130	-1.132	-1.133	-1.134
13	.424	-1.018	-1.032	-1.042	-1.050	-1.057	-1.062	-1.067	-1.071	-1.074	-1.075	-1.076	-1.077	-1.076
14	.470	-.425	-.425	-.426	-.426	-.426	-.426	-.426	-.426	-.426	-.426	-.426	-.426	-.426
15	.497	-1.015	-1.018	-1.020	-1.020	-1.020	-1.020	-1.020	-1.020	-1.020	-1.020	-1.020	-1.020	-1.020
16	.547	-.403	-.403	-.403	-.403	-.403	-.403	-.403	-.403	-.403	-.403	-.403	-.403	-.403
17	.595	-.373	-.373	-.373	-.373	-.373	-.373	-.373	-.373	-.373	-.373	-.373	-.373	-.373
18	.618	-.354	-.354	-.354	-.354	-.354	-.354	-.354	-.354	-.354	-.354	-.354	-.354	-.354
19	.647	-.335	-.335	-.335	-.335	-.335	-.335	-.335	-.335	-.335	-.335	-.335	-.335	-.335
20	.697	-.316	-.316	-.316	-.316	-.316	-.316	-.316	-.316	-.316	-.316	-.316	-.316	-.316
21	.746	-.297	-.297	-.297	-.297	-.297	-.297	-.297	-.297	-.297	-.297	-.297	-.297	-.297
22	.796	-.278	-.278	-.278	-.278	-.278	-.278	-.278	-.278	-.278	-.278	-.278	-.278	-.278
23	.841	-.259	-.259	-.259	-.259	-.259	-.259	-.259	-.259	-.259	-.259	-.259	-.259	-.259
24	.916	-.240	-.240	-.240	-.240	-.240	-.240	-.240	-.240	-.240	-.240	-.240	-.240	-.240
PHASE, DEG	74.5	85.5	91.5	97.5	103.5	109.5	115.5	121.5	127.5	133.5	139.5	145.5	151.5	
ALPHA, DEGR	.481	.464	.443	.427	.410	.393	.373	.351	.328	.304	.279	.254	.229	
1	X/C	*	*	*	*	*	*	*	*	*	*	*	*	*
1	.016	-.240	-.239	-.236	-.233	-.231	-.227	-.224	-.222	-.219	-.216	-.214	-.211	-.207
2	.067	-1.088	-1.088	-1.088	-1.087	-1.086	-1.084	-1.082	-1.080	-1.078	-1.076	-1.074	-1.072	-1.069
3	.092	-1.158	-1.155	-1.152	-1.148	-1.145	-1.140	-1.135	-1.131	-1.127	-1.122	-1.117	-1.113	-1.110
4	.117	-1.138	-1.134	-1.130	-1.126	-1.122	-1.117	-1.112	-1.107	-1.102	-1.097	-1.092	-1.088	-1.085
5	.142	-1.067	-1.063	-1.059	-1.054	-1.049	-1.044	-1.039	-1.034	-1.029	-1.024	-1.019	-1.014	-1.011
6	.164	-1.097	-1.093	-1.089	-1.084	-1.079	-1.074	-1.069	-1.064	-1.059	-1.054	-1.049	-1.044	-1.041
7	.191	-1.067	-1.063	-1.059	-1.054	-1.049	-1.044	-1.039	-1.034	-1.029	-1.024	-1.019	-1.014	-1.011
8	.245	-1.003	-1.000	-.997	-.994	-.991	-.988	-.985	-.982	-.979	-.976	-.973	-.970	-.967
9	.294	-1.033	-1.031	-1.029	-1.026	-1.023	-1.020	-1.017	-1.014	-1.011	-1.008	-.995	-.992	-.989
10	.319	-1.041	-1.039	-1.036	-1.032	-1.029	-1.026	-1.022	-1.019	-1.016	-1.013	-1.010	-1.007	-1.004
11	.345	-1.050	-1.046	-1.043	-1.039	-1.035	-1.031	-1.027	-1.023	-1.019	-1.015	-1.011	-1.007	-1.003
12	.395	-1.074	-1.072	-1.071	-1.069	-1.067	-1.065	-1.063	-1.061	-1.059	-1.057	-1.055	-1.053	-1.051
13	.424	-1.018	-1.016	-1.014	-1.012	-1.010	-1.008	-1.006	-1.004	-1.002	-1.000	-0.998	-0.996	-0.994
14	.470	-.429	-.429	-.429	-.429	-.429	-.429	-.429	-.429	-.429	-.429	-.429	-.429	-.429
15	.497	-1.023	-1.024	-1.024	-1.023	-1.022	-1.021	-1.020	-1.019	-1.018	-1.017	-1.016	-1.015	-1.014
16	.547	-1.012	-1.013	-1.013	-1.012	-1.011	-1.010	-1.009	-1.008	-1.007	-1.006	-1.005	-1.004	-1.003
17	.595	-.355	-.352	-.350	-.347	-.345	-.342	-.340	-.337	-.335	-.332	-.330	-.327	-.325
18	.618	-.337	-.334	-.332	-.329	-.327	-.324	-.322	-.319	-.317	-.314	-.312	-.309	-.307
19	.647	-.319	-.317	-.315	-.312	-.310	-.307	-.305						

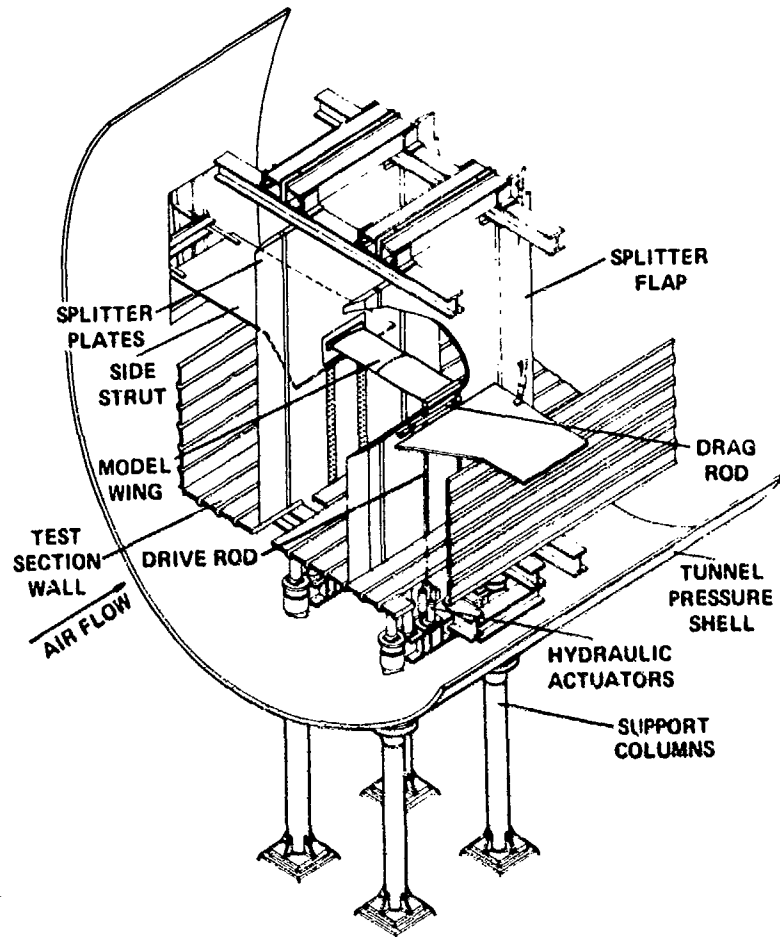


Fig. 5.1. General arrangement of oscillating airfoil test apparatus in NASA AMES 11- by 11-Foot Transonic Wind Tunnel.

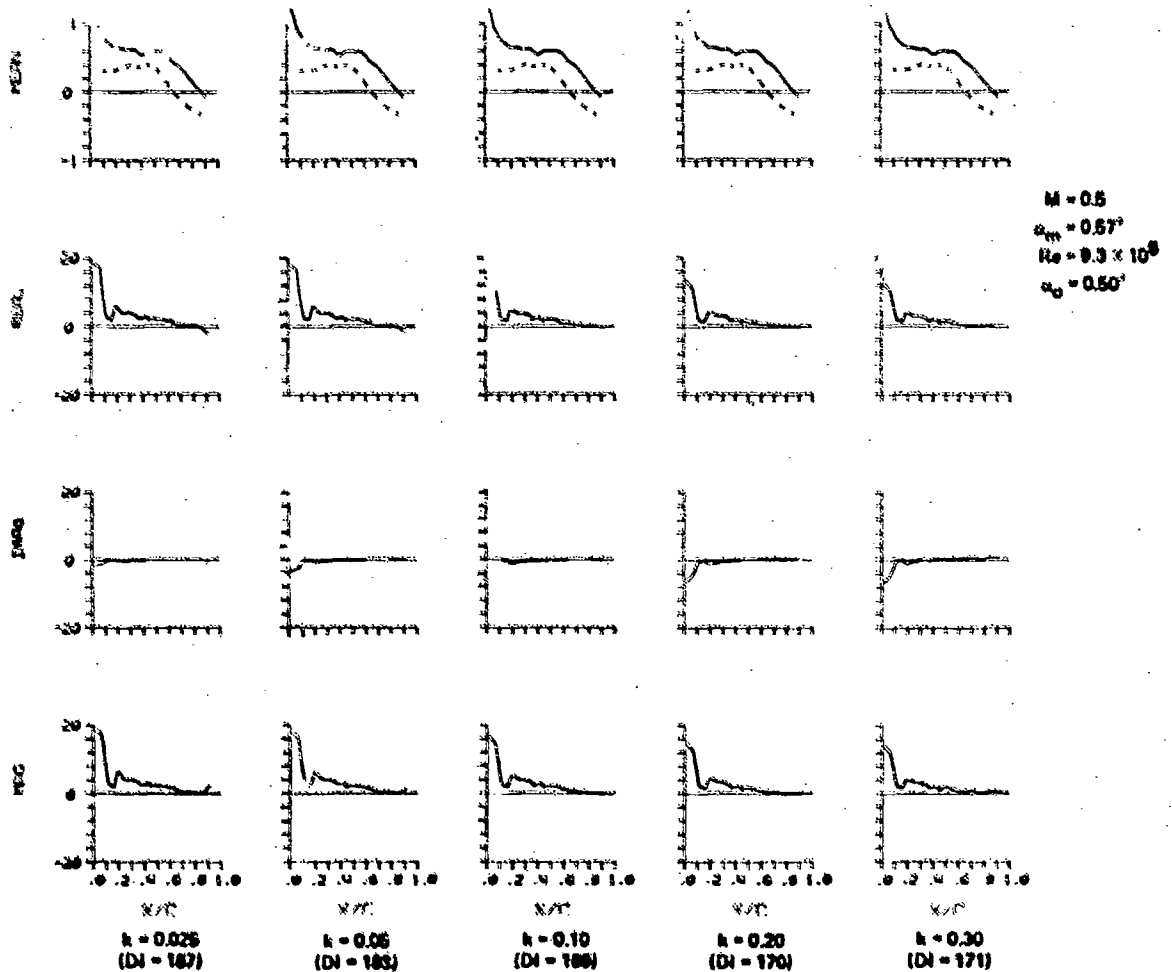


Fig. 5.2. Effect of varying frequency - subsonic flow.

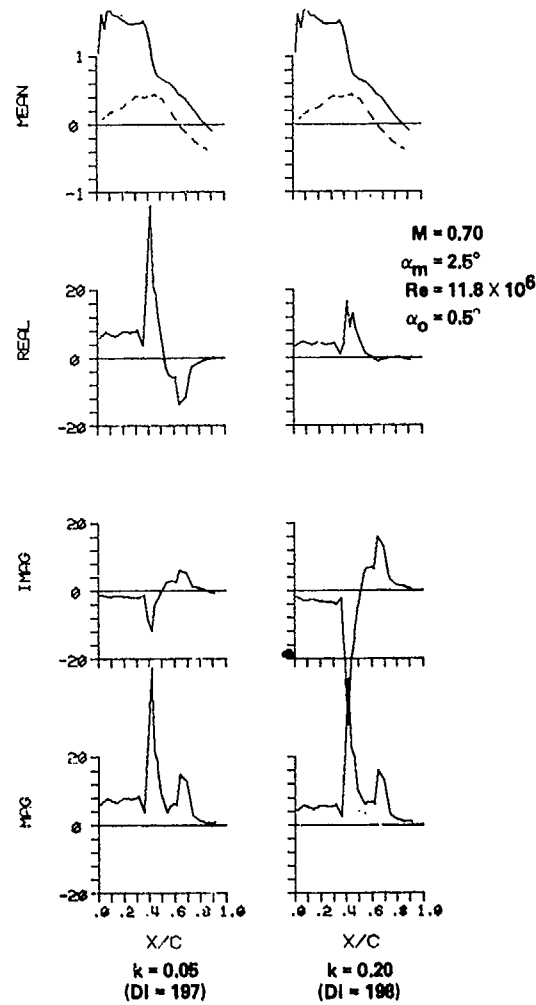


Fig. 5.3. Effect of varying frequency - transonic flow.

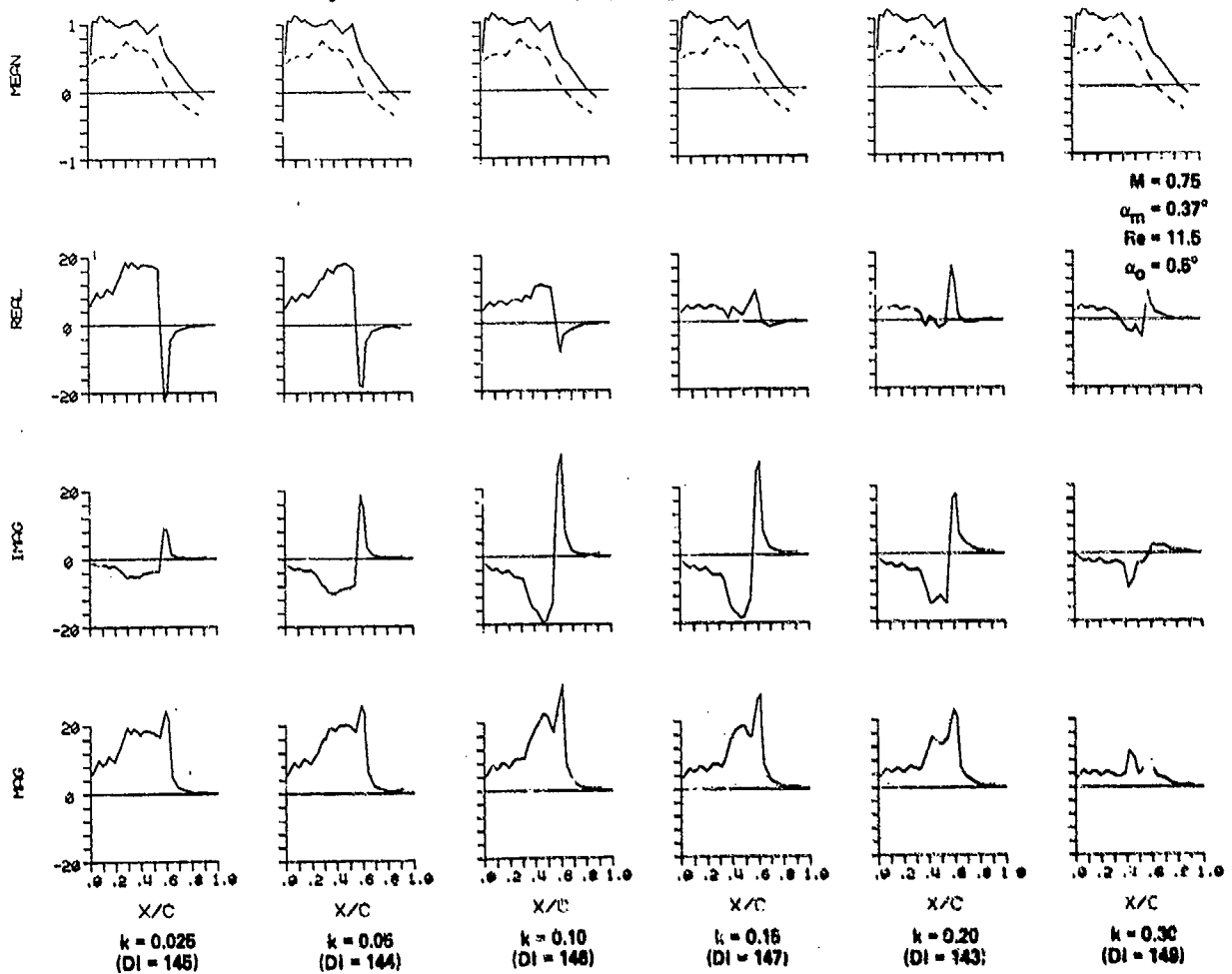


Fig. 5.4. Effect of varying frequency - supercritical design point.

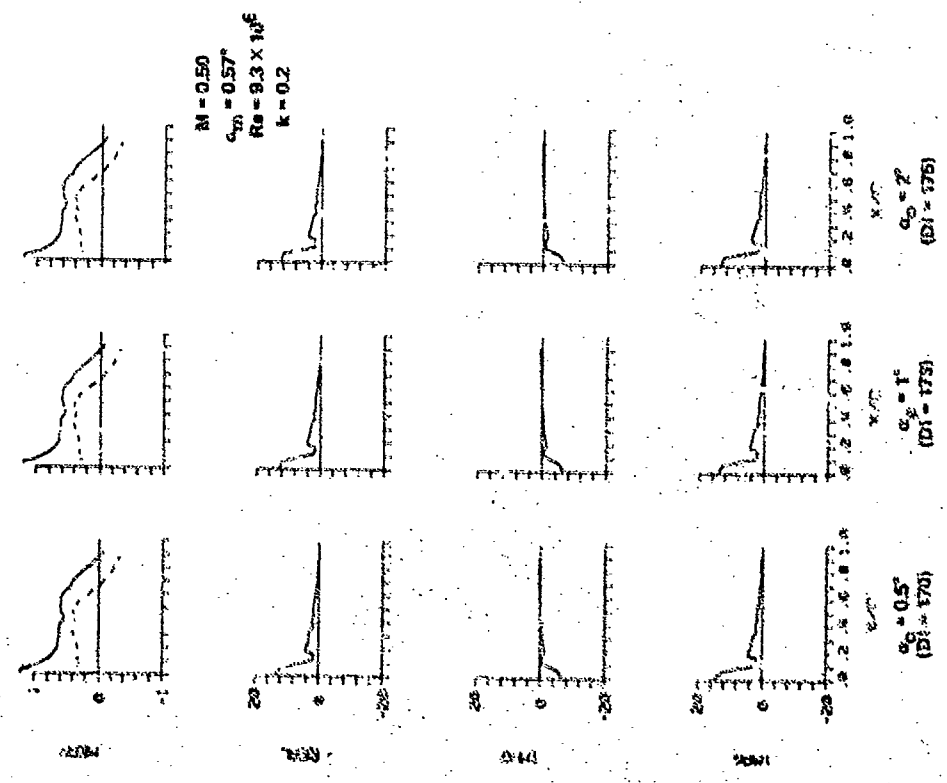
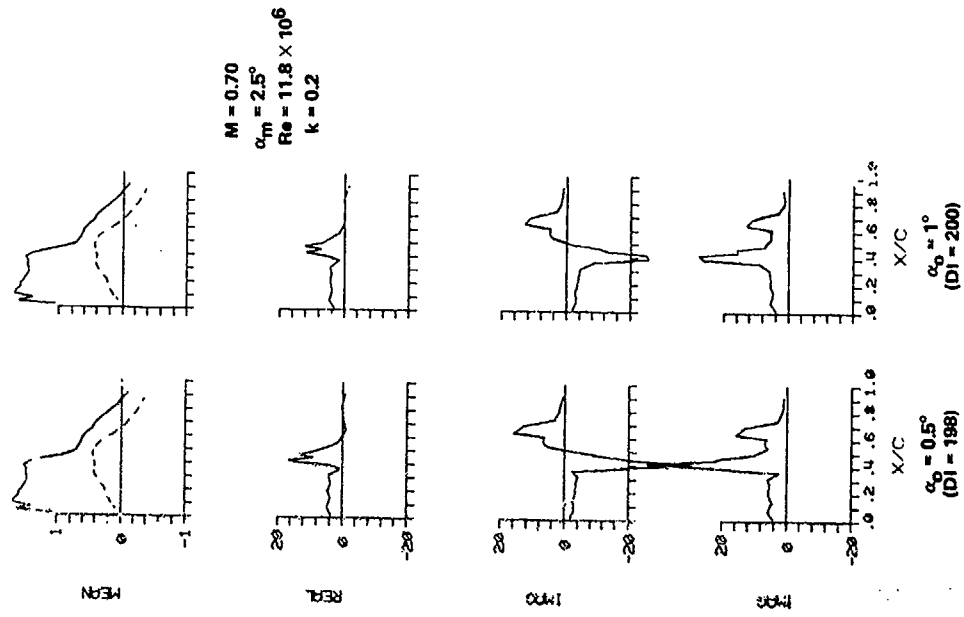


Fig. 5.6. Effect of varying amplitude - transonic flow.

Fig. 5.7. Effect of varying amplitude - subsonic flow.

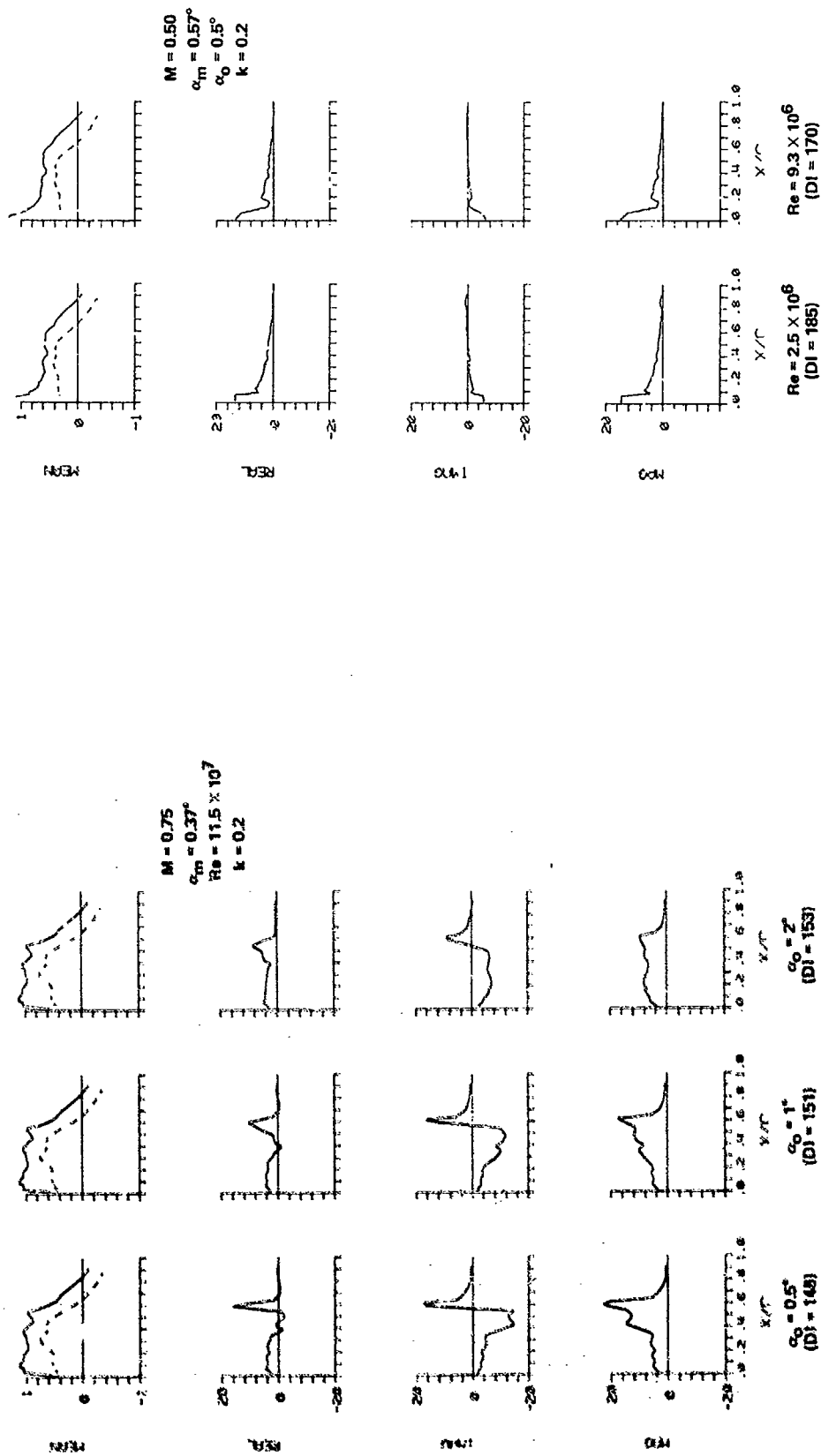


Fig. 5.7. Effect of varying amplitude - supercritical design point.

Fig. 5.8. Effect of varying Reynolds number - subsonic flow.

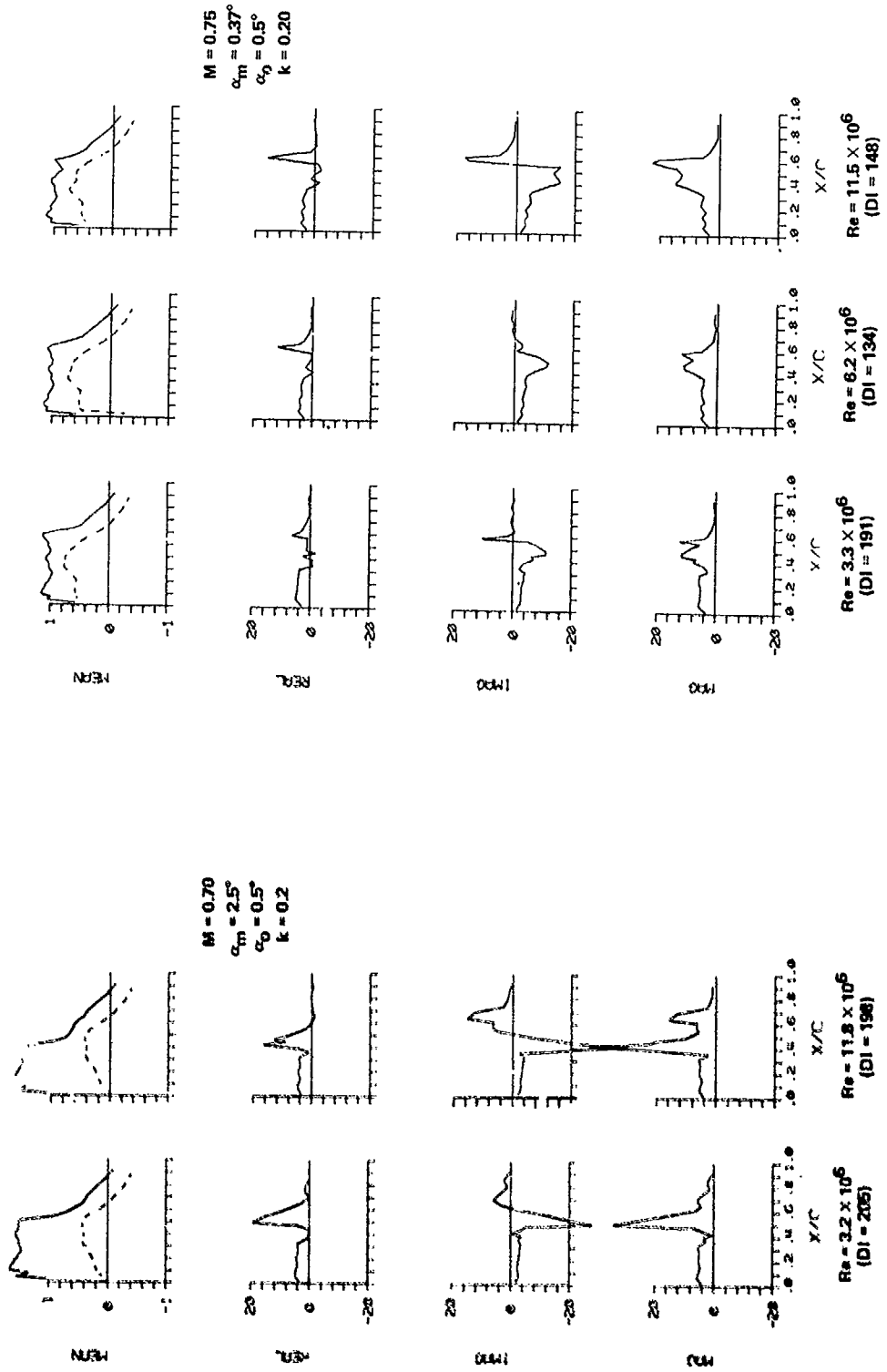


Fig. 5.10. Effect of varying Reynolds number - supercritical design point.

Fig. 5.9. Effect of varying Reynolds number - transonic flow.

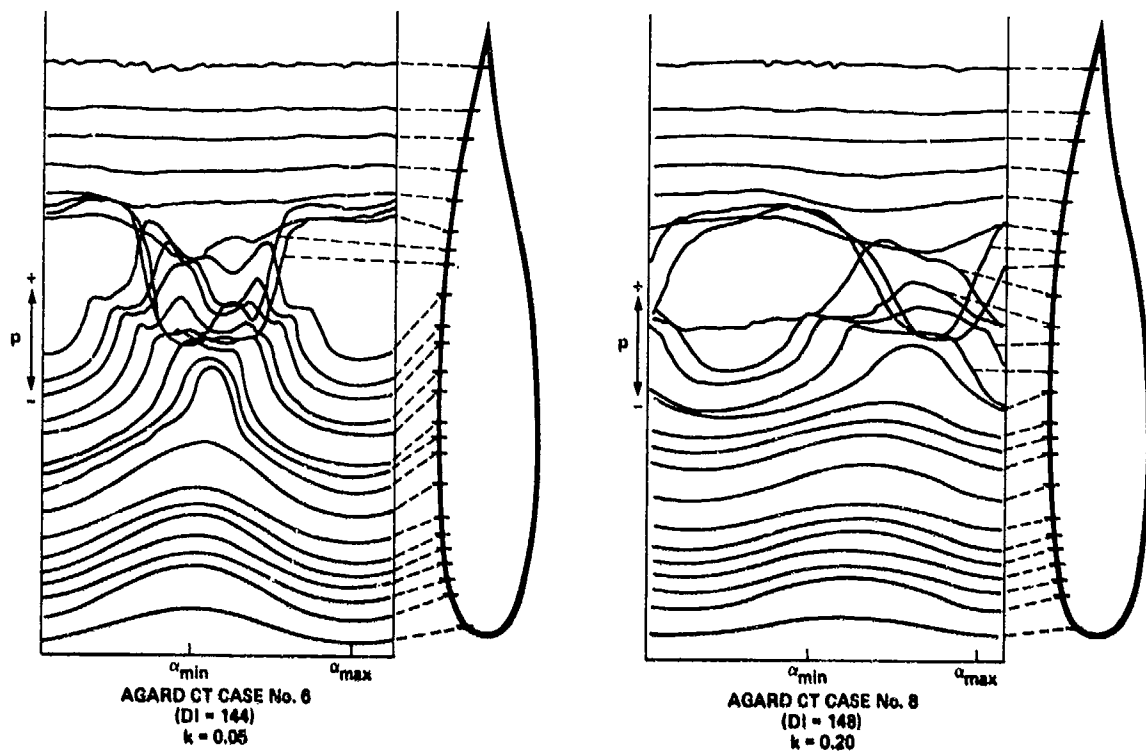


Fig. 5.11. Unsteady pressure time-histories for supercritical design case. $M = 0.721$, $\alpha_m = 0.19^\circ$.

DATA SET 6

RAE WING A. OSCILLATING FLAP

by

D. G. Mabey, RAE Bedford

INTRODUCTION AND DISCUSSION

An extensive series of oscillatory pressure measurements^{6.1,2} was made on a half model of a swept wing with a part-span trailing-edge flap (Fig 6.1), to highlight the uncertainties in linearised theory at transonic speeds and moderately high frequencies and to provide evidence of the importance of boundary-layer thickness. The model thickness-to-chord ratio was selected to ensure that at zero incidence, even at transonic Mach numbers up to $M = 0.9$, the local Mach number, M_e , would be less than 1.2, so that boundary-layer separations were avoided (Fig 6.2). The mean isomach contours are given in Figs 6.2 and 6.3 which illustrates some measurements made for angles of incidence other than zero.

The magnitude of the oscillatory pressures decreases significantly as the boundary-layer displacement thickness, δ_1 , at the flap hinge line increases, consistent with the reduced lift-curve slope of the flap. However, the phase lag of the oscillatory pressure with respect to the flap motion decreases as the boundary-layer thickness increases (Fig 6.4). This large change in phase angle, ϕ , is now attributed to the displacement effect of the time-dependent turbulent boundary layer^{6.3}.

The major uncertainty in the original experiment^{6.1,2} was the absolute value of the flap deflection, which could only be specified to about 5% accuracy because of aeroelastic distortion (both static and dynamic). In the subsequent tests a stiff flap was used made of carbon fibre^{6.3}, together with a new form of optical transducer to measure the flap amplitude^{6.4}. There were also improvements in the measurement of pressures. None of these measurements is included here, for other reasons discussed fully in Ref 6.3.

In the original experiment good comparisons with inviscid linearised theory were obtained at subsonic speeds (Fig 6.4). The principle of superposition of flap frequencies was valid at both subsonic and transonic speeds (Fig 6.5a&b). However, at transonic speeds sinusoidal flap movements do develop significant pressures at harmonic frequencies behind the shock waves, owing to the non-linearity of transonic flows^{6.1} and small aeroelastic distortions (Fig 6.6).

Ref 6.1 gives some details of the original experiment while Ref 6.2 reviews the principal results. Ref 6.3 gives some preliminary measurements on the same model fitted with a modified flap and drive system capable of much higher frequencies. Amongst other results, these tests established that in the original experiments^{6.1,2} the effects of the unwanted wing motion on the oscillatory pressures were small.

The data presented correspond with some of the CT cases in Ref 6.9 chosen for RAE Wing A with an oscillating flap and relate to both subsonic and transonic flows. Of the CT cases, 4 and 5 are for subcritical flow and 11 is for supercritical flow. For CT Cases 8 and 9 the unsteady flow is termed 'critical' because a local supersonic region is present intermittently. (See Table 6.1 and discussion in Ref 6.1.)

No data for the CT Cases with heaving or pitching or for CT Cases 10, 12 and 13 are yet available.

1 GENERAL DESCRIPTION OF MODEL

1.1	Designation	RAE Wing A
1.2	Type	Half model with part-span trailing-edge flap
1.3	Derivation	-
1.4	Additional remarks	-
1.5	References	Ref 6.5

2 MODEL GEOMETRY

2.1	Planform	Straight tapered
2.2	Aspect ratio	6
2.3	Leading-edge sweep	36.65°
2.4	Trailing-edge sweep	22.34°

2.5	Taper ratio	1/3
2.6	Twist	0
2.7	Root chord	240 mm
2.8	Span of model	s = 480 mm
2.9	Area of planform	0.0768 m ²
2.10	Location of reference sections and definition of profiles	RAE 101 - 9% streamwise
2.11	Lofting procedure between reference sections	Straight line generators
2.12	Form of wing-body, or wing-root junction	No body: 0.6 mm gap at root
2.13	Form of wing tip	Straight streamwise chord: no radius
2.14	Control surface details	Trailing-edge flap from $\eta = 0.40$ to 0.70. Hinge line at $x/c = 0.70$ swept 27.05°. Small chordwise and spanwise gaps (see Ref 6.1)
2.15	Additional remarks	-
2.16	References	-
3	WIND TUNNEL	
3.1	Designation	RAE 3 ft x 3 ft
3.2	Type of tunnel	Continuous and pressurised
3.3	Test section dimensions	Height = 640 mm, width = 910 mm, length = 1370 mm
3.4	Type of roof and floor	Slotted
3.5	Type of side walls	Closed
3.6	Ventilation geometry	Four complete slots and two corner half slots in roof and floor, covered with perforated plates. Open area ratio of slots = 8%
3.7	Thickness of side wall boundary layer	$\delta^* = 7$ mm
3.8	Thickness of boundary layers at roof and floor	δ^* less than 7 mm
3.9	Method of measuring Mach number	Plenum chamber pressure
3.10	Flow angularity	About 0.1°
3.11	Uniformity of Mach number over test section	± 0.002
3.12	Sources and levels of noise or turbulence in empty tunnel	Mixing region at ends of working section. Typical levels at transonic speeds $\sqrt{nF(n)} = 0.004$ (Ref 6.6)
3.13	Tunnel resonances	Tunnel resonance frequencies well above flap frequencies
3.14	Additional remarks	-
3.15	References on tunnel	Ref 6.6
4	MODEL MOTION	
4.1	General description	Sinusoidal pitching of flap about swept hinge line
4.2	Reference coordinate and definition of motion	Flap deflection relative to wing chord at $\eta = 0.55$ (mid-flap)
4.3	Range of amplitude	0 to 2°

4.4	Range of frequency	0, 1 Hz, 90 Hz and limited data available at 131 Hz
4.5	Method of applying motion	Semi-resonant motion
4.6	Timewise purity of motion	Good. First overtone 40 dB lower than fundamental
4.7	Natural frequencies and normal modes of model and support system	First bending frequency at 60 Hz, second bending frequency at 143 Hz, minimum model motion at 90 Hz
4.8	Actual mode of applied motion including any elastic deformation	Elastic deformations were not measured but were subsequently shown not to alter the pressures at 1 and 90 Hz
4.9	Additional remarks	Influence of wing motion discussed in Ref 6.3

5 TEST CONDITIONS

5.1	Model planform area/tunnel area	0.13
5.2	Model span/tunnel width	0.53
5.3	Blockage	1.2%
5.4	Position of model in tunnel	685 mm from start of working section
5.5	Range of Mach number	0.40, 0.65, 0.80, 0.85, 0.90, 0.95
5.6	Range of tunnel total pressure	0.95 bar
5.7	Range of tunnel total temperature	278 K to 298 K
5.8	Range of model steady, or mean, incidence	0 to 2°
5.9	Definition of model incidence	Model set to zero geometric incidence (NB up to 0.1° flow deflection)
5.10	Position of transition, if free	Limited data with free transition in Ref 6.2
5.11	Position and type of trip, if transition fixed	x/c = 0.05, roughness elements 0.13 mm high and 2 mm apart
5.12	Flow instabilities during tests	No periodic shock oscillation but some random oscillation associated with unsteadiness in tunnel flow
5.13	Changes to mean shape of model due to steady aerodynamic load	Negligible
5.14	Additional remarks	-
5.15	References describing tests	Refs 6.1, 6.2

6 MEASUREMENTS AND OBSERVATIONS

6.1	Steady pressures for the mean conditions	✓
6.2	Steady pressures for small changes from the mean conditions	-
6.3	Quasi-steady pressures	✓
6.4	Unsteady pressures	✓
6.5	Steady section forces for the mean conditions by integration of pressures	-
6.6	Steady section forces for small changes from the mean conditions by integration	-
6.7	Quasi-steady section forces by integration	-
6.8	Unsteady section forces by integration	-
6.9	Measurement of actual motion at points on model	-

- 6.10 Observation or measurement of boundary layer properties
- 6.11 Visualization of surface flow
- 6.12 Visualization of shockwave movements
- 6.13 Additional remarks

✓
✓
-
-

7 INSTRUMENTATION

- 7.1 Steady pressures
 - 7.1.1 Position of orifices spanwise and chordwise See data tables
 - 7.1.2 Type of measuring system Capsule manometers
- 7.2 Unsteady pressures
 - 7.2.1 Position of orifices spanwise and chordwise See data tables
 - 7.2.2 Diameter of orifices 0.5 mm
 - 7.2.3 Type of measuring system Individual in situ transducers
 - 7.2.4 Type of transducers Kulite type XCQL 093 25A
 - 7.2.5 Principle and accuracy of calibration Steady calibration and tests with oscillatory pressure generator (see Ref 6,7)
- 7.3 Model motion
 - 7.3.1 Method of measuring motion reference coordinates Foil strain gauges on steel flexures at $n = 0.52$ and 0.66 . Average motion at $n = 0.55$
 - 7.3.2 Method of determining spatial mode of motion Not measured
 - 7.3.3 Accuracy of measured motions 5%
- 7.4 Processing of unsteady measurements
 - 7.4.1 Method of acquiring and processing measurements Serial logger to Digital Transfer Function Analyser (DTFA); paper tape input to remote computer; parallel magnetic tape
 - 7.4.2 Type of analysis Harmonic
 - 7.4.3 Unsteady pressure quantities obtained and accuracies achieved Fundamental only
 - 7.4.4 Method of integration to obtain forces Not integrated
- 7.5 Additional remarks -
- 7.6 References on techniques Refs 6.1, 6.3 and 6.4

8 DATA PRESENTATION

- 8.1 Test cases for which data could be made available Table 6.1
- 8.2 Test cases for which data are included in this document Table 6.1
- 8.3 Steady pressures Tables 6.2 to 6.5
- 8.4 Quasi-steady or steady perturbation pressures Tables 6.2 to 6.5
- 8.5 Unsteady pressures Tables 6.2 to 6.5
- 8.6 Steady forces or moments -
- 8.7 Quasi-steady or steady perturbation forces -
- 8.8 Unsteady forces and moments -
- 8.9 Other forms in which data could be made available -

8.10 References giving other presentations of data Refs 6.1, 6.2, 6.3 and 6.8

9 COMMENTS ON DATA

9.1 Accuracy

- 9.1.1 Mach number ± 0.002
- 9.1.2 Steady incidence $\pm 0.1^\circ$
- 9.1.3 Reduced frequency Variations up to $\pm 2\%$ from nominal values due to temperature variations
- 9.1.4 Steady pressure coefficients C_p better than ± 0.006
- 9.1.5 Steady pressure derivatives -
- 9.1.6 Unsteady pressure coefficients Magnitude of \bar{C}_p/δ_0 to $\pm(0.05|\bar{C}_p/\delta_0| + 0.02)$. Phase to $\pm 3^\circ$
- 9.2 Sensitivity to small changes of parameter -
- 9.3 Non-linearities Small (discussed in Refs 6.1 and 6.2)
- 9.4 Influence of tunnel total pressure Not known
- 9.5 Effects on data of uncertainty, or variation, in mode of model motion See Introduction
- 9.6 Wall interference corrections None
- 9.7 Other relevant tests on same model Ref 6.3
- 9.8 Relevant tests on other models of nominally the same shape Ref 6.5 for relevant steady tests
- 9.9 Any remarks relevant to comparison between experiment and theory Some interesting comparisons with subsonic inviscid linearised theory in Ref 6.2
- 9.10 Additional remarks -
- 9.11 References on discussion of data Refs 6.1, 6.2 and 6.3

10 PERSONAL CONTACT FOR FURTHER INFORMATION

D.G. Mabey
Dynamics Laboratory
RAE Bedford
MK41 6AE
UK

11 LIST OF REFERENCES

- 6.1 D.M. McOwat Time-dependent pressure measurements on a swept wing with an oscillating trailing-edge flap.
B.L. Welsh RAE Technical Report 81033 (1981)
B.E. Cripps
- 6.2 D.G. Mabey Aerodynamic characteristics of moving trailing-edge controls at subsonic speeds.
B.L. Welsh AGARD CP 262, Paper 20, May 1979;
D.M. McOwat RAE Technical Memorandum Structures 947 (1979)
- 6.3 D.G. Mabey Further aerodynamic characteristics of moving trailing-edge controls at subsonic and transonic speeds.
B.L. Welsh RAE Technical Report 80134 (1980)
B.E. Cripps
- 6.4 B.L. Welsh A new angular displacement transducer.
RAE Technical Report 79026 (1979)
- 6.5 D.A. Treadgold Pressure distribution measured in the RAE 8ft x 6ft transonic tunnel on RAE Wing 'A' in combination with an axisymmetric body at Mach numbers of 0.4, 0.8 and 0.9.
A.F. Jones AGARD AR 138, Paper B4 (1979)
K.H. Wilson

- 6.6 D.G. Mabey Flow unsteadiness of model vibration in wind tunnels at subsonic and transonic speeds. CP 1155 (1971)
- 6.7 B.L. Welsh Some notes on the measurement of oscillatory pressures. RAE Technical Memorandum Structures 869 (1975)
- 6.8 D.M. McOwat Dynamics Lab Memo 1 (1982)
- 6.9 S.R. Bland AGARD three-dimensional aeroelastic configurations. AGARD-AR-167 (1982)

12 NOTATION

- c_r root chord
- C_p steady pressure coefficient
- \bar{C}_p complex pressure coefficient
- $R(\bar{C}_p)$ real part of \bar{C}_p
- $I(\bar{C}_p)$ imaginary part of \bar{C}_p
- f frequency (Hz)
- k frequency parameter $f \cdot c_r / U$
- M free stream Mach number
- M_e local external Mach number
- Re Reynolds number based on free stream conditions and root chord
- U free stream velocity
- α angle of incidence
- δ_0 flap amplitude in streamwise direction (see Note below)
- δ_1 boundary-layer displacement thickness at hinge line
- δ^* boundary-layer displacement thickness at wall
- n dimensionless spanwise coordinate y/s
- Λ sweepback angle
- ξ dimensionless chordwise coordinate (fraction of local chord)
- ϕ phase angle of pressure with respect to flap motion

NOTE: For consistency with the standard notation suggested by Bland, the symbol δ represents the flap deflection angle measured streamwise. In Refs 6.1 to 6.3, which give other information about the tests, the symbol δ represents the flap deflection measured normal to the hinge line. Thus

$$\begin{aligned} (\delta, \text{ as used here}) &= (\delta \text{ of Refs}) \times \cos \Lambda_{HL}, \quad \text{where } \Lambda_{HL} = 27.05^\circ \\ &= (\delta \text{ of Refs}) \times 0.891. \end{aligned}$$

$$(\bar{C}_p / \delta, \text{ as used here}) = (\bar{C}_p / \delta \text{ of Refs}) \times 1.122.$$

Table 6.1

SUMMARY OF DATA GIVEN AND DATA AVAILABLE

M	Re $\times 10^{-6}$	k	δ_0 (deg)	α (deg)	n				CT or data given	Time- dependent flow	Test No.		
					0.35	0.45	0.60	0.75					
0.40	1.91	Steady	-	0	1	1	1	1			1		
		0.0055	1.78	0	1	1	1	0		A			
		0.50	1.71	0	1	1	1	1		A			
0.65	2.78	Steady	-	0	1	1	1	1			2		
		0.0035	1.75	0	1	1	1	0		A			
		0.32	1.63	0	1	1	1	1		A			
0.80	3.14	Steady	-	+2	1	1	1	1	✓		9		
				+1	1	1	1	1	-		7		
				0	1	1	1	1	✓		3		
				-1	1	0	1	0	-		8		
				-2	1	1	1	1	✓		10		
		0.0029	1.75			+2	1	1	1	0	✓	A	9
						+1	0	1	0	0	-	A	7
						0	1	1	1	0	✓	A	3
						-1	0	1	0	0	-	A	8
						-2	1	1	1	0	✓	A	10
		0.26	1.60			+2	1	1	1	1	5	A	9
						+1	1	1	1	1	-	A	7
0	1					1	1	1	4	A	3		
-1	1					1	0	1	-	A	8		
-2	1					1	1	1	5	A	10		
0.85	3.23	Steady	-	+2	1	1	1	1			13		
				+1	1	1	1	1			11		
				0	1	1	1	1			4		
				-1	1	1	1	1			12		
				-2	1	1	1	1			14		
		0.0028	1.75			+2	1	1	1	0		B	13
						+1	0	1	1	0		A	11
						0	1	1	1	0		A	4
						-1	0	1	1	0		A	12
						-2	1	1	1	0		A	14
		0.25	1.58			+2	1	1	1	1		B	13
						+1	1	1	1	1		A	11
0	1					1	1	1		A	4		
-1	1					1	1	1		A	12		
-2	1					1	1	1		A	14		
0.90	3.32	Steady	-	+1	1	1	1	1	✓		15		
				0	1	1	1	1	✓		5		
				-1	1	1	1	1	✓		16		
		0.0026	1.76			+1	0	1	1	0	✓	C	15
						0	1	1	1	0	8	B	5
						-1	0	1	1	0	✓	A	16
		0.24	1.58			+1	1	1	1	1	11	C	15
						0	1	1	1	1	9	B	5
						-1	1	1	1	1	11	A	16
0.95	3.38	Steady	-	+1	1	1	1	1			17		
				0	1	1	1	1			6		
				-1	1	1	1	1			18		
		0.0036	1.80			+1	0	1	1	0		C	17
						0	1	1	1	0		C	6
						-1	0	1	1	0		C	18
		0.23	1.58			+1	1	1	1	1		C	17
						0	1	1	1	1		C	6
						-1	1	1	1	1		C	18

Type of flow: A Subcritical
 B Critical
 C Supercritical

Data available: 1
 No data: 0
 Data given: ✓

All tests made with fixed transition.
 Results for lower surface are obtained from negative incidences.

Table 6.3 (concluded)

CASE 5

Test M α ξ_0 Surface $k = 2.9 \times 10^{-3} f$
 10 ξ_{00} 2.0 1.75($f=1$) Lower
 $\eta = \xi_{00}$ 1.60($f=90$)

f	data	ξ	ξ_0	ξ_{00}	Surface	k
1.	0.89	0.89	0.89	0.89	0.89	0.89
99.	0.8911(CP/0)	0.8912	0.8913	0.8914	0.8915	0.8916

$\eta = \xi_{00}$

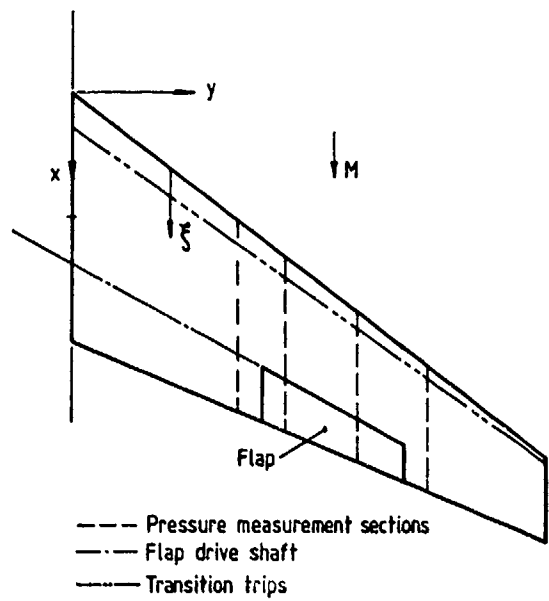
f	data	ξ	ξ_0	ξ_{00}	Surface	k
1.	0.89	0.89	0.89	0.89	0.89	0.89
99.	0.8911(CP/0)	0.8912	0.8913	0.8914	0.8915	0.8916

$\eta = \xi_{00}$

f	data	ξ	ξ_0	ξ_{00}	Surface	k
1.	0.89	0.89	0.89	0.89	0.89	0.89
99.	0.8911(CP/0)	0.8912	0.8913	0.8914	0.8915	0.8916

$\eta = \xi_{00}$

f	data	ξ	ξ_0	ξ_{00}	Surface	k
1.	0.89	0.89	0.89	0.89	0.89	0.89
99.	0.8911(CP/0)	0.8912	0.8913	0.8914	0.8915	0.8916



Aspect ratio	AR	6
Taper ratio	λ	$1/3$
Section		RAE 101
Thickness/chord ratio	t/c	0.09
Sweepback:		
Leading edge	$\Lambda(0)$	36.65°
Mid-chord	$\Lambda(0.5)$	30.00°
Flap LE	$\Lambda(0.7)$	27.05°
Trailing edge	$\Lambda(1.0)$	22.33°
Semi-span	s	0.48m
Root chord	c_r	0.24m
First mean chord	\bar{c}	0.16m
Wing area	$S/2$	$0.0768m^2$
Flap: Span		0.41×0.7
Chord		0.7×1.0
Transition trips:		
Position	ξ	0.05
Height		0.127mm

Fig 6.1 Model geometry: RAE Wing A

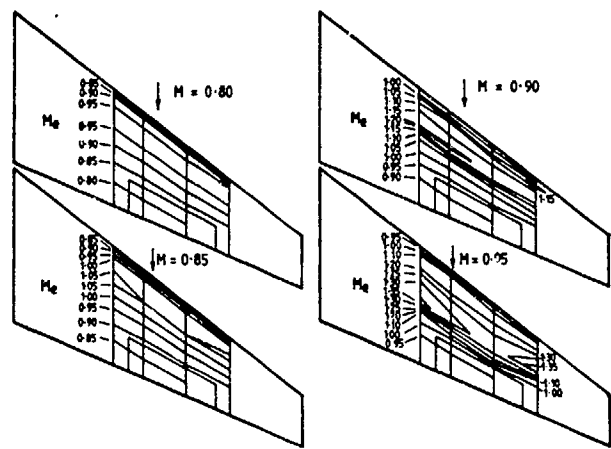


Fig 6.2 Mean isomach contours: $\alpha = 0$

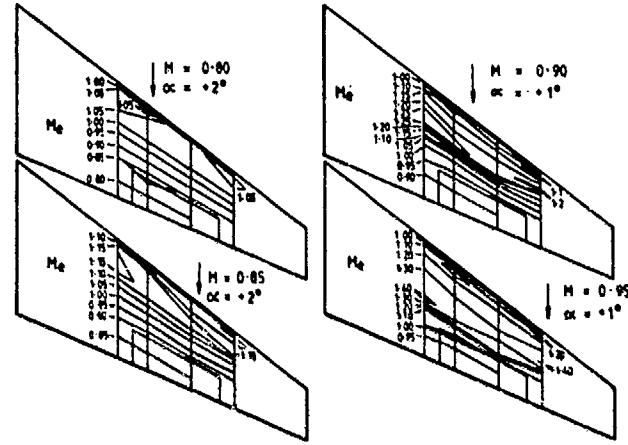


Fig 6.3 Mean isomach contours: suction surface

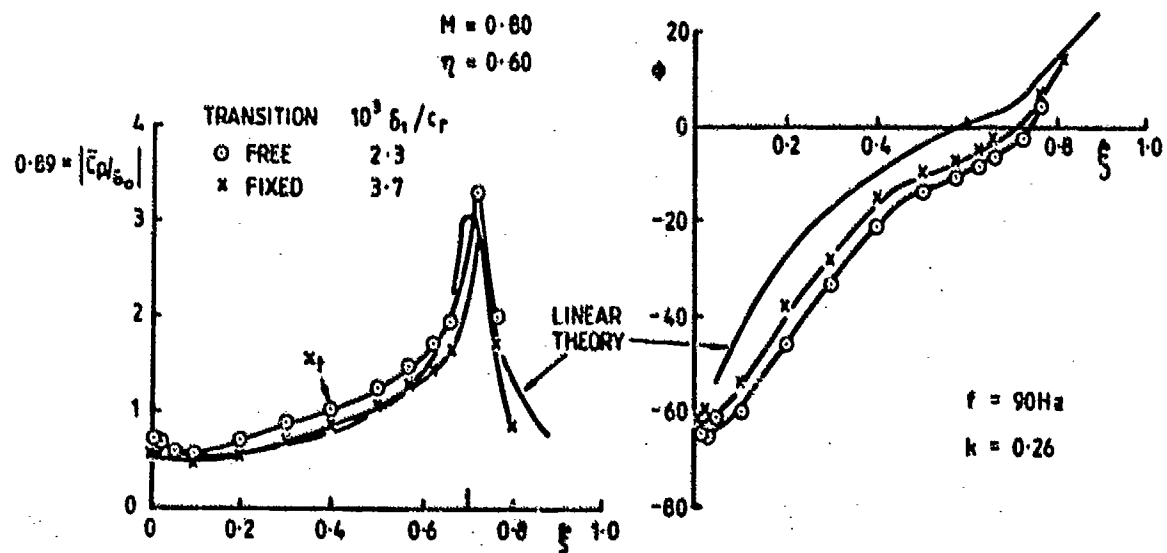


Fig 6.4 Magnitude and phase of subsonic pressure distribution

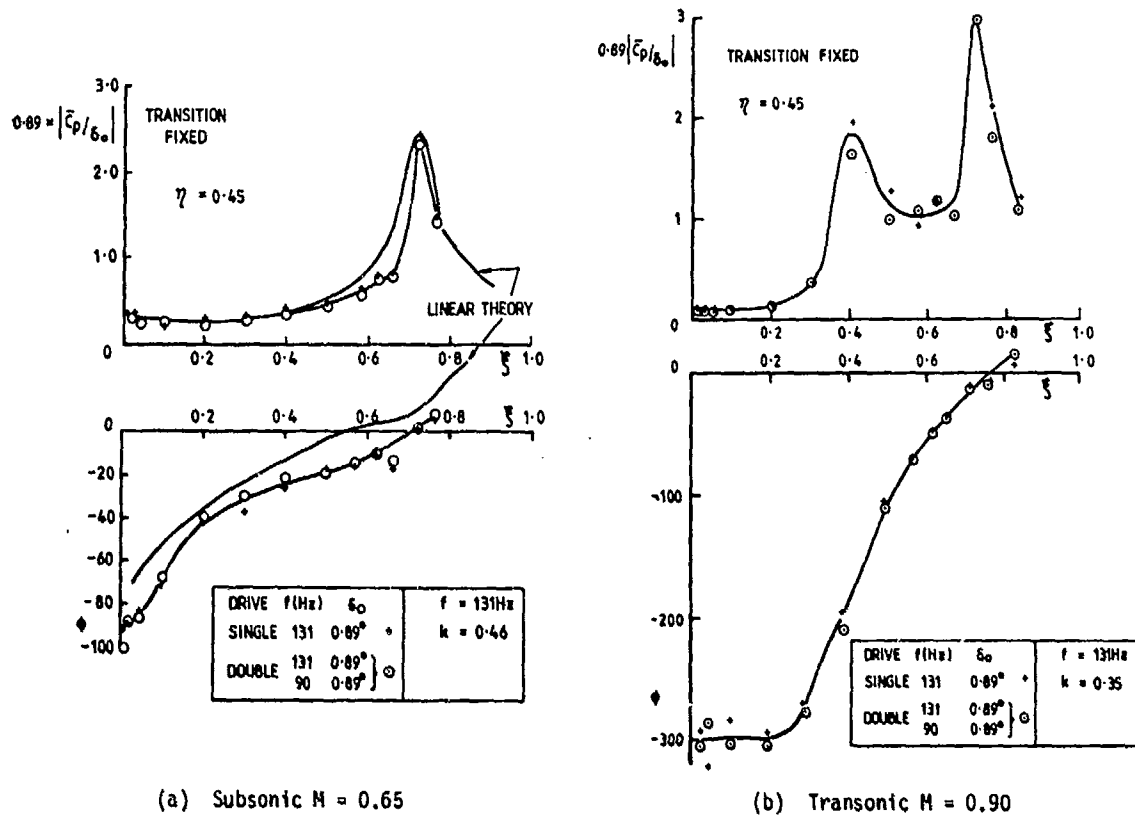


Fig 6.5 Superposition of two frequencies

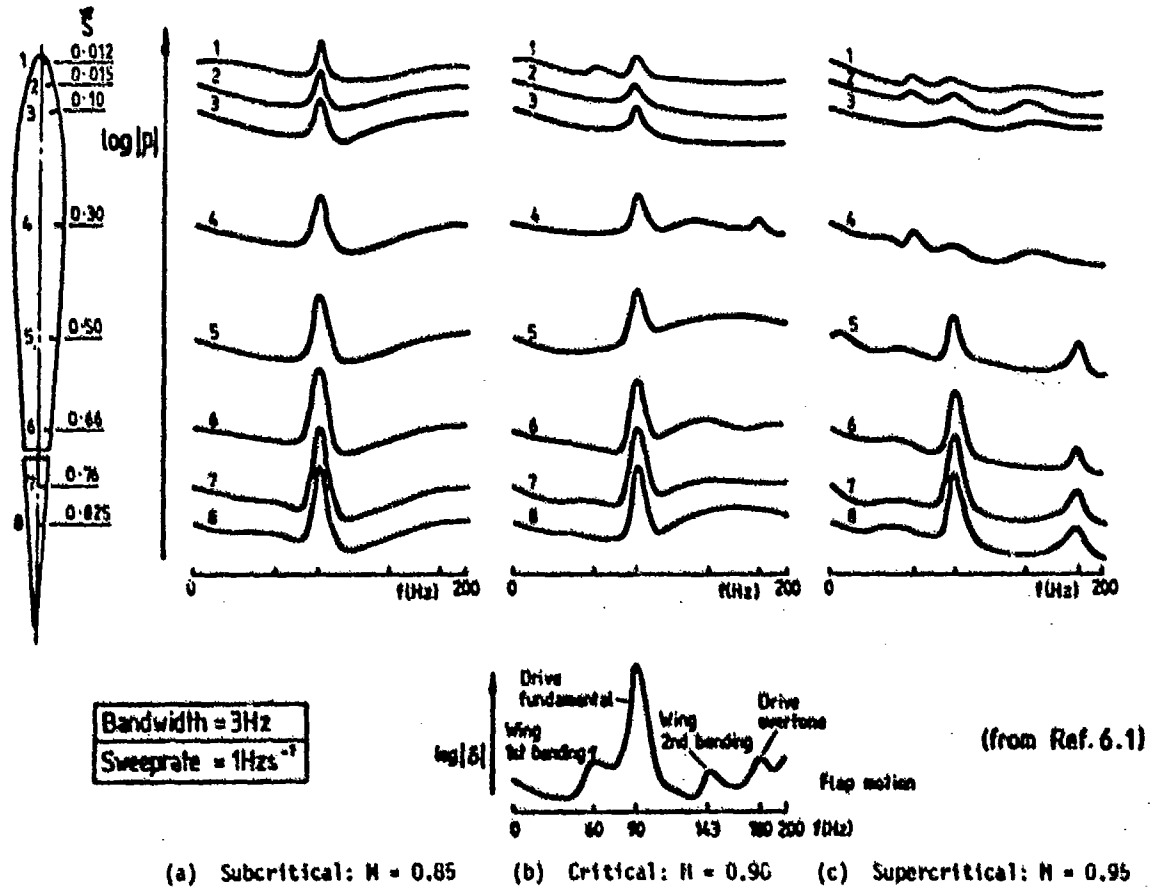


Fig 6.6 Typical spectra: $\alpha = 0, \eta = 0.60$

DATA SET 7

NORA MODEL. OSCILLATION ABOUT A SWEEPED AXIS

by

N. C. Lambourne (formerly with RAE)

INTRODUCTION

This Data Set relates to a low-aspect-ratio model oscillating as a rigid body about a sweptback axis as shown in Fig 7.1. The data were obtained during an international cooperative investigation of wind-tunnel interference on unsteady measurements*. Comparative measurements were made in four different tunnels two of which, the NLR High Speed Tunnel (HST) and the ONERA Modane S2 tunnel, were large in comparison with the model. The results from those tunnels are considered to be free of large interference effects.

The numerical data included here correspond closely with the AGARD CT Cases and come mainly from the HST in which the most extensive tests were made. Where nominally identical conditions were tested in the S2 tunnel, the corresponding data from that source are also included.

Fig 7.2 and Table 7.1 show the parametric combinations for which data could be made available if required. The cases for which data are included here are detailed in Table 7.2; they comprise not only all the CT Cases, but in addition a low-frequency (5 Hz) set of data for every Mach number and mean incidence combination of the CT Cases.

Fig 7.1 and Table 7.3 show the positions at which the steady and unsteady pressures were measured. Because no steady pressures were obtained at the two spanwise positions at which the oscillatory pressures were measured, direct comparisons between unsteady and zero-frequency ($k = 0$) equivalents are not possible. However, oscillatory pressures were measured for an oscillation frequency of 5 Hz ($k \approx 0.035$) and it is considered that the in-phase component of pressure for this frequency is sufficiently close to that which would be obtained for a quasi-steady condition, $k \rightarrow 0$.

For the unsteady measurements, attention was directed mainly to the upper surface (the extrados, denoted throughout by E) whilst only a few measuring positions were provided at the lower surface (the intrados denoted by I).

It should be noted that the measured steady pressures are not expressed as pressure coefficients C_p , but as local Mach numbers M_L . Also the oscillatory pressures have not been converted from their original form of R and I, the real and imaginary components non-dimensionalised using tunnel total pressure, and not dynamic pressure. Multiplying factors for the conversion of these quantities to the more usual C_p'/ρ_0 and C_p''/ρ_0 are included in the tables.

Mode of oscillation

The oscillation imposed on the model was basically rigid-body rotation about the axis shown in Fig 7.1. The motion was defined by the output of a transducer attached to the driving shaft rigidly fixed to the root of the model. The transducer output was calibrated to read angular displacement θ in a streamwise plane parallel to the plane $y = 0$. The oscillatory signal, $\theta = \theta_0 \sin \omega t$, acted as a phase and amplitude reference for all the other oscillatory quantities.

Due to model flexibility, there were slight departures from the design mode of rigid-body motion, and these differences tended to increase with oscillation frequency. Information about the actual motion was obtained from the six accelerometers installed within the model as shown in Fig 7.1 and detailed in Table 7.4.

Because displacements deduced from accelerometers tend to be unreliable for low frequencies, no measurements were made for 5 Hz. However, for this frequency it can be confidently concluded that the differences between the actual motion and the design mode were negligible.

For the 40 Hz tests corresponding to the CT Cases, the complex amplitudes of the normal displacements, z , at each of the accelerometer positions are given in Table 7.5. The severity of the departures from the design mode is more readily appreciated from Table 7.6 which gives, for the three spanwise positions containing accelerometers, local pitching and wing bending (ie the rotation about, and the normal displacements of, the design axis) as deduced on the basis that each chordwise section remains rigid. Not surprisingly, the deformations in twist and bending tend to increase with spanwise position.

* The letters of the acronym NORA refer to the names of the organisations involved: NLR, ONERA, RAE and AVA (a branch of DFVLR).

The bending deformation if it were exactly in phase with the pitching motion would simply amount to a small change in the local position of the pitching axis. A few theoretical calculations made at the time of the experiments to examine the effect of changes of axis position on the unsteady aerodynamics showed that the measured amount of superimposed bending motion for 40 Hz is not likely to produce significant contributions to the oscillatory pressures.

With regard to the effects of the twisting deformation of the model, it can be inferred from Table 7.6 that the actual pitching motion at the sections $\eta = 0.524$ and 0.712 , where the unsteady pressures were measured, has (1) an amplitude rather larger than the reference θ_0 and (2) a small phase lead. The phase lead is never larger than 4° and its effect is probably negligible within the general accuracy of the measurements. Since no corrections for the model deformations have been applied to the tabulated data, which are normalised using the reference θ_0 , the increase in pitching amplitude at the unsteady measuring sections suggests that a user of the 40 Hz data would be justified in reducing the values of the normalised quantities R and I by a few percent.

No numerical data for 60 Hz are presented here but could be made available if required. For this frequency the bending motion of the wing is larger than for 40 Hz, and without an analysis it is not possible to conclude that its effect is insignificant. In the absence of such analysis, the 60 Hz data should be regarded as only qualitatively relating to the design mode of motion.

Steady flow

The steady flow at the upper surface can be inferred from the distributions of M_L shown in Figs 7.3 to 7.6.

When the incidence is near to zero, for all M , there is a small region of high suction and a recompression situated close to the leading edge. With increase of incidence, for each subsonic M the high suction region extends backwards over the chord and is terminated by a steep pressure gradient - the forward recompression. For higher subsonic M this is followed by another expansion region, which for $M = 0.95$ is terminated by a shock wave - the rear shock, aft of mid-chord. The three-dimensional nature of the flow when the model is at incidence can be seen in the isomachs of Fig 7.7.

Whereas there is no doubt about the existence of the rear shock, the exact nature of the flow over the more forward part of the chord is not absolutely clear. Although for some of the test conditions the local Mach numbers in this forward region are supersonic, it is not obvious that the forward recompression involves a shock wave. Certainly there is no possibility of a shock wave for $M = 0.80$ even at the highest incidence. It is therefore important to note that the general shape of the forward recompression remains essentially the same as M is increased up to its highest subsonic value $M = 0.95$. Furthermore, the high angle of sweepback of the isomachs in the forward recompression region, as seen in Fig 7.7, suggests that a shock wave will not be present. Instead it is probable that for much of the incidence range and for all subsonic Mach numbers, a leading-edge separation vortex extends across the upper surface.

Influence of incidence on the oscillatory pressures

An example of the influence of mean incidence on the oscillatory pressures for $M = 0.90$ is shown in Fig 7.8 which gives results for the upper surface (E) at sections 2 and 4 and for the lower surface (I) at section 2. It is the upper surface that is most affected by increasing positive incidence, the lower surface tending to retain the pattern it has for the non-lifting condition. Also, whereas for a non-lifting condition the distributions for the two spanwise positions are basically similar, with increase of incidence the characteristics for the upper surface become more three-dimensional and the leading-edge peaks in $R(X)$ and $I(X)$ move to the rear and broaden. These changes are doubtless related to the rearward displacement with incidence of the steady-flow recompression region, as already seen in Fig 7.4. For $\alpha_m = 3^\circ$, $R(X)$ and $I(X)$ at section 2E each consists of a leading-edge peak followed by several subsidiary peaks or 'crinkles', lying ahead of the rear shock peak which is situated at about 55% chord. With further increase of incidence to $\alpha_m = 5^\circ$, the crinkles have almost disappeared and have been replaced by a more regular distribution of forward and rear peaks. It would seem that this evolution is associated with successive stages in the development locally of high subsonic and eventually supersonic flow.

At section 4E with increase of incidence, $R(X)$ becomes negative over nearly all of the rearward half of the chord. At the highest incidence, $\alpha_m = 5^\circ$, the forward peak extends over much of the fore-chord as a result of the fanning-out of the forward recompression, possibly associated with the separated vortex flow suggested previously.

Influence of oscillation frequency

The effects of changing oscillation frequency are shown, at least qualitatively, for each of the CT combinations of M and α_m in Figs 7.9 to 7.15. For the non-lifting cases, Figs 7.9 to 7.12, results are shown for section 2E only; for the lifting cases, Figs 7.13 to 7.15, results are shown for both sections 2E and 4E.

Changing frequency is generally expected to affect the imaginary component and phase angle. For the non-lifting cases the frequency effects on the real component are not large when the flow is either completely subsonic (Fig 7.9 for $M = 0.8$) or completely supersonic (Fig 7.12 for $M = 1.10$). Greater sensitivity to frequency appears in both real and imaginary components where the local flow is close to sonic (Fig 7.10 for $M = 0.9$, near mid chord) or in the vicinity of the rear shock wave (Fig 7.12 for $M = 0.95$).

For the lifting cases (Figs 7.13 to 7.15) the real and imaginary components show considerable changes, not only at the rear shock wave, but also at the forward peaks.

Sensitivity to small changes in M and α_m

When comparisons between experimental and computational results are being made, it is helpful to be aware of the sensitivity to small variations in the parameters and of the uncertainties in the measurements. For the present model with sonic or near-sonic flow the real and imaginary distributions $R(X)$ and $I(X)$ are sensitive not only to frequency but also to small changes of M and α_m .

As shown in Fig 7.2 the tests for the mean conditions $M = 0.90$, $\alpha_m = 4^\circ$ and $M = 0.95$, $\alpha_m = 4.75^\circ$ corresponding to CT Cases 5 and 7 or 8 are each surrounded by eight neighbouring test cases with small differences in M and α_m . It is from these matrices of tests that information on sensitivity can be obtained.

Fig 7.16 shows for the initial condition $M = 0.90$, $\alpha_m = 4^\circ$, the separate effects of making changes of $\pm 0.2^\circ$ in α_m and ± 0.01 in M . Whilst the forward peaks in $R(X)$ and $I(X)$ show some sensitivity to the incidence change, it is the rear peaks that show most sensitivity to the Mach number change. The increase from $M = 0.89$ to $M = 0.90$ changes the mid-chord crinkles to a distribution with well-defined peaks. A further increase to $M = 0.91$ displaces the peaks to the rear.

For the initial condition $M = 0.95$, $\alpha_m = 4.75^\circ$ the distributions are relatively insensitive to incidence changes of 0.25° , but quite sensitive to the Mach number changes of ± 0.01 as shown in Fig 7.17. The distributions for section 2E demonstrate an important point: when a peak has become very sharp, it may just be detectable from only a single point, as for $M = 0.95$, or may even be 'lost' between measuring positions as we believe has happened for $M = 0.96$. Section 4E shows a highly sensitive negative peak in $R(X)$.

Figs 7.18 and 7.19 may be of special interest when assessing the significance of any differences between computational and experimental data. They show the measurements corresponding to the 40 Hz CT Cases for $M = 0.90$, $\alpha_m = 4^\circ$ and $M = 0.95$, $\alpha_m = 4.75^\circ$ within envelopes that enclose all the data measured for the surrounding test matrices. It is suggested the envelopes could be a help in deciding on the tolerances to be accepted when judging the results of computations.

For CT Cases 1, 4 and 6, as seen in Table 7.2, numerical data obtained in the ONERA S2 tunnel are included for comparison with the data obtained from the main source, the HST of NLR. For the conditions $M = 0.90$, $\alpha_m = 4^\circ$ and $M = 0.95$, $\alpha_m = 4.75^\circ$ corresponding to CT Cases 5 and 7 no measurements are available from the S2 tunnel. However comparisons between the two tunnels are available for the two nearby conditions, $M = 0.90$, $\alpha_m = 5^\circ$ and $M = 0.95$, $\alpha_m = 5^\circ$ and are shown in Figs 7.20 and 7.21. It must be emphasised that the results from both tunnels were obtained using the same techniques and with the same instrumentation, so that from these comparisons it is impossible to draw conclusions about any uncertainties arising from the instrumentation itself. The comparisons do however give some idea of the likely spread in the data from items such as tunnel interference, the character of the tunnel flow and the consistency of the parameter settings.

Since the results from the two tunnels are regarded as having equal 'weight', a theoretical result which, when compared with the results from one tunnel, shows similar discrepancies to those in Figs 7.20 and 7.21 could be regarded as being in general agreement with experiment.

1 GENERAL DESCRIPTION OF MODEL

1.1	Designation	NORA model
1.2	Type	Half model
1.3	Derivation	Horizontal tail surface of Mirage F1
1.4	Additional remarks	-
1.5	References	Ref 7.1

2 MODEL GEOMETRY

2.1	Planform	For the actual model, see Fig 7.1. For the computational model, see Ref 7.2 for modified planform with streamwise tip
2.2	Aspect ratio	2.01
2.3	Leading-edge sweep	50°
2.4	Trailing-edge sweep	13° 26'
2.5	Taper ratio	0.3515 (for the computational model)
2.6	Twist	None
2.7	Root chord	650 mm
2.8	Span of model	442.5 mm
2.9	Area of planform	0.1944 m ² (for the computational model)
2.10	Location of reference sections and definition of profiles	The profile is based on the symmetric NACA 63006 modified to a thickness ratio of about 5% and with a small updroop near the nose. For details of actual model, see Figs 45 and 46 of Ref 7.1. For the computational model, see Ref 7.2
2.11	Lofting procedure between reference sections	
2.12	Form of wing-body, or wing-root junction	Clearance between root and tunnel wall. Small fillet attached to model to cover shaft aperture, see Fig 4a of Ref 7.1
2.13	Form of wing tip	Actual model: sharp Computational model: square cut
2.14	Control surface details	None
2.15	Additional remarks	-
2.16	References	Refs 7.1, 7.2

3 WIND TUNNELS

3.1	Designation	HST: NLR High Speed Tunnel (HST) S2: ONERA Modane S2
3.2	Type of tunnel	HST: Continuous, variable pressure S2: Continuous, variable pressure
3.3	Test section dimensions	HST: Height = 1.60 m, width = 2.00 m, length = 2.50 m S2: Height = 1.77 m, width = 1.75 m, length = 5.40 m (of perforated part)
3.4	Type of roof and floor	HST: Slotted, each having four whole slots and a 1/4-slot at each corner S2: Perforated plates, with holes inclined 60° to the normal. Each plate is backed by a perforated sheet which can be slid to vary porosity
3.5	Type of side walls	HST: Solid S2: Solid
3.6	Ventilation geometry	HST: Roof and floor are 12% open S2: Porosity of roof and floor chosen according to Mach number. 1% open for M = 0.80 and M = 1.10; 6% open for M = 0.9 and M = 0.95
3.7	Thickness of side wall boundary layer	HST: 7 mm approximately S2: 90 to 170 mm
3.8	Thickness of boundary layers at roof and floor	HST: - S2: -
3.9	Method of measuring Mach number	HST: Derived from settling chamber stagnation and plenum chamber static pressures S2: -
3.10	Flow angularity	HST: - S2: -

- 3.11 Uniformity of Mach number over test section
HST: -
S2: $\Delta M/\Delta x = \pm 3 \times 10^{-3} \text{ m}^{-1}$ for $0.70 < M < 0.92$
- 3.12 Sources and levels of noise or turbulence in empty tunnel
HST: Less than 1% in rms p/q for $M = 0.8$
S2: Velocity turbulence: 0.2%
- 3.13 Tunnel resonances
HST: } No evidence of resonance in present tests
S2: }
- 3.14 Additional remarks
HST: Information about flow angularity and Mach number uniformity available only along test section centre-line
S2: Accuracy of Mach number, $\Delta M = \pm 0.001$
- 3.15 References on tunnel
HST: Ref 7.3
S2: Refs 7.4, 7.5, 7.6
- 4 MODEL MOTION
- 4.1 General description
Rigid-body oscillation about swept axis shown in Fig 7.1. Sinusoidal in time
- 4.2 Reference coordinate and definition of motion
Rotation $\theta = \theta_0 \sin \omega t$ measured in streamwise plane $y = 0$ at the root
- 4.3 Range of amplitude
 $0.25^\circ < \theta_0 < 1.00^\circ$
- 4.4 Range of frequency
Standard frequencies for main data: 5, 40 and 60 Hz. A few special tests at other frequencies up to 95 Hz, see Ref 7.1
- 4.5 Method of applying motion
Forced by hydraulic rotary actuator
- 4.6 Timewise purity of motion
Purity of sinusoid considered to be adequate
- 4.7 Natural frequencies and normal modes of model and support system
Lowest natural frequency of system: torsion of drive shaft at 100 Hz approximately
- 4.8 Actual mode of applied motion including any elastic deformation
See Introduction and Tables 7.5 and 7.6
- 4.9 Additional remarks
-
- 5 TEST CONDITIONS
- 5.1 Model planform area/tunnel area
HST: 0.06
S2: 0.06
- 5.2 Model span/tunnel width
HST: 0.22
S2: 0.25
- 5.3 Blockage
HST: } 0.31 for zero incidence
S2: }
- 5.4 Position of model in tunnel
HST: Standard side-wall position
S2: Standard wall mounting position
- 5.5 Range of Mach number
HST: $0.60 \leq M \leq 1.10$, see Table 7.1
S2: $0.80 \leq M \leq 0.95$
- 5.6 Range of tunnel total pressure
 $0.46 \leq p_t \leq 0.9$ bar, see Table 7.1
- 5.7 Range of tunnel total temperature
HST: $30^\circ\text{C} \leq T_0 \leq 38^\circ\text{C}$
S2: $18^\circ\text{C} \leq T_0 \leq 20^\circ\text{C}$
- 5.8 Range of model steady, or mean, incidence
HST: $0.5^\circ \leq \alpha_{\text{mean}} \leq 5.0^\circ$
S2: $-1.0^\circ \leq \alpha_{\text{mean}} \leq 5.0^\circ$
- 5.9 Definition of model incidence
Chord line of basic symmetrical section was datum for incidence
- 5.10 Position of transition, if free
-

5.11	Position and type of trip, if transition fixed	Metal tapes with 'coronets' about 0.09 mm high fixed at 5% local chord on both surfaces
5.12	Flow instabilities during tests	None encountered
5.13	Changes to mean shape of model due to steady aerodynamic load	Not measured, but considered negligible
5.14	Additional remarks	-
5.15	References describing tests	Ref 7.1

6 MEASUREMENTS AND OBSERVATIONS

6.1	Steady pressures for the mean conditions	✓
6.2	Steady pressures for small changes from the mean conditions	-
6.3	Quasi-steady pressures	✓ (5Hz)
6.4	Unsteady pressures	✓
6.5	Steady section forces for the mean conditions by integration of pressures	✓
6.6	Steady section forces for small changes from the mean conditions by integration	-
6.7	Quasi-steady section forces by integration	✓ (5Hz)
6.8	Unsteady section forces by integration	✓
6.9	Measurement of actual motion at points on model	✓
6.10	Observation or measurement of boundary layer properties	-
6.11	Visualization of surface flow	-
6.12	Visualization of shock wave movements	-
6.13	Additional remarks	-

7 INSTRUMENTATION

7.1	Steady pressure	
7.1.1	Position of orifices spanwise and chordwise	See Fig 7.1 and Table 7.3
7.1.2	Type of measuring system	Orifices connected by tubes to conventional tunnel-based system
7.2	Unsteady pressures	
7.2.1	Position of orifices spanwise and chordwise	See Fig 7.1 and Table 7.3
7.2.2	Diameter of orifices	0.8 mm
7.2.3	Type of measuring system	Each orifice closely connected to its own transducer installed within model
7.2.4	Type of transducers	Kulite XCQL 093
7.2.5	Principle and accuracy of calibration	Daily calibration using portable oscillatory pressure generator. Accuracy probably a few percent
7.3	Model motion	
7.3.1	Method of measuring motion reference coordinate	Rotary potentiometer attached to drive shaft, calibrated to give deflection θ
7.3.2	Method of determining spatial mode of motion	Six accelerometers installed within model; see Fig 7.1 and Table 7.4
7.3.3	Accuracy of measured motions	Resolution of θ , about 0.01° . Accelerometers readings, accurate to a few percent

7.4	Processing of unsteady measurements	
7.4.1	Method of acquiring and processing measurements	Pressure and accelerometer signals processed sequentially in groups by ten parallel channels. Each channel consisted of analogue circuitry giving output voltages proportional to Fourier fundamental components. Output voltages digitized and fed to computer for conversion to coefficients, display and disc-storage
7.4.2	Type of analysis	Components in phase and in quadrature with θ , averaged over 8 seconds
7.4.3	Unsteady pressure quantities obtained and accuracies achieved	Fundamental harmonic coefficients of pressure, accurate to a few percent. Chordwise integration to give section lift and moment contributions from upper and lower surfaces, but accuracy low because of wide spacing
7.4.4	Method of integration to obtain forces	Polygonal summation, see Appendix C of Ref 7.1
7.5	Additional remarks	-
7.6	References on techniques	-
8	DATA PRESENTATION	
8.1	Test cases for which data could be made available	Table 7.1
8.2	Test cases for which data are included in this document	Table 7.2
8.3	Steady pressures	Tables 7.7 to 7.13
8.4	Quasi-steady or steady perturbation pressures	Data for 5 Hz in Tables 7.14 to 7.27
8.5	Unsteady pressures	Tables 7.14 to 7.30
8.6	Steady forces or moments	Not included
8.7	Quasi-steady or steady perturbation forces	Not included
8.8	Unsteady forces and moments	Not included
8.9	Other forms in which data could be made available	Unsteady pressures measured at tunnel roof
8.10	References giving other presentations of data	Ref 7.1
9	COMMENTS ON DATA	
9.1	Accuracy	
9.1.1	Each number	± 0.005
9.1.2	Steady incidence	$\pm 0.01^\circ$
9.1.3	Reduced frequency	Better than $\pm 2\%$ of nominal values due to temperature variations
9.1.4	Steady pressure coefficients	M_L to ± 0.005
9.1.5	Steady pressure derivatives	-
9.1.6	Unsteady pressure coefficients	The uncertainties in the coefficients H and I are probably $\pm (0.02 + 0.04Q)$, where $Q = R $ or $ I $
9.2	Sensitivity to small changes of parameter	See Introduction and Figs 7.15 to 7.19
9.3	Non-linearities	Normalised pressure coefficients not sensitive to oscillation amplitude except for positions near the leading edge or a shock wave
9.4	Influence of tunnel total pressure	Effects of Reynolds number not examined

- | | | |
|------|---|--|
| 9.5 | Effects on data of uncertainty, or variation, in mode of model motion | Not large for 5 Hz and 40 Hz. See Introduction and Tables 7.5 and 7.6 |
| 9.6 | Wall interference corrections | No corrections applied to any data. Values of M and α_m are tunnel settings |
| 9.7 | Other relevant tests on <u>same model</u> | - |
| 9.8 | Relevant tests on other models of nominally the <u>same shape</u> | - |
| 9.9 | Any remarks relevant to comparison between experiment and theory | - |
| 9.10 | Additional remarks | - |
| 9.11 | References on discussion of data | Ref 7.1 |

10 PERSONAL CONTACT FOR FURTHER INFORMATION

Mr B.L. Welsh, Royal Aircraft Establishment, Bedford MK41 6AE, England (or, if convenient, any of the authors of Ref 7.1).

11 LIST OF REFERENCES

- | | | |
|-----|--|---|
| 7.1 | N. Lambourne
R. Destuynder
K. Kienappel
R. Roos | Comparative measurements in four European wind tunnels of the unsteady pressures on an oscillating model (the NORA experiments). (1980) Issued in each of the following forms:
RAE Technical Report 80016
ONERA 1589/OR; Note Technique 10/5115 RY
DFVLR-FB 80-30
NLR TR 80066 U
Also published as AGARD-R-673, but this does not contain the Appendices giving full details of the model and tests. |
| 7.2 | S.R. Bland | AGARD three-dimensional aeroelastic configurations.
AGARD-AR-167 |
| 7.3 | - | Users guide to the high speed wind tunnel.
HST of NLR (revised edition) (1977) |
| 7.4 | M. Pierre
G. Fasso | The aerodynamic test center of Modane Avrieux.
ONERA Technical Note 166E (1972) |
| 7.5 | M. Pierre
G. Fasso | Exploitation du centre d'essai aerothermodynamique de Modane Avrieux.
ONERA Note Technique 181 (1971) |
| 7.6 | V. Schmitt
F. Charpin | Experimental data base for computer program assessment.
AGARD AR 138, pp.B1-1 to B1-44 (1979) |

12 NOTATION

General

- | | |
|-----------------------|---|
| c | local chord |
| c_r | root chord |
| $C_p'/q_0, C_p''/q_0$ | normalised fundamental in-phase and in-quadrature components of oscillatory pressure, respectively p'/q_0 and p''/q_0 (rad^{-1}) |
| E | as in 2E, 4E, denotes extrados, or upper surface |
| f | oscillation frequency (Hz), $\omega/2\pi$ |
| I | as in 2I, 4I, denotes intrados, or lower surface |
| i | normalised fundamental in-quadrature component of pressure, $-p''/p_t^{\infty} q_0$ (rad^{-1}) |
| $I(x)$ | chordwise distribution of I |
| k | reduced frequency, $\omega c_r/2V$ |
| M | stream Mach number |

M_L	local Mach number at surface of model, $M_L = \left\{ 5 \left[(p/p_t)^{-2/7} - 1 \right] \right\}^{-1/2}$
p	pressure
p_t	stream total pressure
p', p''	fundamental components of pressure respectively in phase and in quadrature with oscillatory motion θ
q	stream dynamic pressure
R	normalised fundamental in-phase component of pressure $-p'/p_t \theta_0$ (rad^{-1})
$R(X)$	chordwise distribution of R
s	span of model
t	time
T_0	stream total temperature
V	stream velocity
x, y	coordinates in plane of model, see Fig 7.1
$x_{LE}(y)$	coordinate of local leading edge
$x_\alpha(y)$	local chordwise position of oscillation axis
X	local chordwise position, ξ
Z	upward displacement normal to plane of model
α	incidence of model (deg)
α_m	steady, or mean, incidence (deg)
n	non-dimensional spanwise position, y/s
θ	coordinate for specifying angular oscillatory motion, positive nose up, measured in planes parallel to plane $y = 0$. Reference at drive shaft $\theta = \theta_0 \sin \omega t$ (deg)
θ_0	reference amplitude of motion, identical to α_0 of Ref 7.2 (deg)
ξ	non-dimensional chordwise position, $(x - x_{LE})/c$
ω	oscillation frequency (rad^{-1})

Chordwise sections are identified 0E ... 6E and 0I ... 6I ; see Table 7.3 for positions.

Tables 7.7 to 7.13

MLOC	local Mach number, M_L
EXTR	extrados = upper surface
INTR	intrados = lower surface

Tables 7.14 to 7.30

PRESSURE stream total pressure, p_t

The factor $(C'_p/R) \equiv (C''_p/I)$, whose value F is given at the head of each table can be used to obtain C'_p/θ_0 and C''_p/θ_0 , but note that a change of sign is required, thus:

$$\begin{aligned} C'_p/\theta_0 &= -R \times F \\ C''_p/\theta_0 &= -I \times F \end{aligned}$$

Figures 7.8 to 7.12

$$\begin{aligned} \text{Modulus} &= (R^2 + I^2)^{1/2} \\ \tan \phi &= I/R \end{aligned}$$

Table 7.1

TEST NUMBERS OF DATA THAT CAN BE MADE AVAILABLE

Test numbers are necessarily different for different frequencies, but for the steady pressures they are often the same as those for one of the frequencies, usually 40 Hz. Data are included in this document for those numbers underlined.

M	α_m (deg)	P _t (bars)	Steady	5 Hz	40 Hz	60 Hz
0.60	0.4	0.9	2006	2192	2006	2182
	4.5	0.9	2007	2193	2007	2183
0.79	0.4	0.9	2008	2126	2008	2175
	3.8	0.9	2009	2191	2009	2181
0.80	0	0.9	2010	2185/2194	2010	2174/2184
	1.0	0.9	2011	2187	2011	2176
	2.0	0.9	2012	2188	2012	2177
	3.0	0.9	2013	2189	2013	2178
	4.0	0.9	2014	2190	2014	2180
0.89	3.5	0.6	2019	2142	2019	2169
	3.8	0.6	2044	2141	2017/2044	2168
	4.0	0.6	2041	2143	2042	2170
	4.2	0.6	2043	2144	2043	2171
0.90	-0.5	0.6	2024	2122	2024	2157
	-0.3	0.6	2023	2139	2023	2166
	0	0.6	2029	2124	2029	2158
	0.3	0.6	2020	2125	2020	2159
	1.0	0.6	2030	2126	2030	2160
	2.0	0.6	2031	2127	2031	2161
	3.0	0.6	2032	2128	2032	2162
	3.8	0.6	2034	2129/2135	2034	2163
	4.0	0.6	2037	2136	2035	2164
	4.2	0.6	2036	2138	2036	2165
0.91	4.75	0.46	2200	2197	2200	2203
	5.0	0.46	2201	2199	2201	2204/2224
	3.8	0.6	2037	2119	2037	2154
	4.0	0.6	2032	2120	2038	2155
0.92	4.2	0.6	2040	2121	2040	2156
	4.75	0.46	2092	2109	2092	2205
0.93	5.0	0.46	2093	2110	2093	2206
	0	0.6	2027	2134	2027	2153
0.94	4.5	0.46	2085	2102	2085	2207
	4.75	0.46	2086	2103	2086	2208
	5.0	0.46	2087	2104	2087	2211

M	α_m (deg)	P _t (bars)	Steady	5 Hz	40 Hz	60 Hz
0.95	0	0.6	2046	2114	2046	2149
	0.5	0.6	2028	2135	2028	2152
	1.0	0.6	2047	2115	2047	2150
	2.0	0.6	2048	2116	2048	2151
	2.0	0.46	2079	2096	2079	2212
0.96	3.0	0.6	2051	2117	2118	-
	3.0	0.46	2080	2097	2080	2213
	4.0	0.46	2081	2098	2081	2214
	4.5	0.46	2082	2099	2082	2218
	4.75	0.46	2083	2100	2083	2219
	5.0	0.46	2084	2101	2084	2220
	4.5	0.46	2088	2105	2088	2221
1.10	4.75	0.46	2089	2106	2089	2222
	5.0	0.46	2090	2107	2090	2223
	0.6	0.6	2045	2113	2045	2148

Each set of measurements comprises:

- Steady local Mach numbers, as in Tables 7.7 to 7.13
- Oscillatory pressures, as in Tables 7.14 to 7.30
- Accelerometer displacements, as in Table 7.5

Frequency parameter: k (nominal) = $5.8f(0.2 + M^{-2})0.5 \times 10^{-3}$

Reynolds number: the nominal value of $Re \times 10^{-6}$ for any Mach number can be interpolated from the following table:

M	P _t (bar)	
	0.46	0.9
0.60	-	6.6
0.80	-	7.8
0.90	4.2	5.5
0.95	4.3	5.6
1.00	4.4	5.7
1.10	-	5.8

Table 7.2

DETAILS OF EXPERIMENTAL CASES FOR WHICH DATA ARE INCLUDED

CT Case	M	α_m (deg)	$\alpha_0 \equiv \theta_0$ (deg) nominal	f (Hz)	k nominal	P _t (bar)	Re $\times 10^{-6}$	Steady M _L		Oscillatory pressures			
								HST		HST		S2	
								Test No.	Table	Test No.	Table	Test No.	Table
-	0.80	0	0.5	5	0.038	0.90	7.8	2010	7.7	2185	7.14	-	-
1	0.80	0	0.5	40	0.31	0.90	7.8	2010	7.7	2010	7.15	80	7.28
-	0.80	4.0	0.5	5	0.038	0.90	7.8	2014	7.8	2190	7.16	-	-
2*	0.80	4.0	0.5	40	0.31	0.90	7.8	2014	7.8	2014	7.17	-	-
3	0.90	0	0.5	5	0.035	0.60	5.5	2029	7.9	2124	7.18	-	-
4	0.90	0	0.5	40	0.28	0.60	5.5	2029	7.9	2029	7.19	76	7.29
-	0.90	4.0	0.5	5	0.035	0.60	5.5	2035	7.10	2136	7.20	-	-
5*	0.90	4.0	0.5	40	0.28	0.60	5.5	2035	7.10	2035	7.21	-	-
-	0.95	0	0.5	5	0.034	0.60	5.6	2046	7.11	2114	7.22	-	-
6*	0.95	0	0.5	40	0.27	0.60	5.6	2046	7.11	2046	7.23	69	7.30
7	0.95	4.75	0.5	5	0.034	0.46	4.3	2083	7.12	2100	7.24	-	-
8	0.95	4.75	0.5	40	0.27	0.46	4.3	2083	7.12	2083	7.25	-	-
-	1.10	0.55	0.5	5	0.030	0.60	5.8	2045	7.13	2113	7.26	-	-
9	1.10	0.55	0.5	40	0.24	0.60	5.8	2045	7.13	2045	7.27	-	-

* Denotes CT priority case.

Table 7.3

POSITIONS OF PRESSURE HOLES

Section	0	1	2	3	4	5	6								
y/a	0.133	0.389	0.524	0.612	0.712	0.786	0.895								
Pressures	Steady	Steady	Unsteady	Steady	Unsteady	Steady	Steady								
X =	0.0125 0.025 0.05 0.10 0.22 0.30 0.40 0.62 0.75 0.90	0.025 0.05 0.10 0.15 0.22 0.30 0.40 0.50 0.62 0.75 0.90	<u>E. Extrados (upper surface)</u>			0.012 0.05 0.10 0.22 0.30 0.40 0.50 0.62 0.75 0.90	0.05 0.10 0.15 0.22 0.30 0.40 0.50 0.62 0.75 0.90	0.012 0.025 0.05 0.10 0.20 0.28 0.35 0.40 0.45 0.50 0.55 0.60 0.65 0.70 0.80 0.87	0.075 0.15 0.22 0.30 0.40 0.50 0.62 0.75 0.88	0.10 0.15 0.22 0.30 0.40 0.50 0.62 0.75					
			<u>I. Intrados (lower surface)</u>												
			X =	0.0125 0.025 0.05 0.10 0.22 0.30 0.40 0.62 0.75 0.90	0.025 0.05 0.10 0.15 0.22 0.30 0.40 0.50 0.62 0.75 0.88						0.05 0.10 0.20 0.28 0.40 0.50 0.60 0.70	0.05 0.10 0.15 0.22 0.30 0.40 0.50 0.62 0.75 0.87	0.05 0.10 0.20 0.28 0.30 0.40 0.50 0.60 0.70	0.075 0.15 0.22 0.30 0.40 0.50 0.62 0.75 0.85	0.10 0.15 0.22 0.30 0.40 0.50 0.62 0.75

Table 7.4

POSITION OF ACCELEROMETERS IN RELATION TO x_α (y) THE CHORDWISE POSITION OF THE DESIGN AXIS OF OSCILLATION

y/s	Forward position (A)		Rearward position (B)	
	Accel. No.	$x_\alpha - x_A$ (mm)	Accel. No.	$x_B - x_\alpha$ (mm)
0.169	1	260	2	180
0.655	3	110	4	90
0.931	5	55	6	48

Table 7.5

DISPLACEMENTS DEDUCED FROM ACCELEROMETERS. DISPLACEMENTS Z' AND Z'' , MEASURED IN mm, ARE RESPECTIVELY IN-PHASE AND IN-QUADRATURE COMPONENTS PHASE REFERENCED TO DATUM ANGULAR DISPLACEMENT θ

Note: These are taken from Ref 7.1 but a change of sign has been applied throughout

Test No.	$\eta = 0.169$				$\eta = 0.655$				$\eta = 0.931$			
	Accel. No.1 (A)		Accel. No.2 (B)		Accel. No.3 (A)		Accel. No.4 (B)		Accel. No.5 (A)		Accel. No.6 (B)	
	Z'_A	Z''_A	Z'_B	Z''_B	Z'_A	Z''_B	Z'_A	Z''_B	Z'_A	Z''_B	Z'_A	Z''_B
2010	2.322	0.086	-1.602	-0.038	1.148	0.072	-0.672	0.027	0.753	0.089	-0.211	0.084
2014	2.305	0.125	-1.570	-0.080	1.184	0.083	-0.598	-0.009	0.847	0.077	-	0.056
2029	2.314	0.104	-1.614	-0.058	1.116	0.073	-0.708	0.009	0.709	0.086	-0.271	0.056
2035	2.271	0.150	-1.567	-0.100	1.138	0.089	-0.639	-0.023	0.769	0.080	-0.153	0.053
2046	2.297	0.079	-1.590	-0.051	1.130	0.052	-0.661	0.009	0.743	0.061	-0.209	0.044
2083	2.282	0.113	-1.584	-0.092	1.124	0.040	-0.653	-0.047	0.756	0.019	-0.203	-0.033
2045	2.323	0.046	-1.390	-0.049	1.173	0.009	-0.621	-0.029	0.802	0.000	-0.143	-0.016

Table 7.6

LOCAL DISPLACEMENTS IN PITCH (θ, ϵ_θ)_n AND NORMAL TRANSLATION OF DESIGN AXIS (Z, ϵ_Z)_n PHASE REFERENCED TO DATUM $\theta = \theta_0 \sin \omega t$. COMPLEX QUANTITIES θ_n AND Z_n ARE DERIVED FROM TABLES 7.4 AND 7.5 ON THE BASIS THAT CHORDWISE SECTIONS DO NOT DEFORM, THUS

$$\theta_n = (Z_A - Z_B) / (x_B - x_A), \quad Z_n = [Z_A(x_B - x_\alpha) + Z_B(x_\alpha - x_A)] / (x_B - x_A)$$

CT Case	M	α_n	Test No.	θ_0	$\eta = 0.169$				$\eta = 0.655$				$\eta = 0.931$			
					θ (deg)	ϵ_θ (deg)	Z (mm)	ϵ_Z (deg)	θ (deg)	ϵ_θ (deg)	Z (mm)	ϵ_Z (deg)	θ (deg)	ϵ_θ (deg)	Z (mm)	ϵ_Z (deg)
1	0.80	0	2010	0.50	0.51	2	0.01	76	0.52	1	0.15	18	0.54	0	0.25	20
2	0.80	4.0	2014	0.50	0.50	3	0.01	14	0.51	2	0.21	9	-	-	-	-
4	0.90	0	2029	0.50	0.51	2	0.01	-49	0.52	2	0.12	19	0.55	2	0.20	21
5	0.90	4.0	2035	0.50	0.50	4	0.00	-	0.51	4	0.16	10	0.51	2	0.28	13
6	0.95	0	2046	0.50	0.51	2	0.00	-	0.51	1	0.15	11	0.53	1	0.24	12
8	0.95	4.75	2083	0.48	0.50	3	0.01	-106	0.51	3	0.15	-3	0.54	3	0.24	-2
9	1.10	0.55	2045	0.50	0.51	1	0.01	-43	0.51	1	0.19	-4	0.53	1	0.30	-2

Table 7.9

X	SECTION 0		SECTION 1		SECTION 3		SECTION 5		SECTION 6	
	EXTR	INTR	EXTR	INTR	EXTR	INTR	EXTR	INTR	EXTR	INTR
.012	.995	.903	1.013	.937	.916	.966	.928	.958	.936	.978
.025	.886	.910	.918	.969	.940	.967	.947	.985	.941	.978
.050	.853	.916			.944	.974	.965	.973	.970	.986
.075					1.001	.972	.974	.984	.978	1.015
.100	.879	.928	.924	.953	.973	.987	.984	.984	.994	.994
.150	.909	.931	.920	.960	1.011	1.010	.984	1.000	.974	.978
.220	.936	.954	.957	.952	1.015	.997	.994	1.004	.960	.970
.300	.936	.954	.968	.976	.993	.994	.960	.970	.943	.949
.400	.946	.964	1.000	.991	.932	.940	.920	.926	.903	.912
.500			1.002	1.016	.866	.890	.861	.883		
.620	.966	.965	.997	1.004						
.750	.899	.913	.944	.952						
.900	.907	.907	.877	.899						

Table 7.10

X	SECTION 0		SECTION 1		SECTION 3		SECTION 5		SECTION 6	
	EXTR	INTR								
.012	1.204	.779	1.212	.795	1.272	.826	1.361	.832	1.390	.856
.025	1.163	.812	1.238	.824	1.299	.861	1.180	.876	1.356	.872
.050	.912	.834			1.186	.878	1.106	.886	1.263	.900
.075					1.041	.840	1.075	.910	1.049	.949
.100	.936	.861	1.113	.865	1.035	.913	1.026	.940	.950	.967
.150	.967	.876	.978	.881	1.073	.941	.999	.969	.949	.981
.220	1.000	.903	1.041	.909	1.050	.946	.964	.963	.938	.959
.300	1.015	.917	1.068	.929	.994	.963	.926	.930	.909	.923
.400			1.057	.955	.932	.933	.877	.887		
.500	.983	.937	1.024	.959	.869	.891				
.620	.904	.906	.949	.935						
.750	.906	.906	.878	.895						
.900	.906	.906								

MACH=.903

MACH=.902

NORA TEST 2029

NORA TEST 2035

Table 7.11

NORA TEST 2046 MACH=.954

X	SECTION 0		SECTION 1		SECTION 3		SECTION 5		SECTION 6	
	EXTR	INTR								
.012	1.048	.945	1.071	.981	.967	1.015	.978	1.011	1.005	1.049
.025	.952	.953	.966	1.017	.992	1.014	1.013	1.063	1.005	1.060
.050	.892	.960	.975	1.006	.995	1.038	1.040	1.046	1.043	1.057
.075	.921	.975	.968	1.013	1.074	1.042	1.055	1.073	1.077	1.111
.100	.954	.976	1.012	1.000	1.033	1.041	1.078	1.088	1.115	1.143
.150	.988	1.008	1.024	1.027	1.088	1.101	1.126	1.138	1.160	1.176
.200	1.000	1.012	1.062	1.061	1.129	1.107	1.021	1.066	.959	.959
.300	1.065	1.062	1.123	1.128	1.121	1.135	.951	.953	.935	.942
.400	.953	.968	1.007	1.015	.977	.984	.895	.915		
.500	.958	.958	.919	.942	.901	.924				

Table 7.12

NORA TEST 2083 MACH=.951

X	SECTION 0		SECTION 1		SECTION 3		SECTION 5		SECTION 6	
	EXTR	INTR	EXTR	INTR	EXTR	INTR	EXTR	INTR	EXTR	INTR
.012	1.276	.794	1.280	.894	1.403	.892	1.457	.862	1.507	.890
.025	1.297	.832	1.113	.911	1.360	.912	1.355	.914	1.493	.912
.050	1.005	.859	1.314	.856	1.203	.926	1.265	.927	1.449	.940
.075	.987	.888	1.073	.917	1.103	.955	1.232	.953	1.341	.998
.100	1.023	.906	1.105	.946	1.158	.991	1.217	.989	1.172	1.045
.150	1.077	.938	1.127	.971	1.201	.998	1.200	1.041	1.051	1.107
.200	1.074	.955	1.145	1.011	1.212	1.033	1.041	1.069	1.022	1.096
.300	1.122	.996	1.188	1.022	.958	1.011	.975	.986	.971	.975
.400	.962	.963	1.060	.999	.901	.938	.922	.931		
.500	.955	.955	.910	.950						

Table 7.13

NORA TEST 2045 MACH=1.102

X	SECTION 0		SECTION 1		SECTION 3		SECTION 5		SECTION 6	
	EXTR	INTR								
.012	1.236	1.040	1.084	1.082	1.120	1.115	1.083	1.109	1.133	1.129
.025	1.212	1.057	1.080	1.123	1.132	1.129	1.124	1.141	1.124	1.147
.050	1.007	1.082	1.137	1.107	1.167	1.145	1.158	1.125	1.142	1.112
.075	1.034	1.099	1.157	1.134	1.140	1.144	1.167	1.150	1.170	1.155
.100	1.064	1.066	1.168	1.145	1.190	1.173	1.178	1.148	1.206	1.206
.150	1.120	1.120	1.172	1.176	1.234	1.191	1.235	1.204	1.252	1.266
.200	1.122	1.142	1.242	1.229	1.260	1.232	1.268	1.280	1.305	1.315
.300	1.248	1.242	1.257	1.236	1.279	1.260	1.326	1.327	1.296	1.315
.400	1.214	1.236	1.224	1.251	1.248	1.316	1.297	1.338		
.500	1.108	1.108								

Table 7.14

NORA TEST 2185 MACH=0.88 FREQUENCY= 5.HZ PRESSURE=0.98 BAR CP*/R=CP*/I=3.48

X	SECTION 2E		SECTION 4E		SECTION 2I		SECTION 4I	
	R	I	R	I	R	I	R	I
.012	3.792	0.227	4.877	0.375	-1.124	-0.886	-0.49	-0.883
.025	-0.782	-0.816	0.916	0.863	-1.826	-0.888	0.188	-0.171
.050	1.213	0.882	1.878	0.129	-0.749	-0.888	0.199	-0.795
.100	0.982	0.878	1.845	0.89E	-0.288	-0.874	0.288	-0.591
.200	0.664	0.263	0.751	0.875	-0.647	-0.874		
.300	0.572	0.868	0.615	0.876				
.400	0.581	0.867	0.529	0.871				
.488	0.428	0.859	0.484	0.859	0.399	-0.531	0.488	-0.473
.588	0.379	0.878	0.363	0.854	0.588	-0.388	0.581	-0.316
.658	0.335	0.866	0.293	0.137	0.688	-0.243	0.688	-0.181
.788	0.289	0.855	0.242	0.843	0.788	-0.138	0.781	-0.887
.878	0.238	0.847	0.191	0.843				
.900	0.173	0.838	0.198	0.835				
.950	0.138	0.839	0.179	0.831				
.988	0.047	0.824	0.116	0.812				
.978	0.088	0.828	-0.888	0.812				

Table 7.15

NORA		TEST 2818	MACH=8.88	FREQUENCY= 48.HZ	PRESSURE=8.98 BAR	CP'/R=CP"/I=3.48
SECTION 2E						
X	R	I	X	R	I	
.812	3.378	-8.935	.812	4.815	-1.196	
.825	-8.515	8.281	.825	8.819	-8.899	
.838	1.132	-8.197	.838	1.781	-8.282	
.851	8.815	-8.849	.851	8.978	-8.881	
.864	8.632	8.835	.864	8.732	8.857	
.877	8.553	8.188	.877	8.588	8.188	
.890	8.478	8.156	.890	8.492	8.128	
.903	8.425	8.183	.903	8.397	8.284	
.916	8.353	8.288	.916	8.353	8.181	
.929	8.331	8.246	.929	8.274	8.284	
.942	8.289	8.219	.942	8.247	8.198	
.955	8.228	8.248	.955	8.178	8.194	
.968	8.183	8.211	.968	8.092	8.284	
.981	8.121	8.234	.981	8.064	8.184	
.994	8.057	8.215	.994	8.014	8.144	
.878	8.887	8.184	.878	-8.814	8.128	
SECTION 4E						
X	R	I	X	R	I	
.849	-1.741	8.373	.849	8.284	-8.113	
.188	-1.152	8.138	.188	8.155	-8.161	
.199	-8.784	8.821	.199	8.828	-8.379	
.288	-8.687	-8.879	.288	-8.835	-8.243	
.488	-8.485	-8.119	.488	-8.515	-8.197	
.581	-8.384	-8.198	.581	-8.379	-8.161	
.688	-8.185	-8.174	.688	-8.243	-8.286	
.781	-8.872	-8.162	.781	-8.131	-8.197	

Table 7.16

NORA		TEST 2198	MACH=8.88	FREQUENCY= 5.HZ	PRESSURE=8.98 BAR	CP'/R=CP"/I=3.39
SECTION 2E						
X	R	I	X	R	I	
.812	1.138	8.113	.812	8.825	8.124	
.825	1.885	8.114	.825	1.887	8.133	
.838	8.992	8.118	.838	1.422	8.144	
.851	3.885	8.235	.851	1.683	8.152	
.864	1.878	8.875	.864	3.285	8.169	
.877	8.884	8.848	.877	2.233	8.199	
.890	8.895	8.855	.890	2.816	8.153	
.903	8.161	8.281	.903	8.516	8.875	
.916	8.288	8.866	.916	8.417	8.869	
.929	8.212	8.868	.929	8.837	8.868	
.942	8.164	8.856	.942	8.155	8.848	
.955	8.125	8.248	.955	-8.254	8.248	
.968	8.876	8.832	.968	-8.127	8.832	
.981	8.868	8.832	.981	-8.159	8.832	
.994	8.848	8.816	.994	-8.892	8.828	
.878	8.844	8.816	.878	-8.818	8.828	
SECTION 4E						
X	R	I	X	R	I	
.849	-1.849	8.876	.849	-8.931	-8.388	
.188	-8.839	8.864	.188	-8.767	-8.866	
.199	-8.688	8.864	.199	-8.598	-8.866	
.288	-8.538	-8.858	.288	-8.538	-8.864	
.488	-8.398	-8.856	.488	-8.439	-8.866	
.581	-8.357	-8.853	.581	-8.361	-8.861	
.688	-8.228	-8.846	.688	-8.287	-8.854	
.781	-8.896	-8.832	.781	-8.185	-8.844	

Table 7.17

NORA TEST 2814 MACH=5.88 FREQUENCY=48.HZ PRESSURE=9.98 BAR CP'/R-CP*/I=3.39

SECTION 2E			SECTION 4E			SECTION 2I			SECTION 4I		
X	R	I	X	R	I	X	R	I	X	R	I
.812	1.888	8.887	.812	8.921	8.274	.858	-8.846	8.185	.849	-1.888	8.189
.825	8.945	8.878	.825	1.398	8.176	.858	1.914	-8.832	.188	-8.881	8.835
.858	1.887	8.891	.858	1.986	-8.866	.288	1.888	-8.786	.199	-8.546	-8.877
.188	1.888	-1.884	.288	2.568	-8.756	.288	2.323	-8.911	.288	-8.528	-8.182
.288	8.156	8.275	.358	1.394	-8.478	.399	-8.481	-8.163	.488	-8.359	-8.178
.358	8.199	8.318	.488	8.715	-8.877	.588	8.317	8.132	.581	-8.326	-8.179
.458	8.248	8.382	.458	8.317	8.132	.688	8.872	8.288	.688	-8.192	-8.177
.588	8.252	8.288	.588	8.864	8.374	.788	-8.138	8.387	.781	-8.878	-8.176
.688	8.183	8.296	.688	-8.864	8.374	.888	8.871	8.294			
.688	8.135	8.382	.688	-8.138	8.387		-8.896	8.311			
.658	8.885	8.266	.651	-8.871	8.294		-8.853	8.229			
.788	8.867	8.254	.881	-8.896	8.311		8.888	8.163			
.888	8.835	8.288	.871	-8.888	8.163						
.878	8.818	8.155									

Table 7.18

NORA TEST 2124 MACH=8.98 FREQUENCY=5.HZ PRESSURE=8.68 BAR CP'/R-CP*/I=2.97

SECTION 2E			SECTION 4E			SECTION 2I			SECTION 4I		
X	R	I	X	R	I	X	R	I	X	R	I
.812	3.939	8.288	.812	5.784	8.383	.858	-1.667	-8.894	.849	-2.239	-8.117
.825	1.888	8.287	.825	3.856	8.227	.858	-1.274	-8.888	.188	-1.471	-8.897
.858	1.236	8.871	.858	1.971	8.187	.288	1.888	-8.883	.199	-1.838	-8.888
.188	1.888	8.876	.288	1.293	8.883	.288	1.888	-8.874	.288	-8.771	-8.876
.288	8.785	8.865	.358	1.888	8.884	.399	-8.849	-8.879	.488	-8.653	-8.891
.358	8.738	8.872	.488	8.831	8.897	.588	-8.794	-8.888	.581	-8.484	-8.884
.488	8.688	8.889	.488	8.815	8.198	.688	-8.558	-8.881	.688	-8.114	-8.835
.488	8.658	8.882	.488	8.659	8.181	.788	-8.298	-8.862	.781	-8.886	-8.824
.488	8.583	8.887	.488	8.479	8.878						
.688	8.523	8.183	.588	8.231	8.176						
.688	8.399	8.877	.651	8.191	8.859						
.688	8.258	8.862	.688	8.887	8.853						
.658	8.132	8.841	.688	-8.821	8.829						
.788	8.854	8.844	.788	-8.833	8.838						
.888	8.854	8.836	.881	-8.851	8.818						
.878	-8.818	8.824	.871	-8.868	8.812						

Table 7.19

SECTION 2E		SECTION 4E		SECTION 2I		SECTION 4I	
X	R	X	R	X	R	X	R
.812	3.458	.812	4.882	.858	-1.417	.849	-1.979
.825	2.755	.825	3.527	.188	-1.119	.188	-1.394
.858	1.122	.858	1.924	.288	-8.866	.199	-8.967
.188	8.957	.188	1.282	.288	-8.888	.288	-8.829
.288	8.768	.288	1.845	.399	-8.811	.488	-8.651
.288	8.744	.288	8.839	.588	-8.579	.581	-8.382
.358	8.739	.358	8.853	.688	-8.268	.688	-8.843
.488	8.734	.488	8.745	.788	-8.832	.781	8.874
.558	8.648	.558	8.519	.888	-8.388	.888	-8.354
.688	8.617	.688	8.333	.988	-8.355	.988	-8.291
.558	8.459	.551	8.215	.788	-8.258	.788	-8.211
.688	8.278	.681	8.887	.888	-8.249	.888	-8.211
.658	8.149	.651	8.849	.888	-8.164	.888	-8.211
.788	8.853	.781	8.622	.888	-8.554	.888	-8.211
.888	8.811	.881	8.854	.888	-8.119	.888	-8.211
.878	8.811	.871	8.844				

NORA TEST 2823 MACH=8.98 FREQUENCY=48.HZ PRESSURE=8.68 BAR CP'/R-CP"/I=2.97

Table 7.20

SECTION 2E		SECTION 4E		SECTION 2I		SECTION 4I	
X	R	X	R	X	R	X	R
.812	1.657	.812	2.487	.858	-1.826	.849	-1.281
.825	1.526	.825	1.832	.188	-8.828	.188	-8.964
.858	1.215	.858	1.154	.288	-8.698	.199	-8.714
.188	2.995	.188	8.755	.288	-8.645	.288	-8.654
.288	4.832	.288	3.498	.399	-8.575	.488	-8.538
.288	8.888	.288	4.223	.588	-8.582	.581	-8.585
.358	8.888	.358	2.686	.688	-8.489	.688	-8.284
.488	8.713	.488	8.258	.788	-8.247	.781	-8.859
.458	8.374	.458	1.331	.888	-8.862	.888	-8.862
.688	8.183	.688	8.839	.888	-8.875	.888	-8.875
.558	8.178	.551	8.151	.888	-8.871	.888	-8.871
.688	8.836	.681	8.282	.888	-8.836	.888	-8.836
.658	8.858	.651	8.812	.888	-8.836	.888	-8.836
.788	8.888	.781	8.131	.888	-8.836	.888	-8.836
.888	8.818	.881	8.845	.888	-8.836	.888	-8.836
.878	8.824	.871	8.836				

NORA TEST 2136 MACH=8.98 FREQUENCY=6.HZ PRESSURE=8.68 BAR CP'/R-CP"/I=2.98

Table 7.21

SECTION 2E		SECTION 4E		SECTION 2I		SECTION 4I	
X	I	X	I	X	R	X	R
.012	-0.243	.012	2.388	.058	-0.938	.049	-1.143
.025	-0.333	.025	1.651	.188	-0.847	.183	-0.973
.058	-0.264	.188	0.828	.288	-0.725	.199	-0.747
.188	-0.291	.288	2.757	.288	-0.692	.288	-0.687
.288	-1.611	.358	3.229	.399	-0.639	.488	-0.575
.352	0.127	.488	2.725	.588	-0.547	.581	-0.467
.488	-0.163	.588	2.178	.688	-0.398	.688	-0.224
.588	-0.417	.651	1.858	.788	-0.181	.781	0.888
.688	0.369	.888	0.226				
.888	1.385		0.586				
	1.122		0.455				
	0.696		0.432				
	0.444		0.253				
	0.128		0.318				
	-0.164		0.816				
	0.811		0.225				
	0.247		0.149				
	0.191						

NORA TEST 2835 MACH=0.98 FREQUENCY= 48.HZ PRESSURE=0.68 BAR CP'/R=CP'/I=2.98

Table 7.22

SECTION 2E		SECTION 4E		SECTION 2I		SECTION 4I	
X	I	X	I	X	R	X	R
.012	0.158	.012	0.878	.058	-1.633	.049	-2.516
.025	0.168	.025	4.969	.188	-1.296	.183	-2.125
.058	0.832	.188	1.458	.288	-0.786	.199	-0.835
.188	0.858	.288	1.384	.288	-0.856	.288	-0.751
.288	0.846	.358	0.988	.399	-0.658	.488	-1.834
.352	0.841	.488	1.826	.588	-0.566	.581	-0.938
.488	0.864	.588	1.846	.688	-0.666	.688	-0.584
.588	0.835	.651	0.754	.788	-0.352	.781	0.464
.688	0.857	.888	0.765				
.888	0.847		0.441				
	0.847		0.677				
	0.856		0.735				
	0.284		0.254				
	0.158		0.138				
	0.836		0.464				
	0.825		0.179				
	0.125		0.188				

NORA TEST 2114 MACH=0.95 FREQUENCY= 5.HZ PRESSURE=0.68 BAR CP'/R=CP'/I=2.82

Table 7.23
 NDRA TEST 2346 MACH=0.95 FREQUENCY= 48.HZ PRESSURE=0.68 BAR CP'/R=CP"/1-2.82

SECTION 2E			SECTION 4E			SECTION 2I			SECTION 4I		
X	R	I	X	R	I	X	R	I	X	R	I
.012	3.249	-1.012	.012	4.048	-1.344	.058	-1.231	0.379	.049	-1.965	0.748
.025	3.037	-0.762	.025	3.947	-1.164	.188	-1.026	0.196	.188	-1.672	0.667
.100	0.915	-0.216	.058	1.267	-0.343	.188	1.054	0.084	.199	-0.697	0.137
.200	0.985	-0.179	.188	0.744	-0.284	.288	0.744	0.084	.288	-0.665	0.185
.350	0.617	-0.227	.288	0.733	-0.284	.399	0.733	0.126	.488	-0.851	0.243
.488	0.467	-0.084	.399	0.748	-0.222	.688	0.627	0.042	.688	-0.781	0.298
.688	0.035	-0.138	.488	0.626	-0.095	.688	0.626	0.032	.688	-1.085	0.054
.888	0.574	-0.059	.688	0.626	-0.125	.788	0.724	0.212	.788	-0.287	-1.214
.988	0.572	-0.079	.888	0.626	-0.032		2.668				
	0.561	-0.121	.988	0.626	-0.153		0.029				
	0.521	-0.083	.012	2.668	-0.317		1.988				
	0.597	-0.321	.025	0.029	1.988		1.027				
	1.287	0.719	.058	0.038	0.247		0.038				
	1.023	0.444	.088	-0.038	0.247		-0.038				
	-0.198	0.318	.077	-0.024	0.127		-0.024				

Table 7.24
 NDRA TEST 2388 MACH=0.95 FREQUENCY= 6.HZ PRESSURE=0.46 BAR CP'/R=CP"/1-2.83

SECTION 2E			SECTION 4E			SECTION 2I			SECTION 4I		
X	R	I	X	R	I	X	R	I	X	R	I
.012	1.097	0.067	.012	1.795	0.073	.058	-0.855	-0.081	.049	-1.105	-0.087
.025	1.023	0.067	.025	1.748	0.067	.188	-0.035	-0.089	.188	-0.974	-0.074
.100	1.515	0.068	.058	1.824	0.068	.288	0.035	-0.085	.199	-0.757	-0.083
.200	2.224	0.117	.188	1.807	0.094	.399	-0.035	-0.085	.288	-0.739	-0.083
.350	2.167	0.141	.288	2.316	0.081	.488	0.035	-0.085	.488	-0.626	-0.111
.488	2.416	0.182	.399	2.222	0.178	.688	-0.035	-0.183	.688	-0.687	-0.102
.688	0.389	0.067	.488	2.378	0.241	.788	0.035	-0.183	.688	-0.574	-0.101
.888	0.281	0.067	.688	2.448	0.117		.399	-0.717	.788	-0.195	-0.113
.988	0.252	0.046	.888	1.558	0.119		.688	-0.682			
	0.362	0.053	.988	0.588	0.368		.688	-0.523			
	2.515	0.047	.012	0.422	0.074		.788	-0.435			
	0.545	0.048	.025	-0.391	0.067						
	0.584	0.047	.058	-0.383	0.127						
	1.072	0.087	.088	0.222	0.078						
	-0.058	0.054	.077	0.195	0.061						
	0.013	0.048	.077	0.203	0.047						

Table 7.25

NORA TEST 2883 MACH=0.95 FREQUENCY= 40.HZ PRESSURE=5.46 BAR CP*/R=CP*/I=2.83

SECTION 2E			SECTION 4E			SECTION 2I			SECTION 4I		
X	R	I	X	R	I	X	R	I	X	R	I
.612	1.178	-0.385	.612	1.243	-0.556	.058	-1.082	0.136	.049	-1.126	0.171
.625	1.168	-0.374	.625	1.283	-0.518	.188	-0.915	0.086	.188	-0.974	0.158
.658	1.068	-0.358	.658	1.242	-0.516	.288	-0.849	0.088	.288	-0.852	0.036
.188	1.788	-0.368	.188	1.297	-0.479	.288	-0.787	0.088	.288	-0.836	0.043
.288	3.231	-1.583	.288	1.768	-0.849	.399	-0.778	-0.029	.399	-0.855	-0.144
.288	1.059	-0.582	.288	2.623	-1.172	.588	-0.855	0.088	.588	-0.851	-0.189
.358	0.587	0.058	.358	2.986	-1.172	.688	-0.937	-0.189	.688	-0.829	-0.245
.488	0.331	0.188	.488	2.328	-0.845	.788	-0.725	-0.273	.788	-0.628	-0.874
.588	0.262	0.071	.588	1.689	-0.483						
.688	0.313	0.029	.688	0.936	-0.014						
.688	0.424	-0.029	.688	0.516	-0.129						
.658	0.442	-0.044	.658	-0.426	0.358						
.788	0.426	-0.073	.788	0.447	-0.685						
.888	1.487	-1.483	.888	0.447	0.181						
.878	0.183	0.252	.878	0.317	0.117						
	0.133	0.191	.878	0.319	0.072						

Table 7.26

NORA TEST 2113 MACH=1.18 FREQUENCY= 5.HZ PRESSURE=0.68 BAR CP*/R=CP*/I=2.52

SECTION 2E			SECTION 4E			SECTION 2I			SECTION 4I		
X	R	I	X	R	I	X	R	I	X	R	I
.612	2.475	0.188	.612	2.643	0.094	.058	-1.451	-0.071	.049	-1.713	-0.065
.625	2.389	0.189	.625	3.053	0.186	.188	-1.074	-0.053	.188	-1.071	-0.068
.658	3.042	0.124	.658	6.782	0.286	.288	-0.817	-0.058	.288	-0.989	-0.053
.188	0.792	0.053	.188	1.128	0.047	.288	-0.758	-0.058	.288	-0.819	-0.041
.288	0.935	0.053	.288	0.784	0.035	.399	-0.813	-0.058	.399	-0.838	-0.012
.288	0.022	0.042	.288	0.698	0.048	.588	-0.695	-0.024	.588	-0.668	-0.066
.358	0.531	0.048	.358	0.621	0.053	.688	-0.639	-0.018	.688	-0.597	-0.077
.488	0.516	0.038	.488	0.502	0.056	.788	-0.579	-0.047	.788	-0.561	-0.074
.488	0.517	0.052	.488	0.788	0.035						
.588	0.597	0.065	.588	0.433	0.229						
.588	0.603	0.047	.588	0.525	0.041						
.688	0.661	0.047	.688	0.559	0.041						
.658	0.634	0.047	.658	0.792	0.035						
.788	0.695	0.052	.788	0.291	0.059						
.888	0.624	0.054	.888	0.482	0.054						
.878	0.073	0.083	.878	0.386	0.059						

Table 7.27

NORA		TEST 2045	MACH=1.10	FREQUENCY= 40.HZ	PRESSURE=0.60 BAR	CP'/R=CP*/I=2.52	
SECTION 2E		SECTION 4E		SECTION 2I		SECTION 4I	
X	R	X	R	X	R	X	R
.012	2.157	.012	2.157	.050	-1.165	.049	-1.366
.025	3.065	.025	2.680	.100	-0.898	.100	-0.988
.050	1.626	.050	4.268	.200	-0.653	.199	-0.818
.100	0.659	.100	1.030	.400	-0.479	.280	-0.722
.200	0.879	.200	0.645	.600	-0.489	.400	-0.521
.400	0.722	.400	0.616	.800	-0.572	.600	-0.588
.600	0.524	.600	0.492	.900	-0.521	.700	-0.500
.800	0.511	.800	0.532				
.900	0.485	.900	0.605				
1.000	0.531	1.000	0.509				
1.100	0.560	1.100	0.480				
1.200	0.546	1.200	0.455				
1.300	0.495	1.300	0.637				
1.400	0.605	1.400	0.378				
1.500	0.598	1.500	0.414				
1.600		1.600	0.395				
1.700		1.700					
1.800		1.800					
1.900		1.900					
2.000		2.000					
2.100		2.100					
2.200		2.200					
2.300		2.300					
2.400		2.400					
2.500		2.500					
2.600		2.600					
2.700		2.700					
2.800		2.800					
2.900		2.900					
3.000		3.000					
3.100		3.100					
3.200		3.200					
3.300		3.300					
3.400		3.400					
3.500		3.500					
3.600		3.600					
3.700		3.700					
3.800		3.800					
3.900		3.900					
4.000		4.000					
4.100		4.100					
4.200		4.200					
4.300		4.300					
4.400		4.400					
4.500		4.500					
4.600		4.600					
4.700		4.700					
4.800		4.800					
4.900		4.900					
5.000		5.000					
5.100		5.100					
5.200		5.200					
5.300		5.300					
5.400		5.400					
5.500		5.500					
5.600		5.600					
5.700		5.700					
5.800		5.800					
5.900		5.900					
6.000		6.000					
6.100		6.100					
6.200		6.200					
6.300		6.300					
6.400		6.400					
6.500		6.500					
6.600		6.600					
6.700		6.700					
6.800		6.800					
6.900		6.900					
7.000		7.000					
7.100		7.100					
7.200		7.200					
7.300		7.300					
7.400		7.400					
7.500		7.500					
7.600		7.600					
7.700		7.700					
7.800		7.800					
7.900		7.900					
8.000		8.000					
8.100		8.100					
8.200		8.200					
8.300		8.300					
8.400		8.400					
8.500		8.500					
8.600		8.600					
8.700		8.700					
8.800		8.800					
8.900		8.900					
9.000		9.000					
9.100		9.100					
9.200		9.200					
9.300		9.300					
9.400		9.400					
9.500		9.500					
9.600		9.600					
9.700		9.700					
9.800		9.800					
9.900		9.900					
10.000		10.000					

Table 7.28

NORA		TEST 80	MACH=0.80	FREQUENCY= 40.HZ	PRESSURE=0.90 BAR	CP'/R=CP*/I=3.40	
SECTION 2E		SECTION 4E		SECTION 2I		SECTION 4I	
X	R	X	R	X	R	X	R
.012	3.783	.012	5.171	.050	-0.673	.049	-1.935
.025	0.393	.025	1.228	.100	-1.009	.100	-1.209
.050	1.396	.050	1.821	.200	-0.715	.199	-0.811
.100	0.925	.100	1.009	.400	-0.531	.280	-0.657
.200	0.684	.200	0.873	.600	-0.400	.400	-0.468
.400	0.576	.400	0.625	.800	-0.376	.600	-0.323
.600	0.506	.600	0.549	.900	-0.230	.700	-0.161
.800	0.450	.800	0.447			.800	-0.003
.900	0.413	.900	0.372				
1.000	0.356	1.000	0.289				
1.100	0.299	1.100	0.230				
1.200	0.238	1.200	0.178				
1.300	0.178	1.300	0.092				
1.400	0.118	1.400	0.069				
1.500	0.041	1.500	0.013				
1.600	0.011	1.600	0.024				
1.700		1.700					
1.800		1.800					
1.900		1.900					
2.000		2.000					
2.100		2.100					
2.200		2.200					
2.300		2.300					
2.400		2.400					
2.500		2.500					
2.600		2.600					
2.700		2.700					
2.800		2.800					
2.900		2.900					
3.000		3.000					
3.100		3.100					
3.200		3.200					
3.300		3.300					
3.400		3.400					
3.500		3.500					
3.600		3.600					
3.700		3.700					
3.800		3.800					
3.900		3.900					
4.000		4.000					
4.100		4.100					
4.200		4.200					
4.300		4.300					
4.400		4.400					
4.500		4.500					
4.600		4.600					
4.700		4.700					
4.800		4.800					
4.900		4.900					
5.000		5.000					
5.100		5.100					
5.200		5.200					
5.300		5.300					
5.400		5.400					
5.500		5.500					
5.600		5.600					
5.700		5.700					
5.800		5.800					
5.900		5.900					
6.000		6.000					
6.100		6.100					
6.200		6.200					
6.300		6.300					
6.400		6.400					
6.500		6.500					
6.600		6.600					
6.700		6.700					
6.800		6.800					
6.900		6.900					
7.000		7.000					
7.100		7.100					
7.200		7.200					
7.300		7.300					
7.400		7.400					
7.500		7.500					
7.600		7.600					
7.700		7.700					
7.800		7.800					
7.900		7.900					
8.000		8.000					
8.100		8.100					
8.200		8.200					
8.300		8.300					
8.400		8.400					
8.500		8.500					
8.600		8.600					
8.700		8.700					
8.800		8.800					
8.900		8.900					
9.000		9.000					
9.100		9.100					
9.200		9.200					
9.300		9.300					
9.400		9.400					
9.500		9.500					
9.600		9.600					
9.700		9.700					
9.800		9.800					
9.900		9.900					
10.000		10.000					

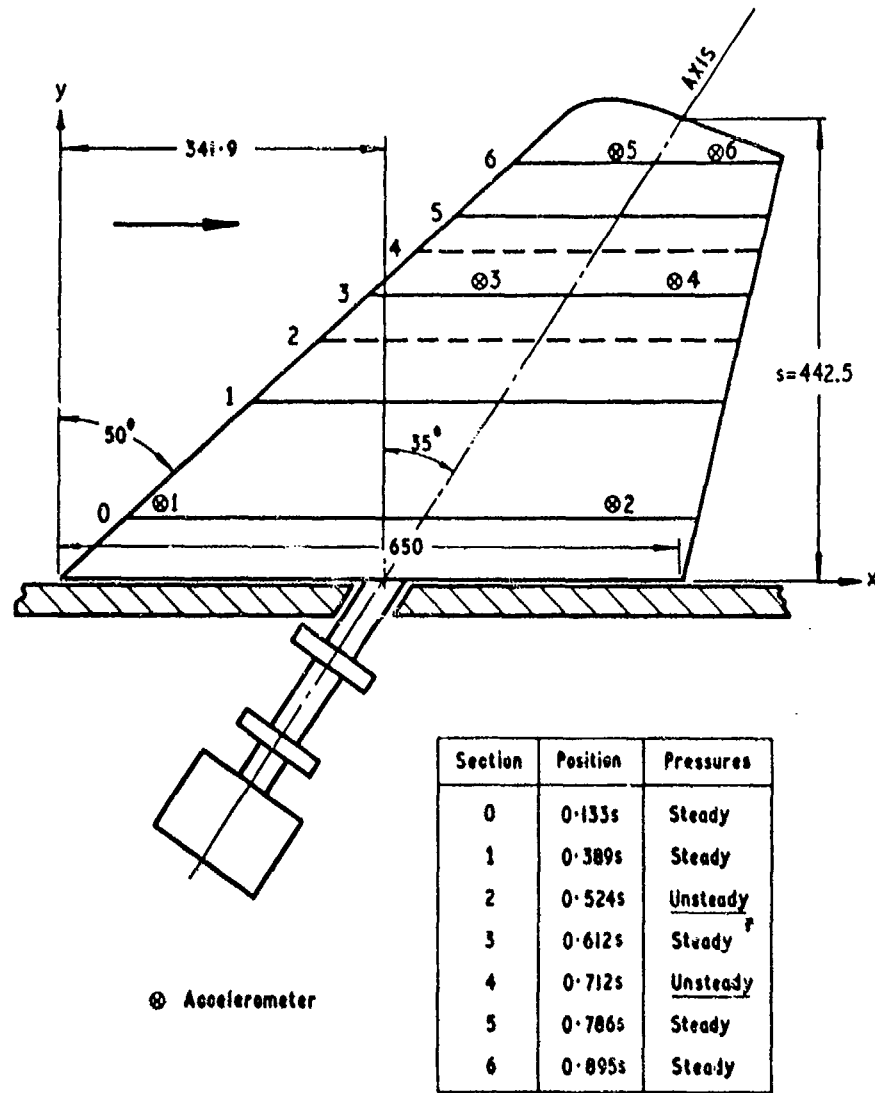


Fig 7.1 Model and rotary oscillator
(dimensions in mm)

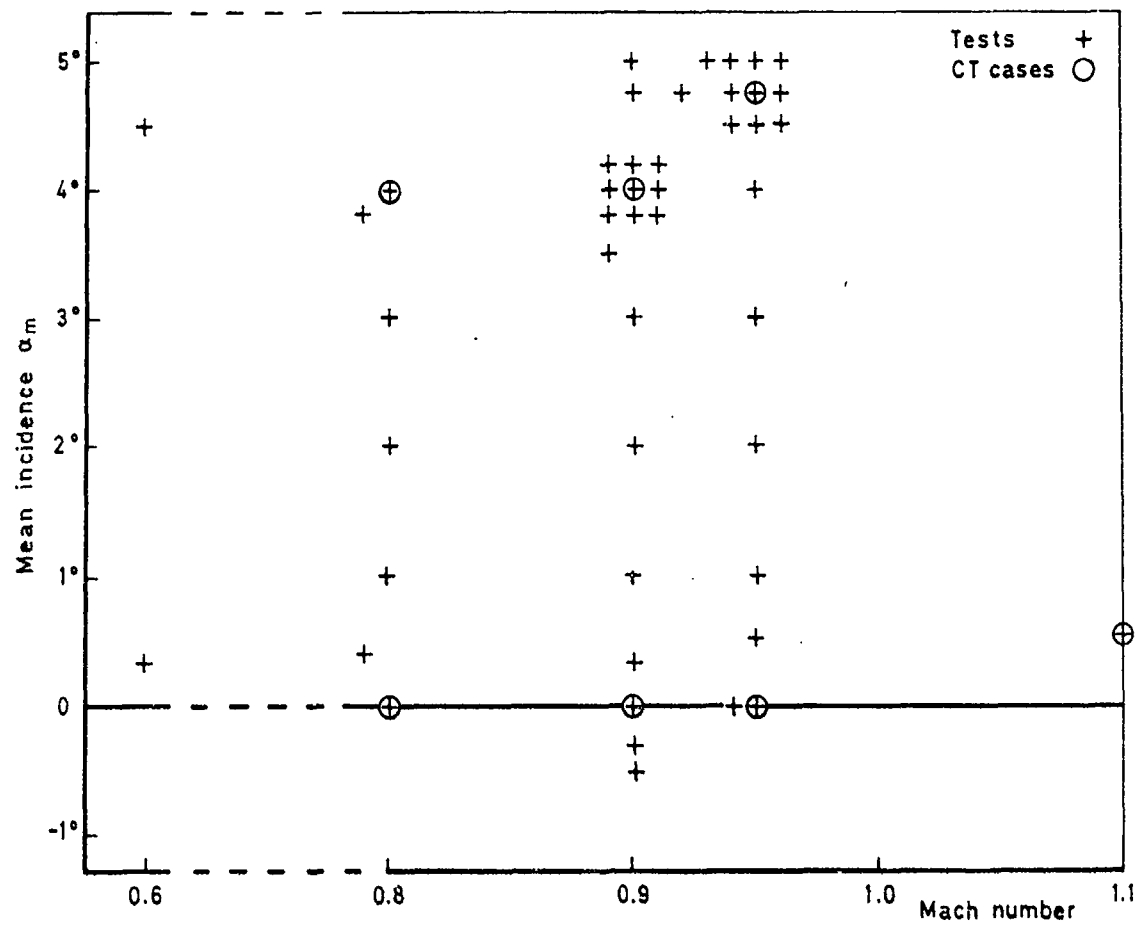


Fig 7.2 Test conditions and computational test cases

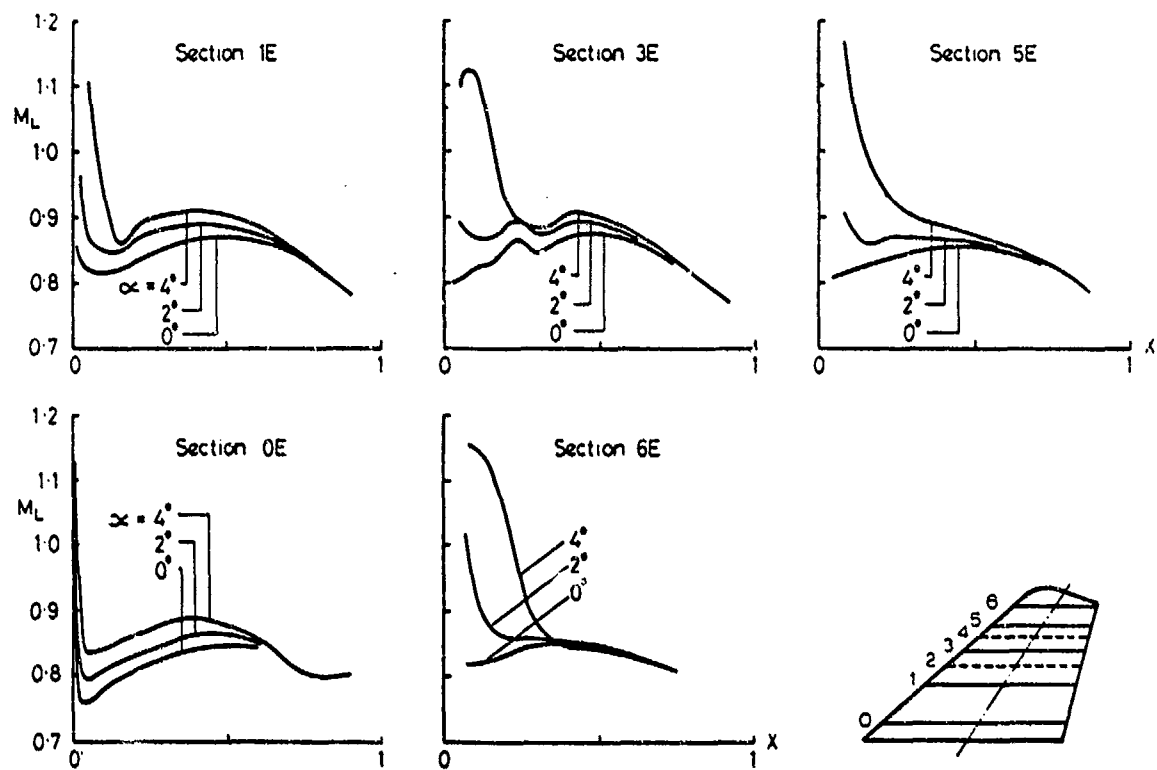


Fig 7.3 Local Mach numbers at upper surface, $M = 0.80$

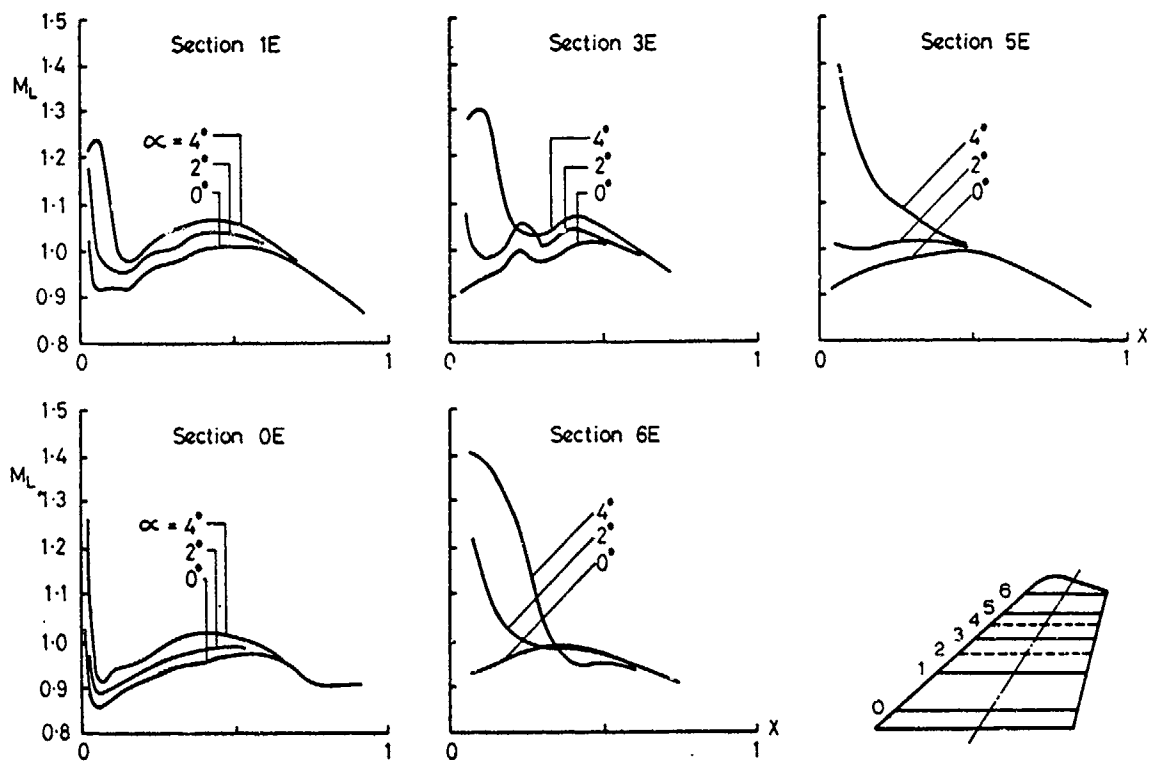


Fig 7.4 Local Mach numbers at upper surface, $M = 0.90$

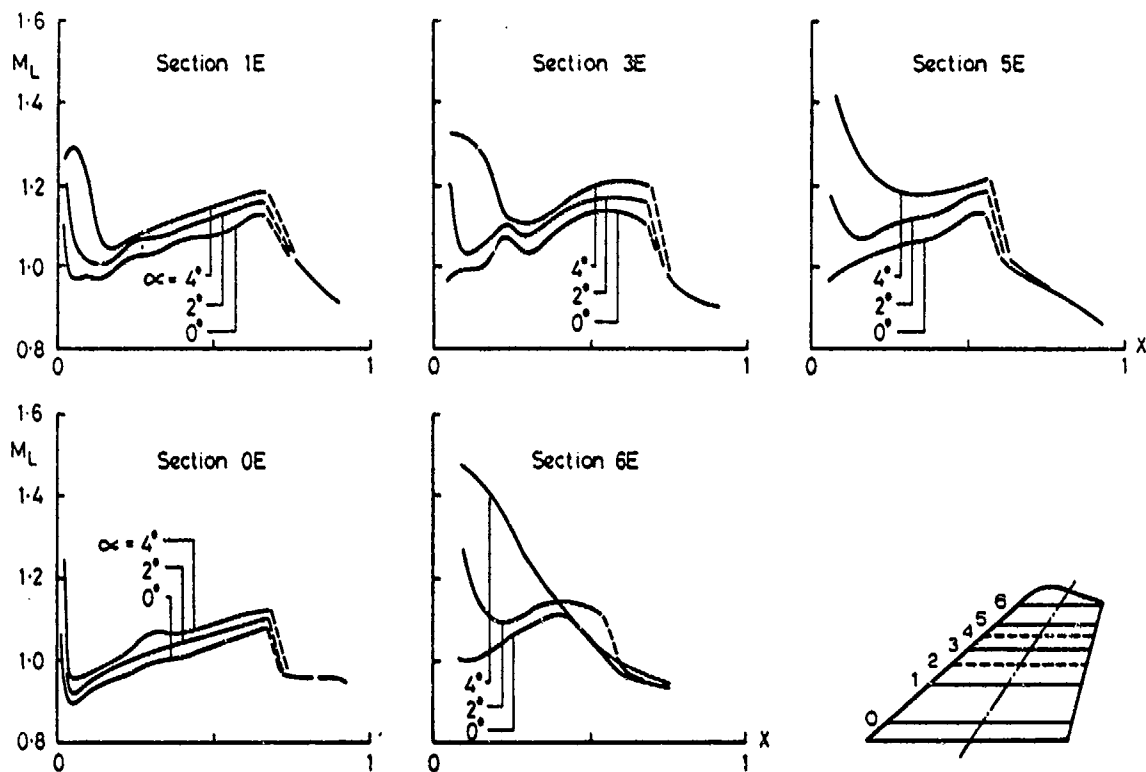


Fig 7.5 Local Mach numbers at upper surface, $M = 0.95$

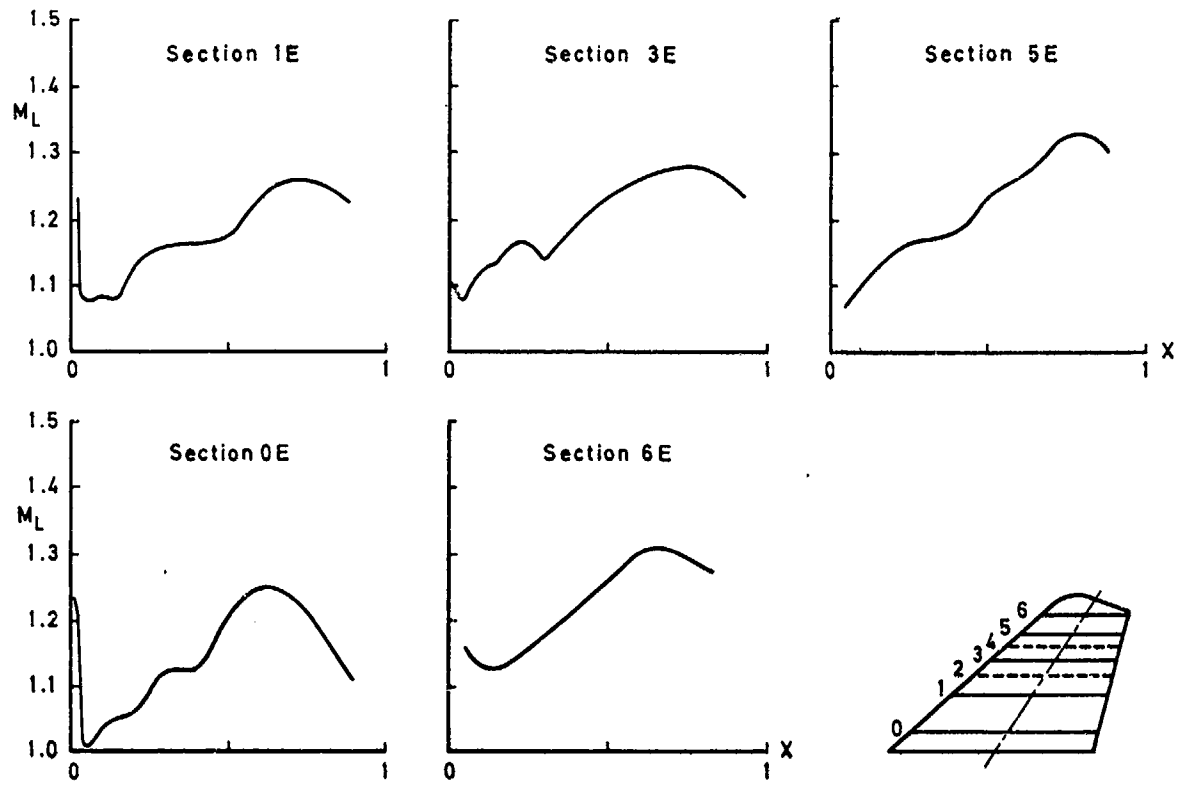


Fig 7.6 Local Mach numbers at upper surface, $M \approx 1.10$, $\alpha \approx 0$

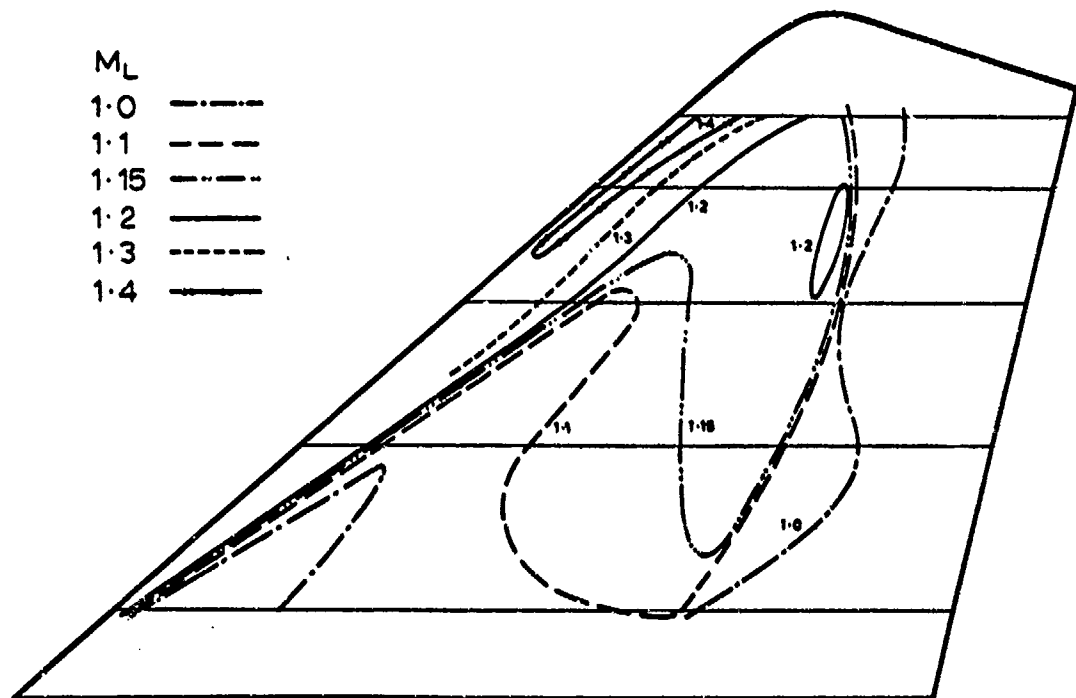


Fig 7.7 Isonachs, $M = 0.95$, $\alpha = 4^\circ$

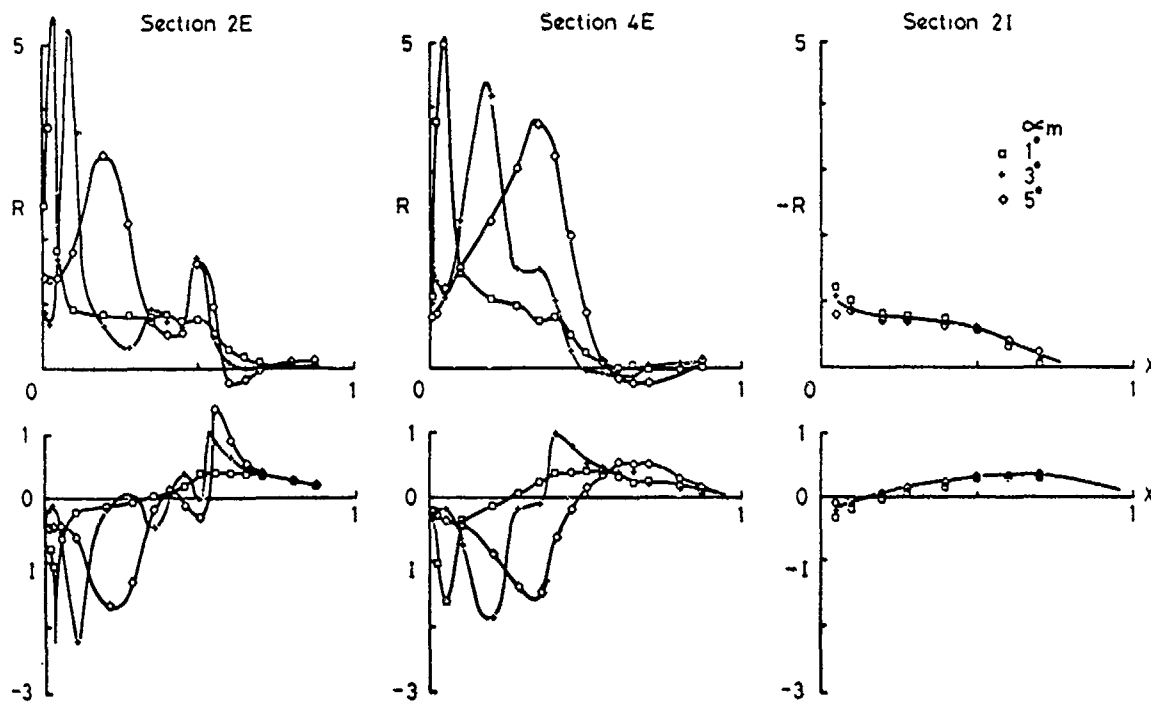


Fig 7.8 Oscillatory pressures. Influence of incidence, $M = 0.90$, $f = 40$ Hz

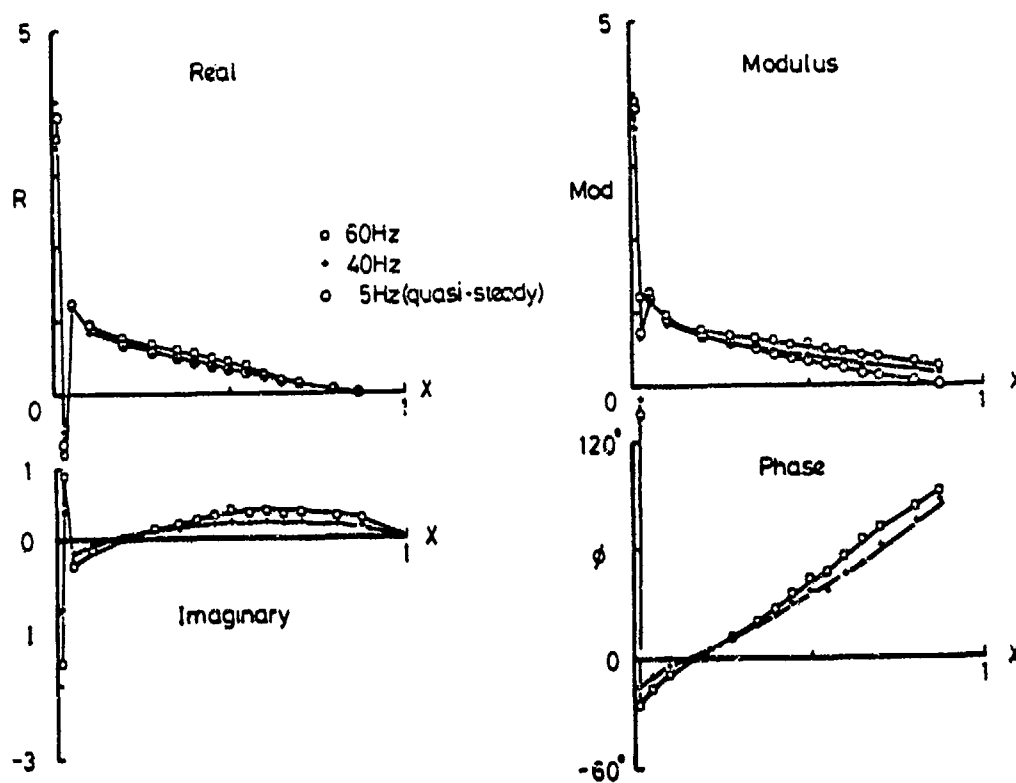


Fig 7.9 Oscillatory pressures, $M = 0.00$, $\alpha_m = 0$. Influence of frequency, Section 2E

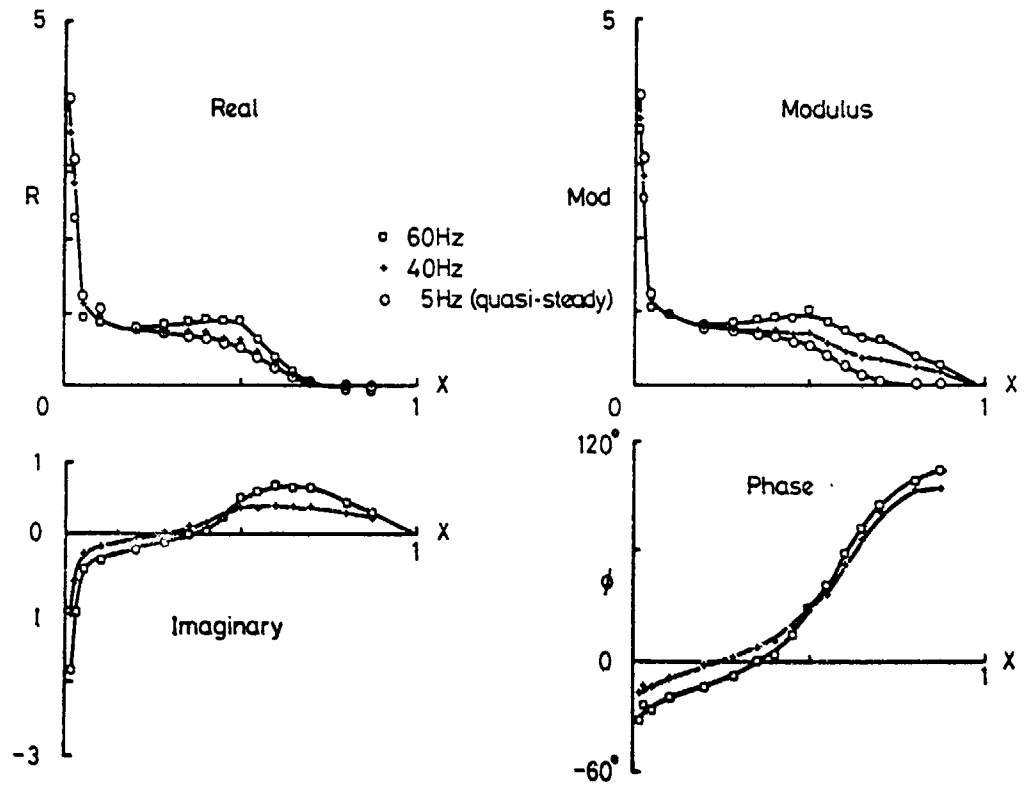


Fig 7.10 Oscillatory pressures, $M = 0.90$,
 $\alpha_m = 0$. Influence of frequency,
 Section 2E

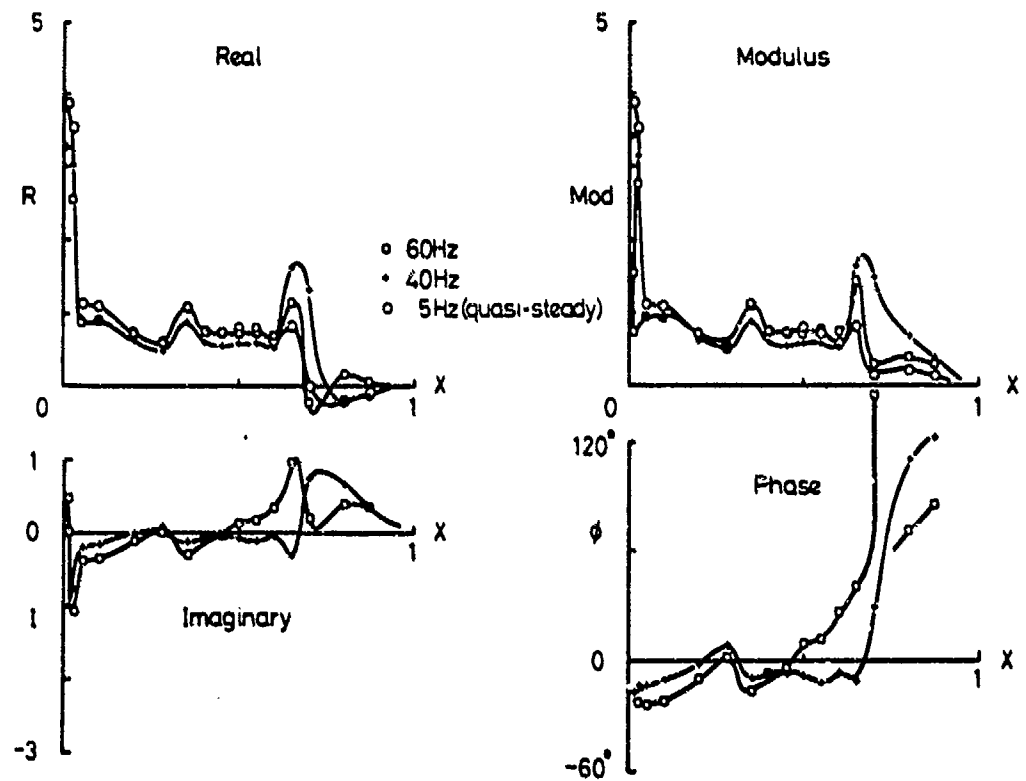


Fig 7.11 Oscillatory pressures, $M = 0.95$,
 $\alpha_m = 0$. Influence of frequency,
 Section 2E

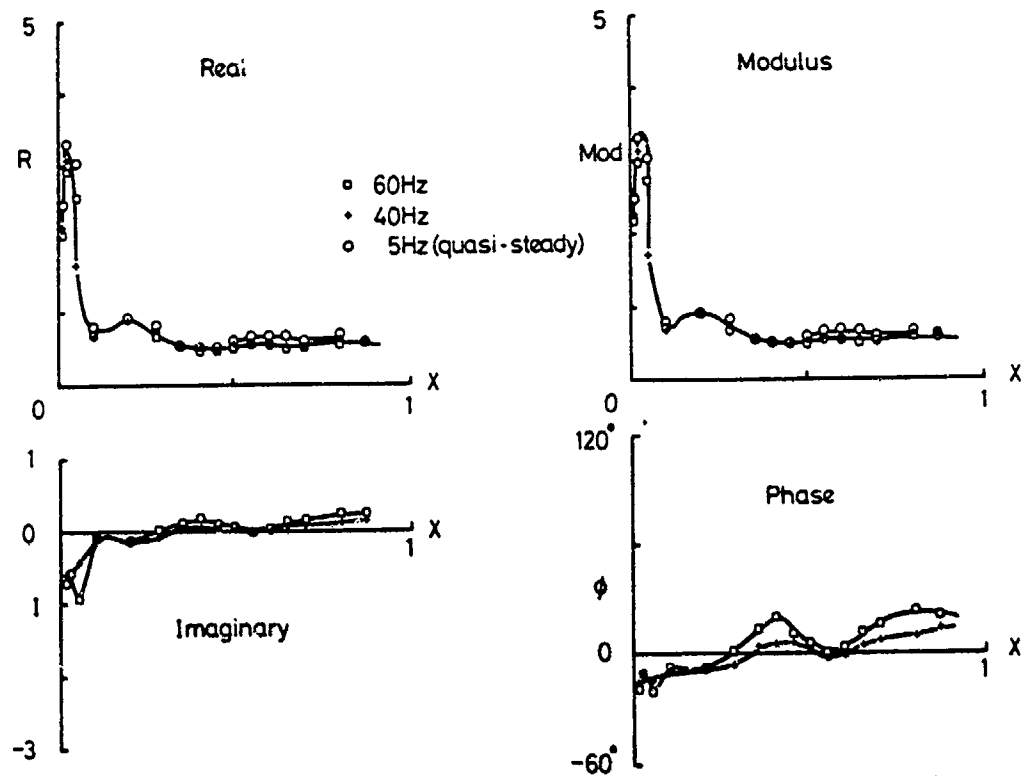


Fig 7.12 Oscillatory pressures, $M = 1.10$,
 $\alpha_m \approx 0.55^\circ$. Influence of frequency,
 Section 2E

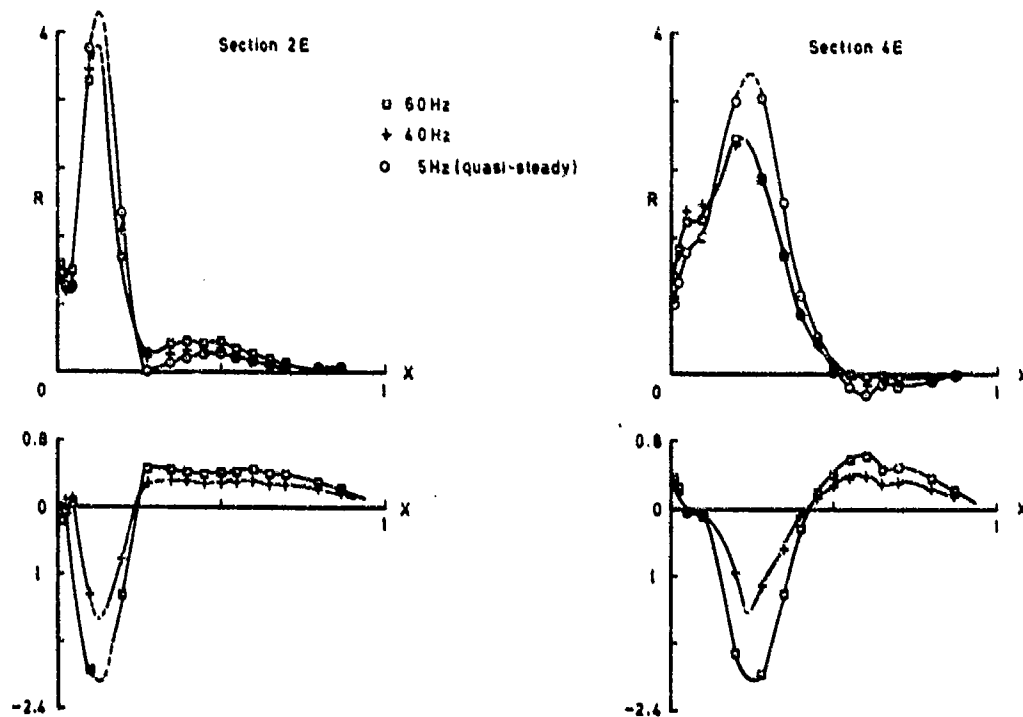


Fig 7.13 Oscillatory pressures, $M = 0.80$, $\alpha_m = 4.0^\circ$.
 Influence of frequency

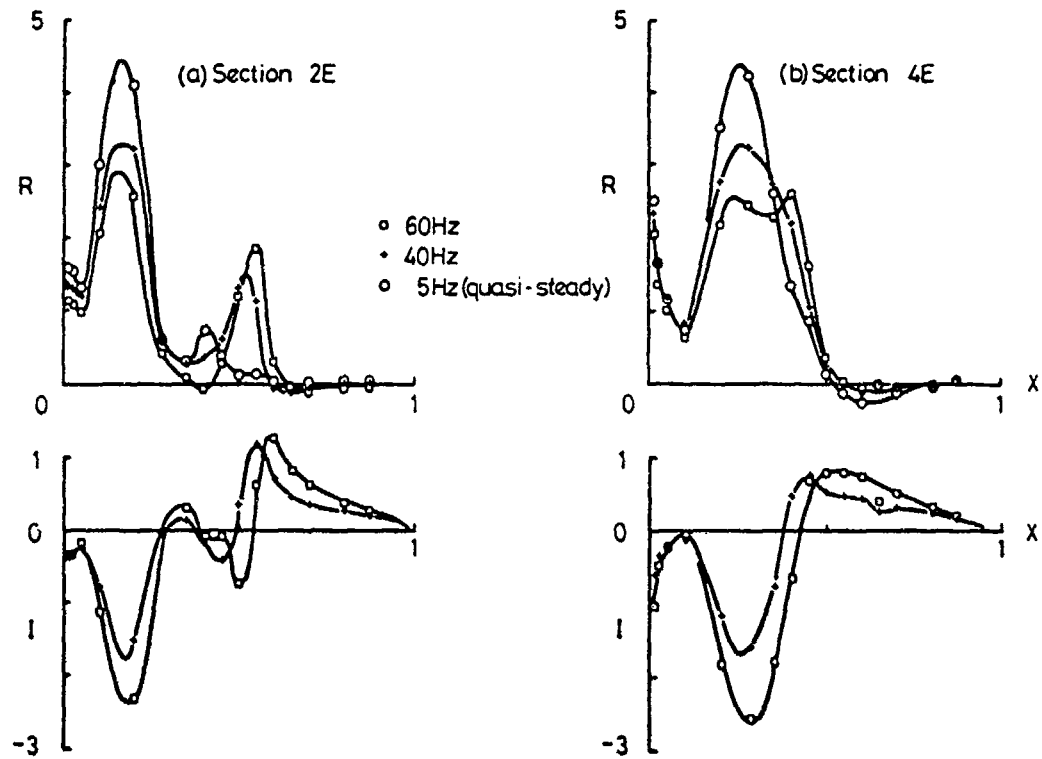


Fig 7.14 Oscillatory pressures, $M = 0.90$,
 $\alpha_m = 4^\circ$. Influence of frequency

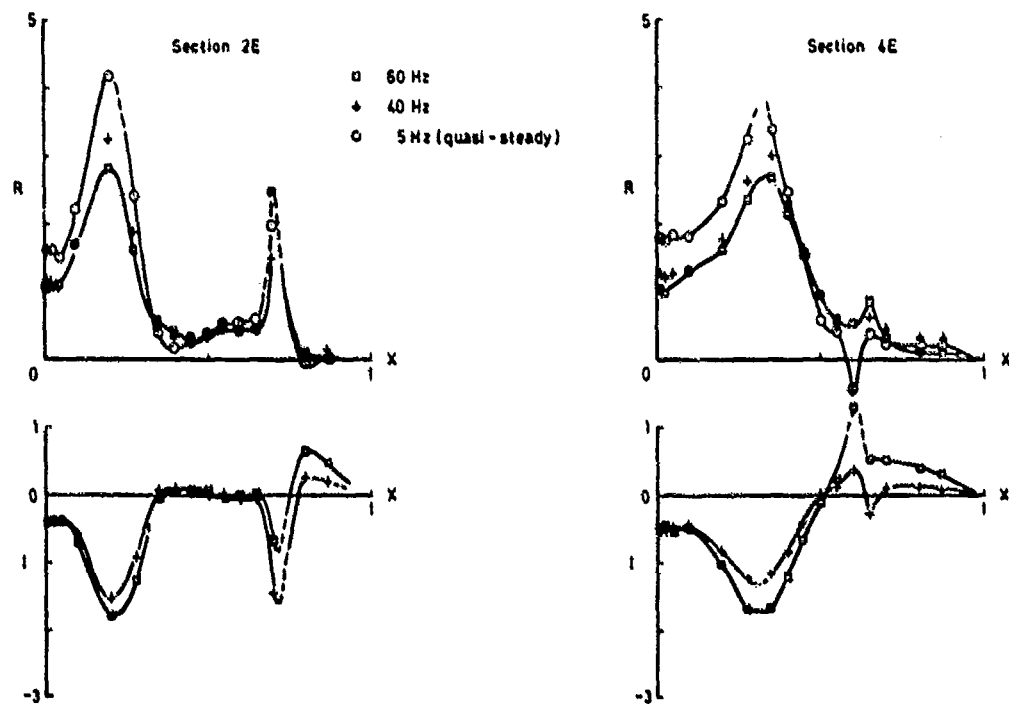


Fig 7.15 Oscillatory pressures, $M = 0.95$, $\alpha_m = 4.75^\circ$.
Influence of frequency

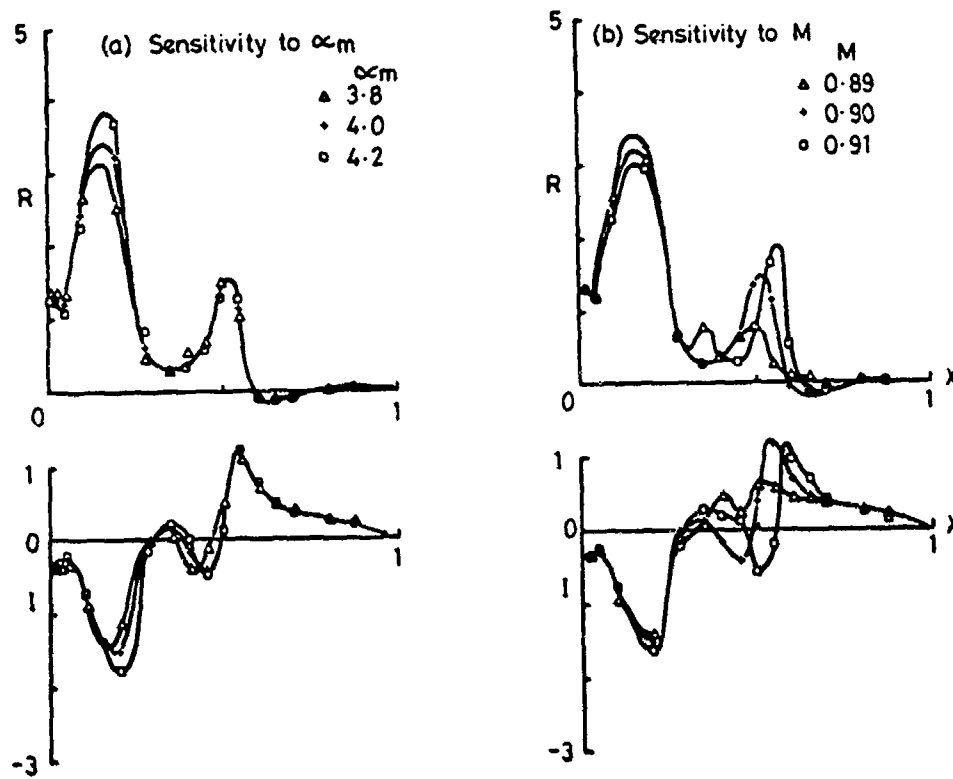


Fig 7.16 Oscillatory pressures. Sensitivity to small changes of incidence and Mach number. $M \approx 0.90$, $\alpha_m \approx 4^\circ$. Section 2E, $f = 40$ Hz

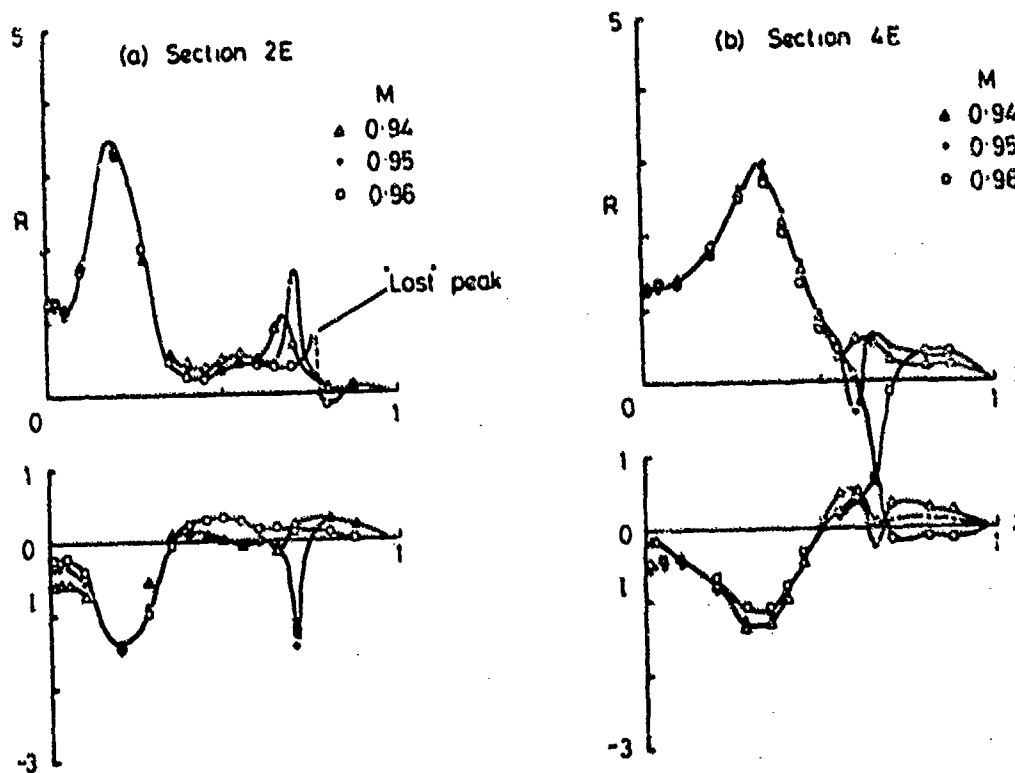


Fig 7.17 Oscillatory pressures. Sensitivity to small changes of Mach number. $M \approx 0.95$, $\alpha_m = 4.75^\circ$, $f = 40$ Hz

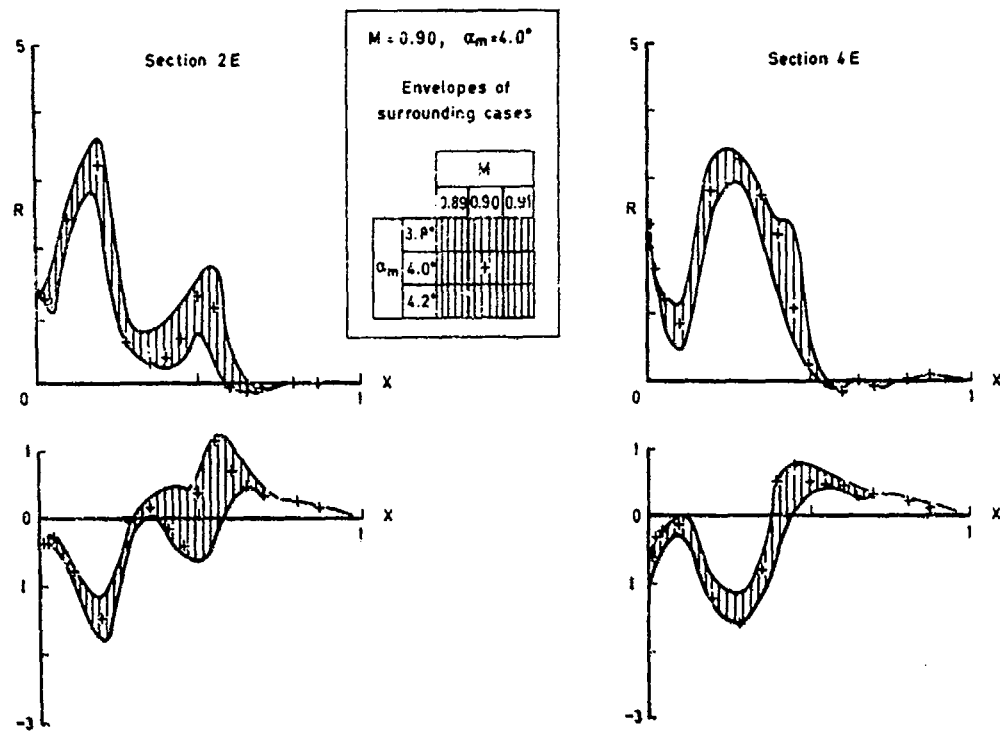


Fig 7.18 Oscillatory pressures for a matrix of cases centred on $M = 0.90, \alpha_m = 4.0^\circ, f = 40 \text{ Hz}$

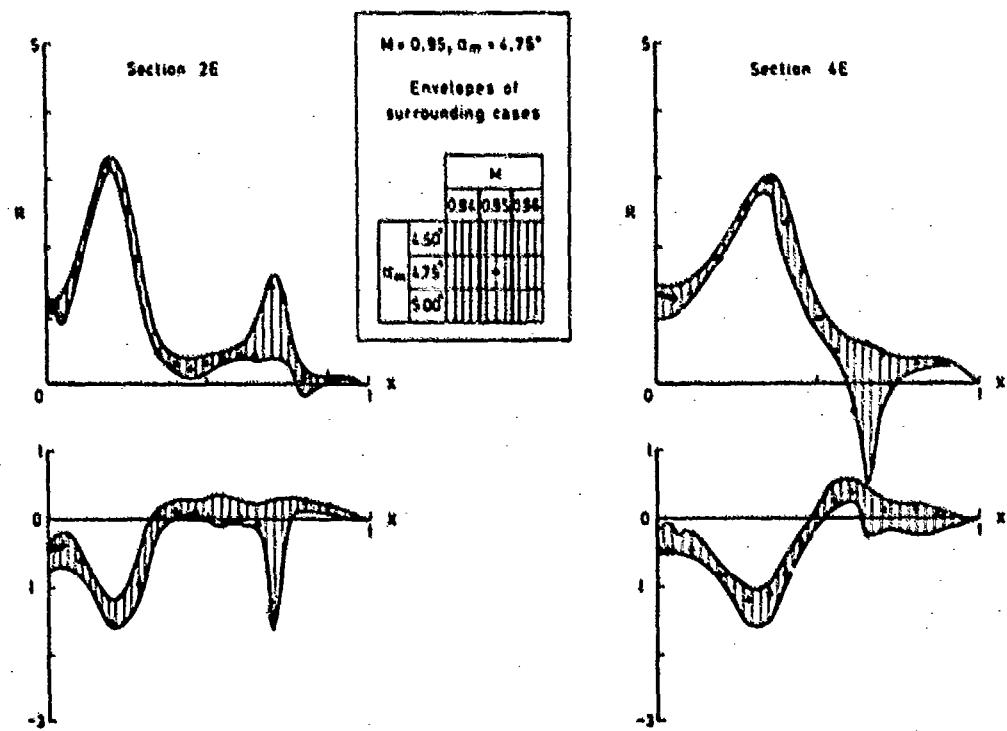


Fig 7.19 Oscillatory pressures for a matrix of cases centred on $M = 0.95, \alpha_m = 4.75^\circ, f = 40 \text{ Hz}$

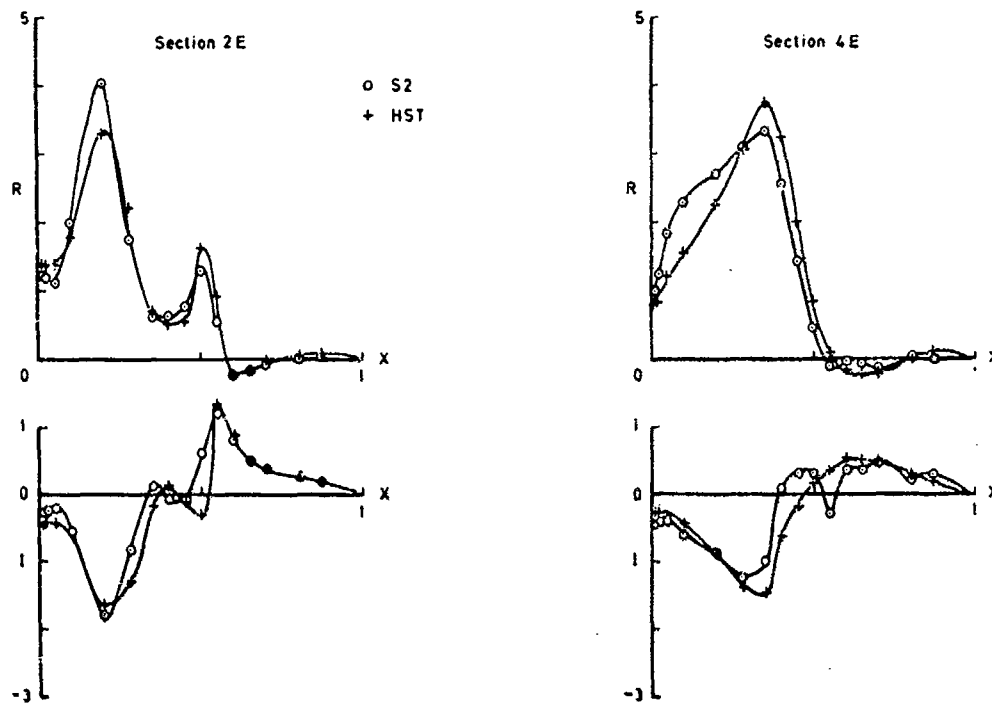


Fig 7.20 Oscillatory pressures. Comparison of data from S2 and HST.
 $M = 0.90$, $\alpha_m = 5^\circ$, $f = 40$ Hz

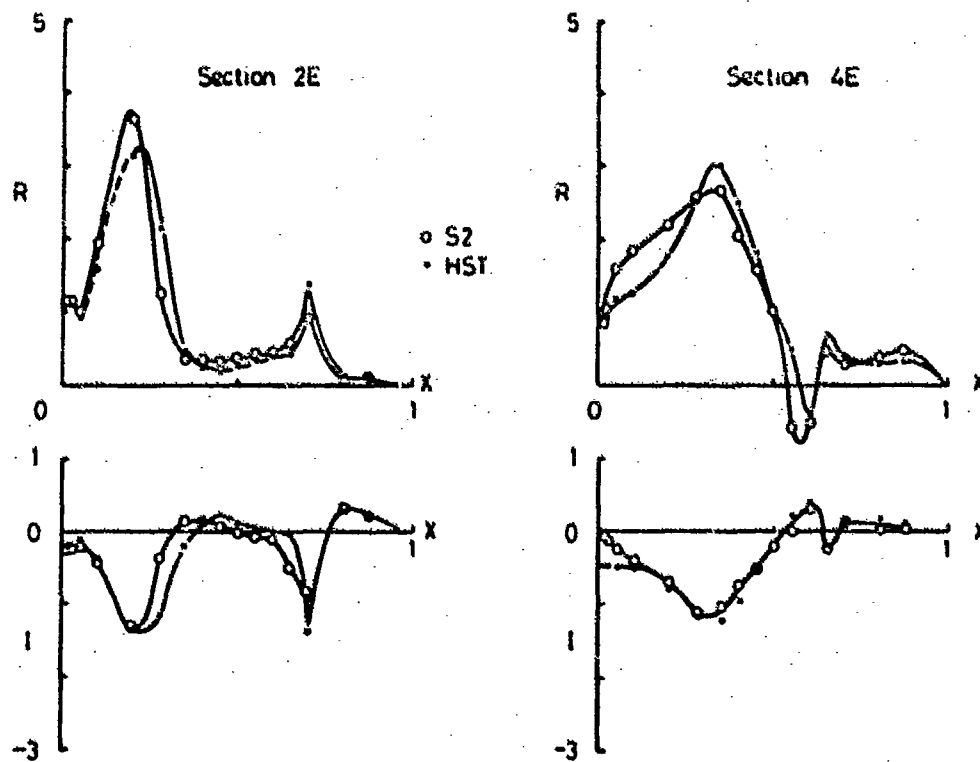


Fig 7.21 Oscillatory pressures. Comparison of data from S2 and HST.
 $M = 0.95$, $\alpha_m = 5^\circ$, $f = 40$ Hz

REPORT DOCUMENTATION PAGE

1. Recipient's Reference	2. Originator's Reference AGARD-R-702	3. Further Reference ISBN 92-835-1430-0	4. Security Classification of Document UNCLASSIFIED								
5. Originator: Advisory Group for Aerospace Research and Development North Atlantic Treaty Organization 7 rue Ancolle, 92200 Neuilly sur Seine, France											
6. Title COMPENDIUM OF UNSTEADY AERODYNAMIC MEASUREMENTS											
7. Presented at											
8. Author(s)/Editor(s) Various			9. Date August 1982								
10. Author's/Editor's Address Various			11. Pages 196								
12. Distribution Statement This document is distributed in accordance with AGARD policies and regulations, which are outlined on the Outside Back Covers of all AGARD publications.											
13. Keywords/Descriptors <table border="0" style="width: 100%;"> <tr> <td style="width: 50%;">Aerodynamic characteristics</td> <td style="width: 50%;">Aerodynamic configurations</td> </tr> <tr> <td>Unsteady flow</td> <td>Experimental data</td> </tr> <tr> <td>Transonic flow</td> <td>Applications of mathematics</td> </tr> <tr> <td>Aeroelasticity</td> <td></td> </tr> </table>				Aerodynamic characteristics	Aerodynamic configurations	Unsteady flow	Experimental data	Transonic flow	Applications of mathematics	Aeroelasticity	
Aerodynamic characteristics	Aerodynamic configurations										
Unsteady flow	Experimental data										
Transonic flow	Applications of mathematics										
Aeroelasticity											
14. Abstract <p>The Compendium is intended to assist the development of improved methods of predicting transonic unsteady aerodynamics and aeroelastic response by collecting the known unsteady aerodynamic experimental data for the standard AGARD two-dimensional and three-dimensional aeroelastic configurations published in AGARD Advisory Reports 156 and 167 respectively.</p> <p>This Report was sponsored by the Structures and Materials Panel of AGARD.</p> <p align="center">7-36</p>											

<p>AGARD Report No. 702 Advisory Group for Aerospace Research and Development, NATO COMPENDIUM OF UNSTEADY AERODYNAMIC MEASUREMENTS Published August 1982 196 pages</p> <p>The Compendium is intended to assist the development of improved methods of predicting transonic unsteady aerodynamics and aeroelastic response by collecting the known unsteady aerodynamic experimental data for the standard AGARD two-dimensional and three-dimensional aeroelastic configurations published in AGARD Advisory Reports 156 and 167 respectively.</p> <p>This Report was sponsored by the Structures and Materials Panel of AGARD. ISBN 92-835-1430-0</p>	<p>AGARD Report No. 702 Advisory Group for Aerospace Research and Development, NATO COMPENDIUM OF UNSTEADY AERODYNAMIC MEASUREMENTS Published August 1982 196 pages</p> <p>The Compendium is intended to assist the development of improved methods of predicting transonic unsteady aerodynamics and aeroelastic response by collecting the known unsteady aerodynamic experimental data for the standard AGARD two-dimensional and three-dimensional aeroelastic configurations published in AGARD Advisory Reports 156 and 167 respectively.</p> <p>This Report was sponsored by the Structures and Materials Panel of AGARD. ISBN 92-835-1430-0</p>	<p>AGARD-R-702</p> <p>Aerodynamic characteristics Unsteady flow Transonic flow Aeroelasticity Aerodynamic configurations Experimental data Applications of mathematics</p>	<p>AGARD-R-702</p> <p>Aerodynamic characteristics Unsteady flow Transonic flow Aeroelasticity Aerodynamic configurations Experimental data Applications of mathematics</p>
<p>AGARD Report No. 702 Advisory Group for Aerospace Research and Development, NATO COMPENDIUM OF UNSTEADY AERODYNAMIC MEASUREMENTS Published August 1982 196 pages</p> <p>The Compendium is intended to assist the development of improved methods of predicting transonic unsteady aerodynamics and aeroelastic response by collecting the known unsteady aerodynamic experimental data for the standard AGARD two-dimensional and three-dimensional aeroelastic configurations published in AGARD Advisory Reports 156 and 167 respectively.</p> <p>This Report was sponsored by the Structures and Materials Panel of AGARD. ISBN 92-835-1430-0</p>	<p>AGARD Report No. 702 Advisory Group for Aerospace Research and Development, NATO COMPENDIUM OF UNSTEADY AERODYNAMIC MEASUREMENTS Published August 1982 196 pages</p> <p>The Compendium is intended to assist the development of improved methods of predicting transonic unsteady aerodynamics and aeroelastic response by collecting the known unsteady aerodynamic experimental data for the standard AGARD two-dimensional and three-dimensional aeroelastic configurations published in AGARD Advisory Reports 156 and 167 respectively.</p> <p>This Report was sponsored by the Structures and Materials Panel of AGARD. ISBN 92-835-1430-0</p>	<p>AGARD-R-702</p> <p>Aerodynamic characteristics Unsteady flow Transonic flow Aeroelasticity Aerodynamic configurations Experimental data Applications of mathematics</p>	<p>AGARD-R-702</p> <p>Aerodynamic characteristics Unsteady flow Transonic flow Aeroelasticity Aerodynamic configurations Experimental data Applications of mathematics</p>

AGARD

NATO  OTAN

7 RUE ANCELLE · 92200 NEUILLY-SUR-SEINE

FRANCE

Telephone 745.08.10 · Telex 610176

DISTRIBUTION OF UNCLASSIFIED
AGARD PUBLICATIONS

AGARD does NOT hold stocks of AGARD publications at the above address for general distribution. Initial distribution of AGARD publications is made to AGARD Member Nations through the following National Distribution Centres. Further copies are sometimes available from these Centres, but if not may be purchased in Microfiche or Photocopy form from the Purchase Agencies listed below.

NATIONAL DISTRIBUTION CENTRES

BELGIUM

Coordonnateur AGARD · VSL
Etat-Major de la Force Aérienne
Quartier Reine Elisabeth
Rue d'Evere, 1140 Bruxelles

CANADA

Defence Science Information Services
Department of National Defence
Ottawa, Ontario K1A 0K2

DENMARK

Danish Defence Research Board
Østerbrogades Kaserne
Copenhagen Ø

FRANCE

O.N.E.R.A. (Direction)
29 Avenue de la Division Leclerc
92320 Châtillon sous Bagneux

GERMANY

Fachinformationszentrum Energie,
Physik, Mathematik GmbH
Kernforschungszentrum
D-7514 Eggenstein-Leopoldshafen 2

GREECE

Hellenic Air Force General Staff
Research and Development Directorate
Holargos, Athens

IRELAND

Director of Aviation
c/o Flugrad
Reykjavik

ITALY

Aeronautica Militare
Ufficio del Delegato Nazionale all'AGARD
3, Piazzale Adenauer
Roma/EUR

LUXEMBOURG

See Belgium

NETHERLANDS

Netherlands Delegation to AGARD
National Aerospace Laboratory, NLR
P.O. Box 126
2600 A.C. Delft

NORWAY

Norwegian Defence Research Establishment
Main Library
P.O. Box 25
N-2007 Kjeller

PORTUGAL

Direcção de Serviço de Material
de Força Aérea
Rua da Escola Politécnica 42
Lisboa
Attn: AGARD National Delegate

TURKEY

Department of Research and Development (ARGE)
Ministry of National Defence, Ankara

UNITED KINGDOM

Defence Research Information Centre
Station Square House
St. Mary Cray
Orpington, Kent BR5 3RE

UNITED STATES

National Aeronautics and Space Administration (NASA)
Langley Field, Virginia 23365
Attn: Report Distribution and Storage Unit

THE UNITED STATES NATIONAL DISTRIBUTION CENTRE (NASA) DOES NOT HOLD STOCKS OF AGARD PUBLICATIONS, AND APPLICATIONS FOR COPIES SHOULD BE MADE DIRECT TO THE NATIONAL TECHNICAL INFORMATION SERVICE (NTIS) AT THE ADDRESS BELOW.

PURCHASE AGENCIES

Microfiche or Photocopy

National Technical
Information Service (NTIS)
5225 Fort Royal Road
Springfield
Virginia 22161, USA

Microfiche

Space Documentation Service
European Space Agency
10, rue Mario Nikis
75015 Paris, France

Microfiche or Photocopy

British Library Lending
Division
Boston Spa, Wetherby
West Yorkshire LS23 7BQ
England

Requests for microfiche or photocopies of AGARD documents should include the AGARD serial number, title, author or editor, and publication date. Requests to NTIS should include the NASA accession report number. Full bibliographical references and abstracts of AGARD publications are given in the following journals:

Scientific and Technical Aerospace Reports (STAR)
published by NASA Scientific and Technical
Information Facility
Post Office Box 8757
Baltimore/Washington International Airport
Maryland 21240, USA

Government Reports Announcements (GRA)
published by the National Technical
Information Service, Springfield
Virginia 22161, USA



Printed by Technical Editing and Reproduction Ltd
5-11, Mortimer Street, London W1N 7RH

ISBN 92-835-1430-0